PB88-220496

Electrical Leak Location Method for Geomembrane Liners

Southwest Research Inst., San Antonio, TX

Prepared for

Environmental Protection Agency, Cincinnati, OH

Jun 88

U.S. Department of Commerce
National Technical Information Service
NTIS

TECHNICAL REPORT DATA

(Please read Instructions on the reverse before completing)

1. REPORT NO. EPA/600/2-88/035	2.	3. RECIPIENT'S ACCESSION NO.
4. TITLE AND SUBTITLE The Electrical Leak Location Method for Geomembrane Liners		5. REPORT DATE June 1988
		6. PERFORMING ORGANIZATION CODE
7. AUTHOR(S) Glenn T. Darilek and Jorge O. Parra		8. PERFORMING ORGANIZATION REPORT NO.
9. PERFORMING ORGANIZATION NAME AND ADDRESS Southwest Research Institute 6220 Culebra Road San Antonio, Texas 78284		10. PROGRAM ELEMENT NO.
		11. CONTRACT/GRANT NO. CR811771
12. SPONSORING AGENCY NAME AND ADDRESS Hazardous Waste Engineering Research Laboratory Office of Research and Development U.S. Environmental Protection Agency Cincinnati, Ohio 45268		13. TYPE OF REPORT AND PERIOD COVERED
		14. SPONSORING AGENCY CODE EPA/600/12

15. SUPPLEMENTARY NOTES

Project Officer: Charles C. Moench, Jr. (513) 569-7819

16. ABSTRACT

An electrical method for detecting and locating leaks in geomembrane liners for hazardous waste impoundments and landfills was developed and successfully demonstrated for a wide variety of applications. Geomembrane liners are sheets of polymeric materials used to prevent the leakage of waste and to prevent rainwater from infiltrating solid waste landfills and surface impoundments. When no leaks are present, a voltage applied between the material in the liner and the earth under the liner produces a relatively uniform electrical potential distribution in the material in the liner. Leaks are located by mapping the anomaly in the potential distribution caused by current flowing through a leak.

Tests on a small-scale double-lined model demonstrated the applicability of the method to a wide variety of double liner configurations of drainage layers with various test parameters such as leak size, electrode depth, and protective soil cover. Leaks in the top liner were easily detected and located. Leaks smaller than 0.8 mm in diameter were reliably located. Leaks in the bottom liner were detected, but not located.

17. KEY WORDS AND DOCUMENT ANALYSIS

a. DESCRIPTORS	b. IDENTIFIERS/OPEN ENDED TERMS	c. COSATI Field/Group

18. DISTRIBUTION STATEMENT Release to Public	19. SECURITY CLASS (This Report) Unclassified	21. NO. OF PAGES 177
	20. SECURITY CLASS (This page) Unclassified	22. PRICE

PB88-220496

EPA/600/2-88/035
June 1988

THE ELECTRICAL LEAK LOCATION METHOD FOR GEOMEMBRANE LINERS

by

Glenn T. Darilek
Jorge O. Parra
Southwest Research Institute
San Antonio, Texas 78284

Contract No. CR-811771-01-3

Project Officer

Charles J. Moench, Jr.
Land Pollution Control Division
Hazardous Waste Engineering Research Laboratory
Cincinnati, Ohio 45268

HAZARDOUS WASTE ENGINEERING RESEARCH LABORATORY
OFFICE OF RESEARCH AND DEVELOPMENT
U.S. ENVIRONMENTAL PROTECTION AGENCY
CINCINNATI, OHIO 45268

REPRODUCED BY
U.S. DEPARTMENT OF COMMERCE
National Technical Information Service
SPRINGFIELD, VA. 22161

DISCLAIMER NOTICE

The information in this document has been funded wholly or in part by the United States Environmental Protection Agency under Cooperative Agreement No. CR-811771-01-3 with Southwest Research Institute. It has been subjected to the Agency's peer and administrative review, and has been approved for publication as an EPA document.

Mention of trade names or commercial products is for explanatory purposes only and does not imply specific endorsement or recommendation by the Environmental Protection Agency or Southwest Research Institute.

SAFETY WARNING

EXTREME ELECTRICAL SHOCK HAZARD

THE HIGH VOLTAGES USED FOR THE LEAK DETECTION METHOD AND TEST PROCEDURES DESCRIBED IN THIS REPORT PRESENT A POTENTIAL FOR ELECTRICAL SHOCK. THE POTENTIAL FOR ELECTRICAL SHOCK IS INCREASED IF OPERATIONS ARE BEING PERFORMED NEAR WATER. SAFETY MEASURES MUST BE TAKEN TO MINIMIZE THE RISK OF INJURY TO OR DEATH OF PERSONNEL. THE TECHNIQUES SET FORTH IN THIS REPORT SHOULD BE ATTEMPTED ONLY BY QUALIFIED PERSONNEL WHO ARE EXPERIENCED IN PERFORMING MEASUREMENTS UNDER SIMILAR CONDITIONS.

FOREWORD

Today's rapidly developing and changing technologies and industrial products and practices frequently carry with them the increased generation of solid and hazardous wastes. These materials, if improperly dealt with, can threaten both public health and the environment. Abandoned waste sites and accidental releases of toxic and hazardous substances to the environment also have important environmental and public health implications. The Hazardous Waste Engineering Research Laboratory assists in providing an authoritative and defensible engineering basis for assessing and solving these problems. Its products support the policies, programs, and regulations of the Environmental Protection Agency, the permitting and other responsibilities of State and local governments, and the needs of both large and small busineses in handling their wastes responsibly and economically.

This report describes methodologies which have been found useful for locating leaks in the geomembrane liner of hazardous waste impoundments and landfills, and will be useful to industrial and engineering firms which have occasion to deal with waste handling and disposal. It should also be of value for regulatory and environmental groups to assess the technical solutions proposed for specific sites requiring remedial action. For further information, please contact the Land Pollution Control Division of the Hazardous Waste Engineering Laboratory.

Thomas R. Hauser, Director
Hazardous Waste Engineering Research Laboratory

ABSTRACT

An electrical method for detecting and locating leaks in geomembrane liners for hazardous waste impoundments and landfills was developed and successfully demonstrated for a wide variety of applications. Geomembrane liners are sheets of elastomeric materials used to prevent the leakage of waste and to prevent rainwater from infiltrating solid waste landfills and surface impoundments. When no leaks are present, a voltage applied between the material in the liner and the earth under the liner produces a relatively uniform electrical potential distribution in the material in the liner. Leaks are located by mapping the anomaly in the potential distribution caused by current flowing through a leak.

A computer simulation model was developed to efficiently predict the effect of a wide range of parameters on the leak signature. The model can accommodate a layered earth sequence above and below an insulating liner with a leak. The model was used to determine leak signatures under a wide variety of measurement parameters for both liquid impoundments and liner cover systems. These determinations allow the design of leak location surveys on an individual basis.

Tests on a small-scale double-lined model demonstrated the applicability of the method to a wide variety of double liner configurations of drainage layers with various test parameters such as leak size, electrode depth, and protective soil cover. Leaks in the top liner were easily detected and located. Leaks smaller than 0.8 mm in diameter were reliably located. Leaks in the bottom liner were detected, but not located. Other auxiliary tests of various electrode materials and geometries were performed to further optimize the method.

The electrical leak location method was adapted for locating leaks in the geomembrane liners of waste impoundment or landfill final cover systems. A scale model was used to test various techniques for improving the detection capabilities under a wide range of cover soil thicknesses, leak sizes, and cover soil resistivities. By using special non-polarizing electrodes, the method proved to be very successful in locating leaks as small as 3 mm under 60 cm of soil cover.

Other methods for locating leaks in cover system liners were investigated and analyzed. The most promising methods include injection and detection of tracer gas and ground-penetrating radar. Limited testing using infrared imaging was unsuccessful in detecting localized areas of low thermal conductivity caused by drainage of soil moisture through a leak.

Testing of the electrical leak location method at one full-scale impoundment site was partially successful. Subsequent improvements in the measurement method and hardware were made to improve the detection and location capabilities. The second full-scale test, at a different impoundment, was successful in finding a leak that had remained undetected by the vacuum box method.

The project has proven the effectiveness of the electrical leak location method for detecting and locating leaks in single and double liners and for cover liners for both pre-service quality assurance testing and in-service performance monitoring.

This report was submitted in fulfillment of the U.S. Environmental Protection Agency Cooperative Agreement No. CR-811771-01-3 by Southwest Research Institute. This report covers a period from September 1984 to December 1987. Work was completed as of December 1987.

CONTENTS

Page

FOREWORD iii
ABSTRACT iv
FIGURES ix
TABLES xv
TABLE OF CONVERSION FACTORS xvi
ABBREVIATIONS xvii

1 INTRODUCTION 1
  BACKGROUND 1
  OBJECTIVES 2

2 CONCLUSIONS 4

3 RECOMMENDATIONS 6

4 TECHNICAL DISCUSSION 8
  CONCEPT DEVELOPMENT 8
  INSTRUMENTATION 10

5 COMPUTER SIMULATION MODEL 13
  BACKGROUND 13
  OBJECTIVES 13
  RESEARCH APPROACH 13
    Theoretical Analysis to Simulate the Response of a Leak in a Lined Impoundment 14
      Formulation 14
      Multiple Leaks 25
    Theoretical Analysis to Simulate the Response of a Leak in the Geomembrane of a Cover System . . 27
    Comparison of Model Results with Field Data 33
    Application of the Computer Model 35
      Parametric Study 35
      Anomaly effects of a leak. 35
      Effect of dipole spacing 38
      Effect of impoundment depth. 38
      Effect of waste material and soil resistivity. . 38
      Effect of offset distance from the leak center . 44
      Comparison of horizontal and vertical dipole surveys 44
      Leak resolution. 44
  SUMMARY 50

CONTENTS (Continued)

Page

6 DOUBLE LINER MODEL TESTS 55
  BACKGROUND 55
  OBJECTIVE 55
  RESEARCH APPROACH 55
    Initial Feasibility Demonstration Tests 55
      Test Procedures 55
      Results of Tests 60
    Tests with Various Drainage Layers, Leak Size and Geometry, and Protective Covers 64
      Test Procedures 64
      Results of Tests 64
    Electrode Material and Type 74
      Test Procedures 74
      Results of Tests 81
    Electrode Geometry 81
      Test Procedures 81
      Results of Tests 82
    Leak Resistance versus Leak Size 82
      Discussion 82
      Test Procedures 82
      Results of Tests 82
  SUMMARY 82

7 LOCATING LEAKS IN COVER SYSTEMS 85
  BACKGROUND 85
  OBJECTIVE 85
  RESEARCH APPROACH 85
    Electrical Leak Location Method 85
      Discussion 85
      Test Procedures 88
      Results of Tests 88
    Other Leak Location Methods for Cover Systems 102
      Infrared Imaging 102
      Ground-Penetrating Radar 103
      Tracer Gas 103
      Electromagnetic Induction 104
      Encapsulated Chemicals or Gas 104
      Electronic Transponders 105
  SUMMARY 105

8 LINER RESISTIVITY TESTS 107
  BACKGROUND 107
  OBJECTIVE 107
  RESEARCH APPROACH 107
    Test Procedures 107
    Resistivity Calculations 110
    Results of Tests 110

Page

SUMMARY 116

9 FIELD DEMONSTRATION SURVEYS 118
  BACKGROUND 118
  OBJECTIVE 118
  RESEARCH APPROACH 118
    Site Selection 118
    Results of Site Selection 119
    General Field Demonstration Test Procedures 120
    Tests at the EPA Land Treatment Research Demonstration Facility 120
      Test Procedures 120
      Results of Tests 120
    Equipment and Survey Procedure Modifications 128
      Modifications 128
      Results of Equipment and Survey Procedure Modifications 129
    Tests at Facility in the Vicinity of San Antonio, Texas 133
      Test Procedure 133
      Results of Tests 136
  SUMMARY 136
REFERENCE 139
BIBLIOGRAPHY 140

APPENDICES

A GREEN'S FUNCTION FOR A LEAK IN A GEOMEMBRANE LINER A-1
B ELECTRICAL POTENTIAL FOR A CURRENT SOURCE LOCATED IN A THREE-LAYER MEDIUM B-1
C SITE SURVEY PLAN FOR FULL-SCALE FIELD TESTS FOR TESTING OF THE GEOMEMBRANE SURVEY TECHNIQUE - EPA LAND TREATMENT RESEARCH FACILITY. C-1
D SITE SURVEY PLAN FOR FULL-SCALE FIELD TESTS FOR TESTING OF THE GEOMEMBRANE SURVEY TECHNIQUE - SITE IN THE VICINITY OF SAN ANTONIO, TEXAS. D-1

FIGURES

Number Page

1 The electrical leak location method detects the electrical potential anomaly associated with electrical current flowing through a leak.......................... 9

2 Simplified block diagram of the instrumentation for testing the electrical leak location method............... 11

3 Three-dimensional diagram of the electrical probing method for a circular leak in a geomembrane liner......... 15

4 Plane $z = h$ of the geomembrane liner showing a circular leak and its geometrical relationship to a field point at (x,y) on the liner.. 18

5 The fraction of current flowing through a leak of radius a versus the surface impoundment size.................... 23

6 Plane $z = h$ of the geomembrane liner showing multiple leaks of radius a_i for $i = 0,1,2,...n$.......................... 26

7 Comparison of experimental leak response and theoretical response predicted for the same field conditions.......... 34

8 Three-dimensional view of a pole-dipole survey arrangement and a circular leak of radius a in a geomembrane-lined liquid waste impoundment................................ 36

9 Anomaly measured over a leak of radius a = 0.0004 m for a pole-dipole array with a horizontal spacing of s = 1 m.. 37

10 Peak-to-peak voltage anomaly of a leak as a function of the electrical survey depth, z_m, for various horizontal dipole electrode spacings................................ 39

11 Anomaly measured over a leak of radius a = 0.0004 m for various horizontal dipole electrode spacings.............. 40

12 Peak-to-peak voltage anomaly as a function of dipole detector electrode spacing for various liquid layer depths, h.. 41

13 Peak-to-peak voltage anomaly as a function of waste material resistivity for various liquid layer depths, h... 42

14 Peak-to-peak voltage anomaly as a function of soil resistivity for various waste material resistivities, $_w$.. 43

FIGURES (continued)

Number		Page
15	Peak-to-peak voltage anomaly as a function of height above liner, $h-z_m$, for various offset distances, x, from the leak center	45
16	Comparison of horizontal dipole and vertical dipole responses over a leak of radius a = 0.0004 m	46
17	Anomaly measured over a leak of radius of a = 0.4 mm using a vertical dipole array having an electrode spacing of s_v = 30 cm	47
18	Potential profiles over two leaks of radius a for electrical surveys conducted at the surface and at depths of 50 cm and 75 cm. The leak centers are located in the liner at positions A and B corresponding to y_c = 8 m and 12 m, respectively, in the plane x = 0. The horizontal dipole detector spacing is s = 2 m	48
19	Potential profiles measured over two leaks of radius a for electrical surveys conducted at the surface and at depths of 50 cm and 75 cm. The leak centers are located in the liner at positions A and B corresponding to y_c = 9 m and 11 m, respectively, in the plane x = 0. The horizontal detector dipole spacing is s = 2 m	49
20	Potential contour plot for two identical leaks of radius a for a pole-dipole electrical survey conducted at a depth of 75 cm. The separation between the leaks is 2 m and the detector dipole spacing is s = 2 m	51
21	Potential profiles measured over two leaks of radius a for electrical surveys conducted at the surface and at depths of 50 cm and 75 cm. The leak centers are located in the liner at positions A and B corresponding to y_c = 9 m, respectively, in the plane x = 0. The horizontal detector dipole spacing is s = 1 m	52
22	Potential contour plot for two identical leaks of radius a for a pole-dipole electrical survey conducted at a depth of 75 cm. The separation between the leaks is 2 m and the detector dipole spacing is s = 1 m	53
23	Double-lined model construction detail	56
24	Plan view of the double-lined model showing simulated leak positions. Leak 6 is above the top liner. Leaks 1-5 are in the sand layer below the top liner	57

FIGURES (continued)

Number		Page
25	Construction details of the dipole probe used for double-lined model..	59
26	Contour plot of potential gradient data for simulated leak in top liner of double-liner model. Data taken using pivot point 1..	61
27	Contour plot of potential gradient data for simulated leak in top liner of double-liner model. Data taken using pivot point 2..	62
28	Plot of potential measurements from pivot point 1 along the 95 degree survey line..............................	63
29	Plot of potential measurements from pivot point 2 along the 90 degree radial line..............................	63
30	Contour plot of the double liner model data taken with a 5.1 mm diameter leak with a geotextile mat drainage layer..	65
31	Contour plot of the double liner model data taken with a 5.1 mm diameter leak with a drainage layer consisting of a geotextile mat placed over geonet........................	66
32	Contour plot of the double liner model data taken with a 5.1 mm diameter leak with a drainage layer consisting of a sandy loam soil layer placed over geotextile mat which is placed over geonet..................................	68
33	Contour plot of the double liner model data taken with a 25 mm diameter leak with a drainage layer consisting of a sandy loam soil layer placed over geotextile mat which is placed over geonet..................................	69
34	Contour plot of the double liner model data taken with a 15 cm long slit cut in the top liner with the potential scans parallel to the slit............................	70
35	Contour plot of the double liner model data taken with a 15 cm long slit cut in the top liner with the potential scans perpendicular to the slit.........................	71
36	Contour plot of the double liner model data taken with a simulated section of a faulty seam with the potential scan parallel to the slit..............................	72

FIGURES (Continued)

Number Page

37 Contour plot of the double liner model data taken with leaks with diameters of 5 mm in the top liner and the bottom liner and the current return electrode in the earth outside the model.................................. 73

38 Contour plot of the double liner model data taken with a protective soil layer with a thickness of 25 mm placed over the geomembrane liner............................... 75

39 Contour plot of the double liner model data taken with a protective soil layer with a thickness of 15 cm placed over the geomembrane liner 76

40 Scan data taken with 15 cm protective soil cover over geomembrane.. 77

41 Contour plot of the double liner model data taken with a protective soil layer 30.5 cm thick placed over the geomembrane liner....................................... 78

42 Scan data taken with 30 cm protective soil cover over geomembrane.. 79

43 Additional scan data taken with 30 cm protective soil cover over geomembrane................................. 80

44 Plot of leak resistance versus circular leak diameter..... 83

45 Half-cell electrode used to measure electrical potentials on soil cover................................. 87

46 Cover system physical model geometry..................... 89

47 Comparison of leak signatures for cover system with various thicknesses of soil cover........................ 90

48 Comparison of leak signatures for cover system with various thicknesses of soil cover plotted on a larger scale... 91

49 Raster plots of leak location data for cover system for scan lines west of leak................................. 92

50 Raster plots of leak location data for cover system for scan lines east of the leak.............................. 94

51 Raster plots of leak location data for cover system for scan lines north of the leak............................. 95

FIGURES (continued)

Number		Page
52	Raster plots of leak location data for cover system for scan lines south of the leak	96
53	Leak location data taken on survey lines spaced 60 cm apart indicate the presence of a 3.2 mm diameter leak under 60 cm of soil cover	97
54	Comparison of leak signature versus leak diameter with 60 cm of soil cover	98
55	Electrode contact noise can be reduced significantly by inserting the electrodes into the soil or removing the dry surface soil near the electrodes	99
56	The survey of the cover system with 60 cm soil cover and 6.4 mm diameter leak has excessive electrode contact noise when the electrodes are simply placed on the dry soil	100
57	When the same survey as shown in Figure 56 is repeated with the dry soil near the electrodes removed, electrode contact noise is reduced greatly	101
58	Test cell design for measuring liner resistivity during exposure to selected liquids	109
59	Resistivity versus time of 1.5 mm HDPE samples exposed to water, salt water, acid, and base	111
60	Resistivity versus time of 1 mm PVC samples exposed to water, salt water, acid, and base	112
61	Resistivity versus time of 0.91 mm CPER samples exposed to water, salt water, acid, and base	113
62	Resistivity versus time of 0.91 mm CSPE samples exposed to water, salt water, acid, and base	114
63	Resistivity versus time of 1.14 mm CSPE samples exposed to water, salt water, acid, and base	115
64	Equipotential contour plot of the conventional array data taken on 10 degree radials at the Ada South Pond	121
65	Equipotential contour plot of the conventional array data taken on 5 degree radials at the Ada South Pond	122
66	Equipotential contour plot of the conventional array data taken on 10 degree radials at the Ada South Pond	123

FIGURES (continued)

Number Page

67 Equipotential contour plot of the conventional array data taken on 5 degree radials over a 3.2 cm^2 simulated leak. A slight perturbation occurred in the area of the leak where the lines begin to curve around the leak location... 125

68 Equipotential contour plot of the conventional array data taken on 5 degree radials over the simulated 3.2 cm^2 leak. The closed contour lines indicate the presence and location of the leak.................................... 126

69 A plan view of the test impoundment showing the location of four 0.76 mm diameter leaks, survey lines 10 and 29, and positions of the current source and return electrodes. 130

70 A plot of the potential measurements taken along survey line 10 over leaks 1, 2, and 3 clearly shows the leak signatures.. 131

71 A plot of the potential measurements taken along survey line 29 directly over leak 4 clearly shows the leak signature... 131

72 The locations of four 0.81 mm diameter leaks are indicated by electrical dipole patterns shown in the potential gradient contour data................................ 132

73 The instrumentation set-up for the full-scale tests in the vicinity of San Antonio included the system control unit, computer, and dual-drum winch...................... 134

74 The electrode assembly is being towed along a survey line.. 134

75 Diagram of impoundment with leak located................. 135

76 Scan data taken near leak................................ 137

TABLES

Number		Page
1	Model parameters for predicting leak signatures	35
2	A comparison of leak anomaly amplitude for various electrode geometries and materials	81
3	Field verification results Ada North Pond	128

TABLE OF CONVERSION FACTORS

AREA

1 cm^2 = 0.155 in.^{2}
1 m^2 = 10.8 ft^2 = 1.20 yd^2
1 in.^{2} = 5.45 cm^2

1 hectare = 2.47 acres
1 acre = 0.405 hectare
1 ft^2 = 0.0929 m^2

LENGTH

1 mm = 0.0394 in.
1 cm = 10 mm = 0.394 in.
1 m = 100 cm = 39.4 in. = 3.28 ft

1 in. = 2.54 cm
1 ft = 0.305 m

VOLUME

1 cm^3 = 0.0610 in^3
1 m^3 = 35.3 ft^3 = 1.31 yd^3
1 in.^{3} = 16.4 cm^3

1 liter = 1.057 quart
1 quart = 0.946 liter

ABBREVIATIONS

AC -- alternating current
Amp -- Ampere

C -- Celsius
cm -- centimeter
CPER -- chlorinated polyethylene
CSPE -- chlorosulfonated polyethylene

DC -- direct current

EPA -- Environmental Protection Agency

F -- Fahrenheit
FML -- flexible membrane liner

HDPE -- high-density polyethylene
H_2SO_4 -- sulfuric acid

m -- meter
mA -- milliampere
mil -- 0.001 inch
mm -- millimeter

NaCl -- sodium chloride
NaOH -- sodium hydroxide

Ω -- ohm
° -- degrees

pH -- measure of acidity or alkalinity
p-p -- peak-to-peak
PVC -- polyvinyl chloride

SwRI -- Southwest Research Institute

V -- volt
VDC -- volts DC

SECTION 1

INTRODUCTION

BACKGROUND

Industries and municipalities in the United States generate large quantities of solid and hazardous wastes each year. The most common method of disposal of these wastes is in landfills and surface impoundments. Liquids contained in surface impoundments and landfills (leachates) are frequently toxic and contain substances that could cause contamination if released into nearby surface water or groundwater resources.

To prevent contamination, geomembrane liner systems are often installed. These liners, placed beneath the landfill or impoundment, are designed to form an essentially impermeable barrier to prevent the migration of contaminant liquids. Geomembrane liners, also known as flexible membrane liners (FMLs), synthetic liners, and membrane liners, are sheets of polymeric materials fabricated in a factory and seamed together at the field site to form a continuous liner. Installation practices and operational factors can lead to punctures or separated seams, causing loss of physical integrity. Damage can also be caused accidentally by heavy machinery used to place protective bedding material on the liner.

A method was needed to effectively locate leaks in geomembrane liners prior to the introduction of the waste materials to ensure that liners are installed and seamed properly and that no damage has occurred. The development of an in-service leak location method was considered to be very important to determine if the liner is operating properly and to isolate the leaks for subsequent repair.

An electrical leak location method to detect and locate leaks in plastic liners installed in pollution-control facilities was developed and tested for the Environmental Protection Agency (EPA) by Southwest Research Institute under Contract 68-03-3033. A report on the results of this project is available through NTIS as Report No. PB 85-122 414 GAR entitled "Electrical Resistivity Technique to Assess the Integrity of Geomembrane Liners."

The electrical leak location method makes use of the high electrical resistivity of the geomembrane liner material. When no leaks are present, a voltage impressed across the liner produces a very low current flow. The low current density produces a relatively uniform voltage potential distribution in the material above the liner. A leak in the geomembrane liner provides a conductive path for current flow, which produces an increase in the current density at the leak point. The localized current density causes an anomaly in the measured potential in the vicinity of the leak. Therefore, leaks can be located by measuring the potential distribution patterns in the material covering the liner. The electrical leak location method can be used in liquid impoundments, as a pre-service inspection of solid waste landfills, and to locate leaks in the final cover for landfills or impoundments. The method will not damage the liner.

This Final Technical Report documents the performance and usefulness of the electrical leak location method through a multi-faceted study of mathematical modeling, scale-model tests, full-scale field evaluations and related experiments. The method was adapted for locating leaks in the geomembrane liners of waste impoundment or landfill final cover systems. The detection sensitivity and accuracy capabilities were optimized for a wide variety of conditions. Other methods for locating leaks in the liners of cover systems were also investigated and analyzed.

OBJECTIVES

The objectives of the project are:

(1) Computer Simulation Model: Develop a computer model to predict leak signatures, and verify the computer model using full-scale test data. Generalize the model to accommodate a layered earth sequence above and below an insulating liner with a leak. Exercise the computer model to simulate the electrical leak location method under a wide variety of test conditions for liquid impoundments and liner cover systems.

(2) Double-Liner Model Tests: Perform physical model evaluations and optimizations of the electrical leak location method for surveying double-lined impoundments. Test the effect of type of drainage layer using drainage layers comprised of various combinations of geotextile, geonet, and soil. Determine the effect of various test parameters such as leak size, electrode depth, and protective soil cover. Test various electrode materials and geometries to further optimize the method.

(3) Cover System Model Tests: Perform an evaluation of the electrical leak location method and other techniques for evaluating the integrity of the landfill geomembrane for cover systems. Perform scale model tests to improve the detection capabilities under a wide range of cover soil thicknesses, leak sizes, and cover soil resistivities. Investigate and analyze other methods for locating leaks in geomembrane liners of cover systems. Conduct test evaluations if the techniques appear to be viable.

(4) Liner Resistance Study: Test the electrical resistivity of typical geomembrane liner materials exposed to various liquids to determine if the resistivity decreases, thereby reducing the usefulness of the electrical leak location method.

(5) Field Demonstration Surveys: Demonstrate the electrical leak location method in full-scale liner systems. Assess and develop the field operational procedures for performing full-scale surveys.

SECTION 2

CONCLUSIONS

An electrical method for detecting and locating leaks in geomembrane liners for hazardous waste impoundments and landfills has been developed and successfully demonstrated in a wide variety of applications. The project demonstrates the validity and usefulness of the electrical leak location method for testing the integrity of the geomembrane for single and double geomembrane liners and final cover systems. The technique is cost effective for construction quality assurance and in-service performance monitoring. The technology has been documented for use by industry.

The computer simulation model efficiently and accurately predicts the potential field due to a leak in an insulating liner. The computer model can efficiently and accurately predict the effect of a wide range of measurement parameters on the leak signature. The computer simulation model indicates that leak location sensitivity is increased very significantly when the electrodes are scanned as close to the liner as possible. For a given level of injected current, leak location sensitivity increases proportionally with the resistivity of the material on the liner. For impoundments with low resistivity liquids, the injected current must be increased to obtain higher leak location sensitivity.

Tests on a small-scale double-lined model demonstrated that the method can be applied to a wide variety of double liner configurations of drainage layers with various test parameters such as leak size, electrode depth, and protective soil cover. Leaks smaller than 0.8 mm in diameter can be reliably located. Within reason, the shape and size of the leak have little effect upon the shape of the leak signature. However, the leak size affects the leak current, thereby increasing the amplitude of the leak signature. Leaks can be detected from distances of 1.5 m and greater from the leak. Linear electrodes scanned perpendicular to the scan direction, with scans offset by approximately the length of the electrodes, produce a lower likelihood of missing a leak compared with surveys using localized electrodes. A simple continuity test can indicate the presence, but not location, of leaks in the bottom liner.

The electrical leak location method is less sensitive for locating leaks in geomembrane liners with a protective soil cover and liquid over the liner. The lower sensitivity is probably because the electrodes cannot be scanned close to the leak, and the liquid shunts the measured potential field to some proportion.

The electrical leak location method is also an effective method for locating leaks in geomembrane liners of waste impoundment or landfill final cover systems. Non-polarizing half-cell electrodes are used to greatly reduce the polarization voltage noise. The method proved to be very successful in locating leaks as small as 3 mm under 60 cm of soil cover.

The most promising method studied for locating leaks in final cover systems, other than the electrical leak location method is ground-penetrating radar. Limited testing using infrared imaging was unsuccessful in detecting localized areas of low thermal conductivity caused by drainage of soil moisture through a leak.

Laboratory tests indicated that there was no significant decrease in the resistance of high-density polyethylene (HDPE), chlorosulfonated polyethylene (CSPE), chlorinated polyethylene (CPER), and polyvinyl chloride (PVC) liner materials during a 13-week exposure to water, salt water, acidic solution, and basic solution. Exposure of typical liner materials to these chemicals had no effect on the applicability of the electrical leak location method.

Improvements in the measurement method and hardware were made to increase the detection and location capabilities. The modified equipment and procedures can detect leaks with a diameter of 0.8 mm up to 1.5 m away from the leak. These leaks can be located with an accuracy of less than 15 cm when the electrodes pass 15 cm above the leaks.

The system found a 20 mm long crack in the liner of an impoundment that had been fully tested using the vacuum box method. No false indications were obtained. The electrical leak survey did not delineate a second pinhole leak 32 mm from the crack leak. For practical purposes, there is little need to delineate leaks that are closer than approximately 80 mm apart.

SECTION 3

RECOMMENDATIONS

The electrical leak location method has been developed to a stage ready for industry use for nonhazardous applications including pre-service leak location surveys for impoundments and landfills and surveys of nonhazardous in-service impoundments. Additional research related to specific areas of the electrical leak location method is recommended to bring the method into application for hazardous material impoundments and for cover systems. The specific recommendations are:

(1) Demonstrate the electrical leak location method for final cover systems at one or more field installations. Such demonstrations will serve to reinforce liner industry acceptance of the validity of the electrical method for economic evaluations of cover systems.

(2) Demonstrate the electrical leak location method for pre-service inspections of the primary liners of liquid impoundments and solid waste landfills with a protective soil cover in place. Because the liner can be easily damaged during emplacement of the protective soil cover, a demonstration of the capabilities of the method in a full-scale field installation will be of great benefit.

(3) Proper leak location equipment implementation is very important to obtain the optimum leak detection sensitivity and probability of detection. In addition to the electronic system and sensor designs, survey methodology and human factors design are important for reliable application of the method. The winch-drawn data acquisition system is applicable particularly to in-service hazardous waste impoundments. A more efficient data acquisition system should be implemented to make the application of the system more cost effective.

(4) The ground-penetrating radar technique should be evaluated for detecting leaks in final cover systems. The radar technique has the promise of providing information related to the severity of the leak.

(5) A method is needed for locating leaks in the secondary liner of liquid impoundments with the primary liner in place. The use of ground-penetrating radar for this purpose is promising. Other proprietary methods have been evaluated with initial promising success. These methods should be evaluated fully.

(6) A remotely piloted vehicle should be developed to conduct leak location surveys in hazardous waste impoundments.

(7) Methods are needed to repair in-service geomembranes. Several methods hold the promise of providing the repair capability without the need to drain the impoundment. The most promising techniques should be developed.

(8) The Environmental Protection Agency and state regulatory offices should be made aware of the capabilities of the electrical leak location method to allow regulatory requirements protecting the environment to be formulated and enforced in the most beneficial and cost effective manner.

(9) The Environmental Protection Agency and state regulatory offices should be made aware of the impact of existing and future regulations on the successful application of the electrical leak location method for guidance in setting the most beneficial regulatory requirements for environmental protection.

SECTION 4

TECHNICAL DISCUSSION

CONCEPT DEVELOPMENT

Figure 1 shows the basic electrical leak location method for detecting and locating leaks in a geomembrane liner. Geomembrane liners made from impervious plastics exhibit very high electrical resistance. When a liner is installed in a landfill or surface impoundment, it effectively acts as an electrical insulator between the materials contained in the facility and the surrounding earth. A voltage source is used to impress a voltage across the liner. If the liner is punctured or separated physically, conductive fluid flows through the leak and establishes an electrical current through the liner. The increase in the current density at the leak forms an electrical anomaly that can be mapped to detect and locate the leak.

The success of the electrical leak location method depends upon the liner material having a high resistance per unit area compared with that of a leak path. If the liner were a perfect insulator and there were no current conducting paths over the edges of the liner, no current would flow. However, geomembrane liner materials have a high but finite resistivity. Therefore, some current will flow through the liner. If the current density through the liner is assumed to be uniform, then the total resistance which the liner presents as a load across the source can be computed from the formula:

$$R_L = \frac{\rho_L t}{A} \qquad (1)$$

where R_L = the total liner resistance (ohms);

ρ_L = the volume resistivity of the liner material (ohm-meters);

t = the thickness of the liner (meters); and

A = the total surface area of the liner (square meters).

While the total resistance of the liner at a large site may be small, the resistance per unit area of liner material is still very high compared with a leak. The current density at a leak will therefore be many times greater than that at any point on the liner. A leak will have a strong effect on the localized potential measured within the impoundment. For practical liner

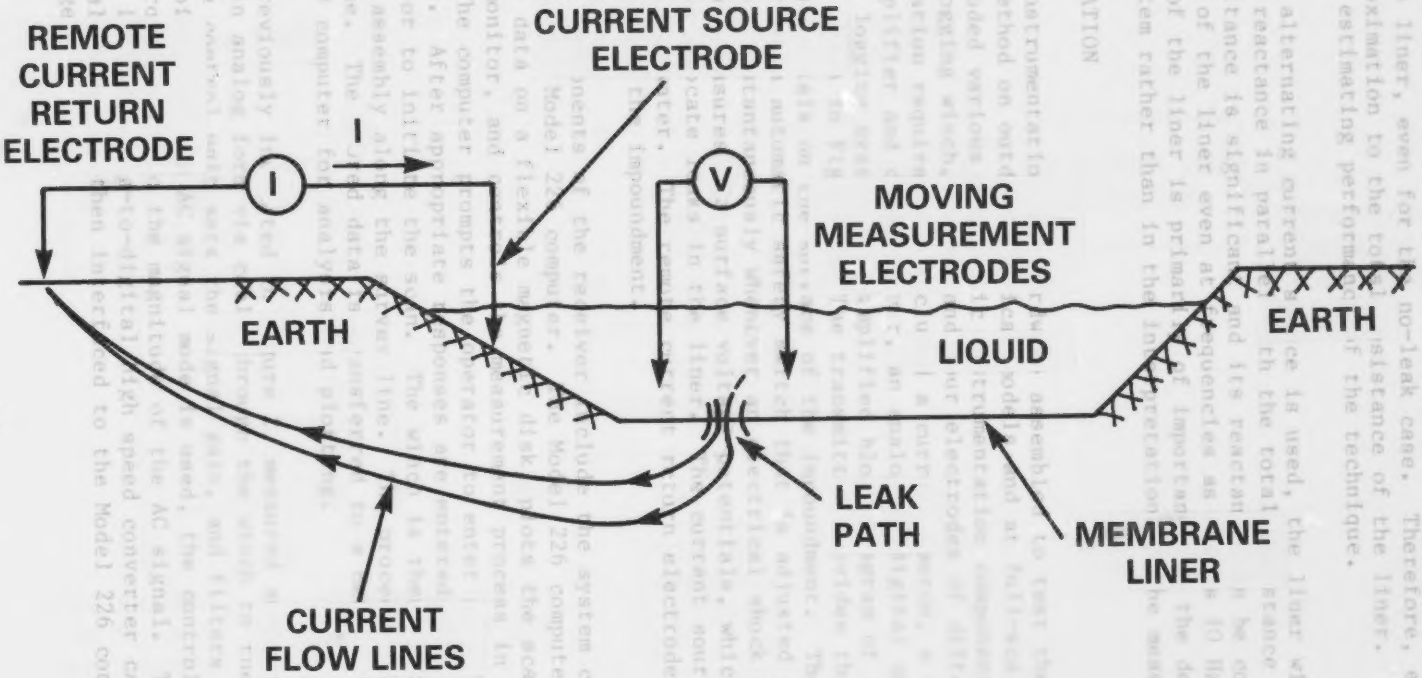
REMOTE CURRENT RETURN ELECTRODE
CURRENT SOURCE ELECTRODE
I
I
V
MOVING MEASUREMENT ELECTRODES
EARTH
LIQUID
EARTH
LEAK PATH
MEMBRANE LINER
CURRENT FLOW LINES

Figure 1. The electrical leak location method detects the electrical potential anomaly associated with electrical current flowing through a leak.

materials and resistivity of the contents of the impoundment or landfill, the location of the current electrode within the lined landfill or impoundment and the shape of the containment area will result in a nonuniform current density through the liner, even for the no-leak case. Therefore, equation (1) is a first approximation to the total resistance of the liner. Nevertheless, it is useful for estimating performance of the technique.

If an alternating current source is used, the liner will exhibit a capacitive reactance in parallel with the total resistance described above. This capacitance is significant and its reactance can be comparable to the resistance of the liner even at frequencies as low as 10 Hz. This capacitive reactance of the liner is primarily of importance in the design of the current source system rather than in the interpretation of the measurements.

INSTRUMENTATION

The instrumentation and hardware assembled to test the electrical leak location method on outdoor physical models and at full-scale field installations included various electronic instrumentation components, an electrically operated logging winch, cable, and four electrodes of different designs. Instrumentation requirements included a current source, a precision voltage sensing amplifier and cable driver, an analog-to-digital converter, and a computer data logging system. A simplified block diagram of the electronic components is shown in Figure 2. The transmitter provides the current needed to generate potentials on the surface of the impoundment. The transmitter is equipped with an automatic safety switch that is adjusted to disconnect the DC power source instantaneously whenever an electrical shock condition is sensed. The receiver measures the surface voltage potentials, which are then analyzed to detect and locate leaks in the liner. The current source electrode is located in the water. The remote current return electrode is placed in the earth away from the impoundment.

Major components of the receiver include the system control unit and a Hewlett-Packard Model 226 computer. The Model 226 computer automatically stores the data on a flexible magnetic disk, plots the scanned data on the computer monitor, and controls the measurement process in response to operator inputs. The computer prompts the operator to enter all of the measurement parameters. After appropriate responses are entered, the computer instructs the operator to initiate the scan. The winch is then switched on to move the electrode assembly along the survey line. The procedure is repeated for each survey line. The stored data is transferred to a Hewlett-Packard HP 9000 Series 500 computer for analysis and plotting.

As previously indicated in Figure 2, measured surface potential voltages are sent in analog form via cable through the winch to the system control unit. The control unit sets the signal gain, and filters the signal to remove ambient noise. If the AC signal mode is used, the control unit generates a DC voltage proportional to the magnitude of the AC signal. The DC signal is coupled to a 12-bit analog-to-digital high speed converter card in the computer. The digital output is then interfaced to the Model 226 computer for display and storage.

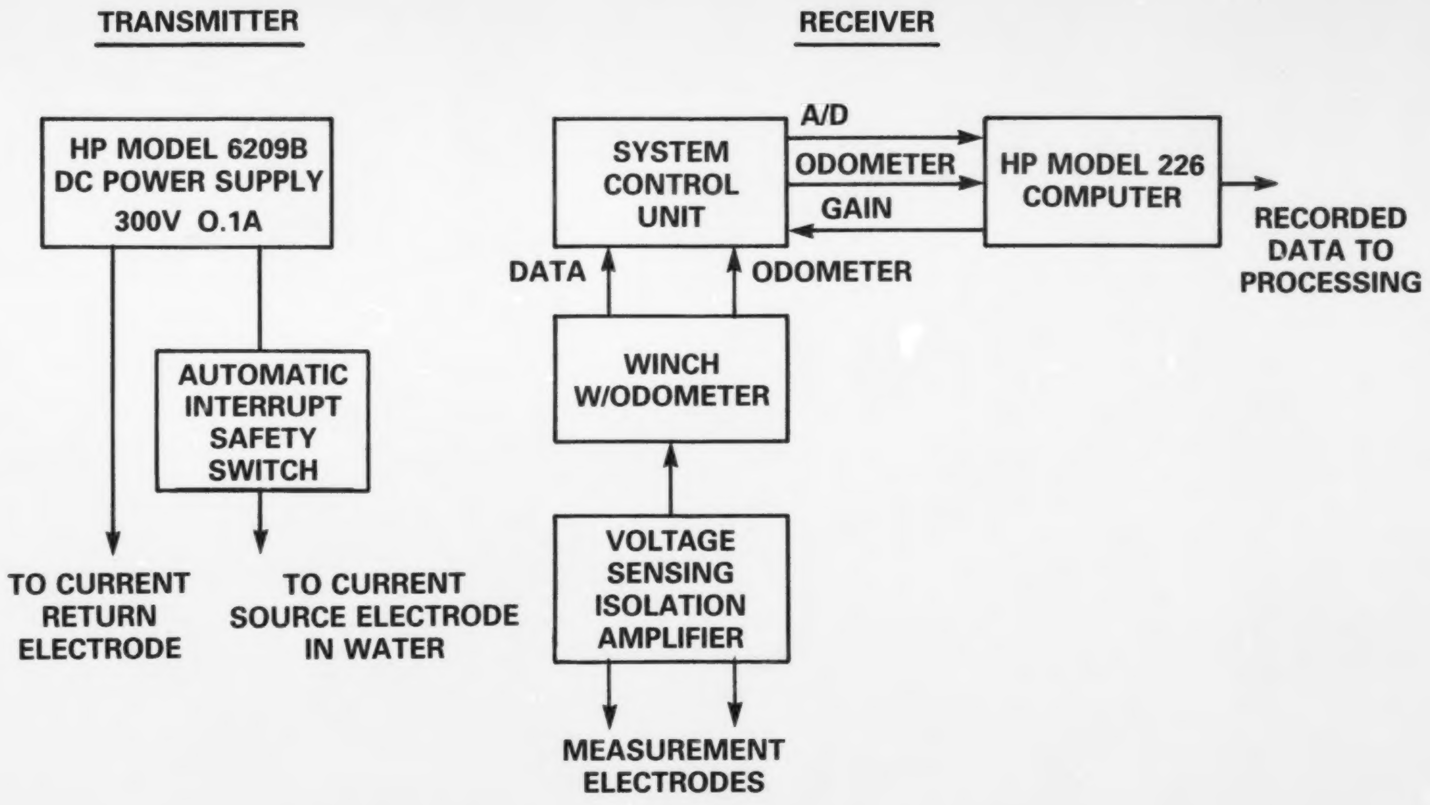
TRANSMITTER
RECEIVER
HP MODEL 6209B DC POWER SUPPLY 300V O.1A
AUTOMATIC INTERRUPT SAFETY SWITCH
TO CURRENT RETURN ELECTRODE
TO CURRENT SOURCE ELECTRODE IN WATER
SYSTEM CONTROL UNIT
A/D
ODOMETER
GAIN
HP MODEL 226 COMPUTER
RECORDED DATA TO PROCESSING
DATA
ODOMETER
WINCH W/ODOMETER
VOLTAGE SENSING ISOLATION AMPLIFIER
MEASUREMENT ELECTRODES

Figure 2. Simplified block diagram of the instrumentation for testing the electrical leak location method.

For full-scale field surveys, an electric logging winch draws the potential measuring electrode along the surface of the water. The dual-drum winch is equipped with variable speed control, a photoelectric odometer, and an electric slip-ring. One winch drum is equipped with 150 m of 4-conductor data logging cable, which is reeled in to make surface potential measurements. The other winch drum is equipped with a nylon rope which is drawn through a remote pulley to reel out the potential measuring electrodes. The voltage sensing amplifier is connected to the end of this cable and is mounted on a support bar between two floats. Electrodes are suspended from the two floats to make potential gradient measurements. The output of the odometer is connected to a computer interface to allow the computer to read and indicate the position of the measurement electrode. The computer inputs potential readings at fixed distance intervals in response to the odometer inputs. The odometer allows the location of leaks to be determined.

The high voltages used for the leak detection method and test procedures described in this report present a potential for electrical shock. The potential for electrical shock is increased if operations are being performed near water. Safety measures must be taken to minimize the risk of injury to or death of personnel. The techniques set forth in this report should be attempted only by qualified personnel who are experienced in performing measurements under similar conditions.

SECTION 5

COMPUTER SIMULATION MODEL

BACKGROUND

Experimental investigations demonstrated the practicality of the electrical survey technique for locating leaks in the geomembrane-lined impoundment test site at Southwest Research Institute. The range of test conditions for these experiments was limited necessarily. Additional investigations are needed to evaluate the success of the technique under the wide range of conditions expected in actual field installations. An experimental measurement program intended to evaluate the electrical survey technique under a wide range of parameters such as liquid depth, liquid conductivity, liner resistance, and earth resistivity is impractical. For the measured data and general theoretical considerations, the results of a limited number of experiments can be extrapolated to other conditions. A more practical alternative is to formulate a computer simulation model to obtain numerical computations of expected results for the range of survey parameters corresponding to the practical field installations. The ability to obtain numerical results prior to measurements at in-service impoundments also increases the level of confidence in the measured results. The predicted results can be used to improve the accuracy of leak signature determinations and to plan liner surveys.

OBJECTIVES

The objectives of Task 1 - Computer Simulation Modeling were to:

(1) Exercise the computer model to catalog leak signatures for a wider variety of field conditions; and

(2) Modify the model to simulate the electrical response of a leak in the geomembrane of a cover system for a landfill.

A three-dimensional modeling technique was developed to predict how a leak in a liner will affect the electrical current distribution in the liquid above the liner. The model was then modified to simulate a cover system consisting of one or more earth layers under the insulating liner, an insulating liner, and one or more layers of earth above the insulating liner. This modification was to accommodate typical solid waste landfill cover systems.

RESEARCH APPROACH

To investigate the performance capabilities of the electrical leak location method, a theoretical model was developed to accommodate various electrical and dimensional parameters in the three layers comprising the lined impoundment or landfill, as well as in the number of leaks and the locations of the current source and potential measurement electrodes. To simplify the model, the physical boundaries of the lined impoundment are assumed to be at a large distance from the leak center; hence, the impoundment, the liner, and the soil under the geomembrane liner are represented as infinite horizontal layers. In addition, the liner thickness and the leak size are assumed to be much smaller than the other linear dimensions. The current flow through the leak is determined by imposing the condition that the total current distribution flows vertically across a finite surface area of the infinite horizontal liner layer containing the leak. This condition is similar to neglecting currents flowing through the lined walls of a waste disposal site with physical boundaries. To demonstrate the validity of the electrical potential solution for predicting leak signatures, synthetic signatures are compared with pole-dipole measurements taken at a 0.4-hectare lined impoundment test site at Southwest Research Institute.

Theoretical Analysis to Simulate the Response of a Leak in a Lined Impoundment

Formulation--

The potential theory problem associated with the response of a leak in a geomembrane liner of thickness, t, and resistivity, ρ_ℓ, is illustrated in Figure 3, which shows the geometry in a three-dimensional view. The liquid impoundment of depth, h, and resistivity, ρ_w, is excited by a point source of current, I_s, located at (x_s, y_s, z_s). The current return electrode is located in the soil layer of resistivity, ρ_s, at a large distance from the source.

To simulate a leak, a circular hole of radius, a, is located in the liner at the position, (x_o, y_o, z_o), which permits a current, I_o, to flow from the waste material to the soil layer under the liner. An expression for the secondary potential associated with the current flow, I_o, entering the leak at (x_o, y_o, z_o), is developed by considering the leak to be a current source. The product of the leak current density, $j(x_o, y_o)$, and the lined impoundment Green's function, $G(x, y, z; x_o, y_o, z_o)$, is integrated over the surface of the leak, S. Thus, the solution for the secondary potential can be written in terms of the Green's function for the three-layer medium (i.e., waste material, liner, and soil) as

$$\phi_s = \frac{\rho_\ell}{4\pi} \int_S j(x_o,y_o)\, G(x,y,z;\, x_o,y_o,z_o)\, dx_o\, dy_o. \tag{2}$$

The Green's function in terms of the potential due to a point current source, I_o, at (x_o, y_o, z_o), gives

$$G(x,y,z;\, x_o,y_o,z_o) = \frac{4\pi}{\rho_\ell I_o}\, \phi_s\, (x,y,z;\, x_o,y_o,z_o), \tag{3}$$

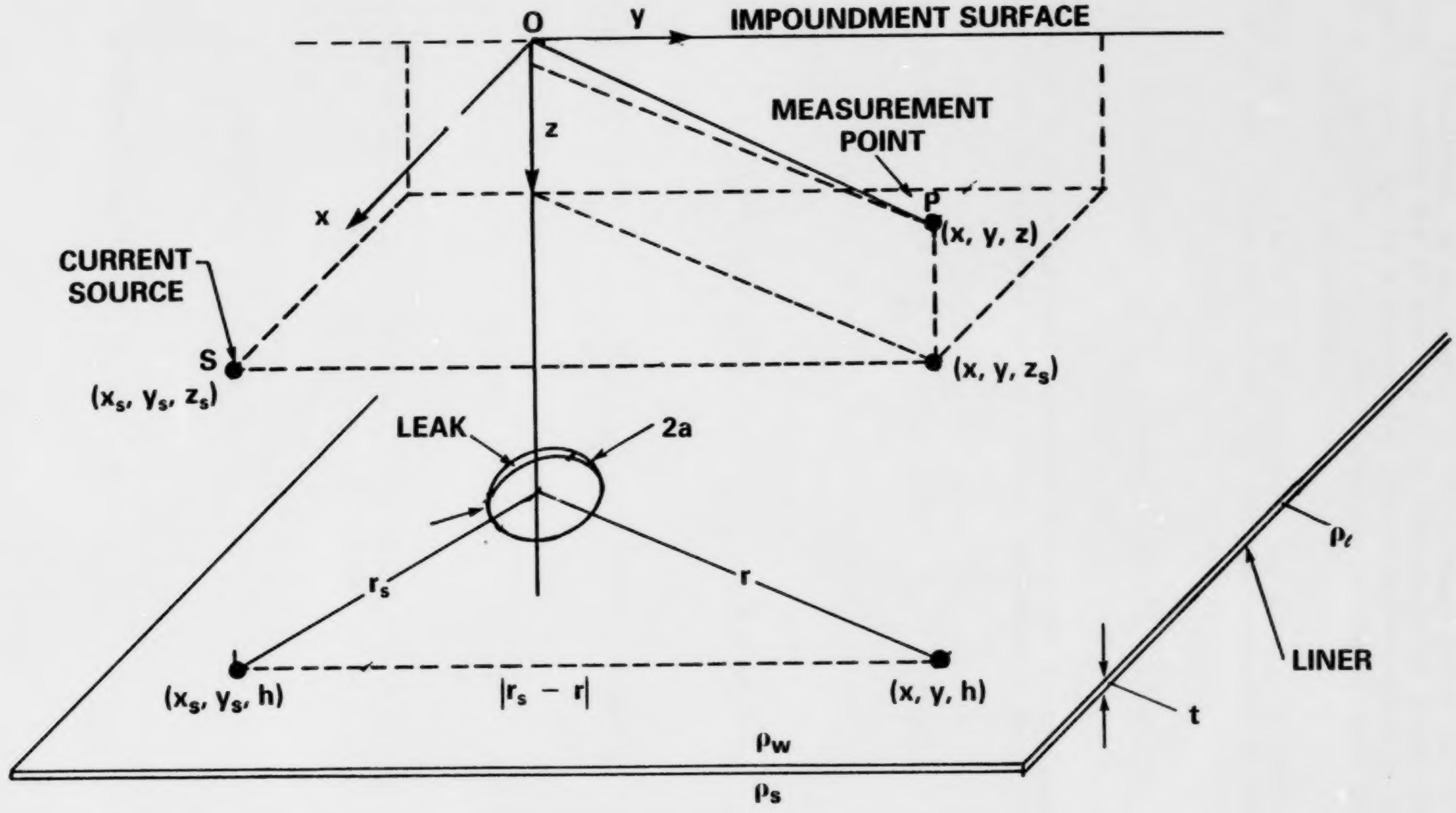
O
y
IMPOUNDMENT SURFACE
MEASUREMENT POINT
P
(x, y, z)
z
x
CURRENT SOURCE
S
(x_s, y_s, z_s)
(x, y, z_s)
LEAK
2a
r_s
r
(x_s, y_s, h)
$|r_s - r|$
(x, y, h)
ρ_ℓ
LINER
t
ρ_w
ρ_s

Figure 3. Three-dimensional diagram of the electrical probing method for a circular leak in a geomembrane liner.

where the location of the source point, (x_o, y_o, z_o), has been included to emphasize the fact that the potential depends on the position of the source. The solution of the Green's function for a source located at the position, (x_o, y_o, z_o), in the liner layer of a three-layer medium is presented in Appendix A. In addition, an expression of the primary potential is required in the general solution and is assumed to be the potential associated with a point source current, I_s, in a three-layer medium representing an impoundment which contains a leak-free liner. The derivation of the primary potential function is presented in Appendix B.

The total potential field at any position, (x, y, z), is obtained by the superposition of the primary potential, ϕ_p, and the secondary potential, ϕ_s,

$$\phi = \phi_p(x,y,z;\ x_s,y_s,z_s) + \frac{\rho_\ell}{4\pi}\int_S j(x_o,y_o)\ G(x,y,z;\ x_o,y_o,z_o)dx_o\ dy_o. \tag{4}$$

The solution of the electrical potential for a leak in the geomembrane liner at $z_o = h$ may be expressed in cylindrical coordinates as

$$\phi = \phi_p(r,z;\ r_s,z_s) + \frac{\rho_\ell}{4\pi}\int_S j(r_o)\ G(r,z;\ r_o,h)\ r_o dr_o d\theta_o, \tag{5}$$

where

$$r_s = (y_s^2 + x_s^2)^{1/2},\ r = (y^2 + x^2)^{1/2},\ r_o = (y_o^2 + x_o^2)^{1/2},$$

$$G(r,z;\ r_o,h) = \frac{\rho_w}{\rho_\ell}\int_0^\infty \frac{T(\lambda)}{1 - R(\lambda)e^{-2\lambda h}}\left[e^{-\lambda(h-z)} + e^{-\lambda(h+z)}\right] \times J_o(\lambda|r - r_o|)\ d\lambda, \tag{6}$$

$$\phi_p = \frac{I_s\rho_w}{4\pi}\left\{\frac{1}{\sqrt{|r - r_s|^2 + (z + z_s)^2}} + \frac{1}{\sqrt{|r - r_s|^2 + (z - z_s)^2}} + \int_0^\infty R(\lambda)\frac{\left[e^{-\lambda(h+z_s)} + e^{-\lambda(h-z_s)}\right]}{1 - R(\lambda)e^{-2\lambda h}} \times \left[e^{-\lambda(h+z)} + e^{-\lambda(h-z)}\right] J_o(\lambda|r - r_s|)\ d\lambda\right\}, \tag{7}$$

$$T(\lambda) = \frac{2(\rho_s + \lambda t \rho_\ell)}{\rho_s + \rho_w + \lambda t \rho_\ell} = 1 + R(\lambda), \tag{8}$$

and

$$R(\lambda) = \frac{\rho_s - \rho_w + \lambda t \rho_\ell}{\rho_s + \rho_w + \lambda t \rho_\ell} . \tag{9}$$

In Equation (5), r_o is the distance from the center of the leak to any point in the leak, and r is the distance from the leak center to an arbitrary point on the geomembrane liner. This situation is illustrated in Figure 4 when rectangular coordinates (x,y) are adapted for the plane $z_o = h$. To perform the integration over the leak surface (in the Θ_o and r_o polar coordinates), the Bessel function, $J_o\ (\lambda|r - r_o|)$, can be expanded using the addition theorem for Bessel functions of the first kind,

$$J_o(\lambda|r - r_o|) = \sum_{m=-\infty}^{\infty} J_m(\lambda r)\ J_m(\lambda r_o) e^{im(\theta)}. \tag{10}$$

To simplify the analysis, the leak radius is assumed to be small compared with other linear dimensions such as r and h. Thus, substituting Equation (10) with m = 0 into Equation (6) then yields from Equation (5)

$$\phi = \phi_p(r,z;\ r_s,z_s) + \left(\frac{\rho_w}{4\pi}\right) \int_0^\infty \frac{T(\lambda)}{1 - R(\lambda)e^{-2\lambda h}} [e^{-\lambda(h+z)} + e^{-\lambda(h-z)}]$$

$$\times\ J_o(\lambda r)\ d\lambda \int_0^{2\pi} \int_0^a j(r_o)\ J_o(\lambda r_o)\ r_o\ dr_o\ d\theta_o. \tag{11}$$

Assuming a uniform current density, j_o, in a leak of radius, a, the integral associated with the variable, r_o, in Equation (11) is reduced to

$$\int_0^a j(r_o)\ J_o(\lambda r_o)\ r_o\ dr_o \cong j_o \int_0^a J_o(\lambda r_o)\ r_o\ dr_o$$

$$= j_o a \frac{J_1(\lambda a)}{\lambda}, \tag{12}$$

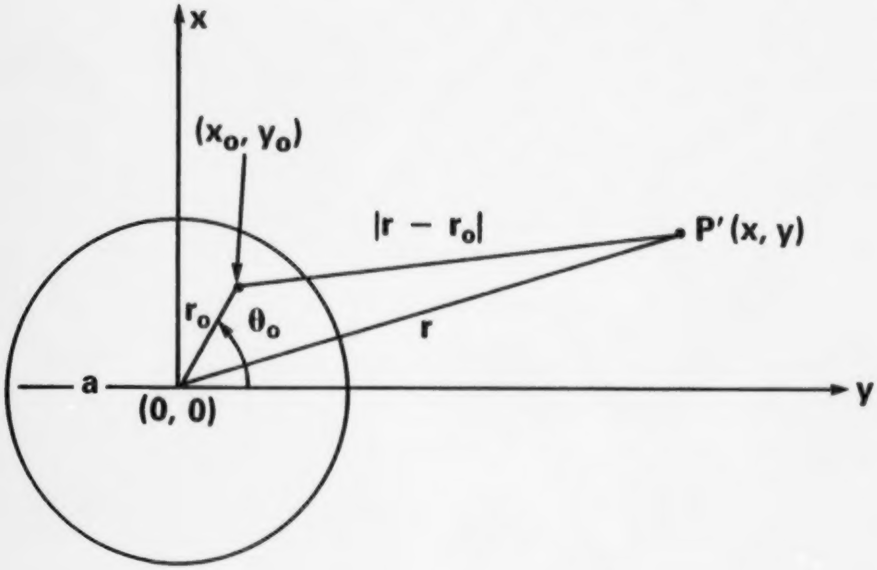
x
(x_o, y_o)
$|r - r_o|$
$P'(x, y)$
r_o
θ_o
r
a
(0, 0)
y

Figure 4. Plane z = h of the geomembrane liner showing a circular leak and its geometrical relationship to a field point at (x,y) on the liner.

and the current entering the leak may be obtained by integrating the current density, $j(r_o)$, over the leak surface as

$$I_o = \int_0^{2\pi} \int_0^{a} j(r_o)\, r_o\, dr_o\, d\theta_o \cong j_o \pi a^2. \tag{13}$$

Then, substituting Equation (12) into Equation (11), the electrical potential becomes

$$\phi = \phi_p(r,z;\, r_s,z_s) + 2 j_o \pi a^2 \left(\frac{\rho_w}{4\pi}\right) \int_0^{\infty} T(\lambda)\, \frac{[e^{-\lambda(h+z)} + e^{-\lambda(h-z)}]}{1 - R(\lambda)e^{-2\lambda h}} \times \frac{J_1(\lambda a)}{\lambda a} J_o(\lambda r)\, d\lambda. \tag{14}$$

When the radius of the leak is small (that is, when $\lambda a << 1$), it is assumed that $J_1(\lambda a)/\lambda a \approx 1/2$ and $j_o \pi a^2$ is replaced by I_o; hence, Equation (14) is reduced further and becomes independent of the leak radius. Therefore, the electrical potential as a function of the unknown current flow, I_o, through the leak is given by

$$\phi = \phi_p(r,z;\, r_s,z_s) + I_o \frac{\rho_w}{4\pi} \int_0^{\infty} T(\lambda)\, \frac{[e^{-\lambda(h+z)} + e^{-\lambda(h-z)}]}{1 - R(\lambda)e^{-2\lambda h}} \times J_o(\lambda r)\, d\lambda. \tag{15}$$

The current flow, I_o, may be derived from the total vertical current distribution associated with the geomembrane liner and the leak at $z = h$. This analysis requires determination of the negative gradient of the electrical potential, given by Equation (15), with respect to the variable, z, and division of the resulting expression by the waste liquid resistivity. This yields the total current density distribution between the waste material and the geomembrane liner,

$$j(r) = j_p(r) - \frac{I_o}{4\pi} \int_0^{\infty} \frac{T(\lambda)}{1 - R(\lambda)e^{-2\lambda h}} (1 - e^{-2\lambda h})\, \lambda J_o(\lambda r)\, d\lambda, \tag{16}$$

where the current density, $j_p(r)$, is deduced from Equation (7) and is given by

$$j_p(r) = \frac{I_s}{4\pi} \int_0^\infty \lambda[1 - R(\lambda)] \left[\frac{e^{-\lambda(h+z_s)} + e^{-\lambda(h-z_s)}}{1 - R(\lambda)e^{-2\lambda h}}\right]$$

$$\times J_o(\lambda r)\, J_o(\lambda r_s)\, d\lambda. \tag{17}$$

The function, $j_p(r)$, is the vertical current density in the absence of the leak and represents the total current density distribution associated with a liner of infinite horizontal dimensions.

In a lined impoundment or landfill, the current flows through the waste material, the liner, and the leaks to return to the current electrode in the soil layer. The landfill or surface impoundment sites of interest are generally less than a few meters in depth and may have surface areas of several hectares so that lateral currents flowing across the lined walls are much smaller than those flowing through the lined bottom and through the leaks. Therefore, the total current distribution which returns to the sink current electrode may be assumed to be equal to the currents flowing across the lined bottom of the impoundment plus the currents flowing through the leaks. This situation suggests that an approximate lined impoundment model may be simulated by infinite horizontal layers, and that the unknown current flow through the leak may be determined from the expression for the current density by assuming that the total current distribution flows vertically across a finite surface area of the infinite horizontal liner layer containing the leaks. Such a finite surface is equivalent to that of the surface impoundment or landfill site.

Since polar coordinates have been adopted in the analysis, the current density, $j(r)$, is integrated over the finite surface area equivalent to that of a lined impoundment to yield the current flow, I_ℓ, through the liner. Thus, the current flowing across the undamaged part of the liner is given by

$$I_\ell = \int_0^{2\pi} \int_a^{r_\ell} r j(r)\, dr\, d\theta, \tag{18}$$

where $j(r)$ is the vertical current density distribution at the boundary between the waste material and the geomembrane liner and is given by Equation (16). The upper limit of integration, r_ℓ, is the radius of a circular area equivalent to that of the finite surface of the landfill or surface impoundment and is determined as follows

$$r_\ell = \left(\frac{\text{surface impoundment area}}{\pi}\right)^{1/2}. \tag{19}$$

Next, substituting Equation (17) into Equation (16) and defining the following functions

$$P(\lambda) \equiv \frac{[1 - R(\lambda)]}{1 - R(\lambda)e^{-2\lambda h}} [e^{-\lambda(h+z_s)} + e^{-\lambda(h-z_s)}], \tag{20}$$

and

$$Q(\lambda) \equiv \frac{T(\lambda)(1 - e^{-2\lambda h})}{1 - R(\lambda)e^{-2\lambda h}} , \tag{21}$$

the vertical current density distribution given by Equation (16) is expressed as

$$j(r) = \frac{I_s}{4\pi} \int_0^\infty \lambda P(\lambda)\ J_o(\lambda r_s)\ J_o(\lambda r)\ d\lambda - \frac{I_o}{4\pi} \int_0^\infty \lambda Q(\lambda)\ J_o(\lambda r)\ d\lambda. \tag{22}$$

Then, substituting Equation (22) into Equation (18) and integrating the resulting expression from a to r_ℓ using the integral solution

$$\int rJ_o(\lambda r)dr = rJ_1\frac{(\lambda r)}{\lambda} + C,$$

yields the current flow through the liner

$$I_\ell = \frac{I_s}{2} \int_0^\infty P(\lambda)J_o(\lambda r_s)\ [r_\ell J_1(\lambda r_\ell) - aJ_1(\lambda a)]\ d\lambda$$

$$- \frac{I_o}{2} \int_0^\infty Q(\lambda)\ [r_\ell J_1(\lambda r_\ell) - aJ_1(\lambda a)]\ d\lambda. \tag{23}$$

This result may be used to implement the assumed condition that the total current injection, I_s, is equal to the current flowing through a leak, I_o, plus the current flowing across the liner, I_ℓ. This approximation is equivalent to neglecting currents flowing through the lined walls of a waste disposal site having physical boundaries. Thus, the fraction of current flow through a leak is derived as

$$f_o \equiv \frac{I_o}{I_s} = \frac{1 + u + v}{1 + p + w}; \qquad \text{for } 1 + p + w > 1, \tag{24}$$

where

$$u = -\frac{r_\ell}{2} \int_0^\infty P(\lambda)\, J_o(\lambda r_s)\, J_1(\lambda r_\ell)\, d\lambda, \tag{25}$$

$$v = \frac{a^2}{4} \int_0^\infty \lambda P(\lambda)\, J_o(\lambda r_s)\, d\lambda, \tag{26}$$

$$p = -\frac{r_\ell}{2} \int_0^\infty Q(\lambda)\, J_1(\lambda r_\ell)\, d\lambda, \tag{27}$$

and

$$w = \frac{a}{2} \int_0^\infty Q(\lambda)\, J_1(\lambda a)\, d\lambda. \tag{28}$$

Equation (24) predicts the portion of the total current which flows from the waste material through the leak into the underlying soil. The fraction of current, f_o, is plotted in Figure 5 as a function of the radius, r_ℓ [defined by Equation (19)], for a leak located in a waste disposal site having a depth of 1 m and in which the waste resistivity is 15 ohm-m and the underlying soil resistivity is 30 ohm-m. As expected, for damaged lined impoundments of large sizes, the relative amount of source current flowing through the leak decreases as the size of the geomembrane liner increases. For example, for a waste disposal site having a surface area of 100,000 m^2 (r_ℓ = 178 m), only 56 percent of the total source current flows through the leak. Alternatively, for lined impoundments of approximately 10,000 m^2 surface area (r_ℓ = 56 m), 90 percent of the source current flows through the leak, and for small impoundments of about 1000 m^2 area or less ($r_\ell \leq$ 17 m), almost 100 percent of the current flows directly through the leak.

Superposition of primary and secondary potentials yields the solution at measurement points above the leak. The primary potential is given in Appendix B and the secondary potential is obtained from the second term of Equation (15). The magnitude of the current, I_o, flowing through the leak, and defined by Equation (24), is used to calculate the electrical potentials at measurement points having coordinates (x,y,z). Thus, the general electrical potential solution for predicting signatures caused by a circular leak in a geomembrane liner may be written explicitly as

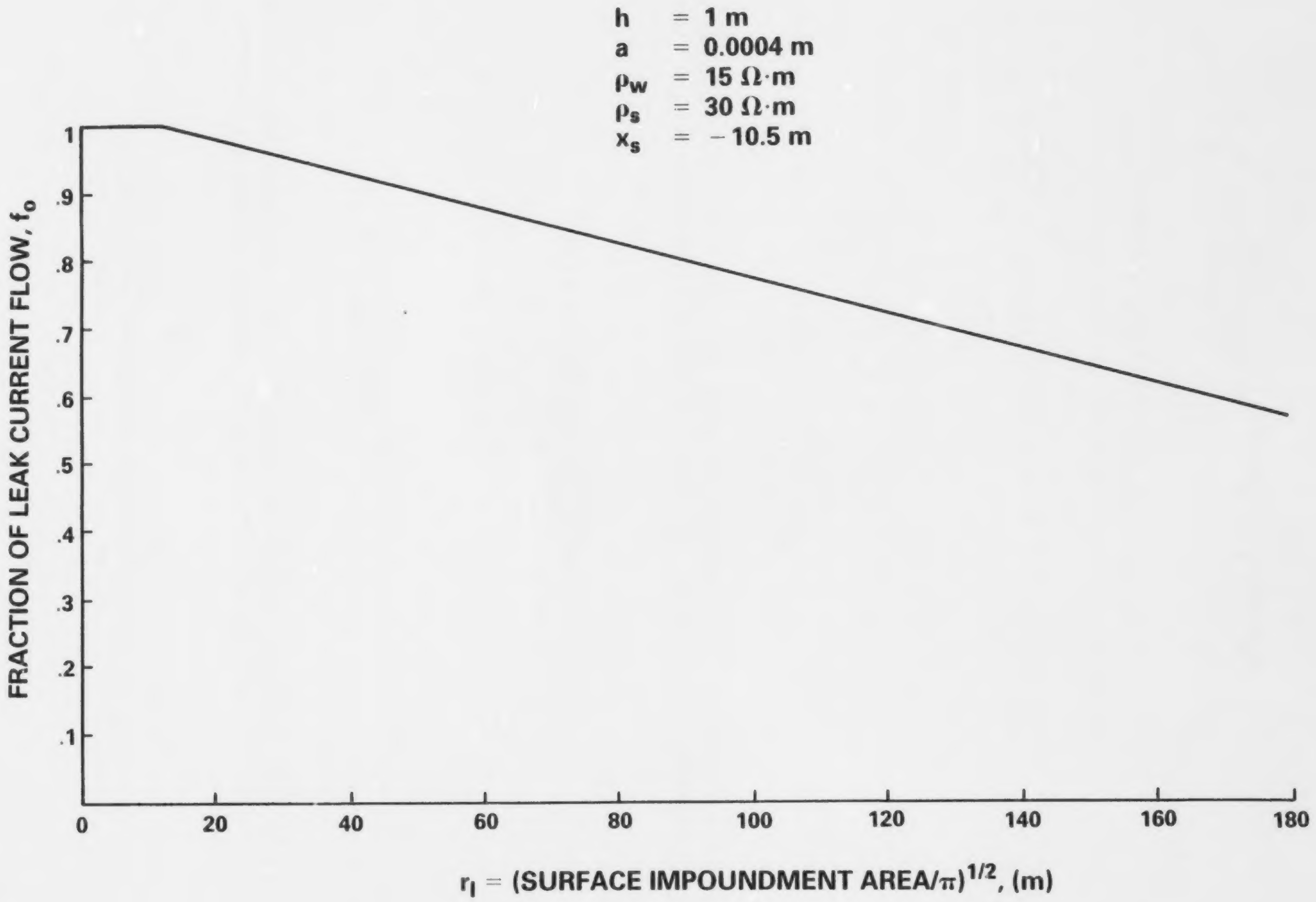

Figure 5. The fraction of current flowing through a leak of radius a versus the surface impoundment size.

$$\phi(r,z) = \frac{I_s\rho_w}{4\pi} \left\{ \frac{1}{\sqrt{|r - r_s|^2 + (z + z_s)^2}} + \frac{1}{\sqrt{|r - r_s|^2 + (z - z_s)^2}} \right.$$

$$+ \int_0^\infty \frac{R(\lambda)}{1 - R(\lambda)e^{-2\lambda h}} [e^{-\lambda(h+z_s)} + e^{-\lambda(h-z_s)}]$$

$$\left. \times [e^{-\lambda(h+z)} + e^{-\lambda(h-z)}] J_o(\lambda|r - r_s|)d\lambda \right\}$$

$$+ \frac{I_o\rho_w}{4\pi} \int_0^\infty f(\lambda)[e^{-\lambda(h+z)} + e^{-\lambda(h-z)}] J_o(\lambda r) d\lambda;$$

$$\text{for } t \ll h, \quad \text{and } \lambda a \ll 1 , \tag{29}$$

where

$$f(\lambda) = \frac{T(\lambda)}{1 - R(\lambda)e^{-2\lambda h}} . \tag{30}$$

The function, $T(\lambda) = 1 + R(\lambda)$, as given by Equation (8), is substituted into Equation (30) to express the function, $f(\lambda)$, in terms of the function, $R(\lambda)$, as

$$f(\lambda) = \frac{R(\lambda)\ (1 + e^{-2\lambda h})}{1 - R(\lambda)e^{-2\lambda h}} + 1,$$

or

$$f(\lambda) = 1 + \left\{ \frac{R(\lambda)}{1 - R(\lambda)e^{-2\lambda h}} [e^{-\lambda(h+z_o)} + e^{-\lambda(h-z_o)}]\right\}_{z_o=h} . \tag{31}$$

This form of the function, $f(\lambda)$, is substituted into Equation (29) to yield the electrical potential solution in a more convenient form for calculations such as

$$\phi(r,z) = \frac{\rho_w I_s}{4\pi} [G(r,z;\ r_s,z_s) + \frac{I_o}{I_s} G(r,z;\ 0,\ h)], \tag{32}$$

where

$$G(r,z;\ r',z') = \frac{1}{\sqrt{|r - r'|^2 + (z + z')^2}} + \frac{1}{\sqrt{|r - r'|^2 + (z - z')^2}}$$

$$+ \int_0^\infty \frac{R(\lambda)}{1 - R(\lambda)e^{-2\lambda h}} [e^{-\lambda(h+z')} + e^{-\lambda(h-z')}]$$

$$\times [e^{-\lambda(h+z)} + e^{-\lambda(h-z)}]\ J_o(\lambda|r - r'|)\ d\lambda. \qquad (33)$$

The function, $G(r,z;\ r',z')$, is the Green's function of a three-layer medium containing a thin, highly resistive layer of thickness, t, for a point source at the position, $(r',\ z')$, and an observer at (r,z). The first term of Equation (32) represents the electrical potential associated with a point source current, I_s, at $(r_s,\ z_s)$ in the absence of leaks; the second term is the electrical potential associated with the current flow, I_o, entering a leak in a geomembrane liner at $(0,h)$. In addition, Equation (32) clearly shows that when $I_o/I_s = 1$, the current injection at the source position $(r_s,\ z_s)$ flows directly through the leak, and when $I_o/I_s = 0$, the potential at the measurement points represents the effect of a leak-free liner.

The integrals given in Equations (25) through (26) and Equation (33) were evaluated numerically using a Hankel transform subroutine called ZHANKS developed by Anderson (1979). Although the integral of Equation (25) has an oscillatory kernel defined by

$$k(\lambda) = P(\lambda)J_o(\lambda r_s),$$

it is rapidly convergent for values of $r_s < r_\ell$.

Multiple Leaks--

Thus far, only the effect of a single leak has been investigated, but the analysis can be extended to incorporate more than one leak in a geomembrane liner of thickness, t, and resistivity, ρ_ℓ. The geometry of multiple leaks in the plane, $z = h$, is illustrated in Figure 6. For any finite number of circular leaks in a liner, the resultant potential distribution at a field point having coordinates x,y,z is

$$\phi = \phi_p(r,z_s;\ r_s,z_s) + \sum_{i=0}^{m} I_i \int_0^\infty F(\lambda)\ [e^{-\lambda(h-z)} + e^{-\lambda(h+z)}]$$

$$\times J_o(\lambda|r - r_i|)\ d\lambda, \qquad (34)$$

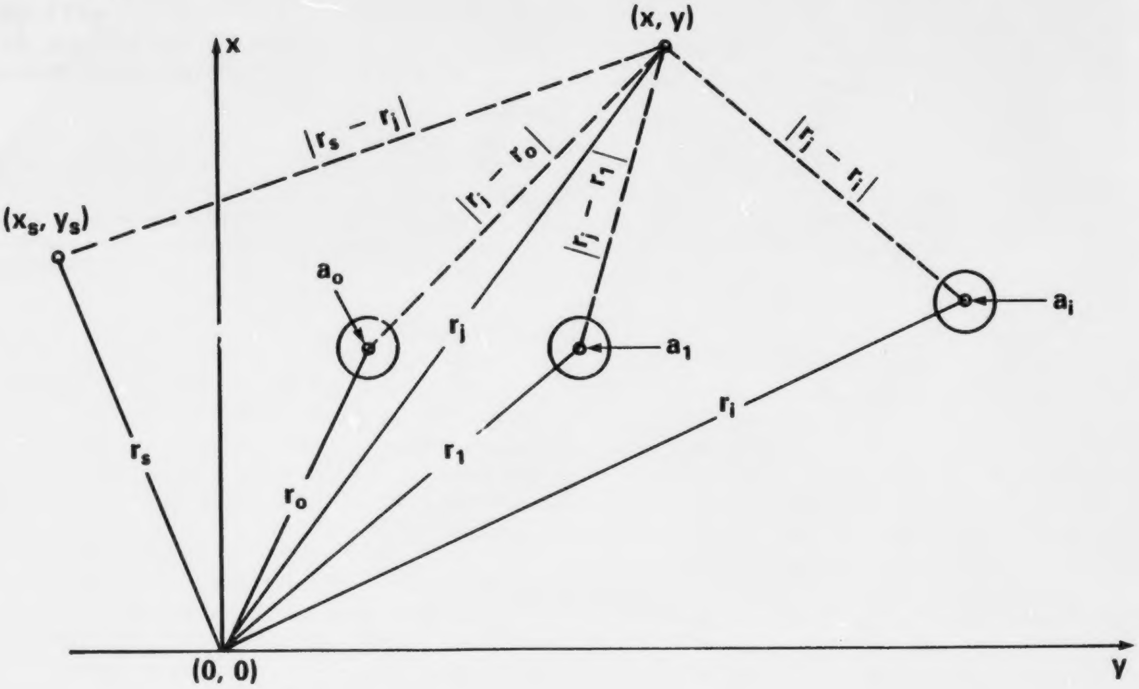

(x, y)
x
$|r_s - r_j|$
$|r_j - r_o|$
$|r_j - r_1|$
$|r_j - r_i|$
(x_s, y_s)
a_o
r_j
a_1
a_i
r_i
r_s
r_1
r_o
(0, 0)
y

Figure 6. Plane z = h of the geomembrane liner showing multiple leaks of radius a_i for i = 0,1,2,...n.

where

$$|r - r_i| = [(x_i - x)^2 + (y - y_i)^2]^{1/2},$$

$$F(\lambda) = \frac{\rho_w}{4\pi}\left(\frac{T(\lambda)}{1 - R(\lambda)e^{-2\lambda h}}\right),$$

and m is the number of leaks.

The first term in Equation (34) is the primary potential given by Equation (7); I_o, I_1, ... I_m are currents passing through the circular leaks and $F(\lambda)$ corresponds to the last term of Equation (15). The current flowing through each leak may be calculated directly using the expression

$$I_i = \frac{f_o I_s}{m}\ ; \qquad \text{for } i = 1,2, \ldots m,$$

which assumes that, for small leaks of the same size, the current flowing through each leak is the same when a constant current distribution is injected.

In a typical leak detection survey, the current source maintains a constant current. The total current flow, I_s, in the lined impoundment is equal to the sum of the current flowing through each individual leak plus the background current flowing through the undamaged part of the liner as well as a small lateral current flow through the waste material layer. Since plastic geomembrane liners have a high resistance per unit of area, the current flowing through the undamaged liner bottom and side walls is negligible compared with the current flowing through one or more leaks for lined impoundments having surface areas of about 10,000 m^2 or less. In addition, the potential driving force varies as a function of the distance between the leak and the source current electrode. However, this variation is small when surveys are performed in typical impoundments. Therefore, the total value of the leak resistance, associated with the leak current density, may be determined by connecting the leak resistances in parallel. Thus, in a lined impoundment or landfill containing a damaged geomembrane liner with multiple leaks, the amplitude of the signatures measured at a given survey depth will depend directly on the amount of current flowing through each individual leak. In general, the presence of multiple leaks results in less current per leak and, therefore, a decrease in detector sensitivity.

Theoretical Analysis to Simulate the Response of a Leak in the Geomembrane of a Cover System

The analysis to simulate leaks in lined impoundments has been extended to incorporate a cover system model, which consists of two layers under the insulating liner, an insulating geomembrane liner, and three layer material above the geomembrane liner. In the model, the cover material is represented by a three-layer medium of resistivities, $\rho_c^{(1)}$, $\rho_c^{(2)}$, $\rho_c^{(3)}$, and thicknesses d_1, d_2, and d_3, respectively. The liner is represented by a thin highly resistive layer of resistivity, ρ_ℓ, and thickness, t; and the region under the liner is represented by two-layers to simulate a soil medium of resistivities, $\rho_s^{(1)}$, and $\rho_s^{(2)}$. The size of the leak is assumed to be much smaller than other liner dimensions.

The expression for the secondary potential associated with the current flow, I_o, entering a leak of radius, a, in the geomembrane liner at the position (x_o,y_o,z_o), is developed (as in the previous analysis) by considering the leak as a current source. The product of the leak current density, $j(x_o,y_o)$, and the cover system Green's function, $G_c,(x,y,z;x_o,y_o,z_o)$, is integrated over the surface of the leak, S. Thus, the solution for the secondary potential can be written in terms of the Green's function for the six-layer medium (i.e., the cover material, the liner, and soil) as

$$\phi_s^{(c)} = \frac{\rho_\ell}{4\pi} \int_S j(x_o,y_o)\, G_c(x,y,z;x_o,y_o,z_o)\,dx_o dy_o. \tag{35}$$

In addition, an expression of the primary potential is required in the general solution and is assumed to be the potential associated with a point source current, I_s, in a six-layer medium representing a cover system which contains a leak-free liner.

The total electrical potential at any position, (x,y,z), is obtained by the superposition of the primary potential, $\phi_p^{(c)}$, and the secondary potential, $\phi_s^{(c)}$,

$$\phi^{(c)} = \phi_p^{(c)}(x,y,z;x_s,y_s,z_s) + \frac{\rho_\ell}{4\pi} \int_S j(x_o,y_o)\, G_c(x,y,z;x_o,y_o,z_o)\,dx_o dy_o. \tag{36}$$

The solution of the electrical potential for a leak in the geomembrane liner at $z_o = h$ may be expressed in cylindrical coordinates as

$$\phi^{(c)} = \phi_p^{(c)}\,(r,z;r_s,z_s) + \frac{\rho_\ell}{4\pi} \int_S j(r_o)\, G_c(r,z;r_o,h)\,r_o dr_o d\Theta_o, \tag{37}$$

where

$$r_s = (y_s^2 + x_s^2)^{1/2}, \quad r = (y^2+x^2)^{1/2}, \quad r_o = (y_o^2 + x_o^2)^{1/2},$$

$$G_c(r,z;r_o,h) = \frac{\rho_c^{(3)}}{\rho_\ell}\left(1+R_c^{(12)}\right)\left(1+R_c^{(23)}\right) \int_0^\infty \frac{(1+e^{-2\lambda h})}{[1+e^{-2\lambda(d_1+d_2)}]}\,\frac{U_c(\lambda)T_c(\lambda)}{[1-Q_c(\lambda)e^{-2\lambda h}]}$$

$$\times\ [e^{-\lambda(2d_1+h+z)} + e^{-\lambda(2d_1+h-z)}]\ J_o(\lambda|r-r_o|)\,d\lambda,$$

$$U_c(\lambda) = \frac{(1+W_2\ e^{-2\lambda d_2})}{[1+W_2\ R_c^{(23)}e^{-2\lambda d2}]\ [1+W_3\ e^{-2\lambda d3}]\ [R_c^{(12)}+e^{-2\lambda d2}]},$$

$$W_2 = \frac{R_c^{(12)}+e^{-2\lambda d_1}}{1+R_c^{(12)}e^{-2\lambda d_1}},$$

$$W_3 = \frac{R_c^{(23)}+W_2 e^{-2\lambda d_2}}{1+W_2 R_c^{(23)}e^{-2\lambda d_2}},$$

$$Q_c(\lambda) = \frac{\rho_s^{(1)}-\rho_c^{(3)}+\lambda t\rho_\ell+(\rho_s^{(1)}+\rho_c^{(3)}-\lambda t\rho_\ell)R_1\ e^{-2\lambda b}}{\rho_s^{(1)}+\rho_c^{(3)}+\lambda t\rho_\ell+(\rho_s^{(1)}-\rho_c^{(3)}-\lambda t\rho_\ell)R_1\ e^{-2\lambda b}},$$

$$T_c(\lambda) = \frac{2\ [\rho_s^{(1)}+\lambda t\rho_\ell+(\rho_s^{(1)}-\lambda t\rho_\ell)R_1\ e^{-2\lambda b}]}{\rho_s^{(1)}+\rho_c^{(3)}+\lambda t\rho_\ell+(\rho_s^{(1)}-\rho_c^{(3)}-\lambda t\rho_\ell)R_1\ e^{-2\lambda b}},$$

$$R_1 = \frac{\rho_s^{(2)}-\rho_s^{(1)}}{\rho_s^{(2)}+\rho_s^{(1)}},$$

$$R_c^{(12)} = \frac{\rho_c^{(1)}-\rho_c^{(2)}}{\rho_c^{(1)}+\rho_c^{(2)}},$$

$$R_c^{(23)} = \frac{\rho_c^{(2)}-\rho_c^{(3)}}{\rho_c^{(2)}+\rho_c^{(3)}},$$

$\rho_c^{(1)}$, $\rho_c^{(2)}$, and $\rho_c^{(3)}$ = resistivities of the cover materials;

d_1, d_2, and d_3 = thickness of the cover materials;

ρ_ℓ and t = resistivity and the thickness of the liner;

$\rho_s^{(1)}$ and $\rho_s^{(2)}$ = resistivities of the soil under the liner;

b = thickness of the first soil layer;

h = depth to the liner;

r_s = radial distance from the current source to the leak center;

x_s = depth to the source current electrode; and

I_s = total current injection point.

The primary potential associated with a point source current, I_s, located in the second layer of the cover material is given at the measurement position, (x,y,z), by

$$\phi_p^{(c)} = \frac{I_s}{4\pi}\,\rho_c^{(2)} \int_0^\infty \frac{\left(1+R_c^{(12)}\right)}{\left(1+R_c^{(12)}e^{-2d_1}\right)} \frac{\left[e^{-\lambda x_s} - \varepsilon e^{-\lambda[2(d_1+d_2)-x_s]}\right]}{\left[1-\varepsilon\mu\, e^{-2\lambda d_2}\right]}$$

$$\times \left[e^{-\lambda z} + e^{\lambda z}\right] J_o(\lambda|r-r_s|)\, d\lambda,$$

where

$$\varepsilon = \frac{R_c^{(23)} - Q_c(\lambda)e^{-2\lambda d_3}}{1-Q_c(\lambda)R_c^{(23)}e^{-2\lambda d_3}}, \qquad (38)$$

and

$$\mu = -\frac{R_c^{(12)} + e^{-2\lambda d_1}}{1+R_c^{(12)}e^{-2\lambda d_1}}.$$

Assuming a uniform current density, j_o, in the leak of radius, a, and using the same analysis given by Equations (13) through (15), the electrical potential as a function of the unknown current flow, I_o, through the leak is derived and is given by

$$\phi^{(c)} = \phi_p^c\,(r,z;r_s,z_s) + \frac{I_o\rho_c^{(3)}}{4\pi}\int_0^\infty K(\lambda)J_o(\lambda r)\,d\lambda, \qquad (39)$$

where

$$K(\lambda) = \left(1+R_c^{(12)}\right)\left(1+R_c^{(23)}\right)\frac{\left(1+e^{-2\lambda h}\right)}{\left(1+e^{-2\lambda(d_1+d_2)}\right)}\;\frac{U_c(\lambda)T_c(\lambda)}{\left(1-Q_c(\lambda)e^{-2\lambda h}\right)}$$

$$\times\left[e^{-\lambda(2d_1+h+z)} + e^{-\lambda(2d_1+h-z)}\right].$$

In a landfill cover system, the current flows through the cover material, the liner, and the leaks to return to the current electrode in the soil layer. The cover systems of interest are generally of the order of 2 m in depth and many have surface areas of several hectares so lateral current flowing across the perimeter of the cover is much smaller than current through the lined bottom and the leaks. Therefore, the total current distribution which returns to the sink current electrode may be assumed equal to the currents flowing across the lined bottom of the cover system plus the currents flowing through the leaks. In addition, the current flow through the cover material, the lined bottom, and the leaks is independent of the resistivity variation of the cover material, since the same current injection, I_s, must return to the sink current electrode in the soil layer. Therefore, to determine the current flow, I_o, through a leak in the geomembrane liner of a cover system, the procedure developed for the liquid impoundment model may be applied by calculating the average resistivity, $\bar{\rho}_c$, of the layered cover material of thickness, h, i.e.

$$\bar{\rho}_c = \frac{\rho_c^{(1)} d_1 + \rho_c^{(2)} d_2 + \rho_c^{(3)} d_3}{d_1 + d_2 + d_3} . \tag{40}$$

Thus, the three-layer cover material model is transformed to one layer cover model of resistivity, $\bar{\rho}_c$, and thickness, h. To determine the current flow, I_o, Equation (39), for the total electrical potential, is modified by making $\rho_c^{(1)} = \rho_c^{(2)} = \rho_c^{(3)} = \bar{\rho}_c$; $d_1 = d_2 = h$ and $R_c^{(12)} = R_c^{(23)} = 0$. With these approximations, Equation (39) becomes

$$\bar{\phi}(c) = \bar{\phi}_p^c + \frac{I_o \bar{\rho}_c}{4\pi} \int_0^{\infty} \frac{\bar{T}_c(\lambda)}{1 - \bar{R}_c(\lambda) e^{-2\lambda h}} \left[e^{-\lambda(h+z)} e^{-\lambda(h-z)} \right] J_o(\lambda r) d\lambda ,$$

where

$$\bar{R}_c(\lambda) = \frac{\rho_s^{(1)} - \bar{\rho}_c + \lambda t \rho_\ell + (\rho_s^{(1)} + \bar{\rho}_c - \lambda t \rho_\ell) R_1 e^{-2\lambda b}}{\rho_s(1) + \bar{\rho}_c + \lambda t \rho_\ell + (\rho_s(1) - \bar{\rho}_c - \lambda t \rho_\ell) R_1 e - 2\lambda b} ,$$

$$\bar{T}_c(\lambda) = \frac{2 [\rho_s^{(1)} + \lambda t \rho_\ell + (\rho_s^{(1)} - \lambda t \rho_\ell) R_1 e^{-2\lambda b}]}{\rho_s(1) + \bar{\rho}_c + \lambda t \rho_\ell + (\rho_s(1) - \bar{\rho}_c - \lambda t \rho_\ell) R_1 e - 2\lambda b} , \tag{41}$$

and

$$\bar{\phi}_p^{(c)} = \frac{I_s\bar{\rho}_c}{4\pi} \left\{ \frac{1}{\sqrt{|r-r_s|^2 + (z+z_s)^2}} + \frac{1}{\sqrt{|r-r_s|^2 + (z-z_s)^2}} \right.$$

$$\left. + \int_0^\infty \frac{\bar{R}_c(\lambda)(1+e^{-2\lambda h})[e^{-\lambda(h+z)} + e^{-\lambda(h-z)}]}{1 - \bar{R}_c(\lambda)e^{-2\lambda h}} J_o(\lambda r)d\lambda \right\} .$$

Since the form of the electrical potential expression given by Equation (41) is the same as that of Equation (15), the fraction of current flow through a leak in a geomembrane liner of a cover system may be obtained from

$$f_o = \frac{I_o}{I_s} = \frac{1+\bar{u}+\bar{v}}{1+\bar{s}+\bar{p}} \text{ ; for } 1 + \bar{s} + \bar{p} \geq 1, \tag{42}$$

$$\bar{u} = - \frac{r_\ell}{2} \int_0^\infty P_c(\lambda)J_o(\lambda r_s)J_1(\lambda r_\ell)d\lambda, \tag{43}$$

$$\bar{v} = - \frac{a^2}{4} \int_0^\infty \lambda P_c(\lambda)J_o(\lambda r_s)d\lambda, \tag{44}$$

$$\bar{p} = - \frac{r_\ell}{2} \int_0^\infty \lambda S_c(\lambda)J_1(\lambda r_\ell)d\lambda \ , \tag{45}$$

and

$$\bar{w} = \frac{a}{2} \int_0^\infty \lambda S_c(\lambda)J_1(\lambda a)d\lambda \ . \tag{46}$$

The functions $P_c(\lambda)$ and $S_c(\lambda)$ are defined by

$$P_c(\lambda) = \frac{[1-\bar{R}_c(\lambda)]}{1-\bar{R}_c(\lambda)e^{-2\lambda h}} [e^{-\lambda(h+z_s)} + e^{-\lambda(h-z_s)}] \ , \tag{47}$$

and

$$S_c(\lambda) \equiv \frac{T_c(\lambda)\ (1-e^{-2\lambda h})}{1-R_c(\lambda)e^{-2\lambda h}}\ . \qquad (48)$$

Equation (42) predicts the portion of the total current injection which flows from the cover material through the leak into the underlying soil. The magnitude of the current flow, I_o, is used to calculate the fields at measurement points having coordinates (x,y,z). Thus, the general electrical potential solution for predicting signatures caused by a circular leak in a geomembrane liner of a cover system may be written explicitly as

$$\phi_c = \frac{I_s\rho_c}{4\pi}\int_0^\infty \frac{[1+R_c^{(12)}]}{[1+R_c^{(12)}e^{-2\lambda d_1}]}\ \frac{[e^{-\lambda x_s}-\varepsilon e^{-\lambda[2(d_1+d_2)-x_s]}]}{[1-\varepsilon\mu e^{-2\lambda d_2}]}$$

$$\times\ [e^{-\lambda z}+e^{\lambda z}]J_o(\lambda|r-r_s|)d\lambda$$

$$+\ \frac{I_o\rho_c^{(3)}}{4\pi}\left(1+R_c^{(12)}\right)\left(1+R_c^{(23)}\right)\int_0^\infty \frac{(1+e^{-2\lambda h})}{1+e^{-2\lambda(d_1+d_2)}}\ \frac{U_c(\lambda)T_c(\lambda)}{[1-Q_c(\lambda)e^{-2\lambda h}]}$$

$$\times\ [e^{-\lambda(2d_1+h-z)}+e^{-\lambda(2d_1+h+z)}]J_o(\lambda r)d\lambda\ . \qquad (49)$$

Comparison of Model Results with Field Data

The derived electrical potential solution given by Equation (32) may be used to simulate the field conditions using the pole-dipole array configuration. The dipole array may be oriented parallel or perpendicular to the surface of the impounded liquid. To demonstrate the use of the modeling technique, the pole-dipole array was implemented in the general solution given by Equation (32) and synthetic leak signatures were computed for several practical cases.

Table 1 presents the numerical model parameters for predicting leak signatures. These values represent the test conditions at the 0.4-hectare impoundment facility.

Figure 7 shows the experimental leak detection response and the corresponding predicted response for a dipole array scanned along a line connecting the leak and the source current electrode. Since the voltage responses are plotted as a function of the position of the midpoint of the dipole, the location of the leak is determined by locating the inflection point between the

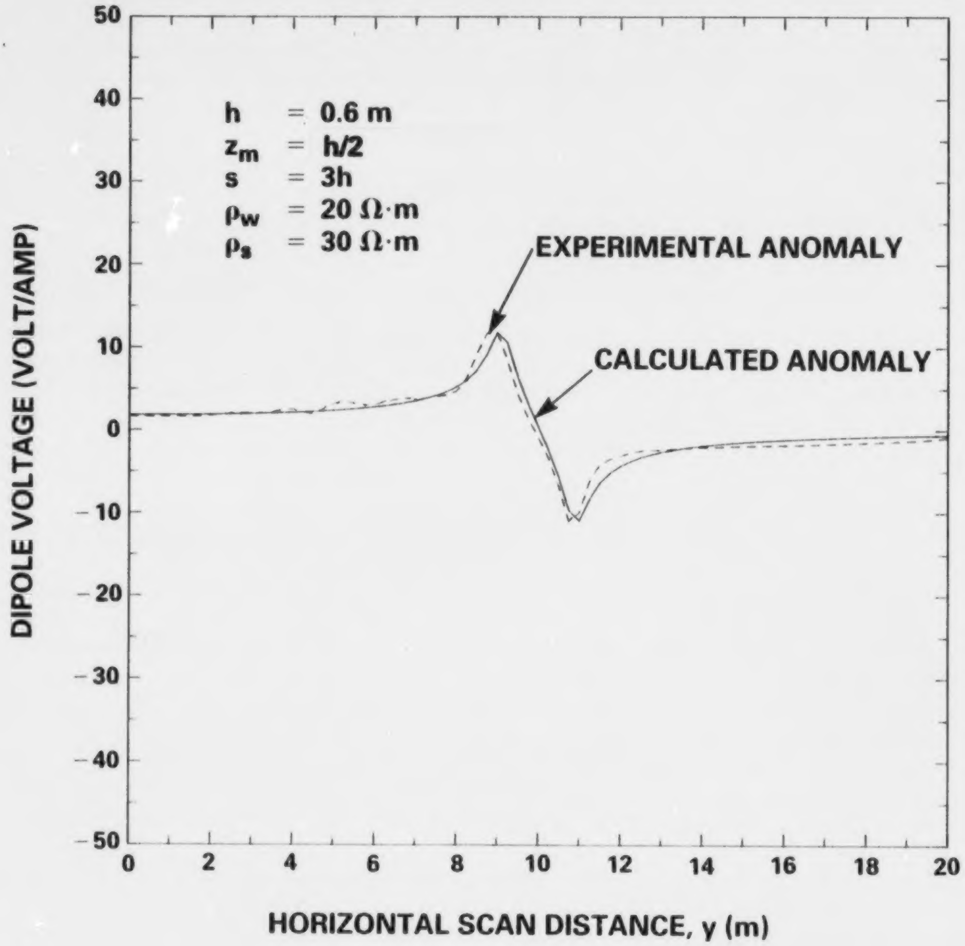

Figure 7. Comparison of experimental leak response and theoretical response predicted for the same field conditions.

TABLE 1. MODEL PARAMETERS FOR PREDICTING LEAK SIGNATURES

Impoundment parameters	
liner resistivity (ρ_ℓ)	10^{14} ohm-m
liner thickness (t)	3 mm
impoundment area (A)	4000 m^2
liquid layer thickness (h)	60 cm
Physical properties	
impoundment liquid resistivity (ρ_w)	20 ohm-m
soil resistivity (ρ_s)	30 ohm-m
Survey parameters	
dipole detector spacing (s)	1.80 m
current source position (x_s, y_s, z_s)	(0, -15.5 m, 0)
survey depth (z_m)	30 cm

minimum and the maximum voltage gradient peaks. The numerical model accurately predicts the measured leak signature at a survey depth of 30 cm. The peak-to-peak anomaly of the voltage gradient signature is 0.2 volt for a source current of approximately 9 mA. In addition, for the 0.4-hectare impoundment area, the amount of current flowing through the leak is about 95 percent of the source current.

Application of the Computer Model

Parametric Study--

The pole-dipole array and the three-layer waste impoundment installation are shown in Figure 8. In this illustration, the current source electrode is located within the waste material layer at the position $(0,0,z_s)$ below the origin of a Cartesian coordinate system (x,y,z). The detector dipole spacing is s. The survey lines containing the dipole detector are oriented parallel to the y-axis. The leak or leaks may be located at any position (x_c,y_c,h) in the geomembrane liner. The waste material is modeled as a layer having a resistivity, ρ_w. The liner is a thin highly resistive layer of thickness, t, and resistivity, ρ_ℓ. The leak is a small circular area of radius a in the thin liner layer and has a resistivity, ρ_w. The soil underlying the liner may be represented by the semi-infinite region of resistivity, ρ_s.

A geomembrane liner of thickness t = 3 mm having a resistivity of $\rho_\ell = 10^{14}$ ohm-m in an impoundment of surface area 5,000 m^2 was assumed for the parametric study and calculations of synthetic leak signatures. The amount of current flow through a leak in a lined impoundment of these characteristics is approximately 93 percent of the total current injection.

Anomaly effects of a leak--

The pole-dipole anomaly of a leak in the geomembrane liner has a characteristic bipolar potential gradient as shown in Figure 9. The detection of such anomalies is dependent upon the various parameters of impoundment depth,

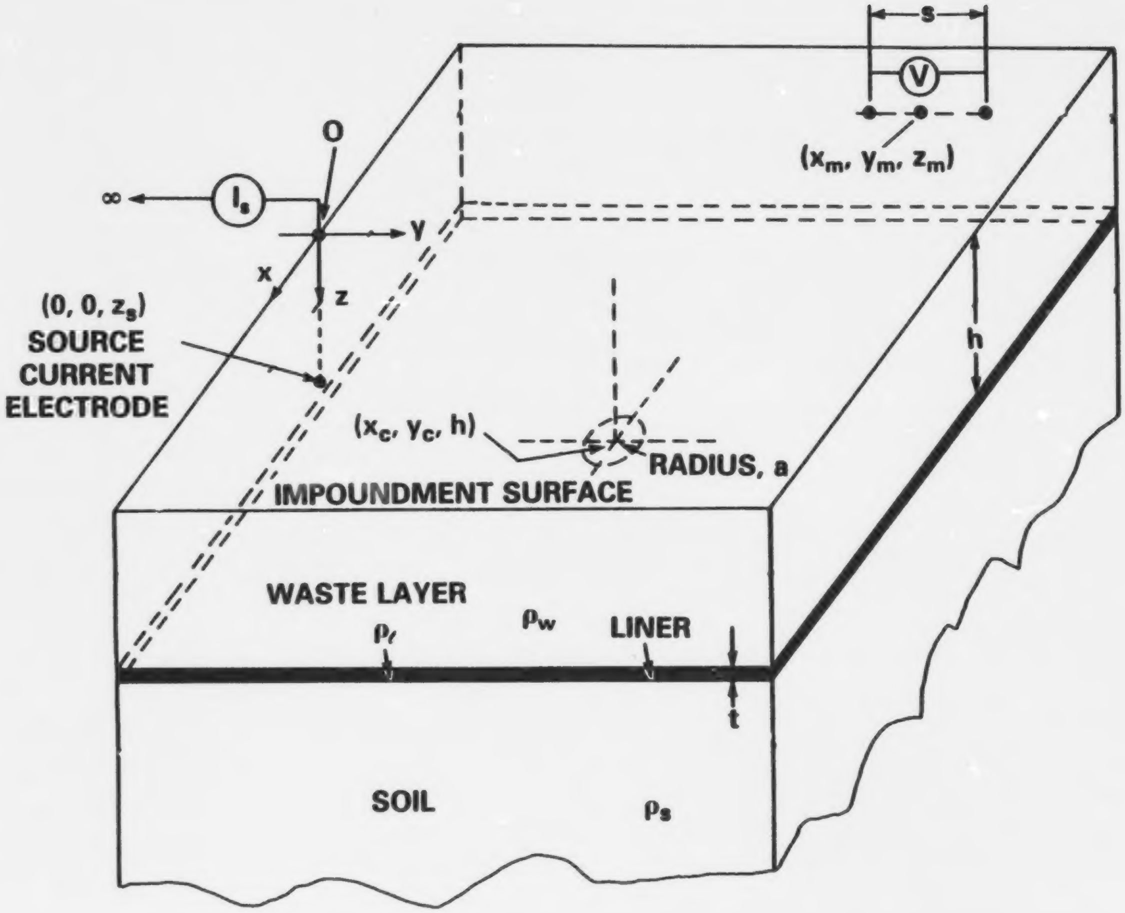

s
V
(x_m, y_m, z_m)
O
∞
I_s
y
x
z
$(0, 0, z_s)$
SOURCE CURRENT ELECTRODE
h
(x_c, y_c, h)
RADIUS, a
IMPOUNDMENT SURFACE
WASTE LAYER
ρ_ℓ
ρ_w
LINER
t
SOIL
ρ_s

Figure 8. Three-dimensional view of a pole-dipole survey arrangement and a circular leak of radius a in a geomembrane-lined liquid waste impoundment.

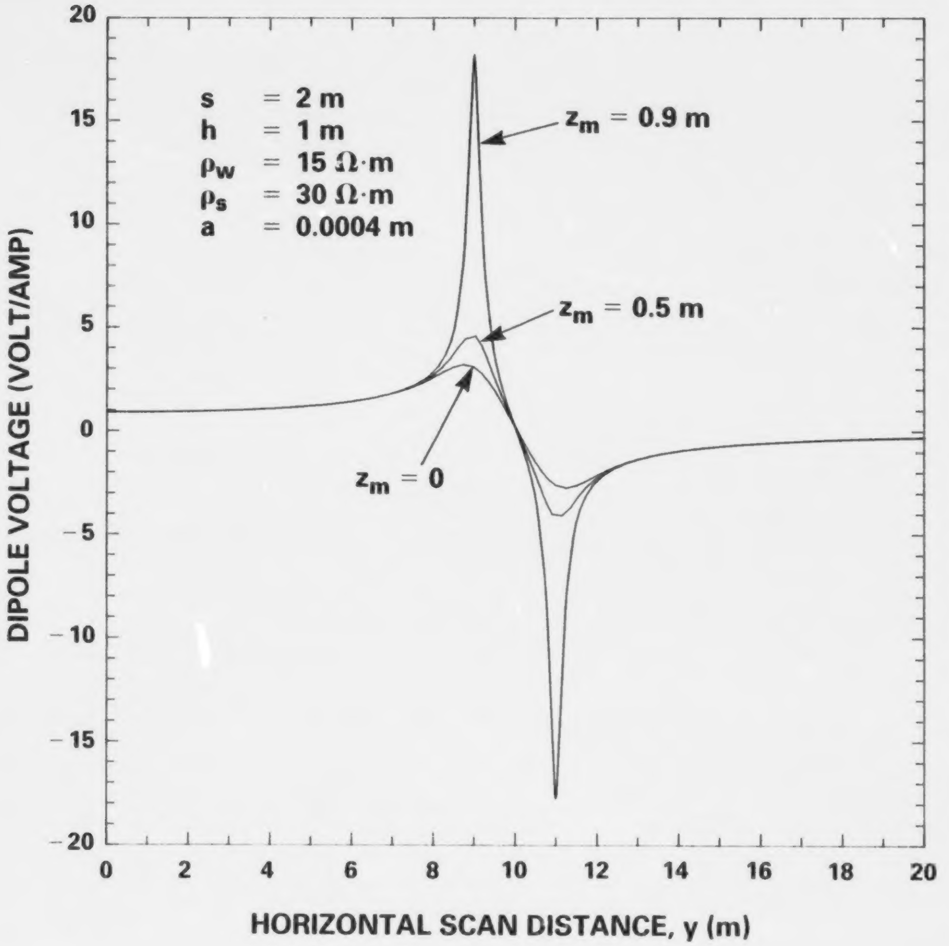

Figure 9. Anomaly measured over a leak of radius a = 0.0004 m for a pole-dipole array with a horizontal spacing of s = 1m.

leak size, waste material resistivity, underlying soil resistivity, the measurement dipole depth and proximity to the leak, and the source excitation current. Figure 9 shows a typical family of leak anomaly responses for a single leak located in a liquid waste impoundment having a depth of 1 m and in which the resistivities of the waste liquid and the underlying soil are 15 ohm-m and 30 ohm-m, respectively.

The family of curves in Figure 9 illustrates the effect of various measurement depths. The curves indicate the substantial improvement gained in detection sensitivity when the potential array is closer to the bottom of the impoundment.

Effect of dipole spacing--

The effect of the detector dipole spacing on the target response was calculated for a circular leak as a function of the survey depth $z = z_m$. The current source electrode is located at a depth of z_s = 50 cm. The peak-to-peak anomaly amplitudes for the three dipole spacings are displayed in Figure 10. As would be expected for large potential dipole spacings, the strength of the detected leak anomaly is increased. In addition, the effect of dipole spacing for a survey line at z = 50 cm is presented in Figure 11 to illustrate the broader effect of the anomaly response when the detector dipole spacing is increased.

Effect of impoundment depth--

Figure 12 shows peak-to-peak anomaly responses computed for various impoundment depths. The pole-dipole survey data is measured at a depth of h/2 below surface of the impoundment. These results confirm that the strength of the anomaly response is increased and leak detectability is improved for large dipole spacings and shallow impoundments. This suggests that for detecting small leaks in deep impoundments, a large receiver dipole spacing is appropriate. Additionally, the waste liquid level should be lowered whenever possible before conducting the pole-dipole survey.

Effect of waste material and soil resistivity--

Peak-to-peak anomaly amplitudes are illustrated for different waste layer resistivity and thickness values in Figure 13. These curves show that when a constant current is injected, the leak detectability is increased essentially linearly with the resistivity of the waste material. These curves together with the parametric curves given in Figure 12 may be used to determine the optimum dipole spacing and liquid level for improving leak detectability in conductive waste materials.

Figure 14 presents the results of submerged dipole measurements (z = 50 cm) illustrating the effect of the underlying soil resistivity for various waste material resistivities. The results show that for constant current injection the leak detection amplitude anomaly is essentially independent of the soil resistivity of the waste material.

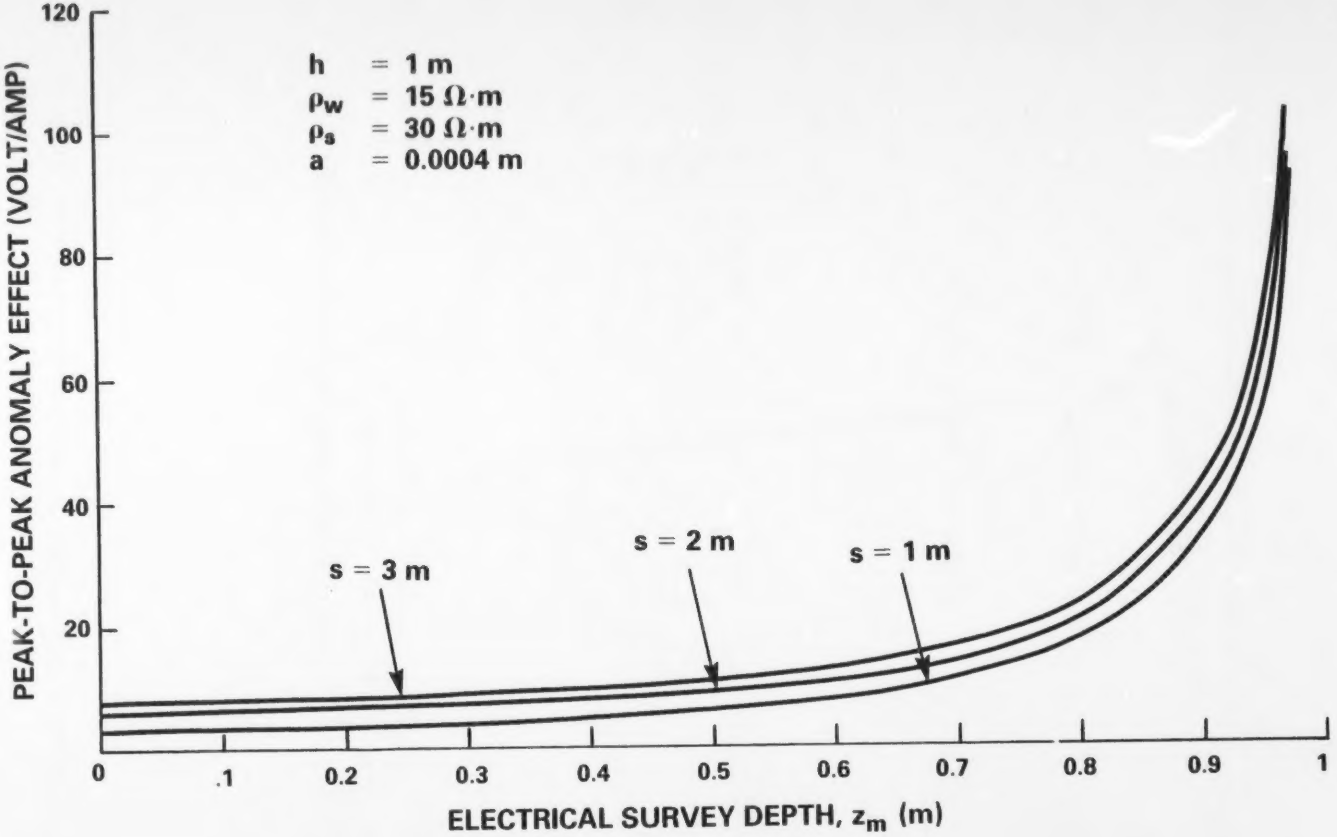

Figure 10. Peak-to-Peak voltage anomaly of a leak as a function of the electrical survey depth, z_m, for various horizontal dipole electrode spacings.

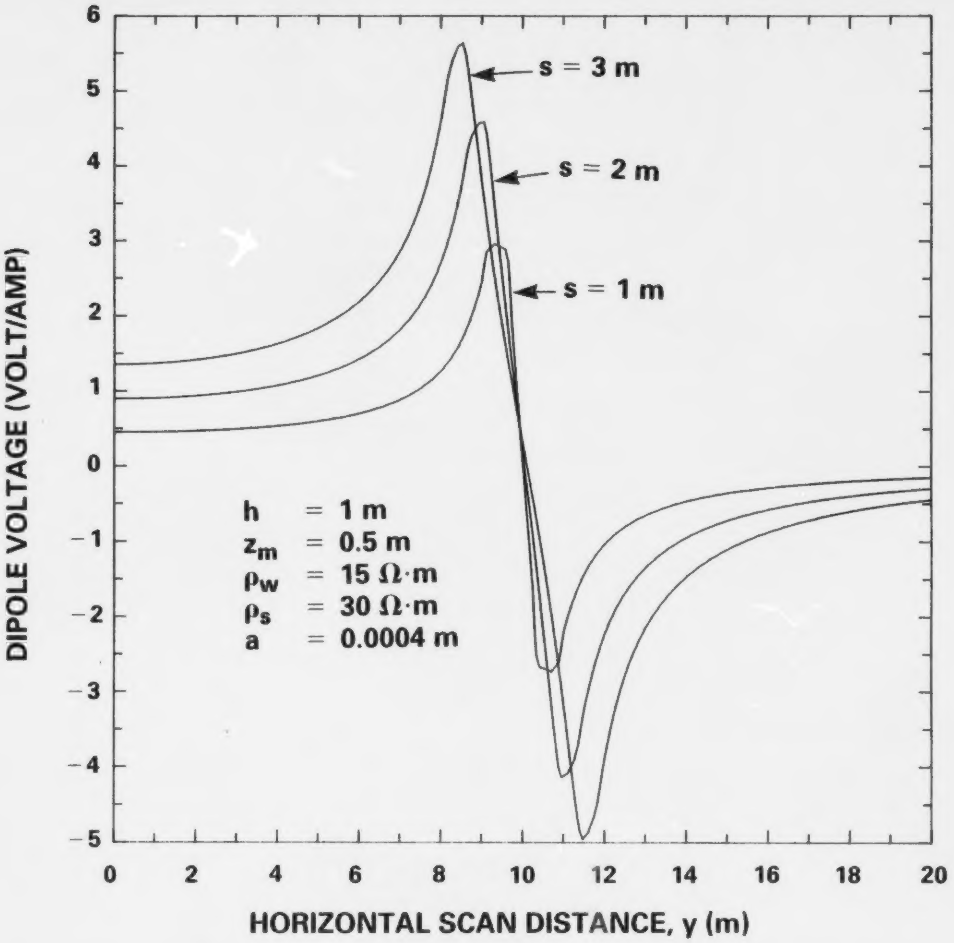

Figure 11. Anomaly measured over a leak of radius a = 0.0004 m for various horizontal dipole electrode spacings.

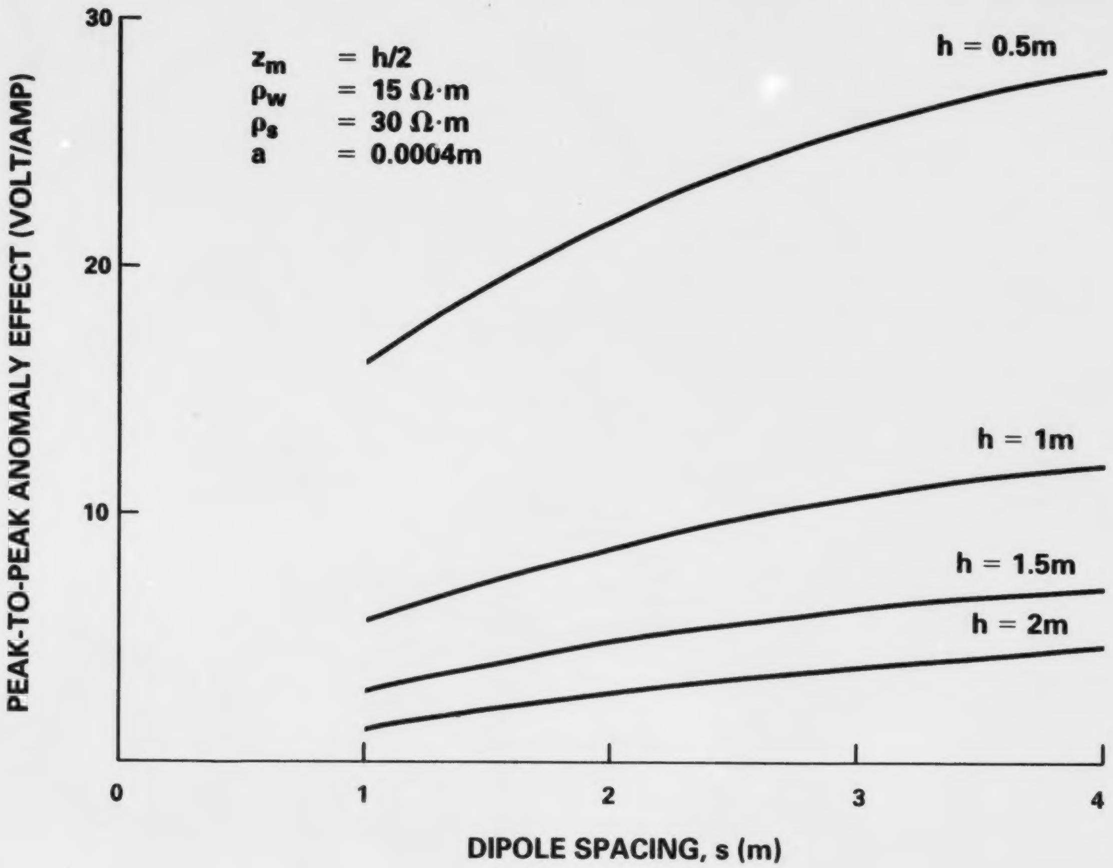

Figure 12. Peak-to-peak voltage anomaly as a function of dipole detector electrode spacing for various liquid layer depths, h.

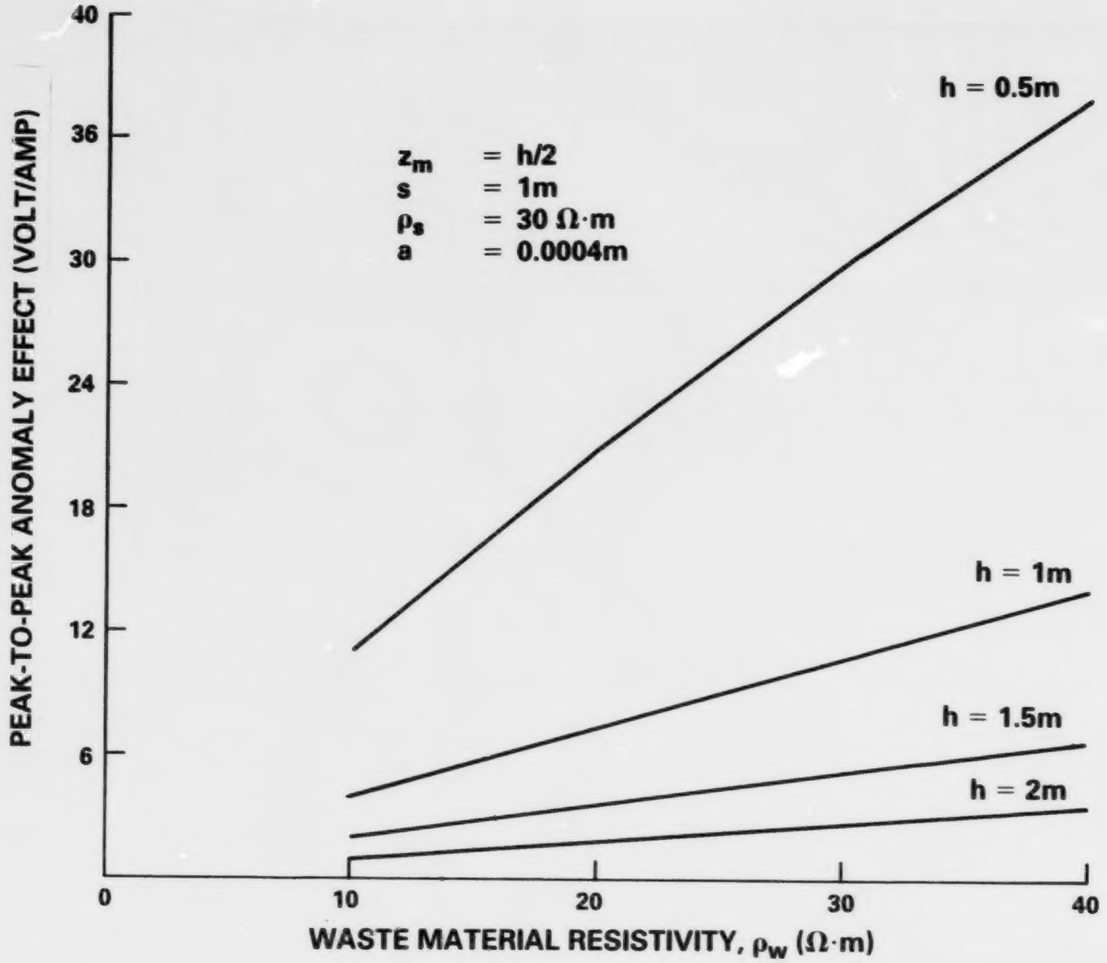

Figure 13. Peak-to-peak voltage anomaly as a function of waste material resistivity for various liquid layer depths, h.

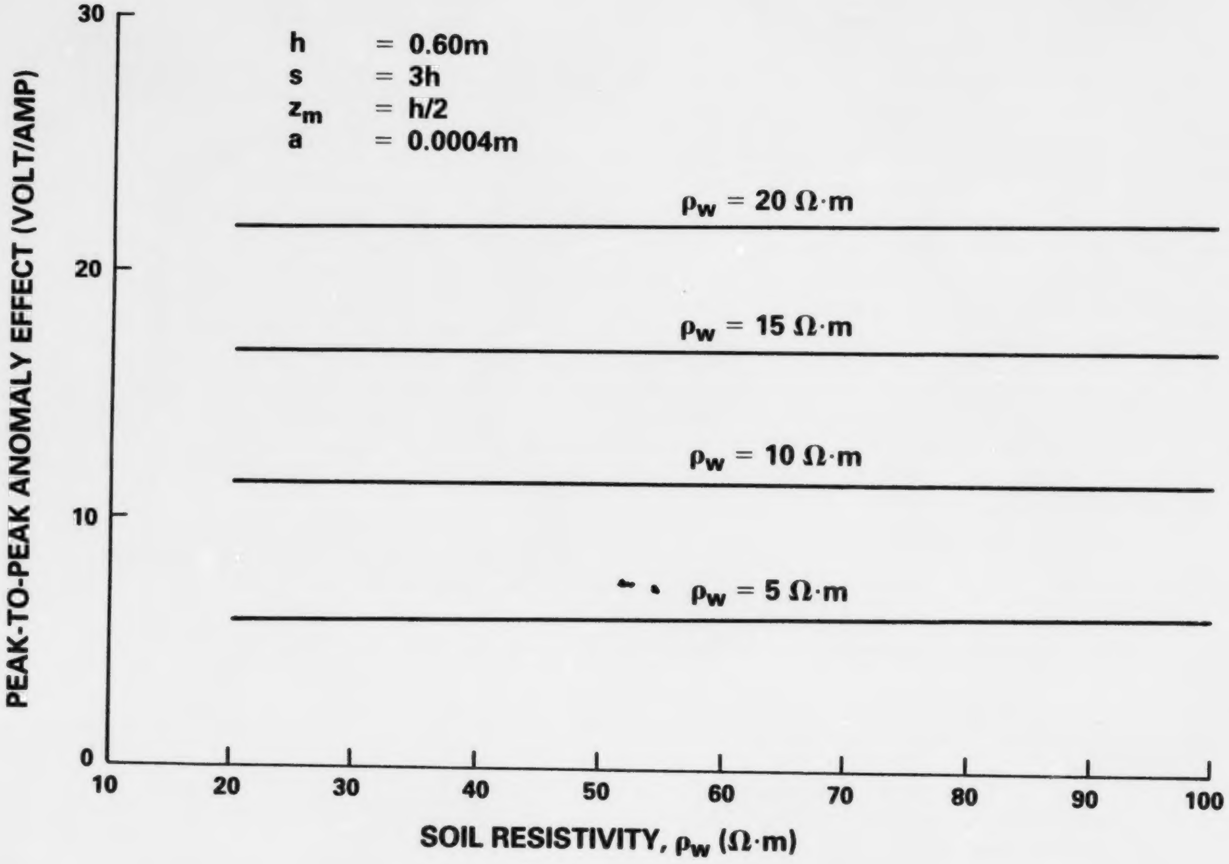

Figure 14. Peak-to-peak voltage anomaly as a function of soil resistivity for various waste material resistivities, ρ_w.

Effect of offset distance from the leak center--

In electrical surveys for leak location it is important to characterize the behavior of the potential gradient anomaly in the horizontal (x,y) plane to determine the optimum spacing between lateral survey lines. To illustrate this characteristic, peak-to-peak anomaly responses are calculated for various dipole offset distances from the leak center as a function of the survey height above the liner and are shown in Figure 15. From these results, the anomaly decays rapidly for small offset distances as the dipole detector depth decreases. An improvement of the leak detectability is observed for survey lines located within a radius of 10 cm from the leak center when the depth of the detector is increased. Conversely, for survey lines located at offset distances greater than 20 cm, the leak detection anomaly essentially is independent of the dipole measurement depth.

Comparison of horizontal and vertical dipole surveys--

Field data may be acquired in geomembrane-liquid impoundments using either horizontal or vertical dipole detectors when it is appropriate. Figure 16 shows that the horizontal dipole response is stronger than the vertical dipole response because of the closer proximity of the two electrodes to the plane of the liner. However, it is usually more practical to conduct subsurface measurements for geomembrane liner integrity using a vertical dipole detector rather than a horizontal dipole detector because the leak can be located more easily and accurately at the peak of the unipolar response of the vertical dipole anomaly whereas the horizontal dipole detector exhibits a bipolar anomaly in which the leak location corresponds to the crossover between the bipolar peaks. Multiple leaks can be resolved with less ambiguity when a vertical dipole is used. Figure 17 illustrates the vertical dipole anomaly response of the leak depicted earlier in Figure 11 for a horizontal dipole detector. In this case, the leak is directly associated with the maximum anomaly response. The depth, z_m, shown in Figure 17 corresponds to the position of the lower electrode of a 0.3-m vertical dipole pair in the 1-m deep waste material.

Leak resolution--

The presence of multiple leaks in a geomembrane-lined impoundment may be easily detectable for large leak separations; however, when leaks are close together, they are more difficult to resolve. To evaluate this resolution problem and to identify the optimum electrical survey parameters, leak signatures are computed for two leaks oriented radially away from the current source. Figures 18 and 19 show horizontal dipole leak signatures computed for two survey depths for leak separations of 4 and 2 m, respectively. As expected, when the horizontal separation between leaks located at positions A and B becomes less than the horizontal dipole spacing, separate resolution of the two leaks is lost. Figure 18 shows the combined response of two leaks located in the liner at positions y = 8 m and 12 m in the plane x = 0. These two leaks are easily detectable and identified at the separation of 4 m using a dipole of spacing of 2 m. The maximum peak-to-peak anomaly signature associated with each leak is 4 volt/amp at a survey depth of 50 cm.

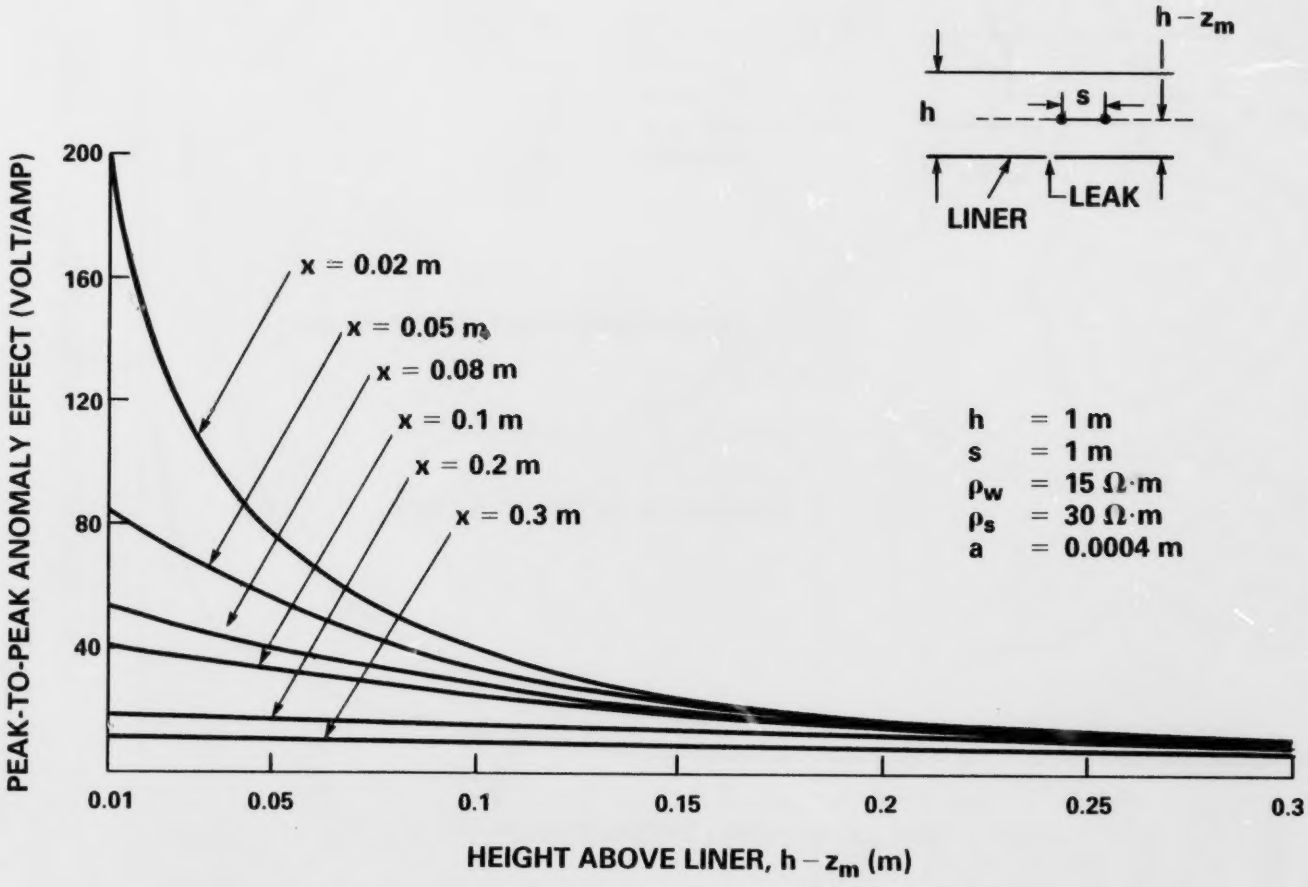

Figure 15. Peak-to-peak voltage anomaly as a function of height above liner, h-z_m, for various offset distances, x, from the leak center.

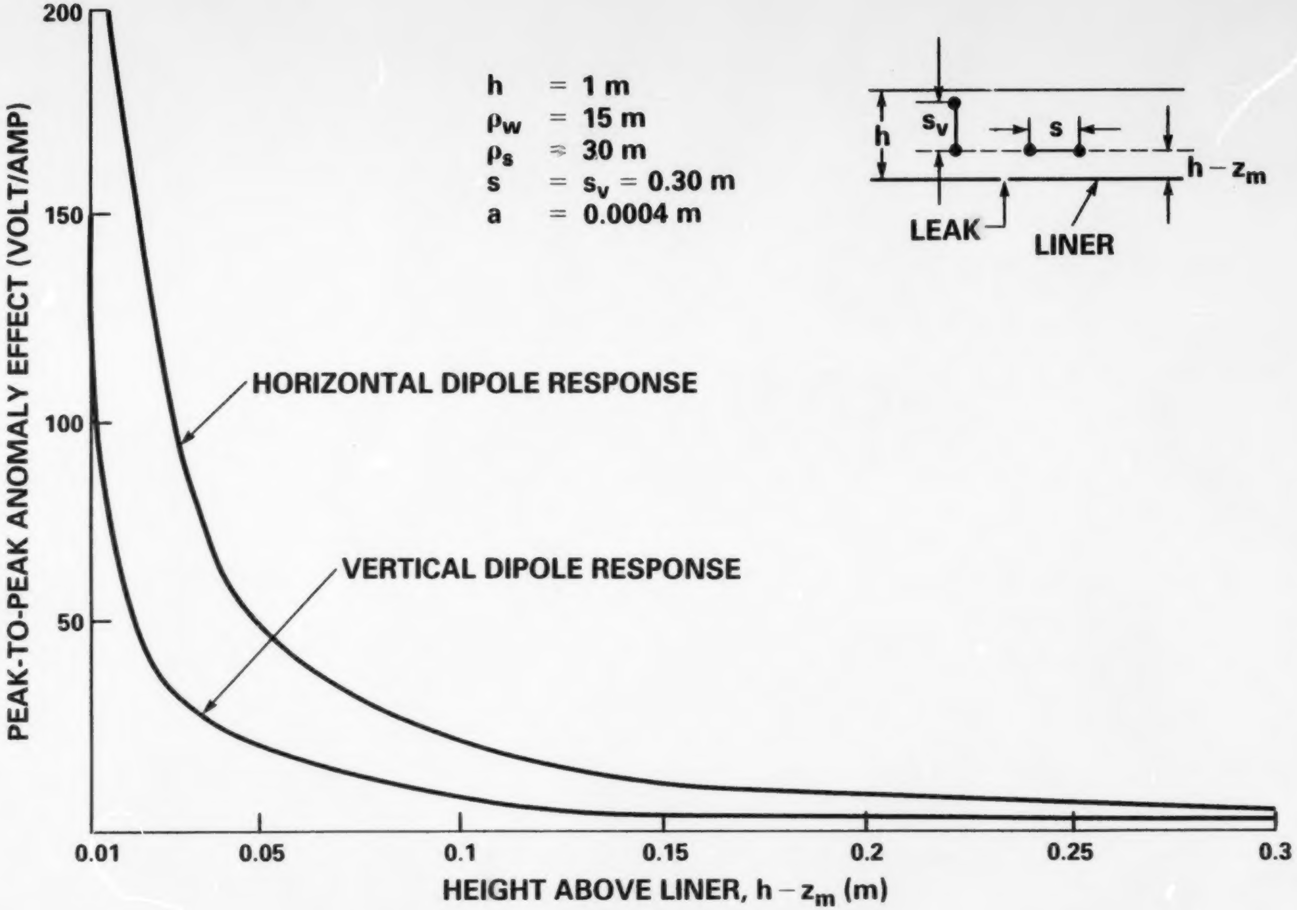

Figure 16. Comparison of horizontal dipole and vertical dipole responses over a leak of radius a = 0.0004 m.

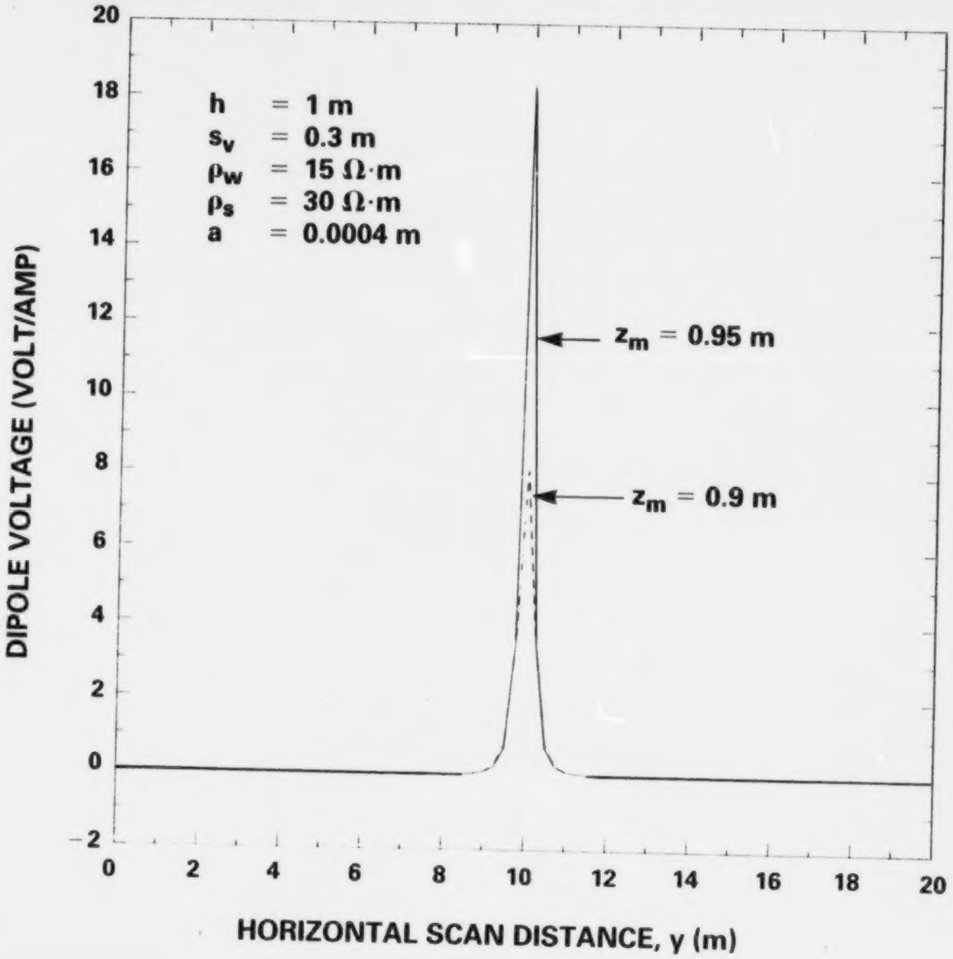

Figure 17. Anomaly measured over a leak of radius a = 0.4 mm using a vertical dipole array having an electrode spacing of s_v = 30 cm.

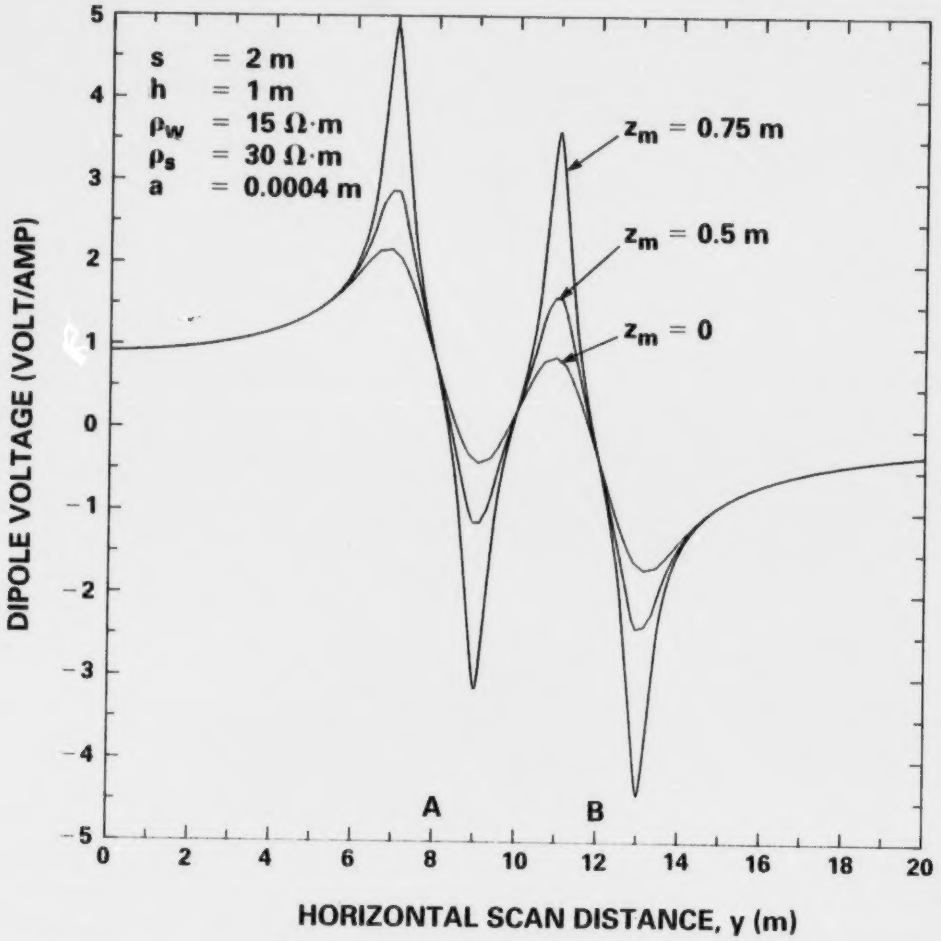

Figure 18. Potential profiles over two leaks of radius a for electrical surveys conducted at the surface and at depths of 50 cm and 75 cm. The leak centers are located in the liner at positions A and B corresponding to y_c = 8 m and 12 m, respectively, in the plane x = 0. The horizontal dipole detector spacing is s = 2 m.

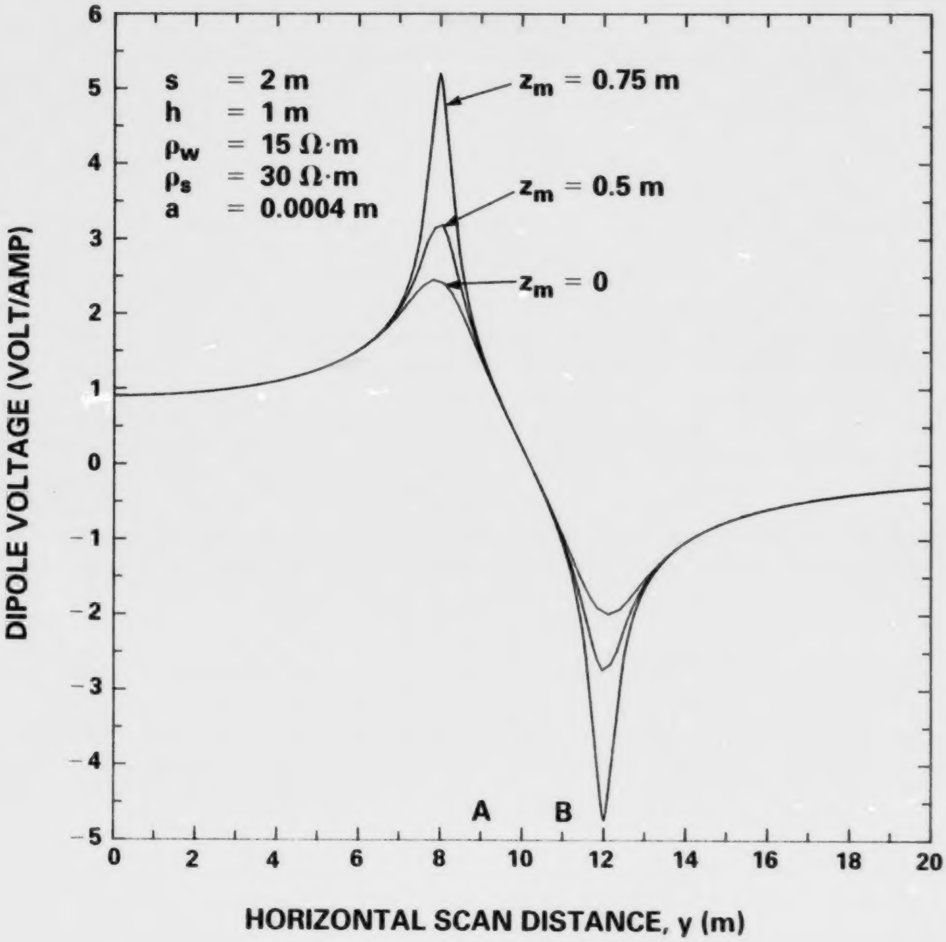

Figure 19. Potential profiles measured over two leaks of radius a for electrical surveys conducted at the surface and at depths of 50 cm and 75 cm. The leak centers are located in the liner at positions A and B corresponding to y_c = 9 m and 11 m, respectively, in the plane x = 0. The horizontal detector dipole spacing is s = 2 m.

Figure 19 shows the horizontal dipole signatures computed for two survey depths for leaks located at positions y = 9 and 11 m in the plane x = 0. For this leak separation of 2 m and dipole separation of 2 m, the individual leak anomalies combine to form a leak signature having an horizontal peak-to-peak separation approximately twice the dipole detector spacing. The peak-to-peak amplitudes of the composite anomalies are 6 and 10 volt/amp at the survey depths of 50 cm and 75 cm, respectively. The contour plot of the composite anomaly response of these two leaks is shown in Figure 20.

The above examples demonstrate that, when leaks are located at separations approximating the dipole detector spacing, the resolution is poor. However, when measurements are acquired using a dipole detector spacing appreciably smaller than that used in the previous example, the resolution improves. To demonstrate this improvement, composite anomaly responses were computed for the two leaks located at the separation of 2 m using a horizontal dipole having a spacing of s = 1 m.

Figure 21 shows the leak survey anomaly profile along horizontal scan lines above the leak center and illustrates the effect of dipole detector depth on the potential gradient anomalies for the two leaks. Although the strength of the anomaly decreases, the resolution of multiple leaks improves for a dipole detector spacing appreciably less than the leak separation. However, for lateral survey lines located at distances greater than one half the dipole detector spacing, the resolution of closely spaced leaks is poor. This is illustrated in the contour plot of parallel survey lines shown in Figure 22. The leak anomalies are difficult to detect on survey lines offset 2 m or more from the line over the leaks.

In general, the above results show that the magnitudes of multiple leak signatures are greater when the leaks are farther apart and the resolution of multiple leaks is improved using a dipole spacing which is smaller than the distance between the leaks. Therefore, with the aid of the present model for the detection of single and multiple leaks, it is possible to specify the subsurface depth at which electrical surveys should be conducted in order to obtain reliable leak detectability as well as the dipole spacing for resolving the presence and locations of multiple leaks. Then, appropriate data for such a survey can be computed and interpreted to facilitate the planning of the optimum leak location survey.

SUMMARY

The derived geomembrane leak detection model is an important and significant adaptation of electrical geophysical analysis techniques to leak location and assessment of damaged geomembrane liners. The current density at the leak plays an essential role in determining the magnitude of the current flow through the leak and the amplitude of the leak anomaly response. The excellent agreement between the experimental and calculated model data validates the practical ability of the model to predict leak signatures. This technique may be implemented as an aid in processing leak survey data acquired in lined impoundments or landfills.

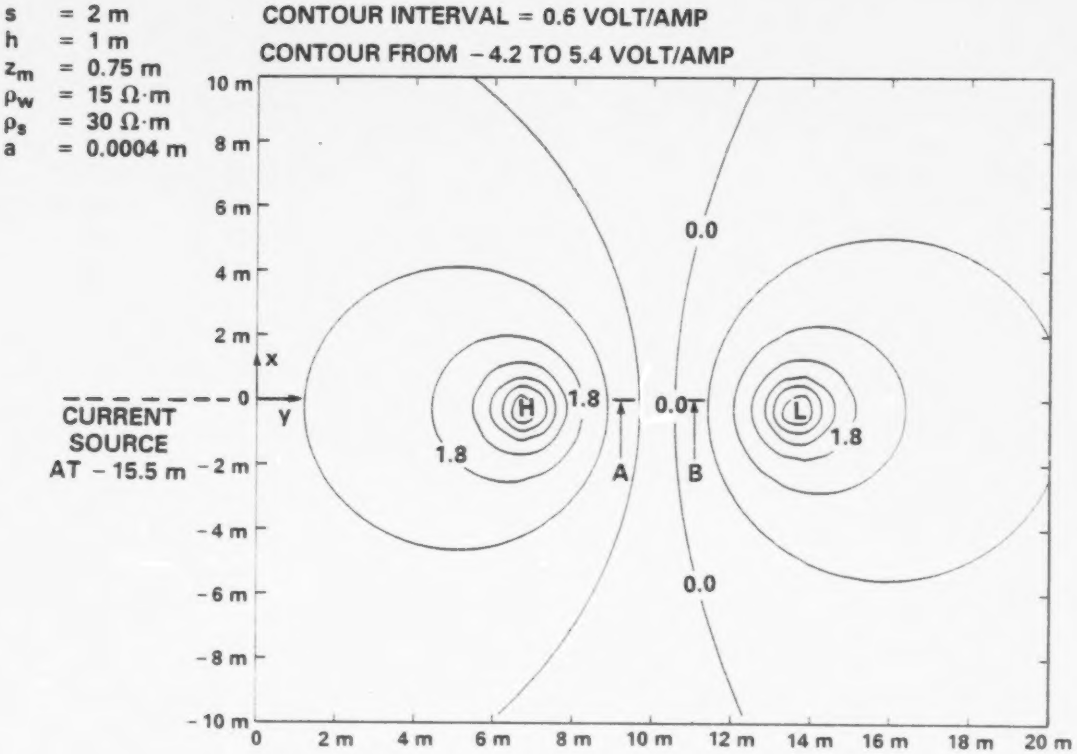

Figure 20. Potential contour plot for two identical leaks of radius a for a pole-dipole electrical survey conducted at a depth of 75 cm. The separation between the leaks is 2 m and the the detector dipole spacing is s = 2 m.

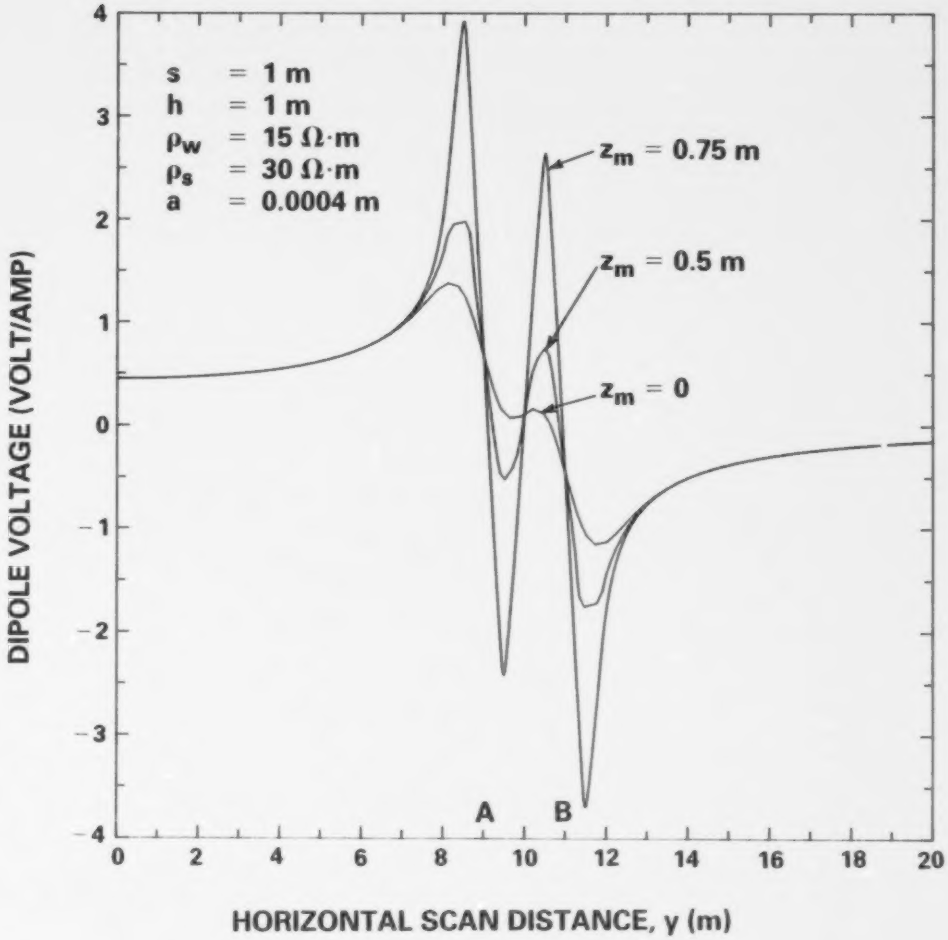

Figure 21. Potential profiles measured over two leaks of radius a for electrical surveys conducted at the surface and at depths of 50 cm and 75 cm. The leak centers are located in the liner at positions A and B corresponding to y_c = 9 m, respectively, in the plane x = 0. The horizontal detector dipole spacing is s = 1 m.

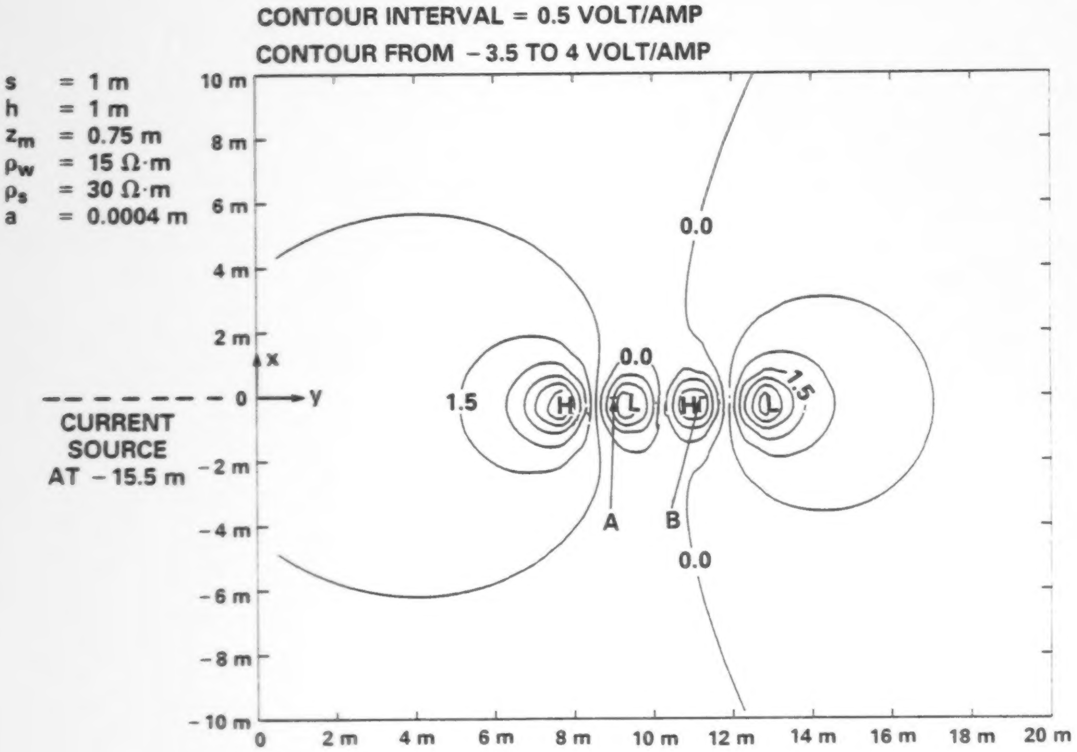

Figure 22. Potential contour plot for two identical leaks of radius a for a pole-dipole electrical survey conducted at a depth of 75 cm. The separation between the leaks is 2 m and the detector dipole spacing is s = 1 m.

The results of this electrical leak detection model study demonstrate the practical application of the model in predicting pole-dipole leak responses in hazardous waste impoundments and for predicting leak signatures associated with the integrity of the geomembrane liners. Parametric curves computed using the modeling program can be used for planning optimum electrical surveys for a wide range of field conditions depending upon the impoundment depth and the resistivity of the waste material. Thus, the surface or subsurface data acquisition depth and the dipole detector spacing can be determined to obtain optimum leak detection results.

The computed leak responses point out the practical importance of performing the survey measurements near the bottom of the impoundment in order to enhance the anomaly. The results also indicate that the dipole detector spacing must be less than the leak separation to improve leak resolution. The injected current must be increased to offset the effect of lower measured leak anomaly attributed to lower resistivity of the liquid. Finally, the results indicate that practical electrical surveys associated with the geomembrane liner integrity may be improved by using a vertical dipole detector.

SECTION 6

DOUBLE LINER MODEL TESTS

BACKGROUND

Double-lined facilities are required to meet EPA minimum technology standards for hazardous waste impoundments. By placing the current return electrode in electrical contact with the liquid-saturated drainage layer located between the two liners, the electrical leak location method is applicable for detecting and locating leaks in the upper liner. Simple electrical continuity tests between the drainage layer and the earth can be used to determine the existence of a significant leak in the bottom liner, but not the location of that leak.

OBJECTIVE

The objective of this task was to economically assess the performance of the electrical leak location method for detecting and locating leaks in the top liner of double liner systems. The double liner model tests evaluated the method with drainage layers comprised of various combinations of geotextile, geonet, and soil; with various types and sizes of leaks; and with a protective cover.

RESEARCH APPROACH

Initial Feasibility Demonstration Tests

Test Procedures--

Initial tests were conducted using a small-scale model equipped with two liners with a sand layer between them. Figure 23 shows the construction details and model layout. The 3 m × 3 m frame for the model was constructed with lumber reinforced with wooden stakes located around the perimeter of the frame. A bed of sandy loam was packed inside the frame and a 0.91-mm (36-mil) chlorosulfonated polyethylene (CSPE) liner was installed over the sandy loam. A 100-mm layer of sandy loam drainage layer was compacted over the bottom liner, and five simulated leaks, constructed from 16-gauge wire with 6 mm of insulation stripped from the ends, were placed in the soil cover. The simulated leaks were used instead of actual leaks to allow testing for leaks in many locations without disassembling and reconstructing the model. A second layer of 0.91-mm (36-mil) CSPE geomembrane was installed over the drainage layer. A sixth simulated leak was positioned over the top liner. The positions of the leaks are shown in Figure 24.

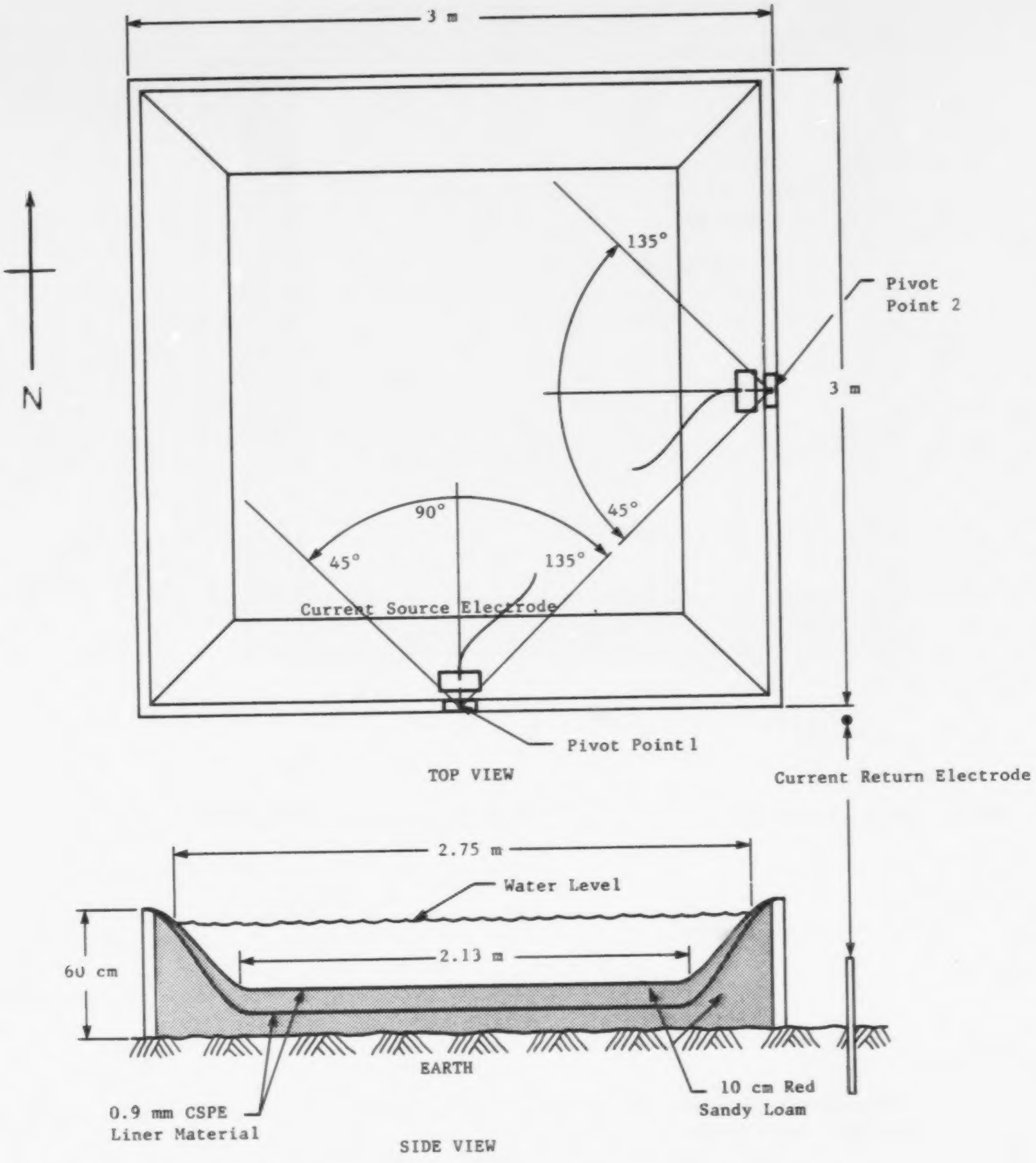
3 m
3 m
N
135°
Pivot Point 2
90°
45°
45°
135°
Current Source Electrode
Pivot Point 1
TOP VIEW
Current Return Electrode
2.75 m
Water Level
60 cm
2.13 m
EARTH
10 cm Red Sandy Loam
0.9 mm CSPE Liner Material
SIDE VIEW

Figure 23. Double-lined model construction detail.

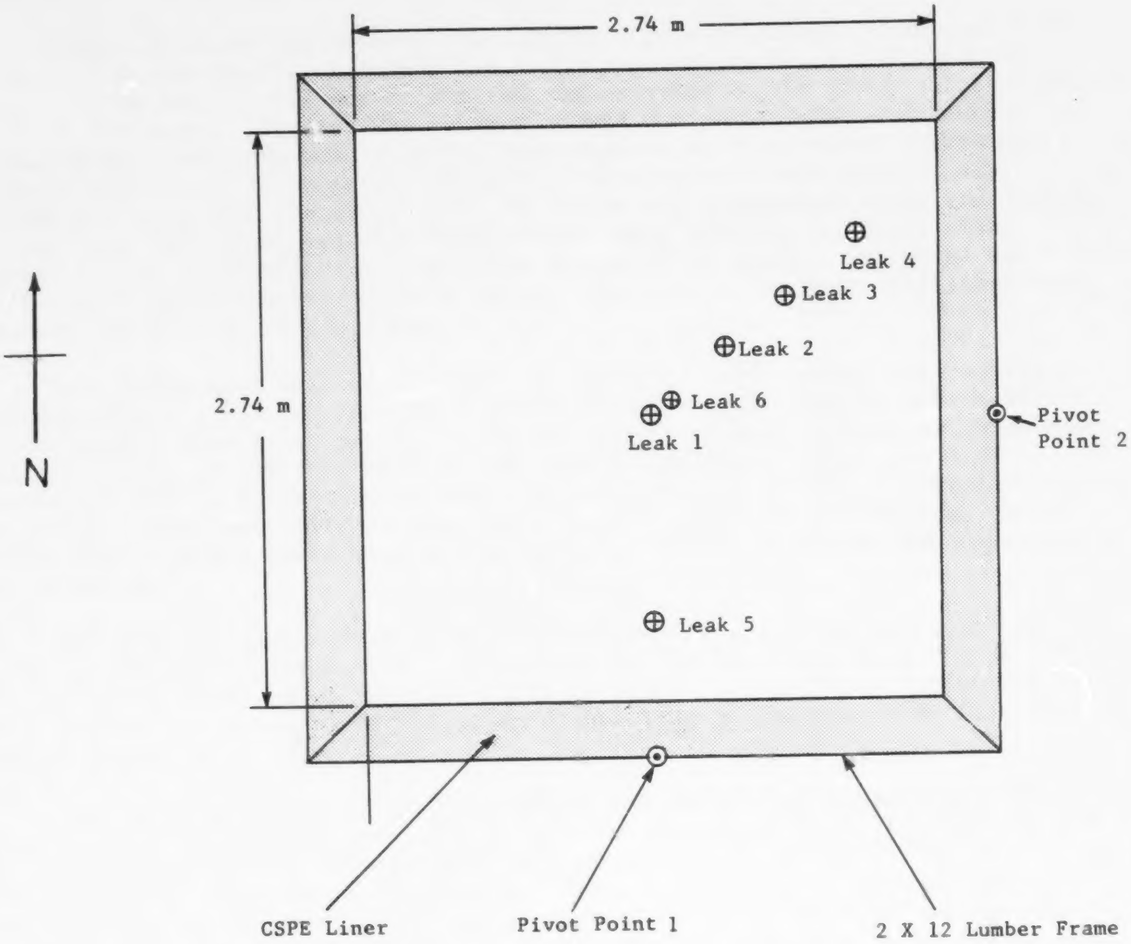
2.74 m
2.74 m
N
Leak 4
Leak 3
Leak 2
Leak 6
Leak 1
Pivot Point 2
Leak 5
CSPE Liner
Pivot Point 1
2 X 12 Lumber Frame

Figure 24. Plan view of the double-lined model showing simulated leak positions. Leak 6 is above the top liner. Leaks 1-5 are in the sand layer below the top liner.

A moveable dipole electrode pair was attached to a fiberglass rod fixed at one of two pivot points located at the center of the south and east sides of the model frame. The dipole pair can be moved along marked radial lines from 45 degrees to 135 degrees for each pivot point.

Figure 25 shows the construction of the dipole electrode probe used for potential measurements. A fiberglass rod supported two brass rod electrodes spaced 76 mm apart. One end of the rod was attached to the pivot point on the side of the model. The rod was rotated around the pivot point. Potential measurement scans were made with the rod oriented at five degree increments from 45 degrees to 135 degrees. Potential measurements were made at any radial distance from the pivot point by moving the electrodes along the length of the rod. Potential gradient measurements were taken 15 mm apart along radial survey lines with the electrodes spaced 76 mm apart. The model was filled with approximately 42 cm of water. The electrodes were positioned just beneath the surface of the water.

The liners were checked for leaks by applying a DC voltage between the current return electrode located in earth ground and the current source electrode located near pivot point 1. The equivalent circuit resistance, measured using voltages of 50, 100, and 200 VDC, was 5.0 megohms. This amount of resistance can be attributed to the finite resistivity of the liner material. Therefore, this test verified that there were no leaks in the liners. Subsequent leak location tests were conducted using 40 VDC to reduce the electrical shock hazard.

The physical model provided the flexibility to study the leak configurations of interest. These were: (1) a leak in the top liner only; (2) a leak in the bottom liner only; and (3) a leak in both liners. These conditions were created in the model by selective connections of the simulated leaks and return electrode.

The first condition of interest was a leak in the top liner only. To simulate this condition, simulated leak 6 was connected to an electrode in the sand layer between the two liners. The current return electrode was placed in the sand layer between the two liners. These connections eliminated the bottom liner and base soil from the electrical circuit. Voltage was applied across the top liner. The simulated leak served as a current shunt across the top liner.

The second condition of interest was a leak in the bottom liner only. To set up this condition, simulated leak 1 (located in the sand drainage layer) was connected to earth ground, the current return electrode was connected to earth ground, and the current source was positioned in the water above the top liner.

The third condition of interest was leaks in the top and bottom liners. Simulated leak 6, above the top liner, was connected to an electrode in the drainage layer. Simulated leak 1, in the drainage layer, was connected to earth ground. The current source electrode remained positioned in the water above the top liner and the current return electrode was grounded to the earth.

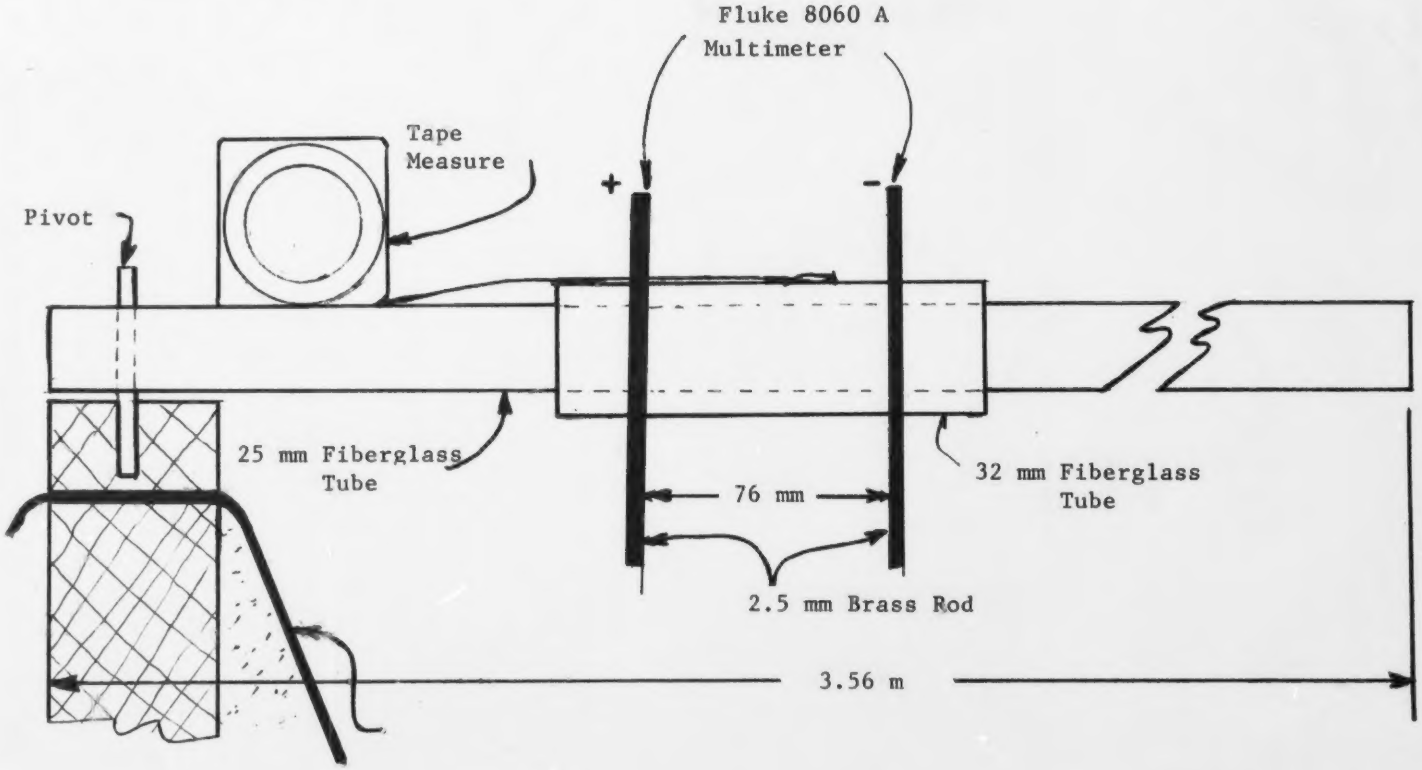
Fluke 8060 A
Multimeter
Tape
Measure
Pivot
+
-
25 mm Fiberglass
Tube
76 mm
32 mm Fiberglass
Tube
2.5 mm Brass Rod
3.56 m

Figure 25. Construction details of the dipole probe used for double-lined model.

Contour plots of the data were generated using the NCAR CONRAC computer software. Contour plots of the data were useful for interpreting the data. These plots are particularly useful for data with low noise. However, for noisy data, particularly with low frequency spatial noise, the contour plots are not as useful as a raster display of adjacent lines of data. Because of the spatial interpolation, spatial filtering, and spline curve fits of the data needed for producing realistic contour plots, the contour maps do not exactly conform to the data. Therefore, the scaling of distances from the contour maps can be unreliable. In some instances, the peaks of the anomalies in the data for the double liner tests plot with a greater separation than that indicated in the data for the survey line directly over the leak.

Results of Tests--

Test with simulated leak in top liner--Figures 26 and 27 show the potential gradient contour plots of the double-lined model data taken with a simulated leak in the top liner. A DC power supply was used to apply 40 volts across the top liner. The current flow was 21 mA. Figure 26 is a contour plot of data taken using pivot point 1. To confirm the results, the experiment was repeated with the pivot point and current source electrode moved to the adjacent edge of the test model. Figure 27 is the contour plot of the data taken using pivot point 2.

The measured anomalous response due to the simulated leak is the characteristic adjacent peaks of opposite polarity. The location of the simulated leak is approximately midway between the positive and negative peaks. Figures 28 and 29 are unscaled plots of the potential gradient measurements along the survey line that passes over the leak from pivot points 1 and 2, respectively. The measured voltage gradient decreases as the electrodes approach the leak. In the near vicinity of the leak, the potential decreases rapidly and reverses polarity. Beyond the leak, the potential gradient asymptotically approaches zero. The simulated leak is a current sink with current flowing into it from all directions. The reverse in the polarity indicates a reverse in the direction of the current flow on either side of the leak. These model measurements are as predicted by the computer simulation model.

Results of test with simulated leak in bottom liner--The test model was configured with no leak in the top liner and one of the simulated leaks in the drainage layer grounded to the earth to simulate a leak in the bottom liner. When the current source electrode was placed in the sand layer and the current return electrode grounded, the voltage and current conditions were similar to those in the top liner experiment. Thus, while the location of the leak in the bottom liner cannot be determined by measurements in the water, the current flow through the bottom liner indicated the presence of a leak.

Results of test with simulated leaks in both liners--The simulated leaks were connected to simulate leaks in both the top and bottom liners. A voltage of 40 VDC was connected between electrodes in the water and earth ground. The resultant current was almost identical to the current with a simulated leak in the top liner only. Potential measurements taken with the electrode pair on the surface of the water indicated approximately the same current distribution

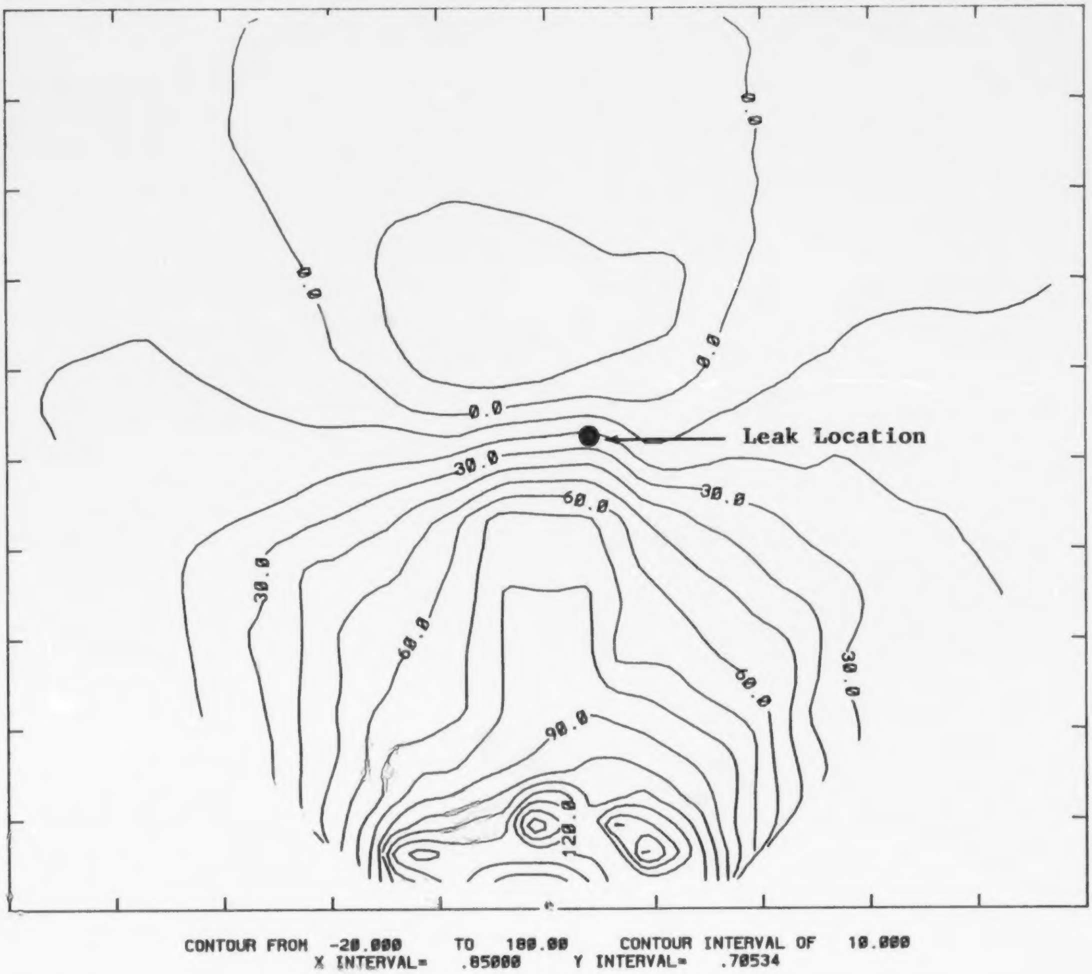

Figure 26. Contour plot of potential gradient data for simulated leak in top liner of double-liner model. Data taken using pivot point 1.

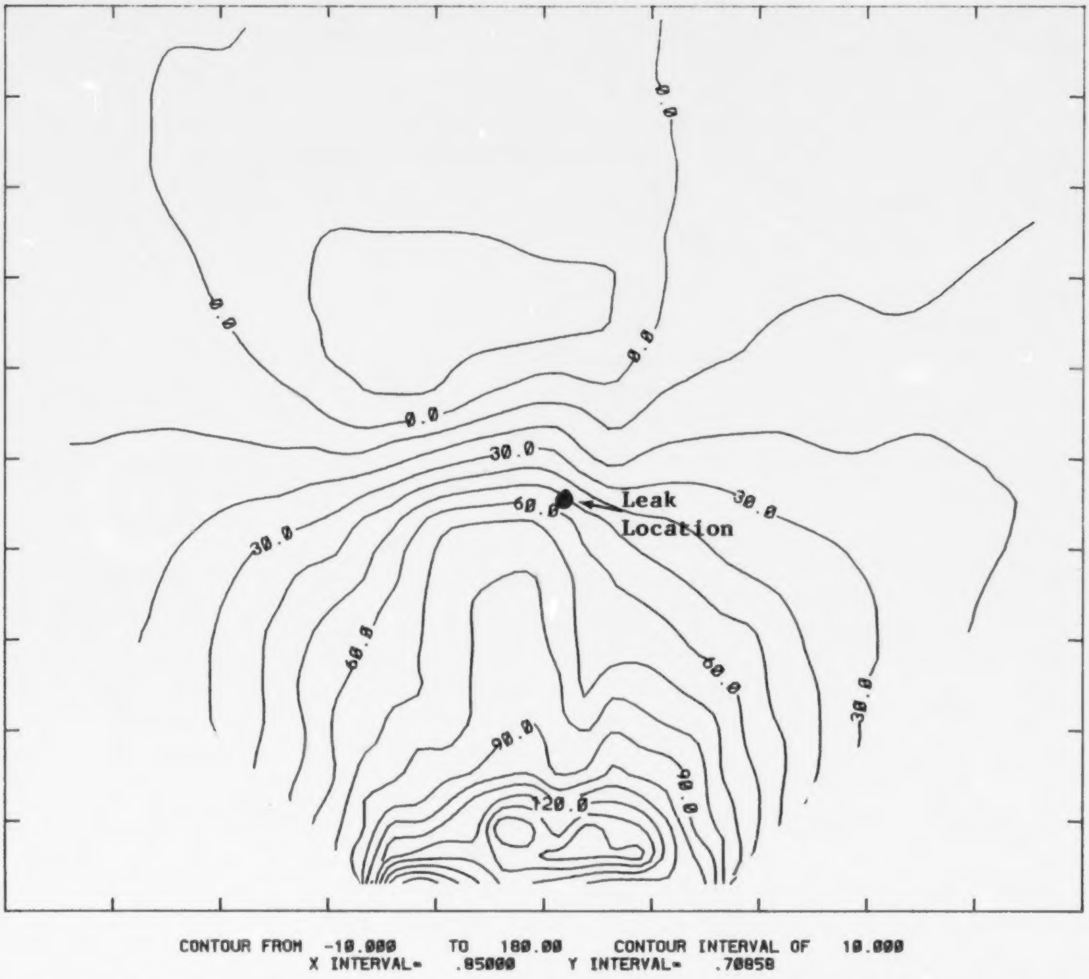

Figure 27. Contour plot of potential gradient data for simulated leak in top liner of double-liner model. Data taken using pivot point 2.

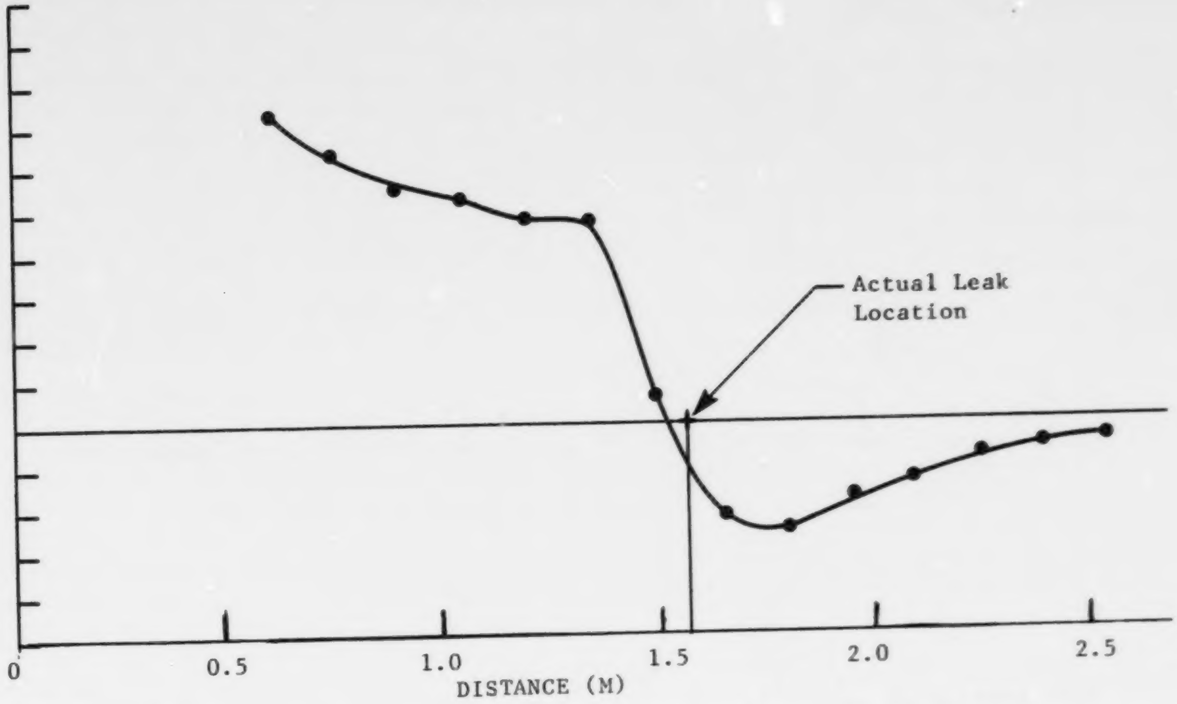

Figure 28. Plot of potential measurements from pivot point 1 along the 95 degree survey line.

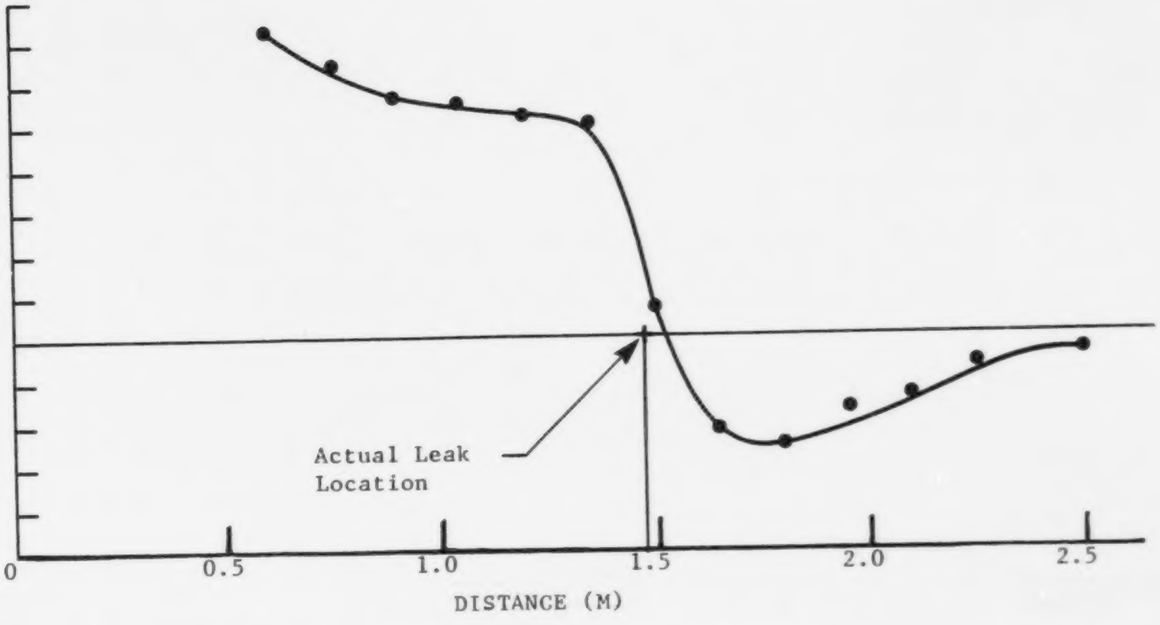

Figure 29. Plot of potential measurements from pivot point 2 along the 90 degree radial line.

as with the single leak in the top liner. The simulated leak in the bottom liner provided a current path between the water in the model and the earth ground. Several tests using different simulated leak locations in the bottom liner did not influence the test results. Thus, the location of the leak in the bottom liner did not influence the top liner leak signature. These results indicate the electrical leak location method can be used to detect and locate a leak in the top liner and only detect a leak in the bottom liner.

Tests with Various Drainage Layers, Leak Size, Leak Geometry, and Protective Covers

Test Procedures--

Additional studies were conducted on the double liner model having dimensions of 3 m × 3 m to test the electrical leak location method for locating leaks with various impoundment configurations including various types of drainage layers, various types of leaks, and a protective soil cover over the primary liner. A computer data acquisition system was used to collect potential gradient data on a rectilinear grid. Data were stored on flexible disk for computer analysis.

A test fixture was used to position the potential electrodes at a constant depth as close as possible to the liner. The potential electrodes were insulated metal rods with a diameter of 1.6 mm, with the last 25 mm of the rod exposed. A potential electrode spacing of 76 mm was used. The electrode support bar was equipped with a microswitch activated by pegs (spaced fixed distances apart) to provide an indication of the electrode position as the electrodes traversed the model. The support bar was modified for collecting data along parallel scan lines.

Drainage layers were configured using various combinations of geotextile, geonet, and sandy loam for the drainage layer. The geotextile was Hoechst non-woven Trevira Spunbond mat with a thickness of 0.38 mm (150 mil). The geonet was Tensar DN-1, square grid net, approximately 5-mm (200-mil) thick. A layer of sandy loam with a thickness of 38 mm simulated a soil drainage layer material. Actual leaks were used instead of simulated leaks. A circular leak with a diameter of 5.1 mm was used. Selected tests were repeated with larger circular leaks and with leaks of other geometries to simulate slits and defective seams. Another test was conducted with various thicknesses of protective sandy loam soil layers over the liner.

Results of Tests--

Results of tests with various drainage layers--Figure 30 is a contour plot of the data taken with a geotextile mat drainage layer. The location of the leak is clearly indicated by the dipolar contour pattern. The peak-to-peak anomaly caused by the leak is 50 volts per ampere. No other anomalies are present in the data.

Figure 31 is a contour plot of the data taken with a drainage layer consisting of geotextile mat placed over geonet. Again, the location of the leak is clearly indicated by the dipolar contour pattern. The peak-to-peak anomaly

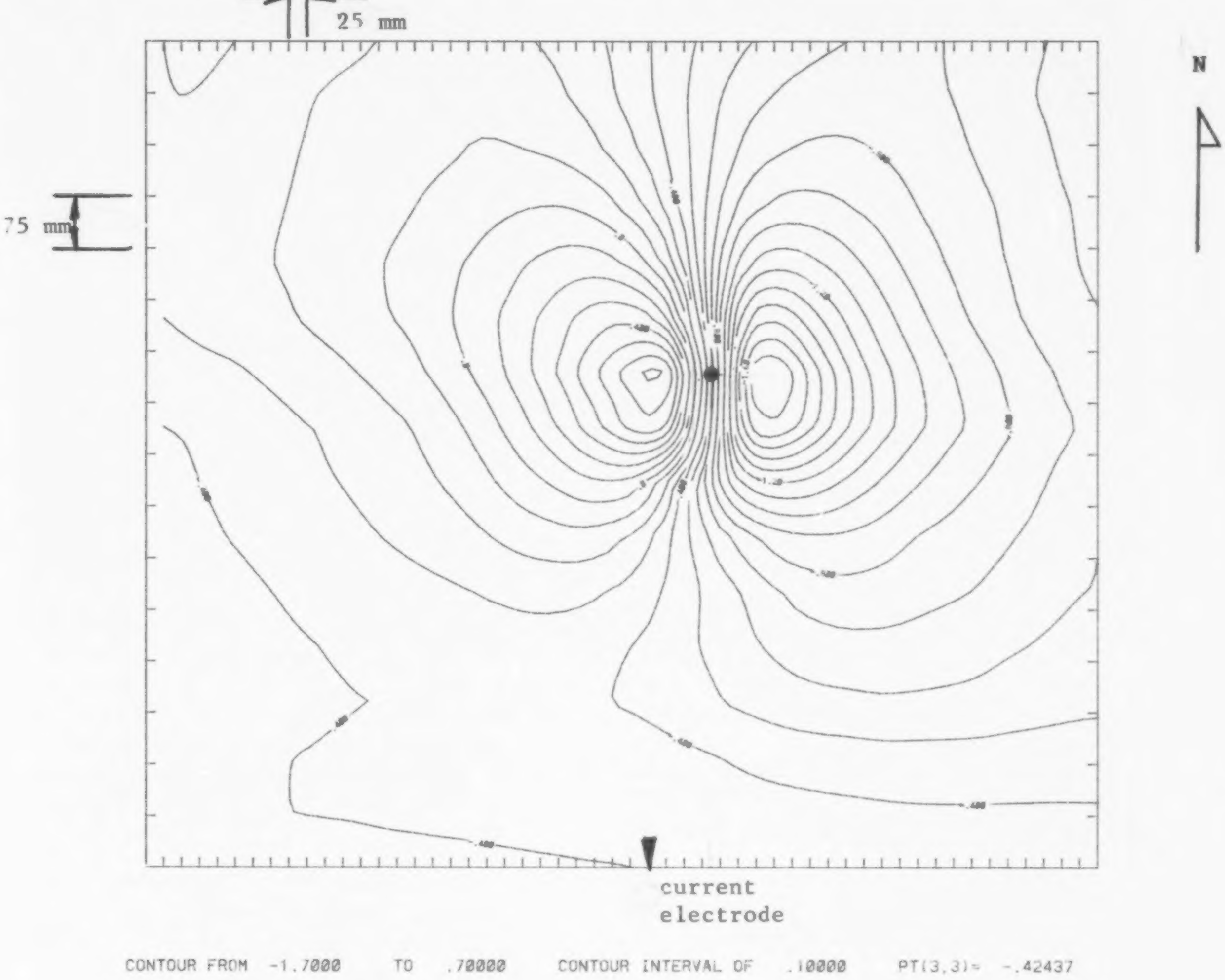

● ● ⟶ Potential Electrode Orientation and Scan Direction
Potential Electrode Separation = 76 mm
Potential Electrode Depth = 51 mm
Water Depth = 76 mm
Current = 9 mA
Voltage = 80 V
Leak Anomaly 0.45 V p-p
Drainage Layer: Geotextile

Figure 30. Contour plot of the double liner model data taken with a 5.1 mm diameter leak with a geotextile mat drainage layer.

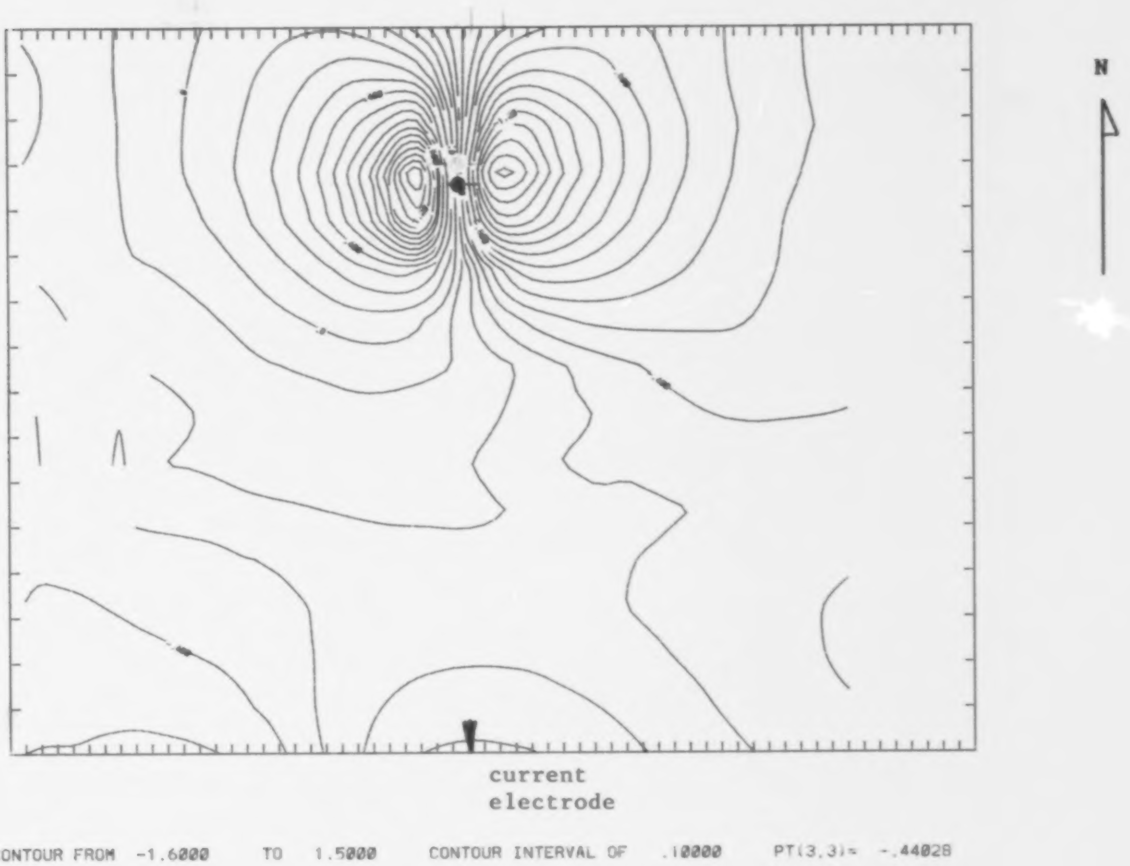

● ● ⟶ Potential Electrode Orientation and Scan Direction
Potential Electrode Separation = 76 mm
Potential Electrode Depth = 51 mm
Water Depth = 75 mm
Current = 8 mA
Voltage = 80 V
Leak Anomaly: 0.68 V p-p
Drainage Layer: Geotextile and Geonet

Figure 31. Contour plot of the double liner model data taken with a 5.1 mm diameter leak with a drainage layer consisting of a geotextile mat placed over geonet.

caused by the leak is 85 volts per ampere. No other anomalies are present in the data.

Figure 32 is a contour plot of the data for a drainage layer consisting of a sandy loam soil layer placed over geotextile mat which is placed over the geonet material. The location of the leak is again clearly indicated by the dipolar contour pattern. The peak-to-peak anomaly caused by the leak is approximately 50 volts per ampere. The potential gradient pattern caused by the current injection electrode is also evident in the data. The characteristic of the anomaly caused by the current injection electrode is clearly different from the anomaly caused by a leak.

Results of tests with various leak sizes and geometries--Figure 33 is a contour plot of the data taken with a drainage layer consisting of a sandy loam soil layer placed over geotextile mat which is placed over the geonet material with a leak diameter of 25 mm. A comparison of Figures 32 and 33 indicates the anomalies caused by leaks with diameters of 5.1 mm and 25 mm are very similar. The leak with a diameter of 25 mm produced a peak-to-peak anomaly of 54.4 volts per ampere. As expected, the larger leak required less voltage to produce the current. An anomalous indication in the southeast corner of the model may have been due to a single wild data point.

Figure 34 is a contour plot of the data taken with a slit with a length of 15 cm cut in the top liner. The potential scans were parallel to the slit. The drainage layer consisted of a sandy loam soil layer placed over a geotextile mat which was placed over a geonet material. Again, the location of the leak is clearly indicated by the dipolar contour pattern. The peak-to-peak anomaly caused by the leak is 67.8 volts per ampere. The characteristic of the anomaly caused by the slit is very similar to the anomaly caused by a circular hole.

Figure 35 is a contour plot of the data taken with a slit with a length of 15 cm cut in the top liner with the potential scans taken perpendicular to the slit. The dipolar contour pattern with the survey lines perpendicular to the leak is very similar to the pattern produced with the survey taken parallel to the leak. Of course, the orientation of the dipolar pattern is rotated 90 degrees. The peak-to-peak anomaly caused by the leak is 44.4 volts per ampere.

Figure 36 is a contour plot of the data taken with a simulated section of a faulty seam. The faulty seam was simulated by partially patching the 15-cm long slit by seaming the patch on only three sides. The potential scans were parallel to the slit. The drainage layer consisted of a sandy loam soil layer placed over a geotextile mat which was placed over a geonet material. The anomalous dipolar pattern due to the leak is indicated clearly. The peak-to-peak anomaly caused by the leak is 78.5 volts per ampere. Another anomalous indication at the eastern edge of the model probably is due to a wild data point.

Results of test with leaks in both liners--Figure 37 is a contour plot of the data taken with leaks with diameters of 5 mm in the top liner and the bottom liner. The current return electrode was placed in the earth outside

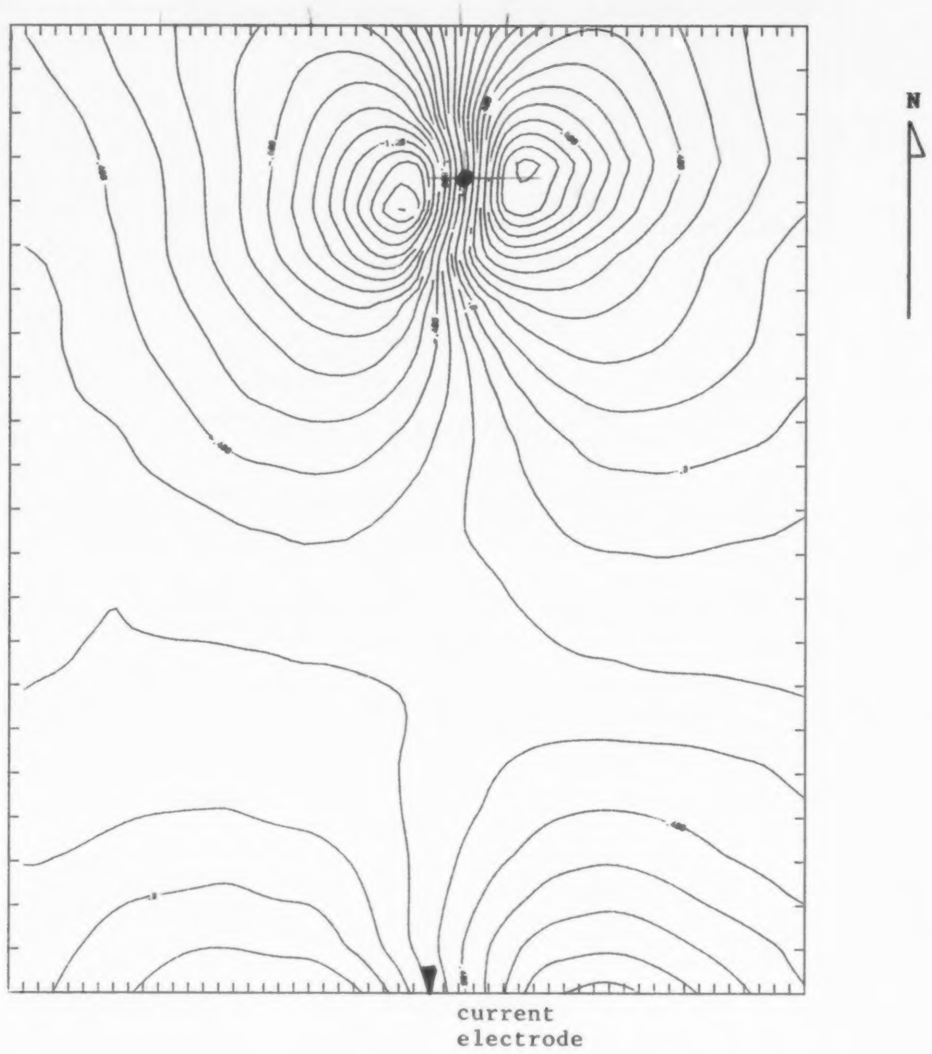

CONTOUR FROM -1.6000 TO 1.1000 CONTOUR INTERVAL OF .10000 PT(3,3)= -.65874E-01

● ● ——► Potential Electrode Orientation and Scan Direction
Potential Electrode Separation = 76 mm
Potential Electrode Depth = 51 mm
Water Depth = 76 mm
Current = 9 mA
Voltage = 50 V
Leak Anomaly: 0.44 V p-p
Drainage Layer: Geotextile and Geonet + 38 mm sandy loam

Figure 32. Contour plot of the double liner model data taken with a 5.1 mm diameter leak with a drainage layer consisting of a sandy loam soil layer placed over geotextile mat which is placed over geonet.

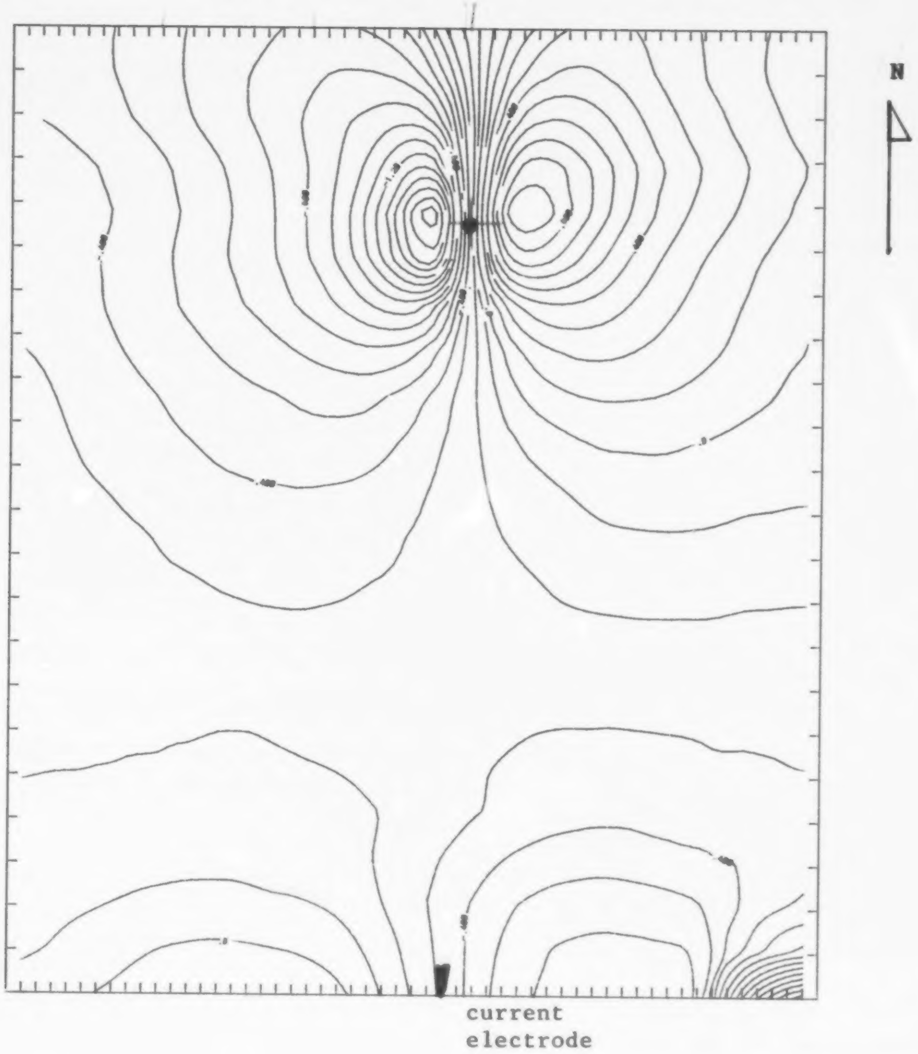

CONTOUR FROM -1.7000 TO .90000 CONTOUR INTERVAL OF .10000 PT(3,3)= -.13356

● ● → Potential Electrode Orientation and Scan Direction
Potential Electrode Separation = 76 mm
Potential Electrode Depth = 51 mm
Water Depth = 76 mm
Current = 9 mA
Voltage = 24 V
Leak Anomaly: 0.49 V p-p
Drainage Layer: Geotextile, Geonet + 38 mm sandy loam

Figure 33. Contour plot of the double liner model data taken with a 25 mm diameter leak with a drainage layer consisting of a sandy loam soil layer placed over geotextile mat which is placed over geonet.

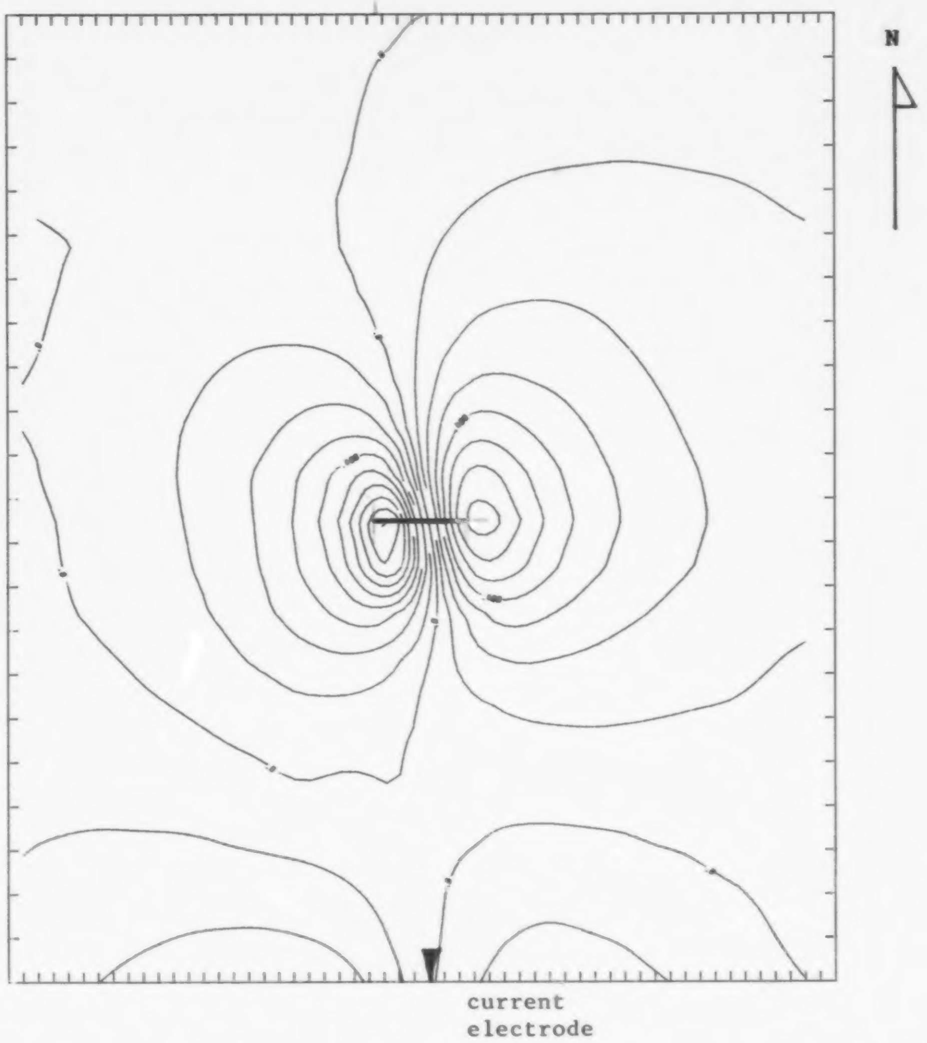

CONTOUR FROM -1.8000 TO 1.4000 CONTOUR INTERVAL OF .20000 PT(3,3)= .25025

● ● ⟶ Potential Electrode Orientation and Scan Direction
Potential Electrode Separation = 76 mm
Potential Electrode Depth = 51 mm
Water Depth = 76 mm
Current = 9 mA
Voltage = 19 V
Leak Anomaly: 0.61 V p-p
Drainage Layer: Geotextile, Geonet, and 38 mm sandy loam

Figure 34. Contour plot of the double liner model data taken with a 15 cm long slit cut in the top liner with the potential scans parallel to the slit.

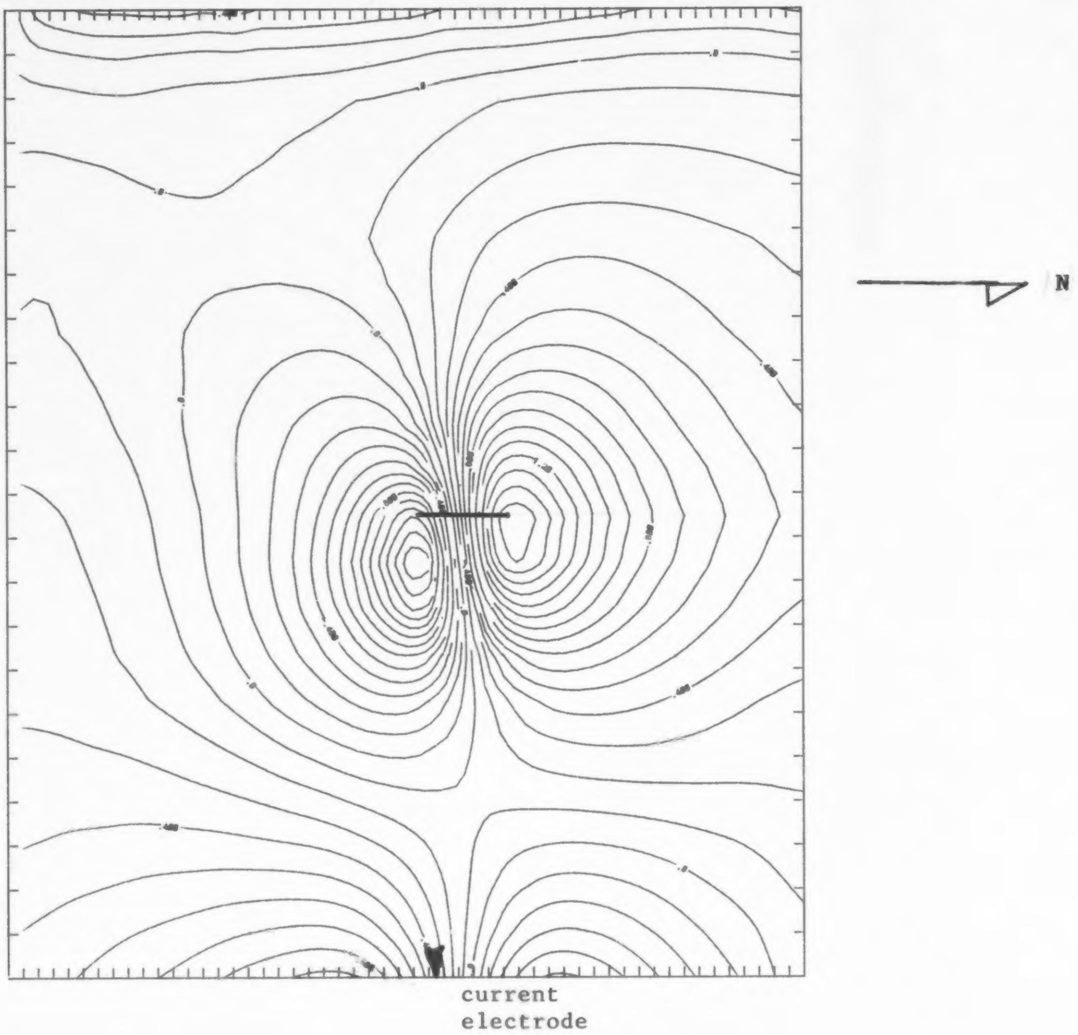

```
CONTOUR FROM  -1.4000     TO   1.5000     CONTOUR INTERVAL OF    .10000     PT(3,3)=   .46876
```

● ● ⟶ Potential Electrode Orientation and Scan Direction
Potential Electrode Separation = 76 mm
Potential Electrode Depth = 51 mm
Water Depth = 76 mm
Current = 9 mA
Voltage = 26 V
Leak Anomaly = 0.38 V p-p
Drainage Layer = Geotextile, Geonet, and 38 mm sandy loam

Figure 35. Contour plot of the double liner model data taken with a 15 cm long slit cut in the top liner with the potential scans perpendicular to the slit.

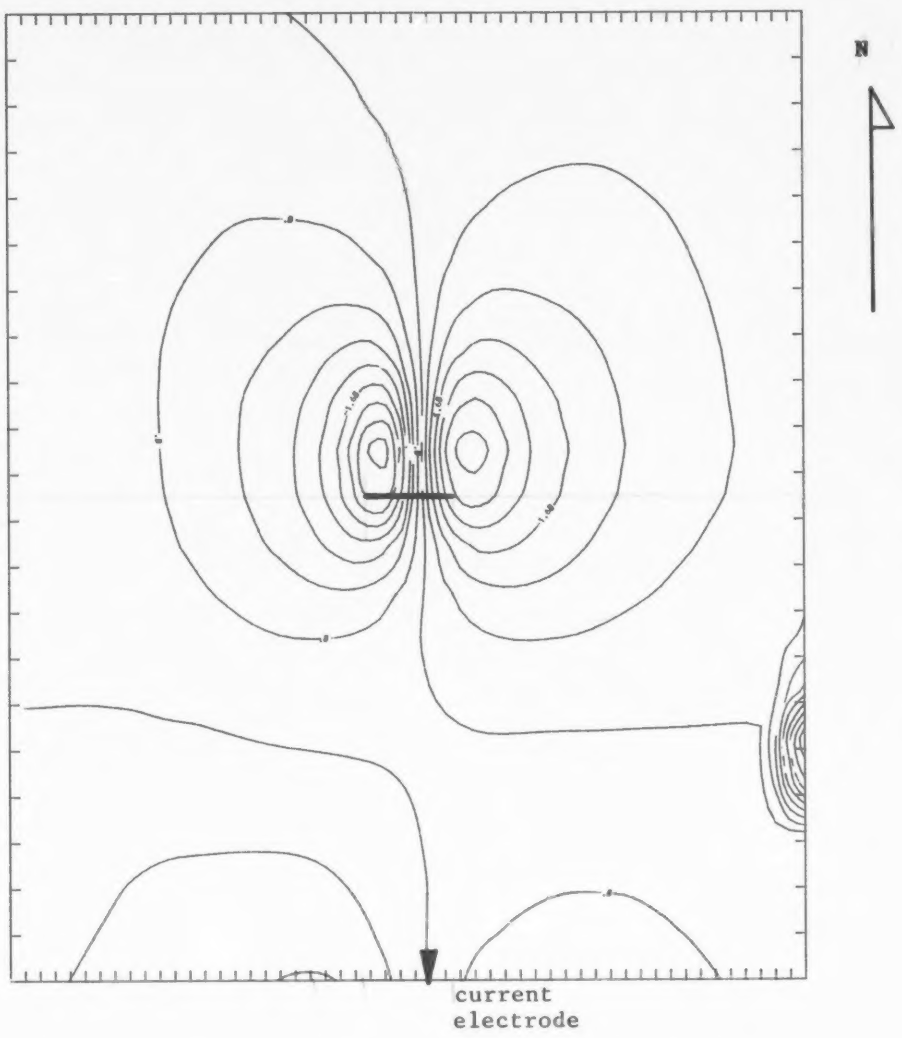

CONTOUR FROM -2.8000 TO 4.0000 CONTOUR INTERVAL OF .40000 PT(3,3)= .65562

● ● ⟶ Potential Electrode Orientation and Scan Direction
Potential Electrode Separation = 76 mm
Potential Electrode Depth = 51 mm
Water Depth = 76 mm
Current = 13 mA
Voltage = 45 V
Leak Anomaly = 1.02 V p-p
Drainage Layer = Geotextile, Geonet, and 38 mm sandy loam

Figure 36. Contour plot of the double liner model data taken with a simulated section of a faulty seam with the potential scan parallel to the slit.

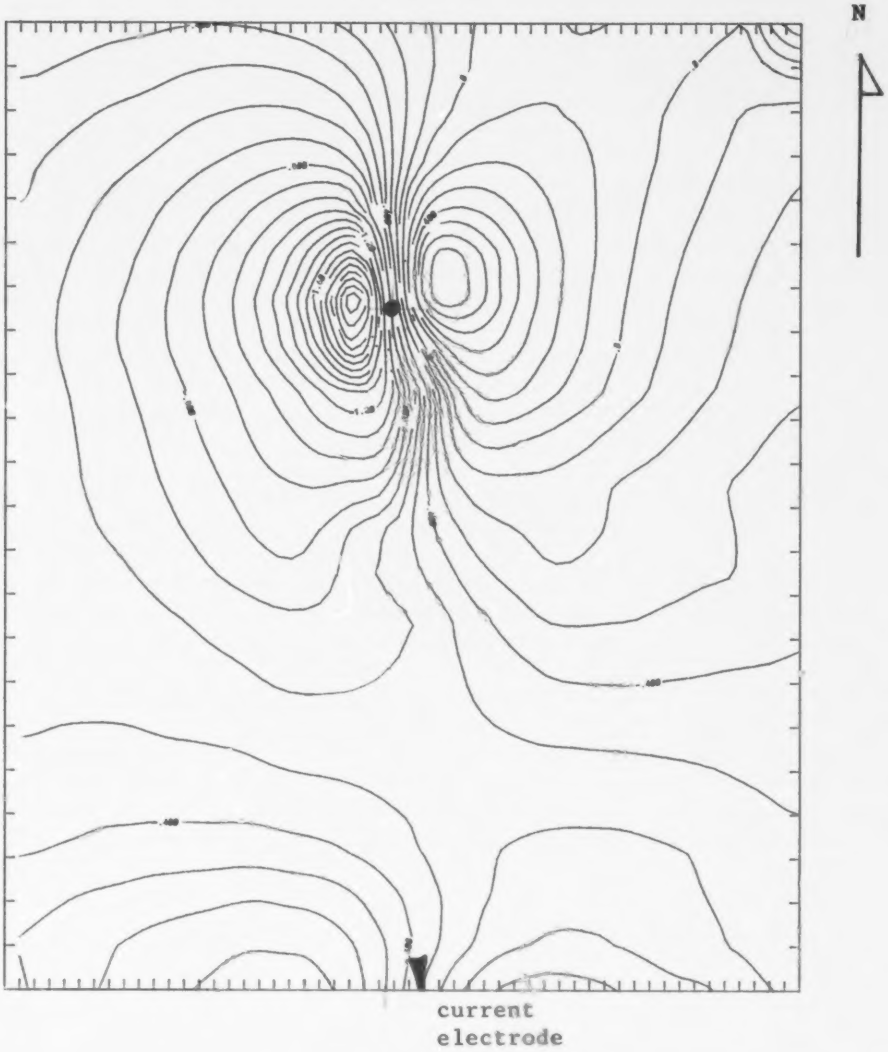

CONTOUR FROM -2.3000 TO .70000 CONTOUR INTERVAL OF .10000 PT(3,3)= -.32105

● ● ⟶ Potential Electrode Orientation and Scan Direction
Potential Electrode Separation = 76 mm
Potential Electrode Depth = 51 mm
Water Depth = 76 mm
Current = 9 mA
Voltage = 80 V
Leak Anomaly = 0.51 V p-p
Drainage Layer = Geotextile, Geonet, and 38 mm sandy loam

Figure 37. Contour plot of the double liner model data taken with leaks with diameters of 5 mm in the top liner and the bottom liner and the current return electrode in the earth outside the model.

the model. The drainage layer consisted of a sandy loam soil layer placed over a geotextile mat which was placed over a geonet material. The anomalous dipolar pattern due to the leak is clearly indicated. The peak-to-peak anomaly caused by the leak is 56.7 volts per ampere.

Results of tests with protective cover on the liner--Figure 38 is a contour plot of the data taken with a protective soil cover with a thickness of 25 mm placed over the geomembrane liner. The drainage layer consisted of a sandy loam soil layer placed over a geotextile mat which was placed over the geonet material. The location of the leak can be determined from the contour data, but the dipolar pattern is weaker than that for the previous tests. The peak-to-peak anomaly caused by the leak is 46.7 volts per ampere.

Figure 39 is a contour plot of the data taken with a protective soil cover with a thickness of 15 cm placed over the geomembrane liner. The approximate location of the leak can be determined from the contour data, but the dipolar pattern is even weaker. The peak-to-peak anomaly caused by the leak is 78.9 volts per ampere. Figure 40 shows plots of the data taken on some of the scan lines. Although some noise is present in the data, the characteristic dipolar negative-to-positive transition of the signal is clearly evident in the data. The peak-to-peak amplitude and sharpness of the transition of the anomaly is highest directly over the leak.

Figure 41 is a contour plot of the data taken with a protective soil cover 30 cm thick placed over the geomembrane liner. The location of the leak cannot be determined from the contour plot. Another stronger anomaly is present along the south edge of the model. Figure 42 shows plots of the data taken on the scan lines near the leak. A very broad anomaly with a peak-to-peak amplitude of only 8.9 volts per ampere is present in the scan line directly over the leak. Because the peaks of the anomaly are separated by approximately 43 cm, this anomaly cannot be attributed to the leak. Figure 43 shows the scan data taken in the vicinity of the other anomaly near the south edge of the model. The anomaly in the scan data taken 1 m south of the leak has a peak-to-peak amplitude of 40 volts per ampere and has the characteristics of a leak.

Electrode Material and Type

Test Procedures--

Tests were conducted using various electrodes to determine the best and most practical electrode material for electrical leak location surveys in liquid-filled impoundments. The electrode materials and configurations that were tested included: (1) carbon, (2) stainless steel, (3) glass half-cells (silver-silver chloride half-cell pH electrodes), and (4) guarded stainless steel.

The guarded stainless steel electrodes consisted of stainless steel electrodes enclosed in perforated plastic covers. Plastic practice golf balls were used for the perforated plastic covers. The electrodes were connected to an isolation amplifier. The output of the isolation amplifier was recorded on a calibrated strip chart recorder.

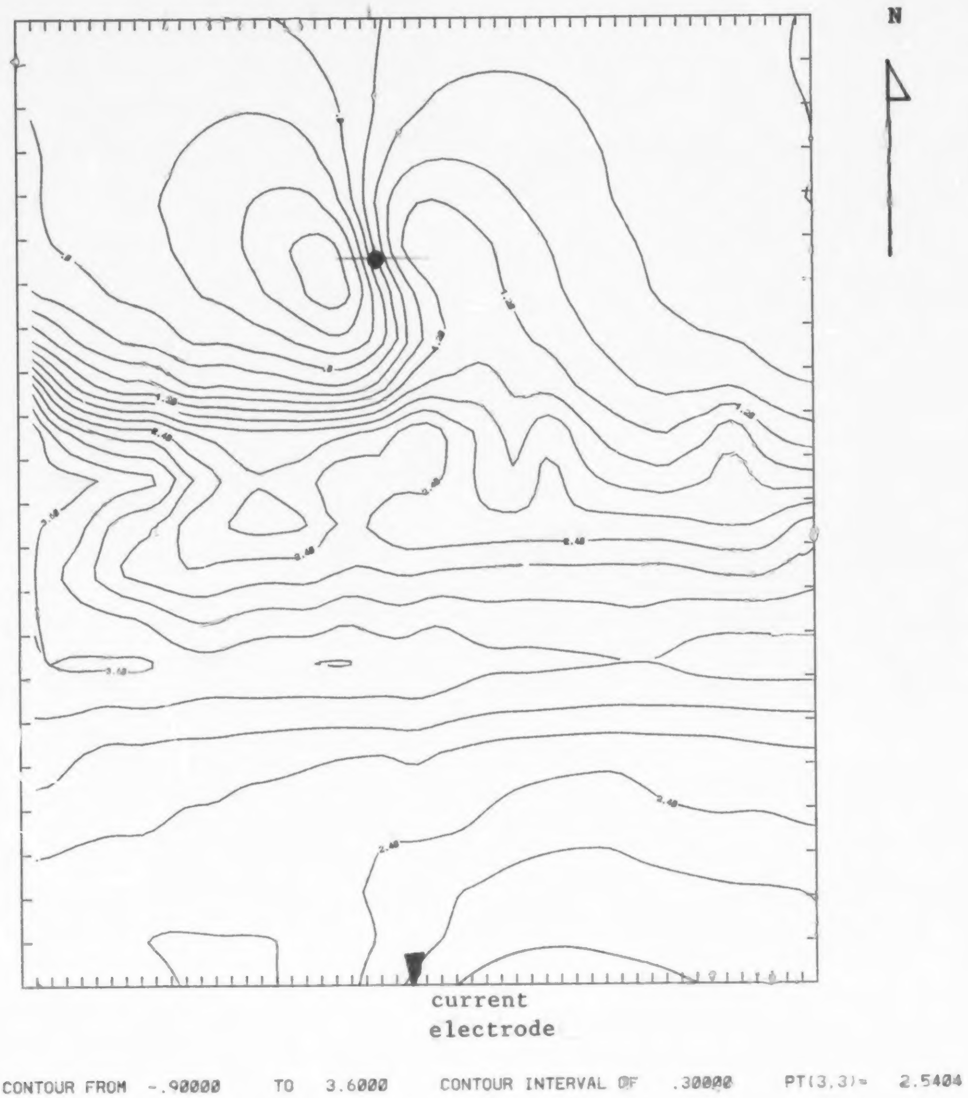

● ● —▶ Potential Electrode Orientation and Scan Direction
Potential Electrode Separation = 76 mm
Potential Electrode Depth = 51 mm
Water Depth = 76 mm
Current = 9 mA
Voltage = 65 V
Leak Anomaly = $0.42\ V_{p-p}$
Drainage Layer = Geotextile, Geonet, and 38 mm sandy loam

Figure 38. Contour plot of the double liner model data taken with a protective soil layer with a thickness of 25 mm placed over the geomembrane liner.

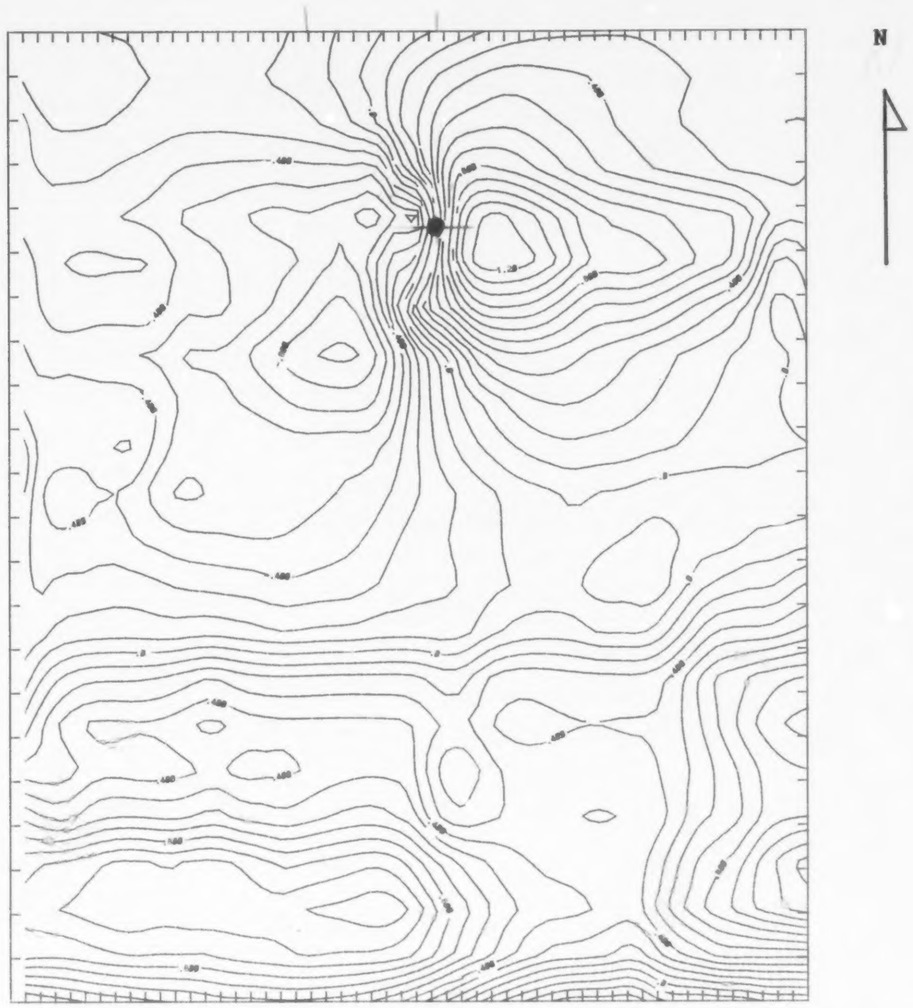

CONTOUR FROM -.90000 TO 1.2000 CONTOUR INTERVAL OF .10000 PT(3,3)= .99655

● ● ⟶ Potential Electrode Orientation and Scan Direction
Potential Electrode Separation = 76 mm
Potential Electrode Depth = 51 mm
Water Depth = 76 mm
Current = 9 mA
Voltage = 65 V
Leak Anomaly = 0.71 V_{p-p}
Drainage Layer = Geotextile, Geonet, and 38 mm sandy loam

Figure 39. Contour plot of the double liner model data taken with a protective soil layer with a thickness of 15 cm placed over the geomembrane liner.

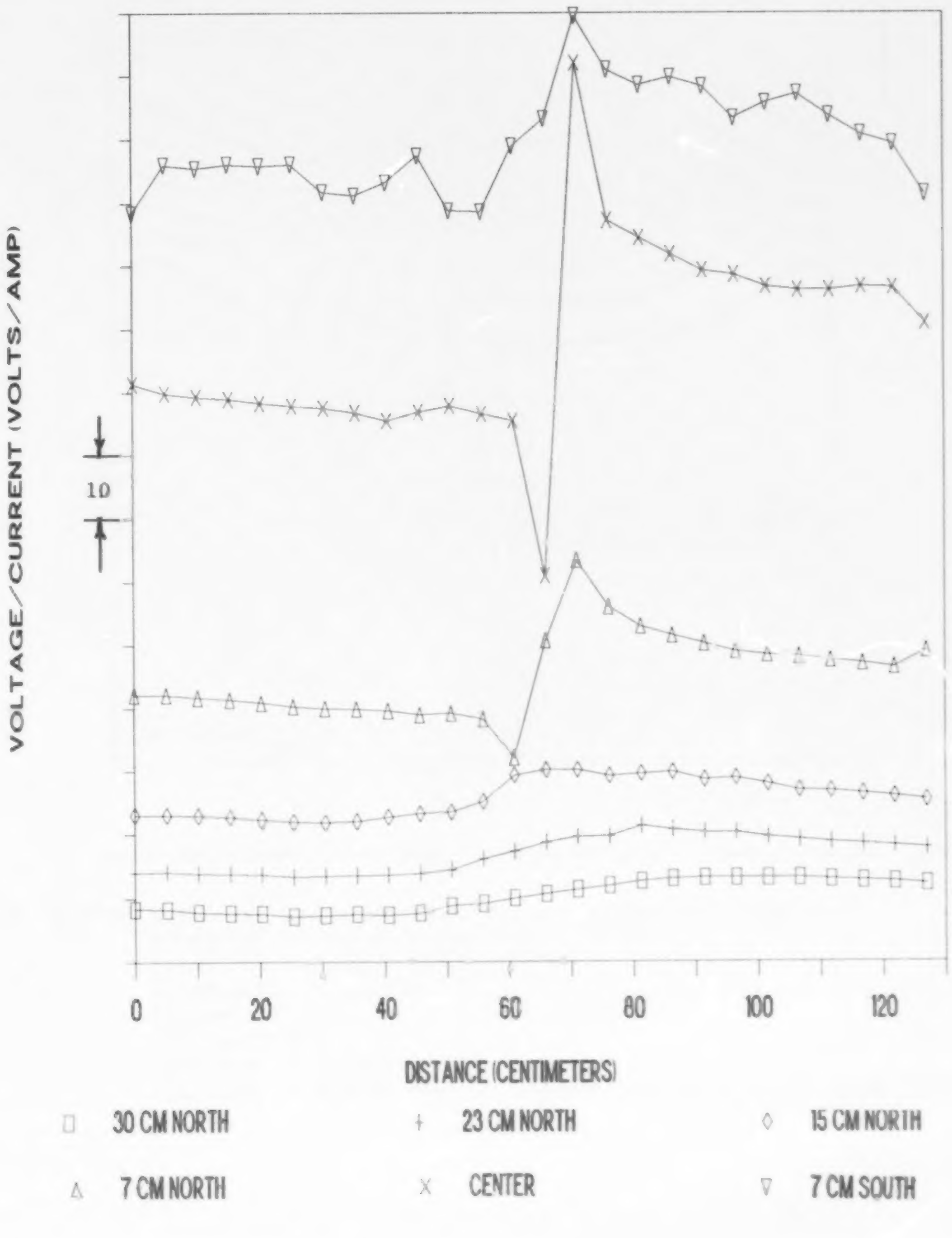

Figure 40. Scan data taken with 15 cm protective soil cover over geomembrane.

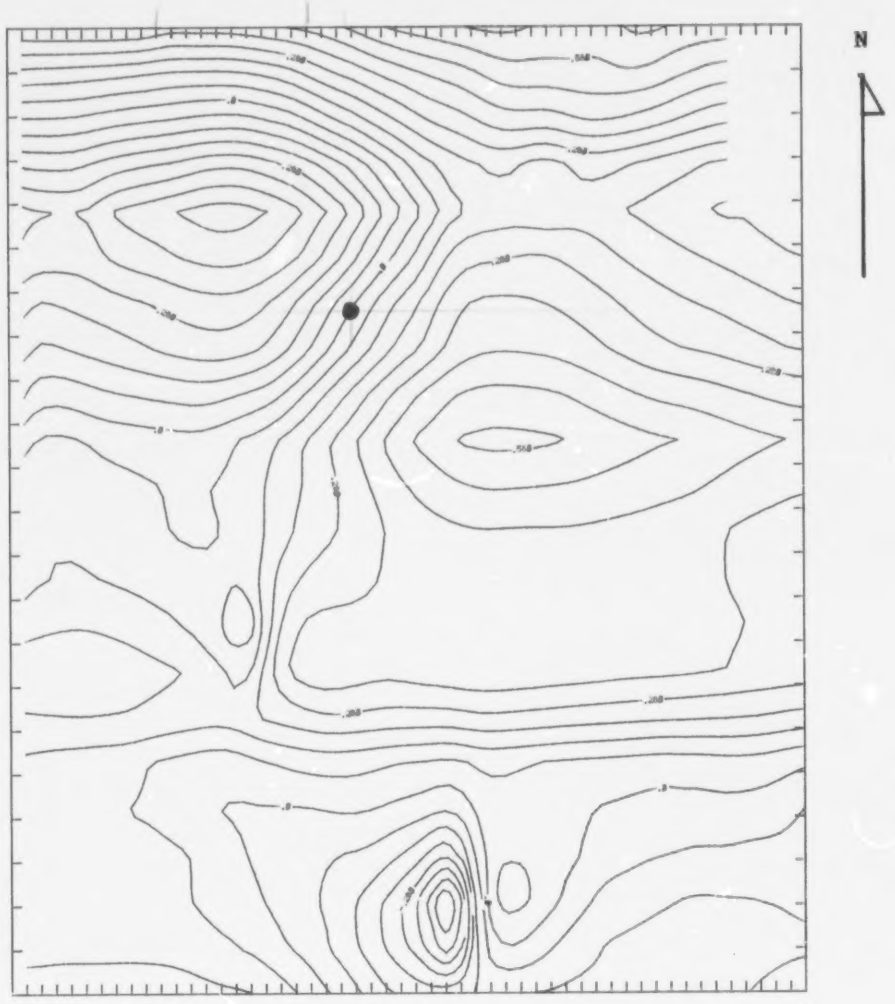

CONTOUR FROM -.56000 TO .63000 CONTOUR INTERVAL OF .70000E-01 PT(3,3)= .12293

● ● ⟶ Potential Electrode Orientation and Scan Direction
Potential Electrode Separation = 76 mm
Potential Electrode Depth = 51 mm
Water Depth = 76 mm
Current = 9 mA
Voltage = 60 V
Leak Anomaly = 0.08 V_{p-p}
Drainage Layer = Geotextile, Geonet, and 38 mm sandy loam

Figure 41. Contour plot of the double liner model data taken with a protective soil layer 30.5 cm thick placed over the geomembrane liner.

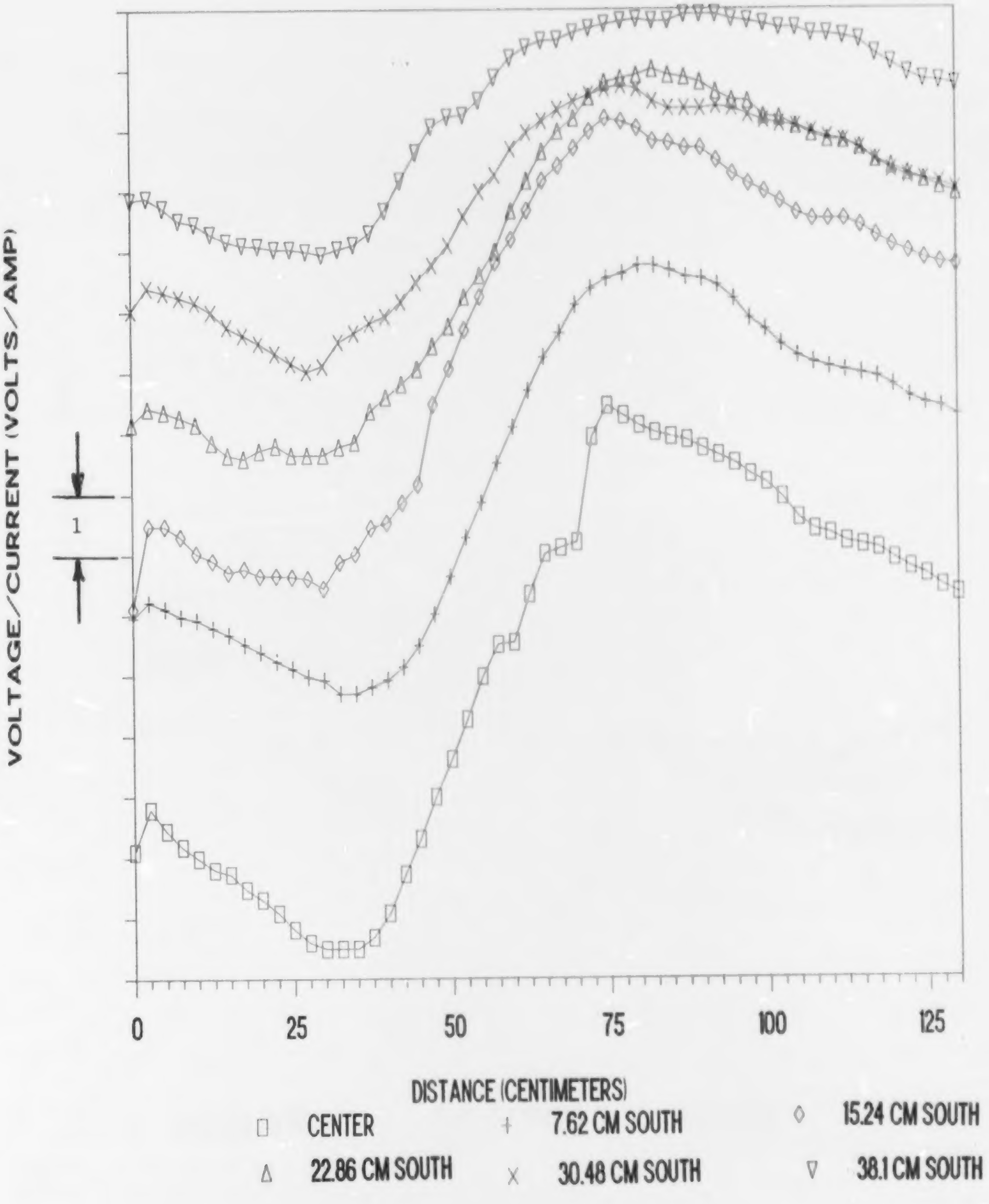

Figure 42. Scan data taken with 30 cm protective soil cover over geomembrane.

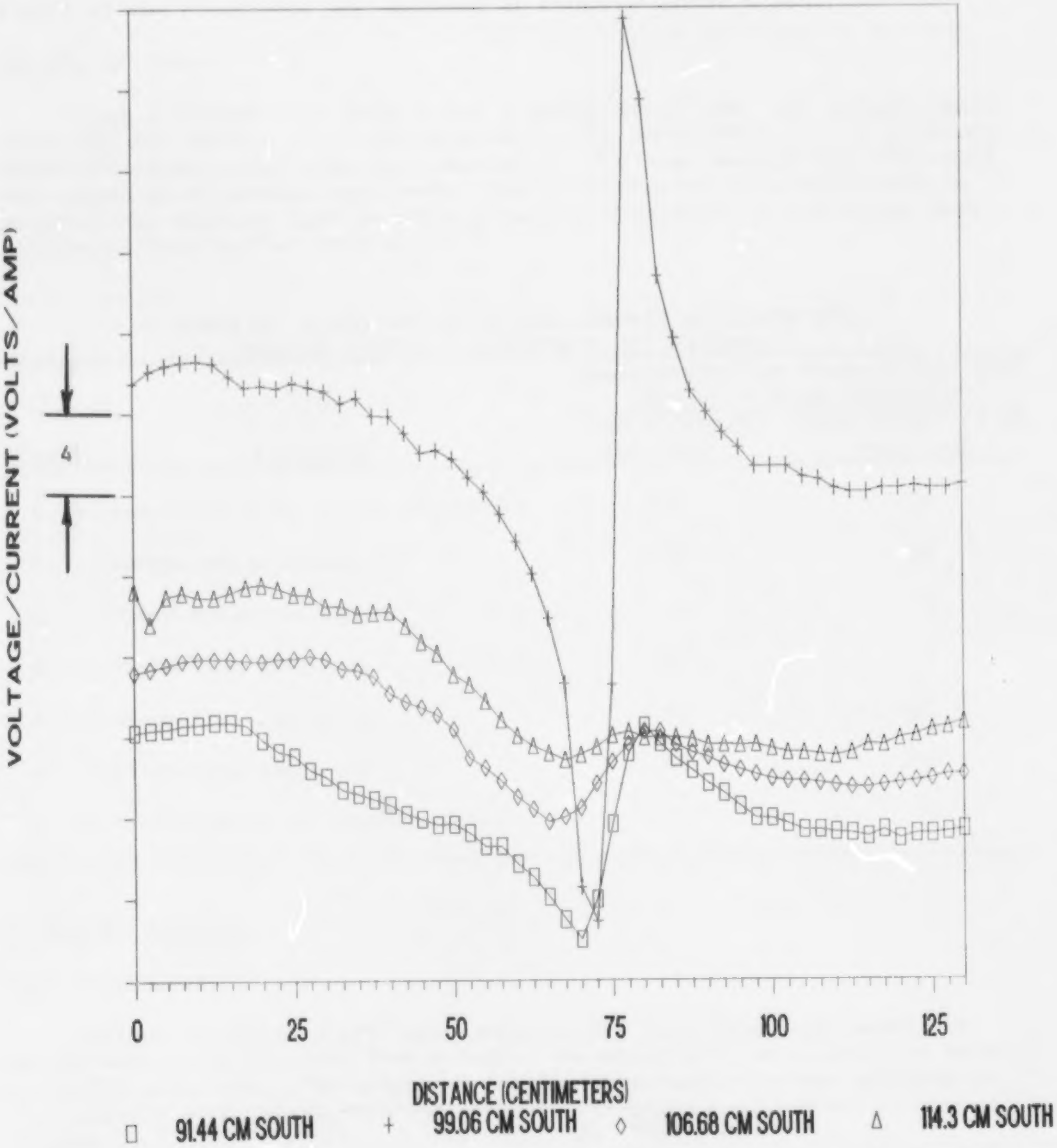

Figure 43. Additional scan data taken with 30 cm protective soil cover over geomembrane.

Tests were conducted by comparing the electrode voltage characteristics of the various electrodes under identical conditions. The relative sensitivity of the electrodes was measured by scanning across a leak.

Results of Tests--

Lines 1 through 3 in Table 2 are a comparison of the leak anomaly amplitudes for the various electrode materials. The sensitivity of the stainless steel and carbon electrodes was comparable. The leak anomaly was very small when glass pH electrodes were used. The resistance of these electrodes is probably too high for leak location purposes; therefore, pH electrodes were eliminated from further evaluation.

TABLE 2. A COMPARISON OF LEAK ANOMALY AMPLITUDE FOR VARIOUS ELECTRODE GEOMETRIES AND MATERIALS

		Approximate Leak Anomaly Amplitude Current = 10 mA (nominal)	
Line	Electrode	Scan Centered Over Leak	Scan Offset 15 cm from Leak
1	Stainless steel point electrodes	200	20
2	Carbon point electrodes	208	12
3	Glass point electrodes	3	0
4	15-cm line electrode	188	20
5	30-cm line electrode	150	175
6	60-cm line electrode	68	150
7	Protected 25 cm line electrodes	130	22

Electrode Geometry

Test Procedures--

Various electrode shapes were compared for leak detection capability versus centerline distance from a leak. The electrodes were connected to an isolation amplifier. The output of the isolation amplifier was recorded on a calibrated strip chart recorder. The leak anomaly was measured as the electrodes were scanned over a leak under identical conditions. The line electrodes were oriented horizontally and perpendicular to the scan direction. The geometries tested were:

(1) A localized electrode consisting of a cylinder approximately 25 mm in diameter and 25 mm long,

(2) A line electrode approximately 10 mm in diameter and 15 cm long, and

(3) A line electrode approximately 10 mm in diameter and 30 cm long.

Results of Tests--

Table 2 lists the measured leak anomaly amplitudes when the centerlines of the electrodes were scanned directly over the leak, and 15 cm offset from the leak. When the electrodes were scanned directly over the leak, the anomaly amplitudes were inversely related to the length of the electrodes. However, when the electrodes were scanned along a line 15 cm from the leak, the 30-cm line electrode produced the largest anomaly. Most importantly, the leak anomaly was barely detected when the localized point electrodes passed within 30 cm of the leak, where the longer electrodes produced easily detectable anomalies.

Leak Resistance versus Leak Size

Discussion--

Simple theoretical models have been formulated to relate leak resistance to leak diameter. The simplest model is based upon the fundamental definition of resistance and predicts the resistance will be inversely proportional to the square of the leak diameter. Another model based upon the equation for a grounded metal plate predicts the resistance will be inversely proportional to the leak diameter. A limited amount of testing was performed to empirically determine which model was more applicable.

Test Procedures--

A test fixture with dimensions of 30 cm × 30 cm was constructed with a geomembrane liner. Tap water was placed above and below the liner. A voltage was impressed between large electrodes in the two layers of water. The electrodes consisted of a metal bar along the entire perimeter of the test fixture. The impressed voltage and resultant current were measured for circular leaks with various diameters. The leak resistance was calculated as the impressed voltage divided by the current.

Results of Tests--

Figure 44 is a plot of the leak resistance versus leak diameter. For comparison, two other lines are drawn on the graph which correspond to the two models. The empirical data can be approximated by the grounded plate model, which predicts that the resistance will be inversely proportional to the leak diameter.

SUMMARY

The double-lined model experiments demonstrate the usefulness of the electrical leak location method for detecting and locating small leaks in the top liner of a double-lined impoundment. The only modification to the test

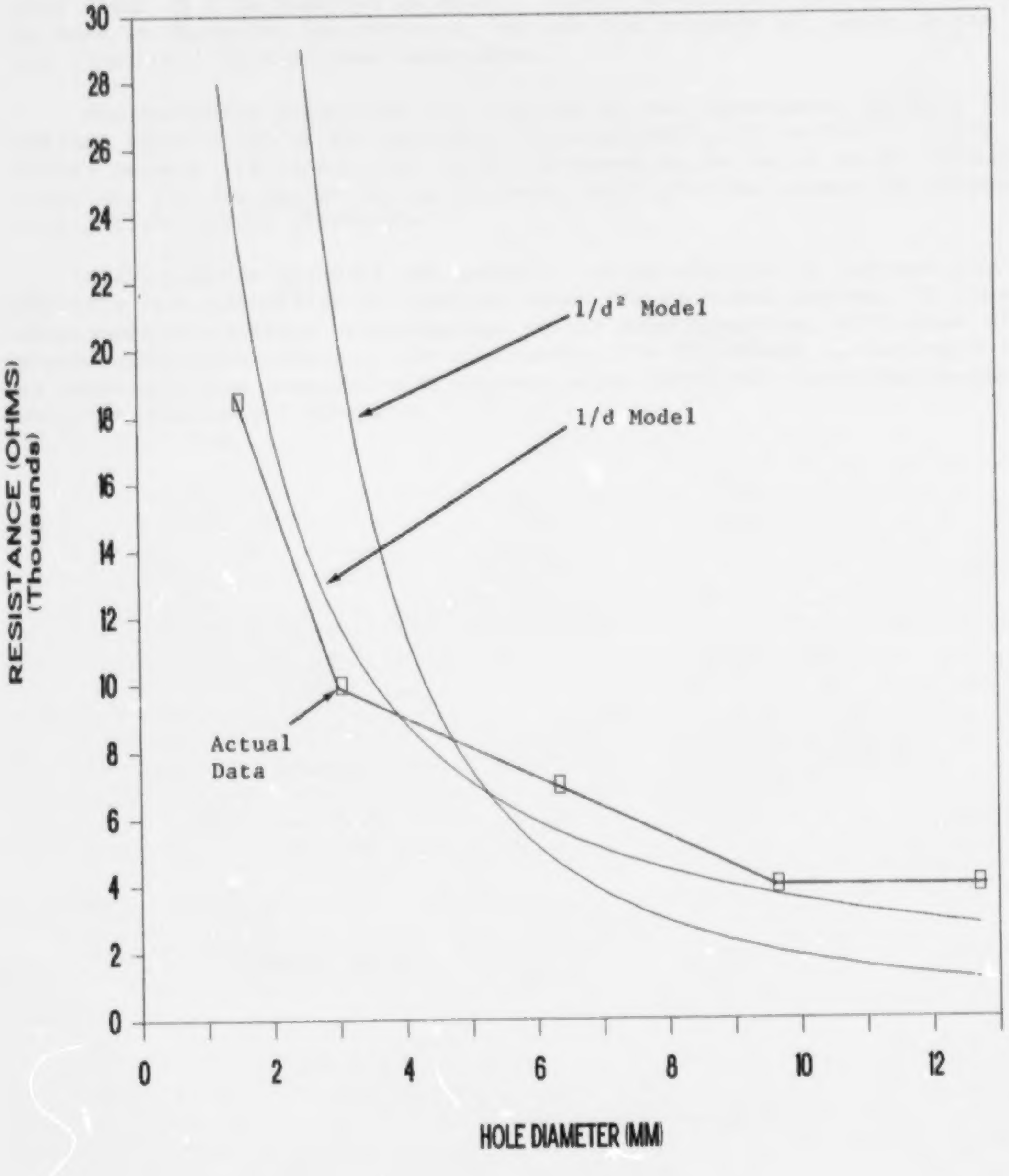

Figure 44. Plot of leak resistance versus circular leak diameter.

method is to place the current return electrode in the flooded drainage layer between the top and bottom liners. The method has been successfully demonstrated with a wide variety of drainage layer types, leak sizes, and geometries. The method is less sensitive for locating leaks under a protective soil cover that is immersed in water. Simple electrical continuity tests can be used to determine the presence, but not the location of, leaks in the bottom liner of a double-lined impoundment.

The following conditions are required at the impoundment facility for optimum application of the method: (1) an electrically conductive layer exists between the liners that is not grounded to the earth except through a leak; and (2) the design of the drainage layer provides access for placement of a current return electrode.

The electrode material and geometry can be selected to increase the sensitivity and probability of locating leaks during a leak survey. If linear electrodes are scanned perpendicular to the scan direction, with scans offset approximately the length of the electrodes, the likelihood of missing a leak is decreased when compared with surveys using localized electrodes scanned with the same offset distance.

SECTION 7

LOCATING LEAKS IN COVER SYSTEMS

BACKGROUND

Geomembrane liner material is widely used for landfill final cover systems. An impermeable cap is placed over the hazardous waste to prevent rainwater from percolating through the waste and leaching chemicals that could migrate into groundwater or surface water. A typical cover system consists of: (1) a low permeability bottom layer consisting of a plastic liner over a layer of clay placed over the waste, (2) a middle drainage layer consisting of layers of sand and gravel, and (3) a vegetated soil top layer.

Such cover systems are intended for long-term storage of hazardous wastes. Periodic inspection and maintenance can be performed to ensure that the cover system is performing as intended. Therefore, methods are needed to evaluate the integrity of these cover systems. The electrical leak location method has been found to be applicable for this purpose. Several alternative leak detection methods were also investigated to determine their applicability for locating leaks in the cover systems of waste landfill sites.

OBJECTIVE

The objectives of this project task were: (1) to evaluate and develop the electrical leak location method for evaluating the integrity of geomembrane cover systems for landfills; and (2) to investigate other techniques for evaluating the integrity of geomembrane cover systems for landfills.

RESEARCH APPROACH

Electrical Leak Location Method

Discussion--

The electrical leak location method can be adapted for making surface soil potential measurements to locate leaks in final cover system geomembrane liners. Decreased sensitivity for finding small leaks is anticipated because potential measurements must be made at the surface, and some geological noise and electrical polarization noise is expected.

The accuracy of the surface earth potential measurements for leak location depends upon several factors. Conditions that decrease accuracy include the presence of instrument noise, poor electrical contact between the ground and the electrodes (measurement noise); localized inhomogeneities of the surface resistivity (geological noise); electrode polarization noise, and the presence of interfering signals such as electrical power line interference (electrical noise). Noise in these cases is defined as the unwanted part of the measured signal that is contributed by phenomena other than the leak signature.

For well-designed surface soil potential measurements using modern equipment, instrument noise and electrical noise usually are insignificant. Measurement noise is caused by poor or unstable electrical contact between the ground and the measurement electrodes. For accurate earth potential measurements, the potential measuring instrument must not perturb the potential being measured. To accomplish this, the instrument is designed with an input resistance very much greater than the electrode contact resistance with the earth. For dry soil, this contact resistance can be comparable with the input resistance of practical potential measurement instruments, resulting in measurement inaccuracies.

Poor electrode contact is commonly caused by dry surface soil or by dry vegetation. In most cases, the nonconductive dry surface is underlain by more electrically conductive soil, so poor electrical contact problems can be overcome if the dry surface material at the measurement point is displaced, or the electrode penetrates through the dry surface layer.

Geological noise caused by small areas of relatively high or low resistivity soil, particularly near the measurement electrodes, can cause disproportionate variations in the measured leak signature. To decrease the effect of geological noise, the measurement electrodes must not be spaced too closely, and the spatial frequency of the measurements must be adequate to properly sample the anticipated leak signature.

Polarization noise is caused by electrochemical reactions at the interface between the soil and metal electrodes and by ion accumulations in the soil near metal electrodes. The oxidation and reduction reactions generate a significant potential when there are differences in the chemical composition of the electrodes and the soil near the electrodes. These potentials stabilize when equilibrium is reached in the ion concentration and exchange reactions next to the electrodes. An adsorbed, relatively thin film of ions forms on the electrode and is held in place by electrical and chemical forces. Next to the electrode and the film layer a thin layer of diffuse ions can form when current flows through the interface. In addition, membrane polarization can be present when charges in clays attract a diffuse cloud of positive ions. The term "membrane" in this case is not associated with geomembranes. Membrane polarization is like electrode polarization superficially, but no chemical reaction takes place. Membrane polarization is caused by ion accumulations within the electrolytic conductor. Other phenomena, including the photoelectric effect, and temperature differences between the electrodes can produce small, but measurable noise voltages.

Polarization noise can be reduced significantly by using half-cell electrodes. These electrodes are also referred to as porous electrodes and nonpolarizing electrodes. Figure 45 shows the construction of a typical

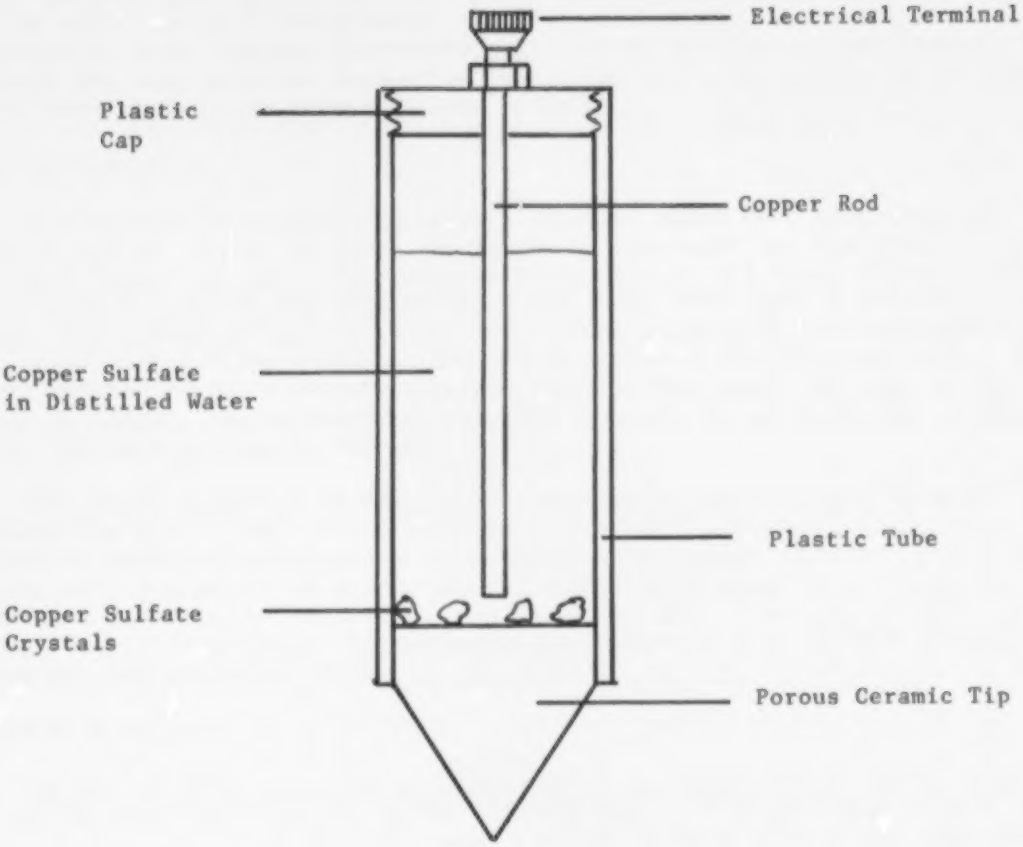
Electrical Terminal
Plastic Cap
Copper Rod
Copper Sulfate in Distilled Water
Plastic Tube
Copper Sulfate Crystals
Porous Ceramic Tip

Figure 45. Half-cell electrode used to measure electrical potentials on soil cover.

half-cell electrode. Although many combinations of metals and salt solutions can be used for half-cells, the copper-copper sulfate half-cell is most commonly used for measuring earth potentials. A saturated salt solution is maintained in the half-cell by maintaining undissolved salt crystals in the half-cell.

The principle of the half-cell electrode is that the chemical conditions of the metal and salt constituents is maintained stable, so no polarization differences exist between electrodes. Electrical contact is established through the salt solution permeating the porous tip. The porous tip is commonly made of unglazed porous ceramic material.

Test Procedures--

Experiments were conducted using a physical model with dimensions of 4.9 m × 4.9 m. Figure 46 shows the layout of the model and the location of the test leak. The model was constructed by placing a 1.02-mm (40-mil) HDPE liner over the ground and then covering the liner with various thicknesses of soil. The ground surface was first prepared by grading it flat and removing all vegetation and large rocks. Sandy loam was used for the cover soil. For these initial tests, a dirt-free border was provided along the edge of the sheet to prevent the current from coupling directly to earth ground. A wooden frame was used to contain the soil.

The tests consisted of using a DC power supply to impress a voltage between the soil on top of the HDPE sheet and earth ground and then making potential gradient measurements on the soil using porous half-cell electrodes. A hole with a diameter of 3.2 mm was drilled in the center of the sheet to provide a known target to detect. Potential gradient measurements were made along a rectilinear grid. Measurements were made every 10 cm with a potential electrode separation of 10 cm.

Results of Tests--

Effect of depth of cover on leak anomaly amplitude--Figure 47 is a plot of the measured leak anomaly versus depth of the soil cover. The anomaly is directly above the leak in every case. Figure 48 is a plot of the same data for soil depths of 15 cm to 60 cm plotted on a larger scale. The leak was easily detected for all of the soil cover depths tested. Although the peak-to-peak amplitude of the anomaly decreases rapidly with increasing soil cover, the anomalous signal is larger than the noise even with 60 cm of soil cover.

The ability to locate a leak with a diameter of only 3.2 mm was much better than originally expected. This is attributed to the use of half-cell electrodes and the increased sensitivity of the electrical leak location method with higher resistivity media.

Effect of scan offset distance on leak anomaly--Additional scans were made with 30 cm of soil cover to measure the anomaly as the scan line was moved away from the leak. Figure 49 shows the data for scan lines over and west of the leak location. The leak anomaly is evident in the data for the scan line over the leak and 60 cm west of the leak. The anomaly was not

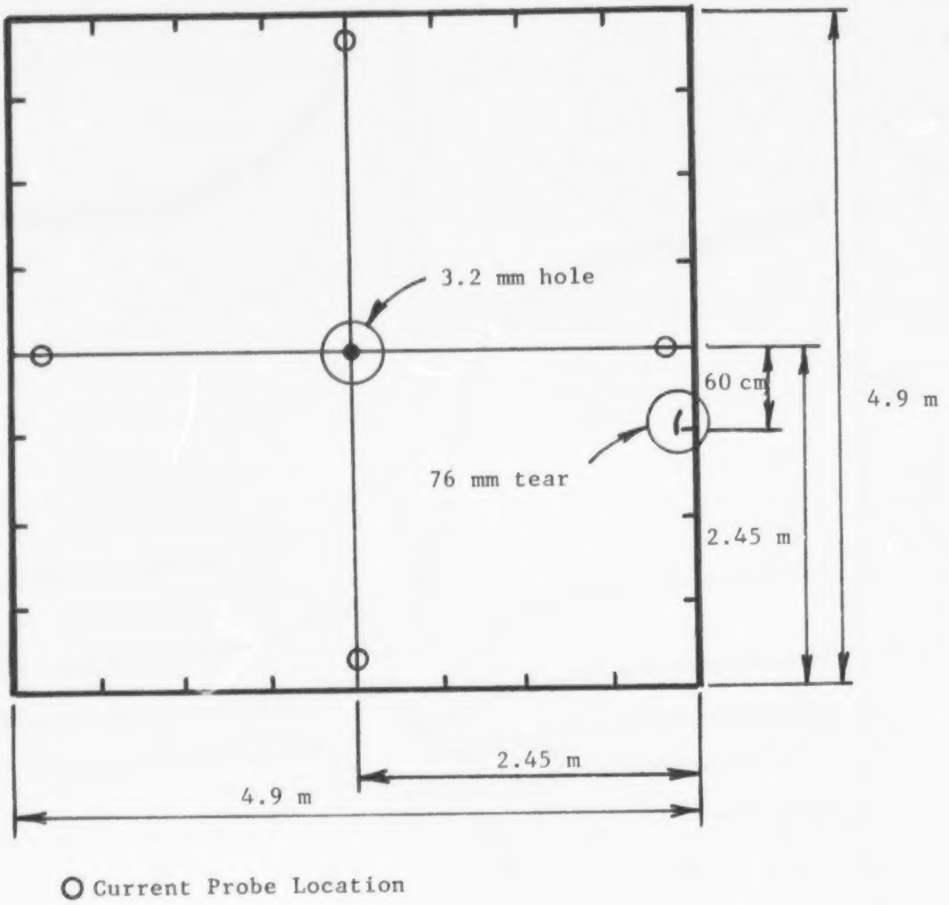
3.2 mm hole
60 cm
4.9 m
76 mm tear
2.45 m
2.45 m
4.9 m
○ Current Probe Location

Figure 46. Cover system physical model geometry.

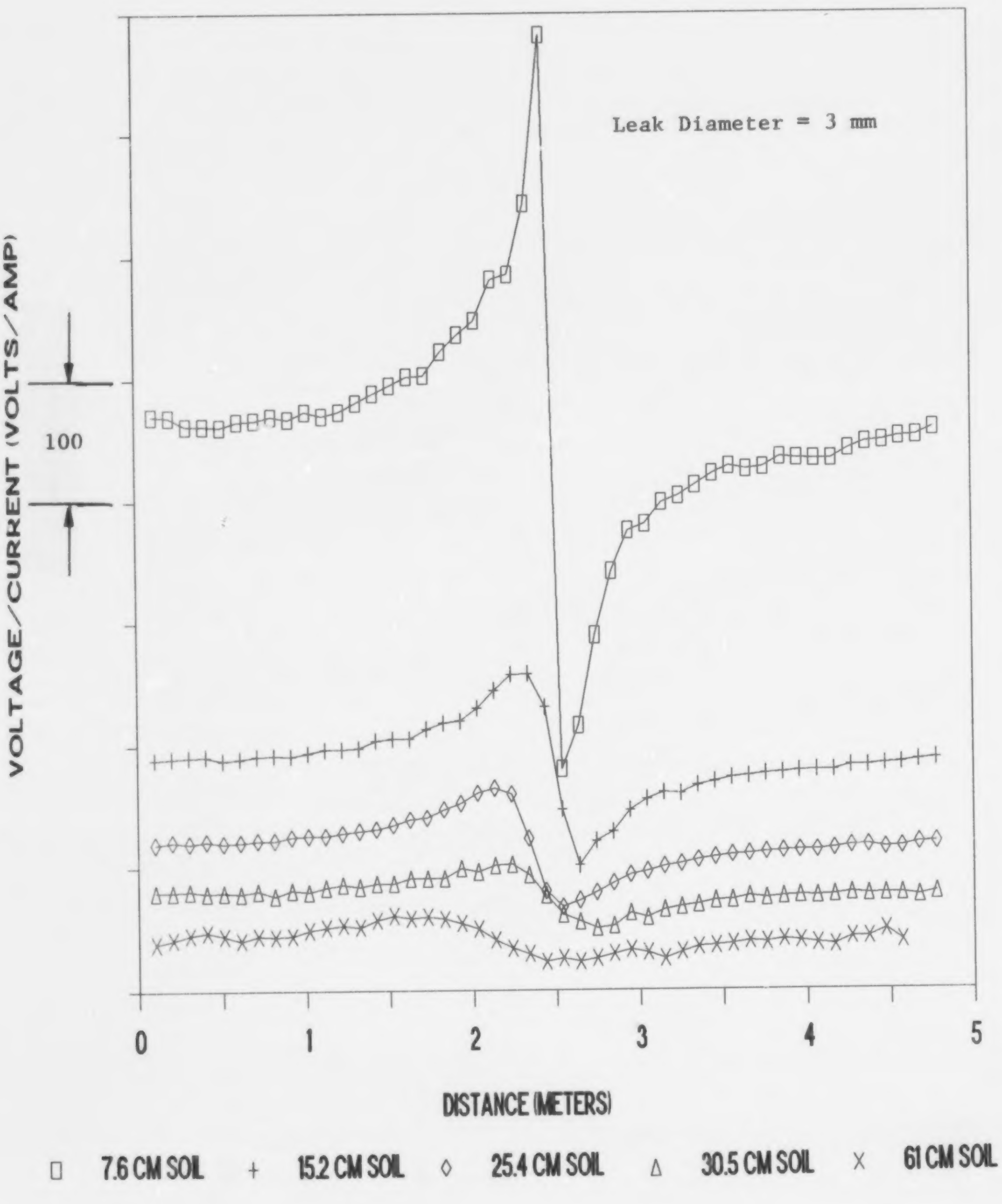

Figure 47. Comparison of leak signatures for cover system with various thicknesses of soil cover.

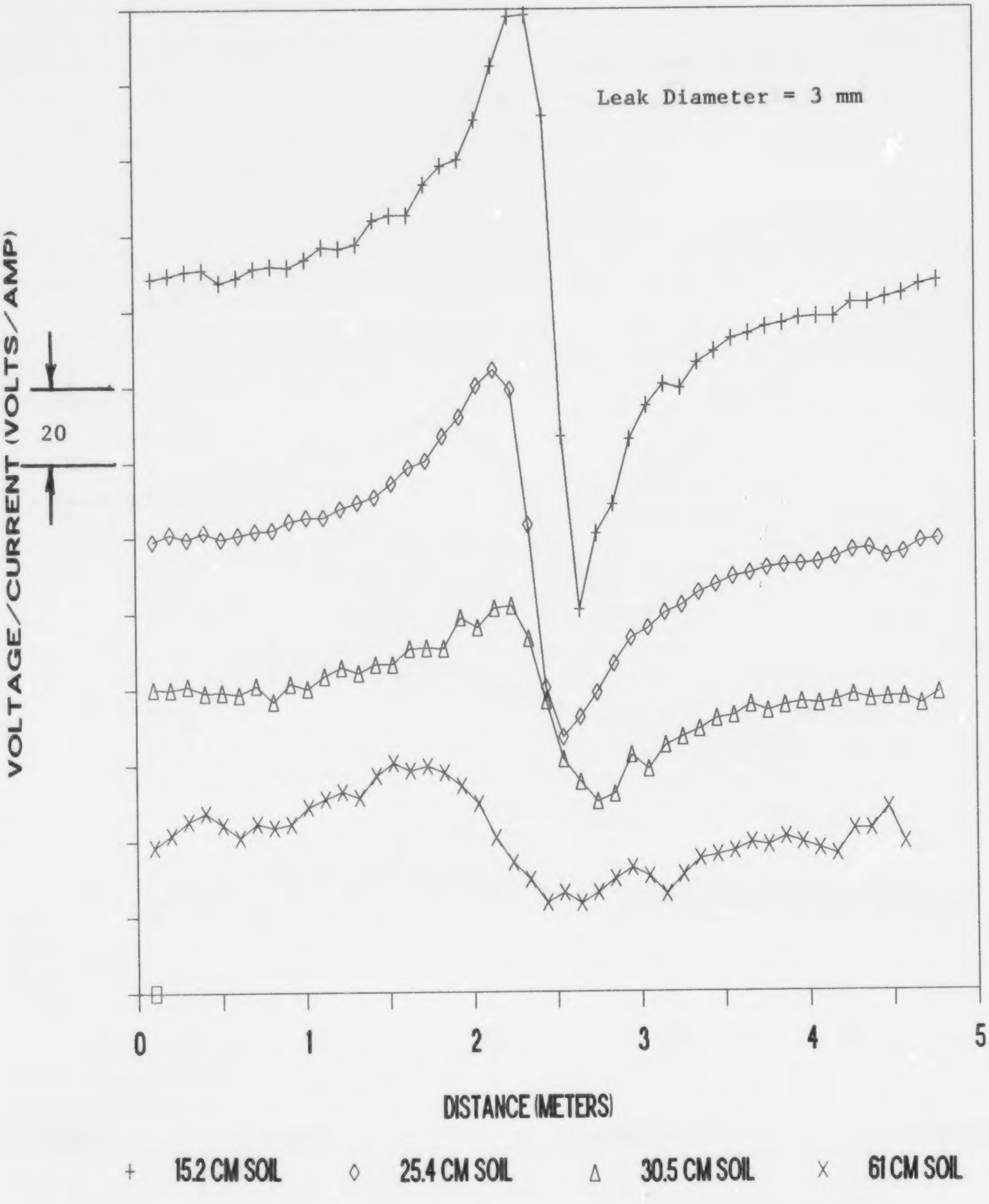

Figure 48. Comparison of leak signatures for cover system with various thicknesses of soil cover plotted on a larger scale.

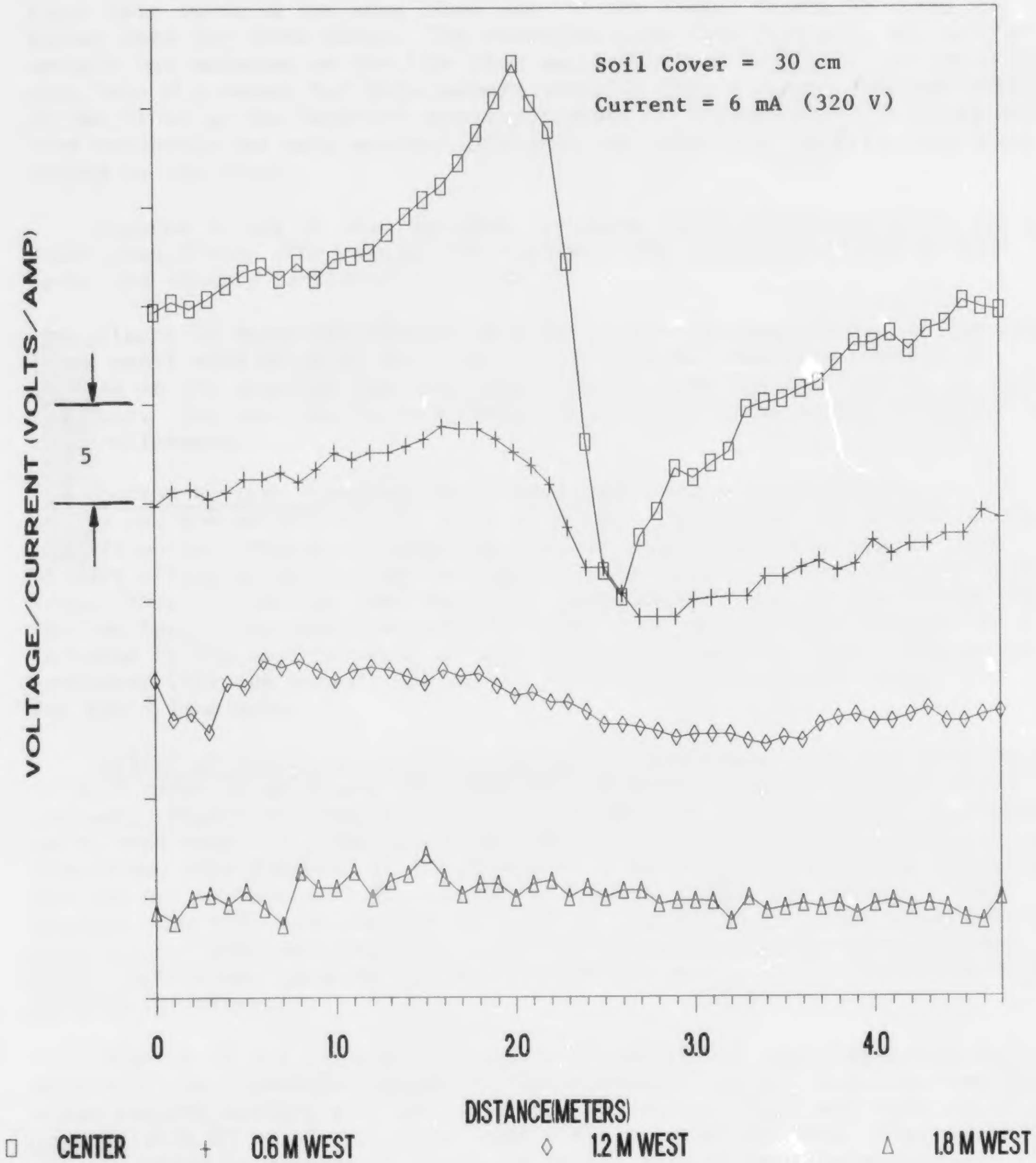

Figure 49. Raster plots of leak location data for cover system for scan lines west of leak.

present in the data for the scan line 1.2 m from the leak. The current injection electrode was moved to the center of the west edge of the model and the tests were repeated for scan lines east of the leak. Figure 50 shows the raster data for these tests. The anomalies were less distinct, and another anomaly was measured on the line that was 1.8 m from the leak. An investigation into the reason for this anomaly revealed that a second leak was present in the liner at the location previously shown in Figure 45. This 76-mm long tear evidently was made accidentally when the cover soil material was being placed on the liner.

Figures 51 and 52 show the data for scans taken perpendicular to the previous scan lines. The results are similar. The anomalies caused by both leaks are clearly indicated in Figure 52.

Figure 53 shows the plotted data for a leak-location survey of the cover liner model with 60 cm of soil over a 3.2-mm leak. The leak anomaly is evident in the data for the scan line directly over the leak and 60 cm east of the leak. The data was taken without taking measures to reduce electrode contact resistance.

Effect of leak diameter--Tests were performed with leak diameters of 3.2 mm and 6.4 mm with a soil cover of 60 cm to determine the effect of the leak diameter. Figure 54 shows the plotted results of these tests. The primary effect of increasing the leak diameter is to increase the leak current. This was not the case for these tests because the current levels for the two tests were approximately the same. This was probably because of differences in the soil moisture or soil compaction near the leak. The tests indicated that the anomaly due to the 6.4-mm hole is slightly larger than that for the 3.2-mm hole.

Effect of electrode contact resistance--Tests were performed with 60 cm of soil cover to determine the measures necessary to obtain good electrode contact. Figure 55 shows a comparison of the leak signatures with measurements made when: (1) the electrodes were simply held on the surface; (2) the electrodes were inserted in the ground to a depth of approximately 25 mm; and (3) the dry surface soil was scraped off prior to the measurements. The results show that measures can be taken to significantly reduce electrode contact noise. When compared with inserting the electrodes in the soil, the minor improvement obtained by scraping the dry soil probably is not worth the additional effort.

Figures 56 and 57 show the results of additional tests comparing surveys made with the electrodes placed on the unprepared surface with a survey made after the dry surface soil was removed. The survey scans were made on 60 cm centers with 60 cm of soil cover over a 6.4 mm diameter leak. The electrode contact noise is evident in Figure 56 in the form of erratic variations between adjacent data points. The electrical contact noise is reduced significantly when the dry surface soil near the electrode is removed.

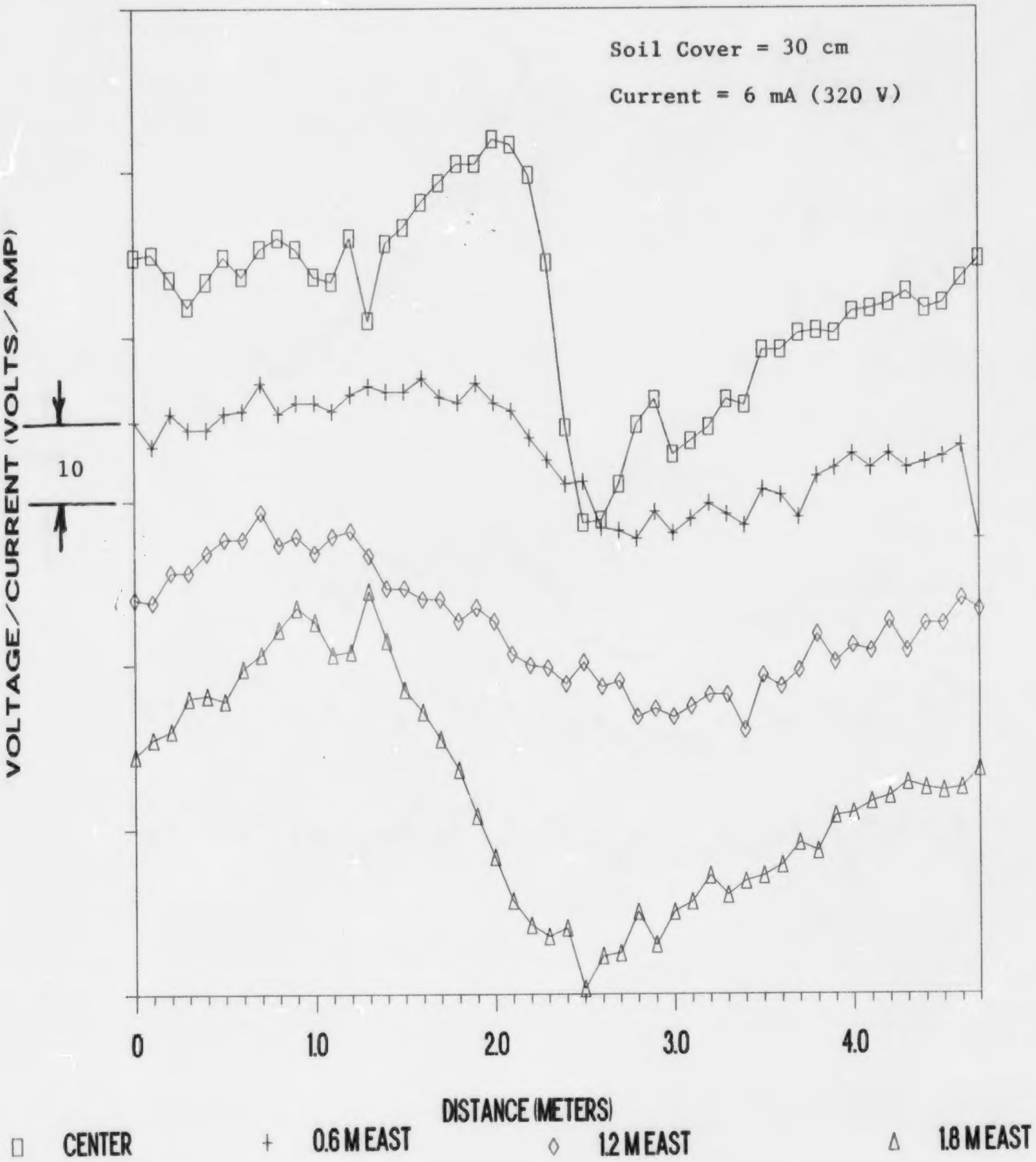

Figure 50. Raster plots of leak location data for cover system for scan lines east of the leak.

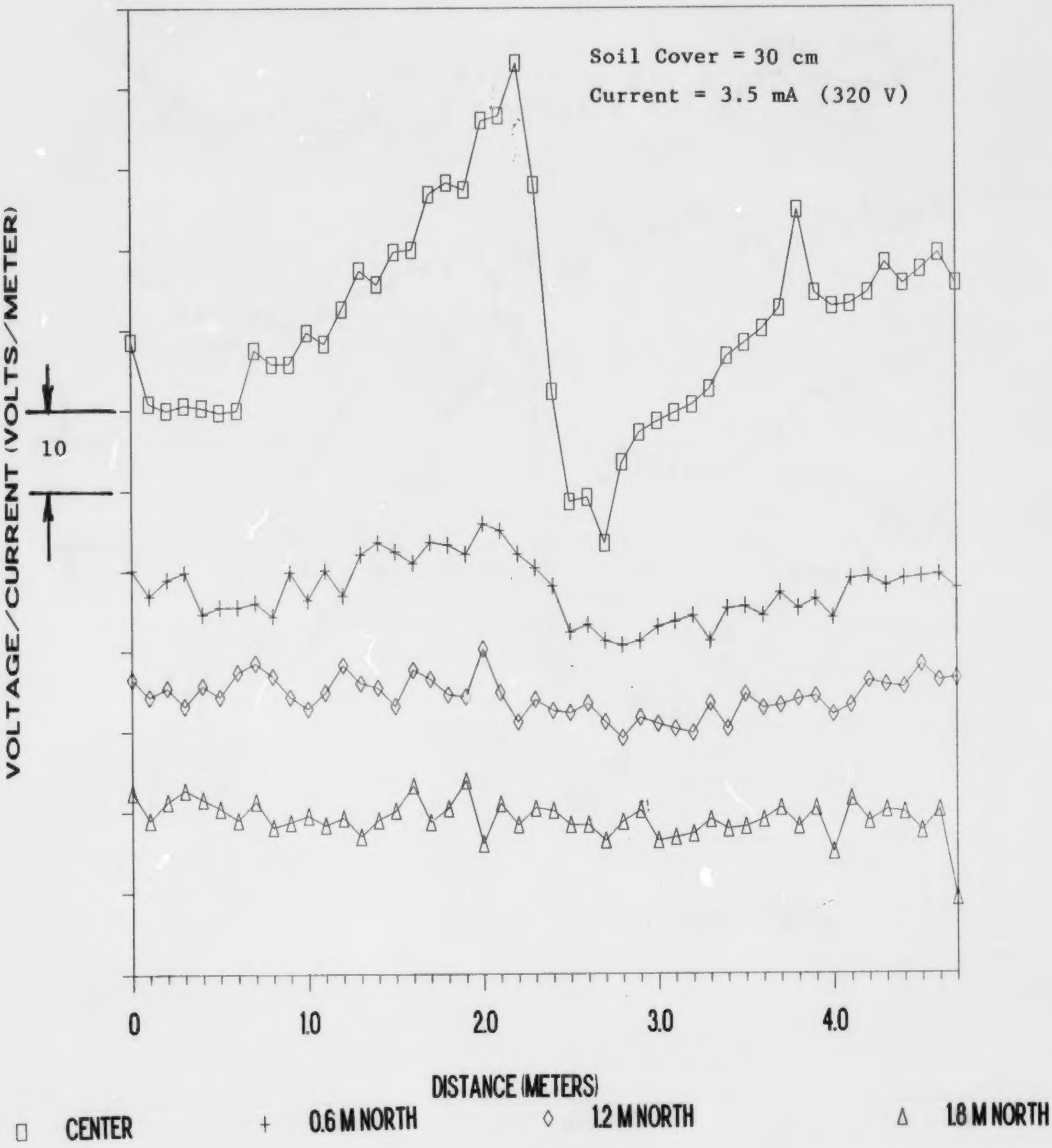

Figure 51. Raster plots of leak location data for cover system for scan lines north of the leak.

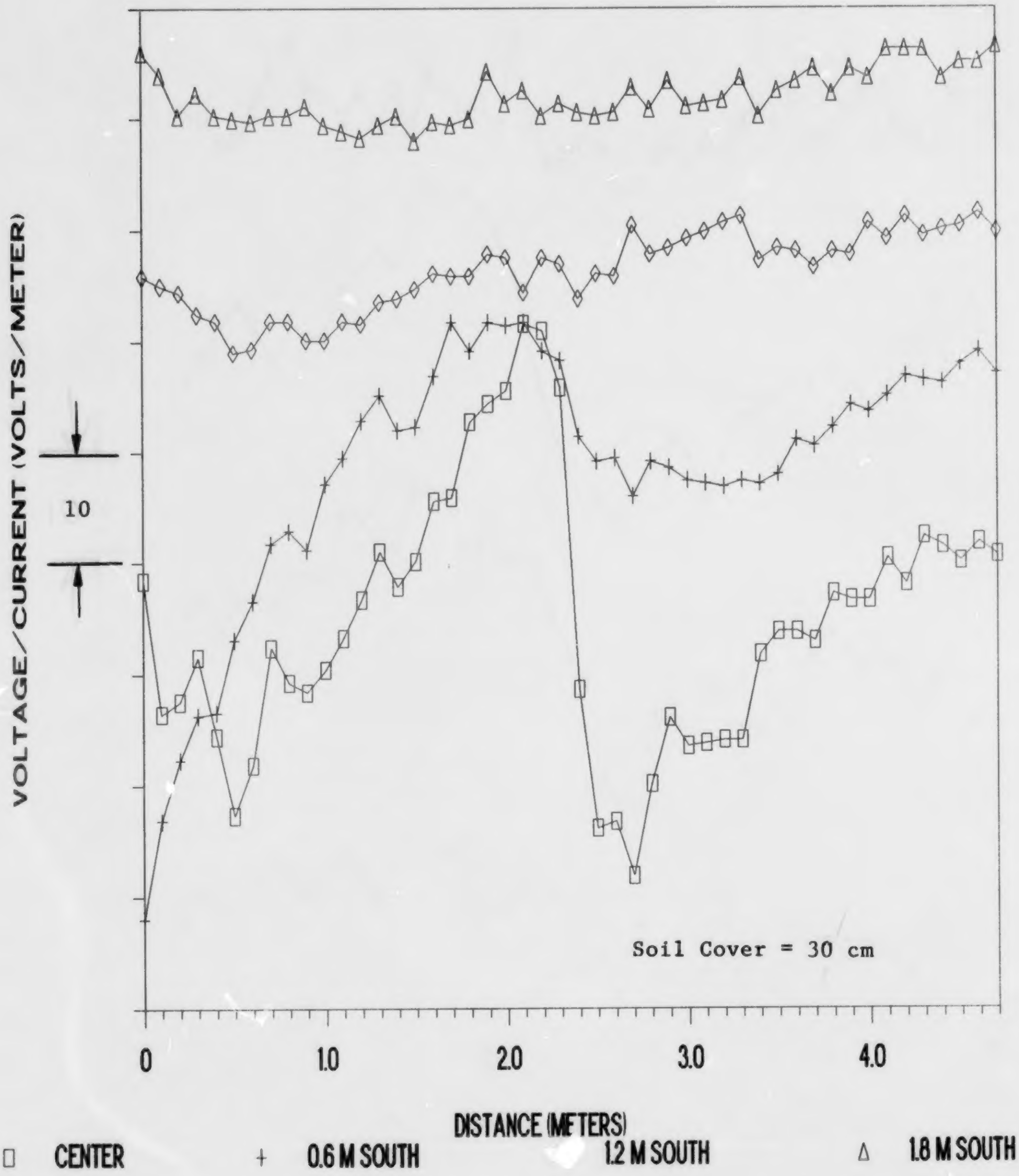

Figure 52. Raster plots of leak location data for cover system for scan lines south of the leak.

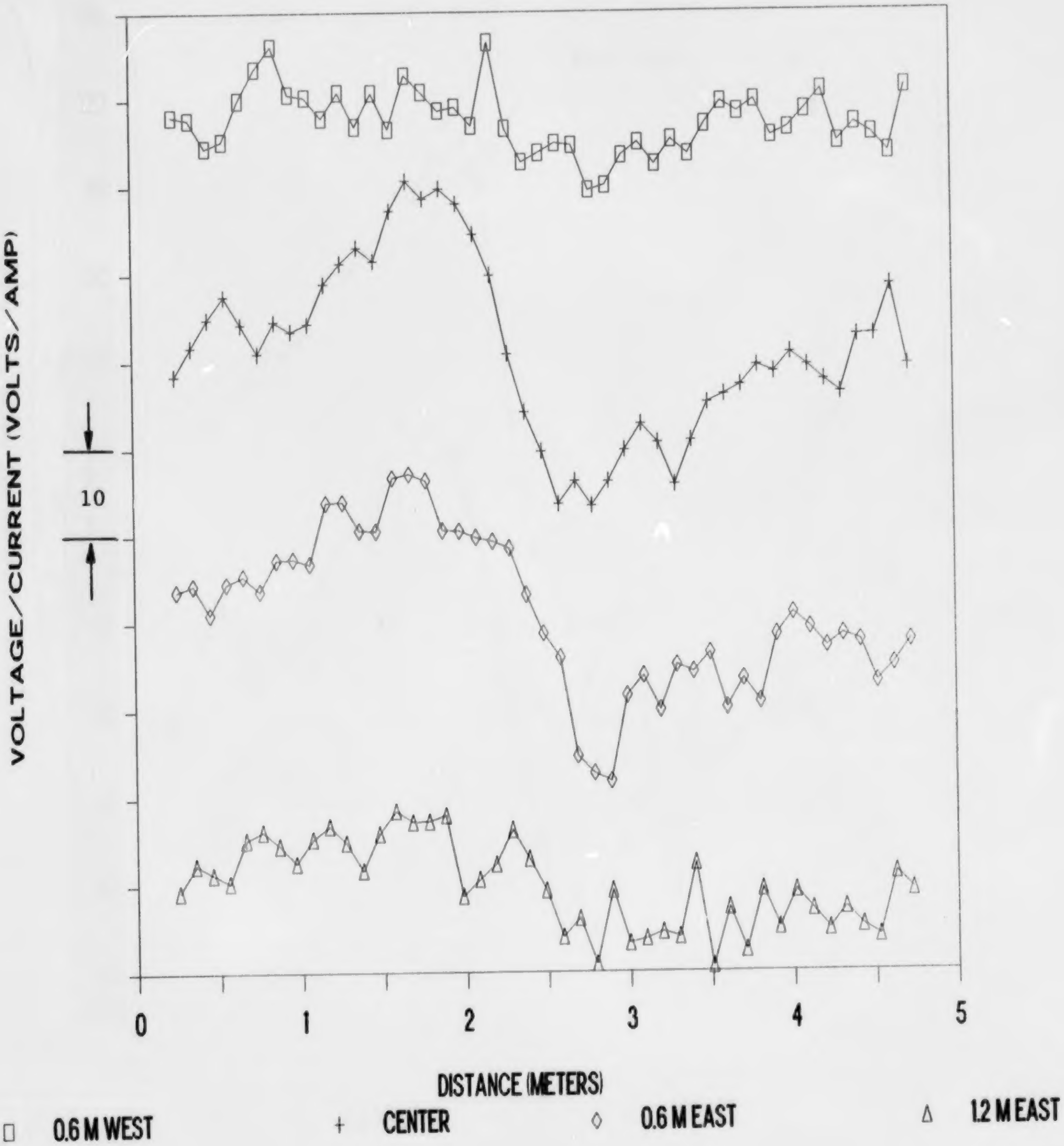

Figure 53. Leak location data taken on survey lines spaced 60 cm apart indicate the presence of a 3.2 mm diameter leak under 60 cm of soil cover.

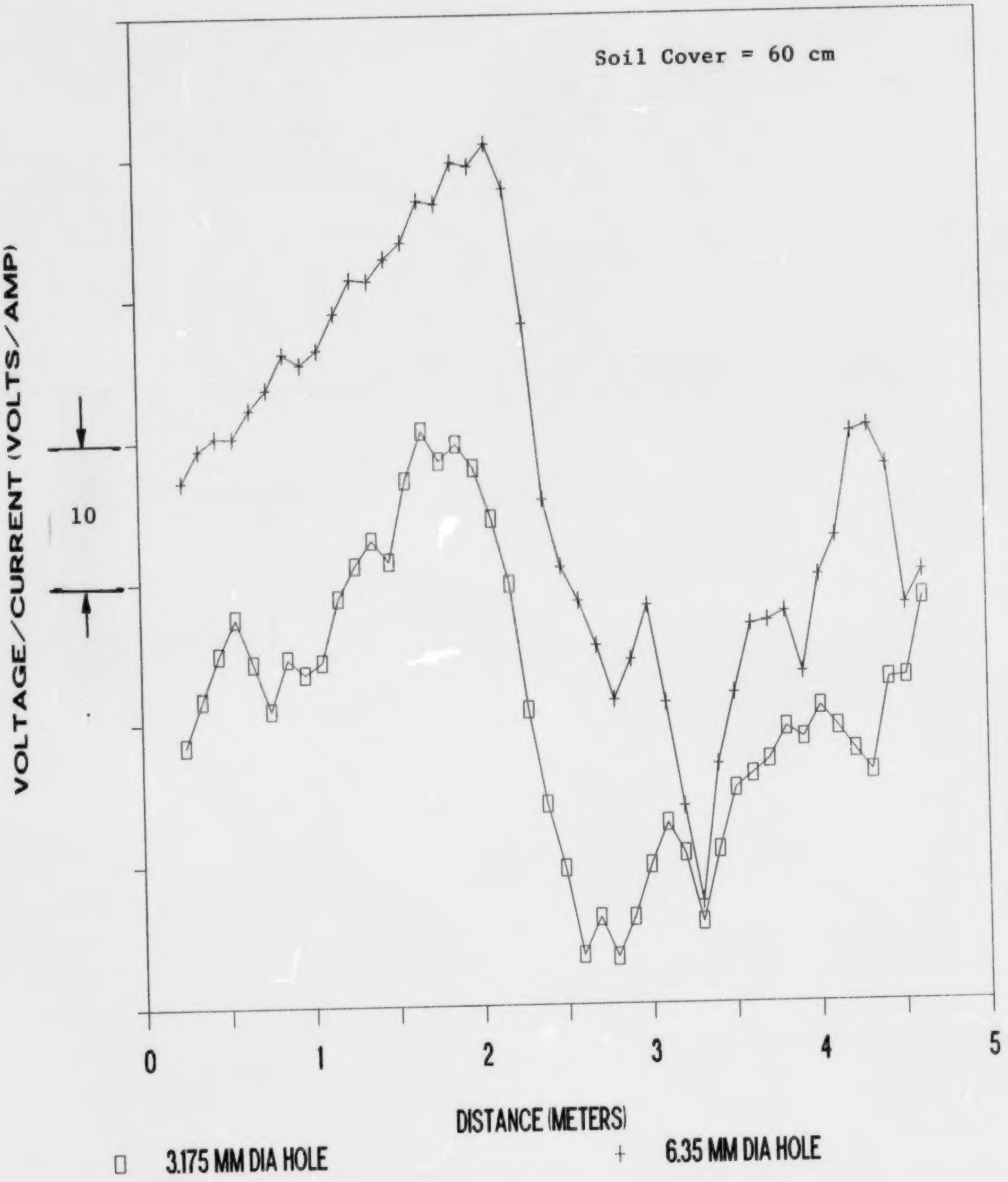

Figure 54. Comparison of leak signature versus leak diameter with 60 cm of soil cover.

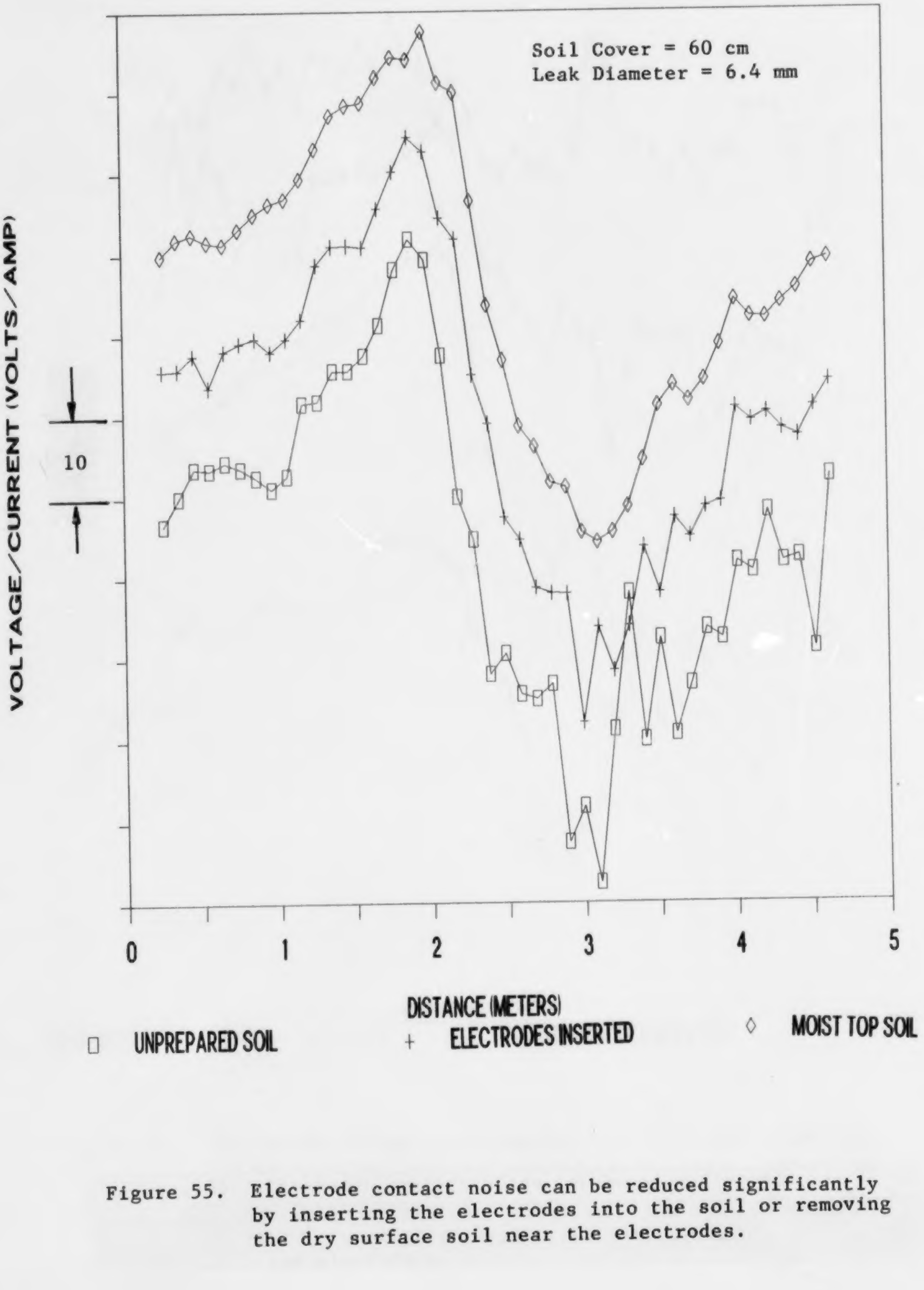

Figure 55. Electrode contact noise can be reduced significantly by inserting the electrodes into the soil or removing the dry surface soil near the electrodes.

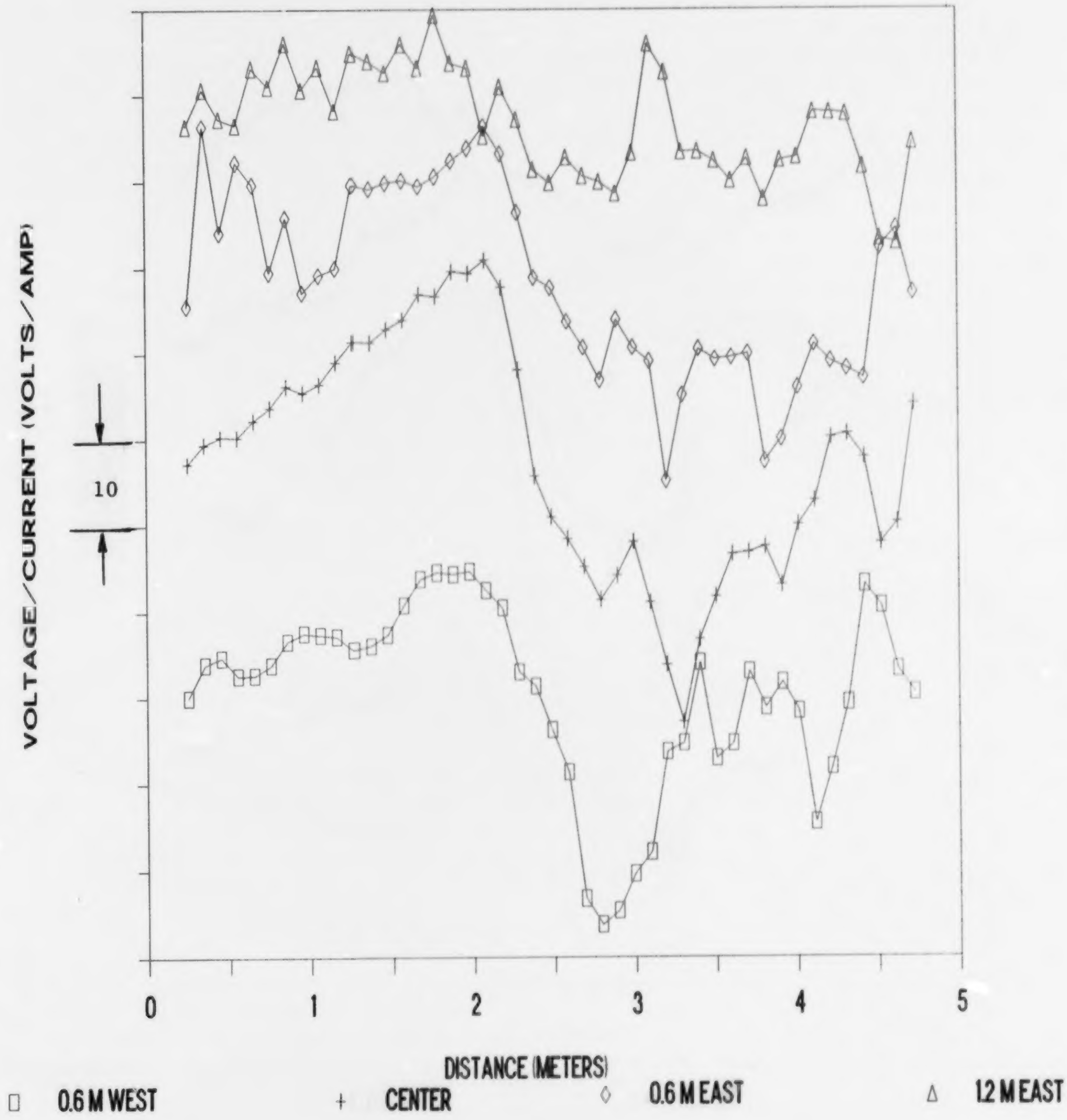

Figure 56. The survey of the cover system with 60 cm soil cover and 6.4 mm diameter leak has excessive electrode contact noise when the electrodes are simply placed on the dry soil.

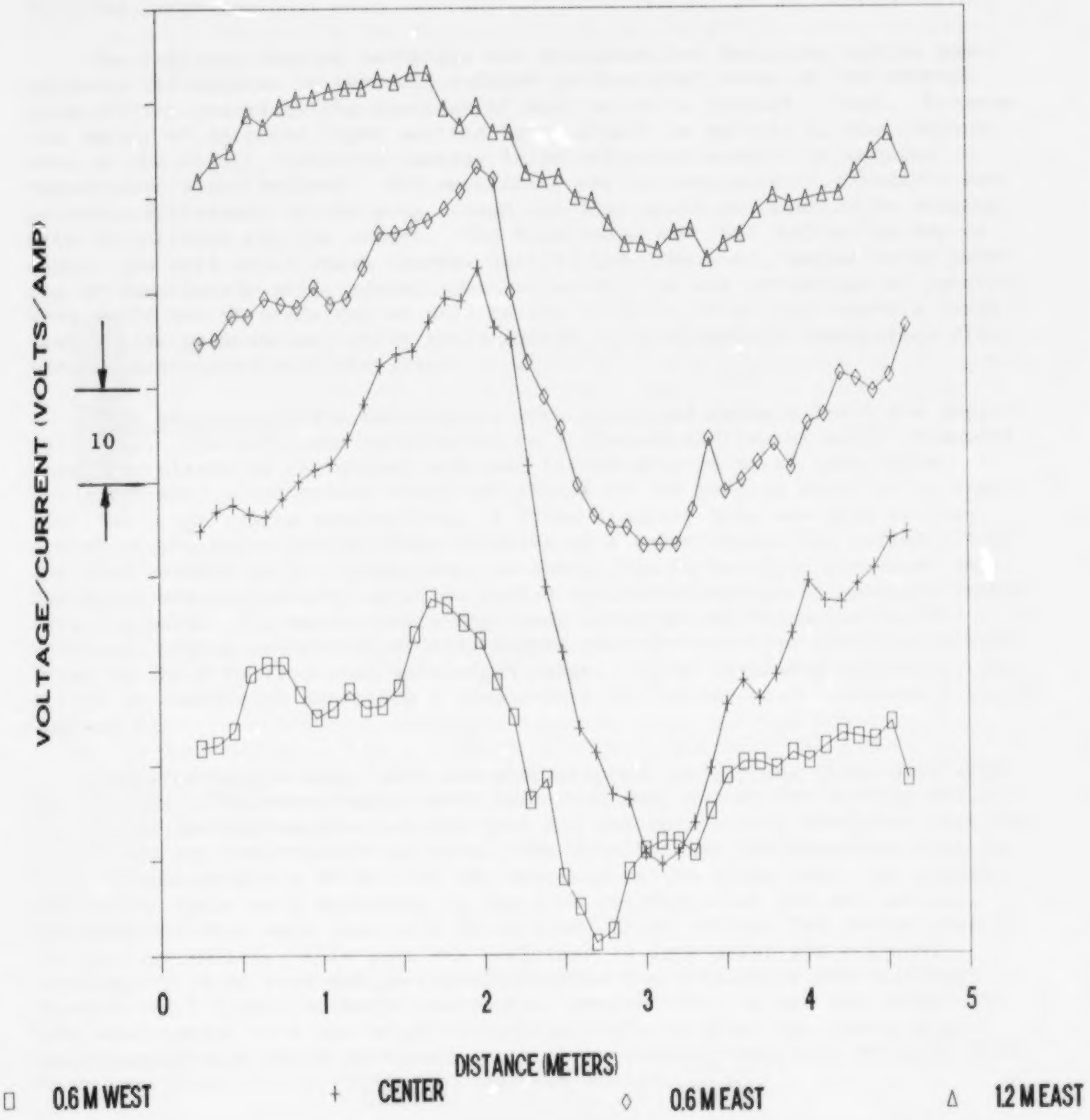

Figure 57. When the same survey as shown in Figure 56 is repeated with the dry soil near the electrodes removed, electrode contact noise is reduced greatly.

Other Leak Location Methods for Cover Systems

Infrared Imaging--

The infrared imaging technique was evaluated for detecting subtle temperature differences on the soil related to localized areas of low thermal conductivity caused by the drainage of soil moisture through a leak. Because the amount of infrared light emitted by an object is related to the temperature of the object, infrared imaging is an efficient method for mapping temperature distributions. The experiment was to determine if a notable temperature difference in the area around the leak could be detected by viewing with an infrared imaging camera. The hypothesis was that during the day or night, the soil would reach thermal equilibrium. However, during early morning or immediately after sunset, when solar heating was introduced or removed, heat would not be conducted as well in the slightly drier soil above a large leak in the geomembrane, which would result in a detectable temperature difference associated with the leak.

Test procedures--The experiments were performed using a 3-m × 3-m physical model. The model was constructed on a cleared section of soil. A wooden frame was placed on the ground and then filled with 76 mm of sandy loam. A 0.1-mm (4-mil) polyethylene sheet was placed on the bedding material to simulate the cover system geomembrane. A 25-mm diameter hole was made in the center of the polyethylene sheet to serve as a known leak. The polyethylene was then covered with a 76-mm layer of sandy loam to serve as the cover soil. The model was soaked with water so that a sufficient amount of moisture leaked into the hole. The measurements were made using an AGA Thermovision 782 infrared imaging camera and display system that is sensitive to infrared radiation in the 8 to 12-micron wavelength range. Under favorable conditions the system is capable of detecting a temperature difference of 0.1 degrees C (0.16 degrees F).

Infrared images were taken and photographed one day and three days after the wetting. Two measurements were made each day; one in the morning while the ground surface temperature was cool and one in the late afternoon when the ground surface temperature was warm. The detector was positioned so that an area of approximately 60 cm × 60 cm, centered on the known leak, was viewed. Additional tests were performed in the late evening after the sun had set. Measurements were made from 8:30 PM to 10:00 PM to monitor the target area as the surface cooled. This test was performed 15 days after the original wetting. A final test was performed in which the soil above the hole was removed and 2 liters of water was poured into the hole to wet the sand. The hole was covered with the original soil and left to stand for three days. Measurements were again performed in the late evening from 8:30 PM until 10:00 PM to watch the target area as the surface cooled.

Results of tests--In all of the tests there was no evidence of a readily identifiable target when viewed with the infrared imaging camera.

Ground-Penetrating Radar--

Ground-penetrating radar surveys can be conducted on the surface of the cover system. Changes in the conductivity of the subsurface media are measurable at the surface as reflected electromagnetic waves. Therefore, ground-penetrating radar can detect areas of concentrated moisture beneath the geomembrane liner caused by leaks in the liner.

Ground-penetrating radar systems are finding wide applications in geophysical and geotechnical studies for the resource development, environmental management, and construction industries. Under favorable soil conditions, ground-penetrating radar systems have been used with good success. Modern signal processing techniques such as synthetic aperture can improve both the detection and location capabilities of the radar.

Advantages--The ground-penetrating radar technique does not require the placement of materials under the liner, either at the time of installation or when testing. Under favorable soil conditions, ground-penetrating radar has proven to be effective for detecting and delineating many subsurface anomalies. Ground-penetrating radar may offer the additional capability of mapping the depth of the soil cover and the lateral extent of the seepage through a leak.

Disadvantages--The depth of investigation of the ground-penetrating radar method depends upon the conductivity of the soil cover. Success of the method depends upon the soil having only moderate conductivity and, hence, reasonably low dissipation of electromagnetic energy. In more conductive soils, the high dissipation of the electromagnetic energy and the very weak signal scattered from leak anomalies can be detected only for shallow cover soil depths.

The data obtained from ground-penetrating radar surveys requires interpretation that is subject to the skills of the interpreter and a knowledge of the conditions of the site that was surveyed. The signature of the impoundment being surveyed will change over time because of factors such as moisture content of the cover system and changes in the vegetation on the cover. Very refined and reliable techniques are needed to distinguish actual leaks from these other factors.

Tracer Gas--

Certain gases, including fluorinated hydrocarbons, can be injected under the cover system below the geomembrane. The gas will migrate in the sand layer and seek a path to the surface through a leak. Gas travelling upward through a leak in the liner can then be detected with available hand-carried sensor instruments scanning the surface of the impoundment. Some types of gas are relatively easy to detect in dilute quantities, so only a small quantity of gas is needed.

Advantages--The tracer gas method would be most successful in determining the presence of leaks in the geomembrane after the installation of the membrane but prior to the addition of any drainage layer or soils. Several injection points could be built into the membrane at the time of installation to ensure uniform gas dispersion.

A survey of the area could be completed quickly and the data would not require technical interpretation. More than one operator could work simultaneously with the gas detecting equipment to survey the area for leaks.

Disadvantages--This method requires injecting the gas under the liner, so it is more difficult to implement in existing systems and for systems that have a thick soil cover above the geomembrane. A closed system (i.e., cover to bottom liner continuous contact around the complete impoundment) is desirable and probably necessary to contain the gas until the leak survey is complete. The leak detection process can be jeopardized by the possibility of non-uniform distribution of the gas caused by preferential gas migration in the drainage layer. For large landfills, the amount of gas needed may be excessive. For example, assuming 25 percent void space in the landfill, if enough Freon R12 is added to raise the pressure by 1.9 mm of mercury (1 in. of water), approximately 340 grams per 1000 cubic meters (9 pounds per acre-ft) of waste would be needed. Environmental concerns over the eventual release of fluorocarbons or other gasses may make this method impractical.

Electromagnetic Induction--

The electromagnetic induction method is used to map the near-surface apparent terrain conductivity. This method is the most frequently used geophysical technique for environmental contamination studies because of its speed and ease of operation. A decrease in conductivity or an increase in resistivity of the soil indicates a decrease in moisture present at the point of a potential leak due to moisture being drained through the leak. Therefore, apparent conductivity measurements may be applicable for locating leaks in the geomembrane.

This method can best be applied if a history of surveys over a period of time is kept and an average of the results maintained. Over a period of time, the localized highs and lows can be identified as the soil and cover signature; any new anomaly is identified as a potential leak and subjected to continued observation and/or further investigation.

Advantages--There is no need for any material to be installed under the cover liner either during construction or prior to a test. The method makes use of conductivity or resistivity measurement procedures that are well established in the environmental protection industry.

Disadvantages--The soil above the liner is subject to localized highs and lows in conductivity or resistivity caused by designed drainage characteristics. Therefore, only very large leaks can be detected. The resolution of the method is relatively limited, and the data requires interpretation.

Encapsulated Chemicals or Gas--

Encapsulated chemicals or gas that are activated by water can be placed under the liner at the time of cover system installation. The capsules will dissolve in the presence of moisture leaks in the cover system and release chemicals or gas, which are then detected on the surface.

Advantages--Portable detection equipment sensitive to the gas or chemical can be used to survey the waste site. With this method, several instrument operators can quickly scan the site. Procedures can be set up for periodic surveys of the site.

Disadvantages--The process of encapsulation is not controllable to the point that uniform encapsulation thicknesses are achievable. This results in unreliability in the release of the gas or chemical. The amount of moisture present in the waste site and the presence of waste materials is likely to be sufficient to dissolve the capsules prematurely.

The capsules must be installed prior to the cover liner and might not withstand the pressures of the cover system. The gas or chemical might dissipate before the survey is performed. Subsequent leaks in the same area cannot be detected, because the capsules are spent after the first leak. New capsules must be installed in the leak area during the repair process.

Electronic Transponders--

If placed under the cover liner at the time of installation, electronic transponders would become energized in the presence of moisture leaking through the liner from above. The transponders could be activated by an external stimulus to conserve battery life. The transponders would emit a detectable electromagnetic or acoustic signal for detection on the surface of the impoundment. Passive sensors are feasible if the sensors are energized by a strong electromagnetic field.

Advantages--Transponder signals can be detected easily. Rapid sweeps of the area can be made by more than one operator. Sensors could de-energize automatically when the moisture level decreases. The transponders can be buried at different levels in order to achieve a longer period of detection in the area of a leak.

Disadvantages--The transponders must be placed under the cover liner at the time of installation. Surveys of the area would need to be performed soon after a saturating rain in order to detect any activated transponder. This method is potentially expensive and batteries for powering the transducers have a low life compared with the intended lifetime of a cover system.

SUMMARY

The scale model tests demonstrated the applicability of the electrical leak location method for locating leaks in the geomembrane liner of final cover systems. Small leaks can be located in a geomembrane covered with soil without the need for an overlying conductive layer of liquid. Half-cell electrodes are required to reduce electrode polarization noise. Electrode contact noise can be reduced significantly if the electrodes are inserted into the soil to penetrate the dry surface soil. A hole with a diameter of 3.2 mm covered with 60 cm of sandy loam can be detected easily.

The electrical leak location method, adapted to make surface soil potential measurements using half-cell electrodes, is particularly well suited for locating leaks in impoundment and landfill geomembranes with protective soil covers. Surveys can be performed after the protective soil cover is put in place, thereby allowing leaks caused by the soil placement operations to be located.

Further advances in ground-penetrating radar systems are needed to make them a viable means of detecting leaks in cover systems. Some of the necessary advancements include signal processing for detection enhancement and antenna improvements.

Limited testing of the infrared imaging technique was unsuccessful in detecting localized areas of low thermal conductivity caused by drainage of soil moisture through a leak. Analyses of the electromagnetic induction technique, tracer gas, and encapsulated chemicals indicate that the methods are not viable alternatives for detecting leaks in the final cover system geomembrane. Electronic transducers may be applicable to some applications, but significant additional development would be needed to reduce the cost and increase the lifetime of the transducers.

SECTION 8

LINER RESISTIVITY TESTS

BACKGROUND

The success of the electrical leak location method for surveying in-service liner installations is influenced by the electrical resistivity of the liner. The liner materials must have a resistivity that is substantially greater than the resistivity of the soil beneath the liner and the resistivity of the liquid above the liner. For example, the HDPE liner at the Southwest Research Institute test facility has a volume resistivity of approximately 10^{16} ohm-cm, the water has a volume resistivity of approximately 2×10^3 ohm-cm, and the soil has an approximate volume resistivity of 3×10^3 ohm-cm. To evaluate whether the electrical resistance of selected liner materials changes after exposure to waste liquids, thereby reducing the usefulness of the survey technique, a series of tests were conducted to measure electrical resistance changes in selected liner materials over a period of time.

OBJECTIVE

The objectives of these tests were: (1) to determine changes in the electrical resistance of various liner materials during exposure to selected liquids at room temperature and atmospheric pressure; and (2) to determine if the changes could impact the usefulness of the electrical leak location method.

RESEARCH APPROACH

Test Procedures

The tests were performed in triplicate using five different types of liner material exposed to four different liquids, requiring a total of 60 test cells.

The liner materials used in the tests were:

(1) Polyvinyl chloride (PVC) - 0.76 mm (30 mil);

(2) High-density polyethylene (HDPE) - 1.52 mm (60 mil);

(3) Chlorosulfonated polyethylene (CSPE) - 0.91 mm (36 mil), with scrim;

(4) Chlorosulfonated polyethylene (CSPE) - 1.14 mm (45 mil), with scrim; and

(5) Chlorinated polyethylene (CPER) - 0.91 mm (36 mil), with scrim.

These materials were selected for testing because they are used frequently in the liner industry. Two thicknesses of CSPE were selected in order to evaluate how the liner thickness affects changes in resistance.

The liquids used in the tests were:

(1) Alkaline: sodium hydroxide solution, pH of 10;

(2) Acidic: sulfuric acid solution, pH of 1;

(3) Brine: sodium chloride solution, 10 percent by weight NaCl dissolved in deionized water; and

(4) Deionized water.

The first three liquids were chosen because they occur frequently in industrial and municipal environments where membrane liners are used. The fourth liquid was chosen because of its aggressive swelling effects on liner materials.

The liner materials were loaded into test cells constructed of acrylic plastic. The design of these cells is shown in Figure 58. A 70-mm-diameter cylinder approximately 90 mm high was enclosed by two 13-cm square acrylic plastic plates. The plates were bolted together with four bolts. The bottom of each liner sample was painted with graphite paste and pressed in contact with brass shim stock. The brass shim stock served as the current return electrode. The plastic cylinder was placed on the liner sample and sealed with a silicone RTV sealant. A rubber stopper was placed into a hole in the top plate. A hole in the center of the stopper provided an airtight insertion point for the current source electrode.

The liner specimens were exposed on one side to the liquid in order to simulate field conditions. Measurements of the electrical resistance were made weekly using a DC power supply, a voltmeter, and picoammeter.

To measure the liner resistance, a brass rod electrode was inserted through the rubber stopper into the liquid. Voltage was applied between the brass rod electrode and the brass shim stock below the liner specimen. Current and voltage readings were recorded after a stable condition was achieved. Thus, the resistance of the entire test cell was calculated from voltage and current data. The resistance of the liquid was assumed to remain constant with time and to be insignificant when compared with the liner material. The resistance of the liner material was calculated from the measured voltage and current. The tests were conducted for 11 weeks.

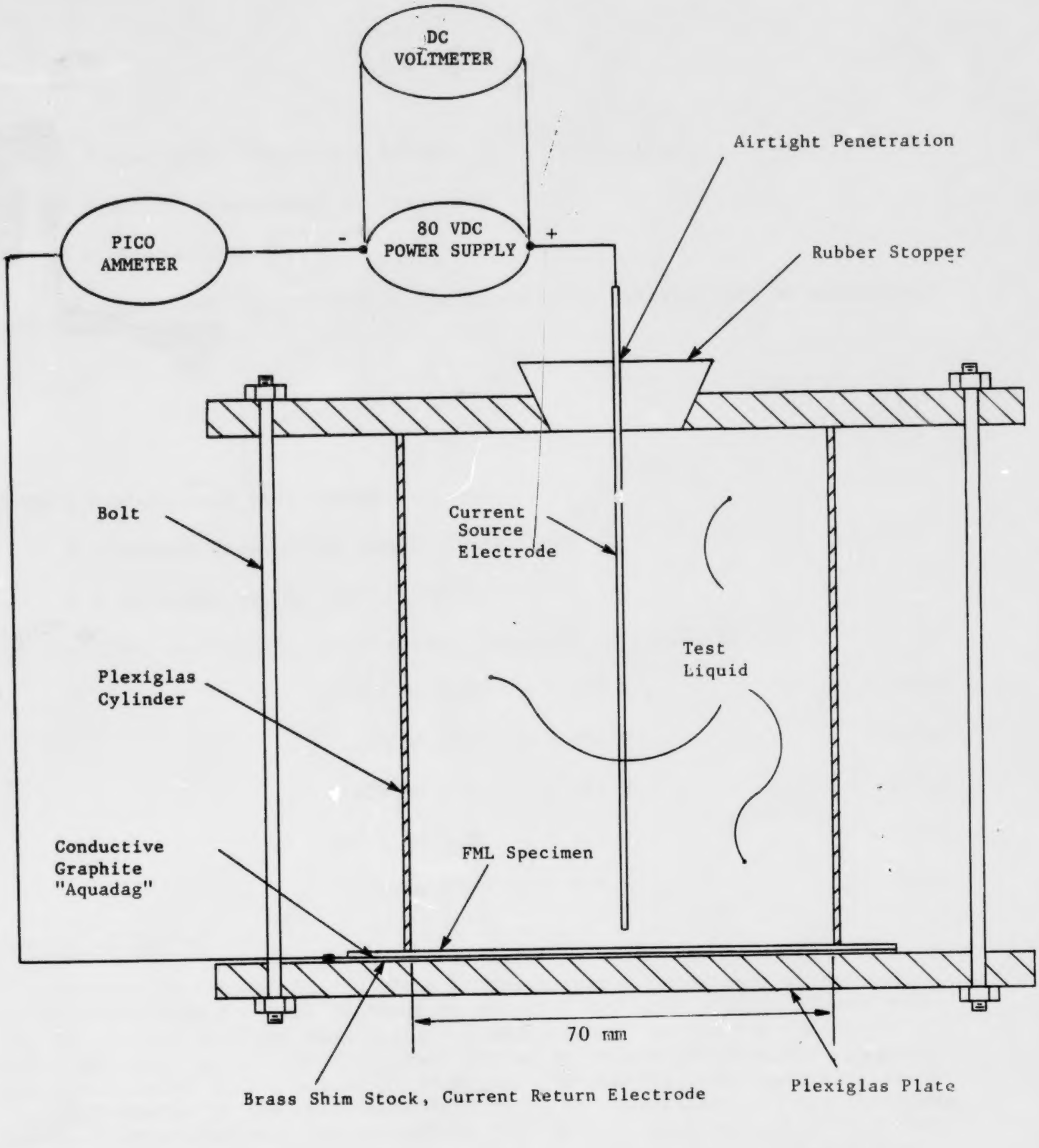
DC VOLTMETER
Airtight Penetration
PICO AMMETER
-
80 VDC POWER SUPPLY
+
Rubber Stopper
Bolt
Current Source Electrode
Test Liquid
Plexiglas Cylinder
Conductive Graphite "Aquadag"
FML Specimen
70 mm
Brass Shim Stock, Current Return Electrode
Plexiglas Plate

Figure 58. Test cell design for measuring liner resistivity during exposure to selected liquids.

Resistivity Calculations

Electrical resistance values for each test measurement have been computed using Ohm's Law:

$$R = \frac{V}{I} \tag{50}$$

where R = electrical resistance (ohms),

V = electric potential (volts), and

I = current (amperes).

The electrical resistivity of the geomembrane material can be calculated using the equation:

$$\rho = \frac{RA}{t} , \tag{51}$$

where ρ = electrical resistivity (ohm-cm)

A = exposed area of the sample (cm^2), and

t = thickness of the sample (cm^2).

For the liner resistivity measurements, Equation (51) reduces to:

1.14 mm CSPE $\rho = 335 R$, (52a)

1.52 mm HDPE $\rho = 251 R$, (52b)

1.02 mm PVC $\rho = 377 R$, (52c)

0.91 mm CSPE $\rho = 419 R$, (52d)

and 0.91 mm CPER $\rho = 419 R$. (52e)

Results of Tests

Figures 59 through 63 are plots of the measured resistance of the test cells versus time for each geomembrane material and each liquid. These data are all plotted with the same scale for comparison. In the few instances where the data was off scale, typical off-scale values are labeled. Measurements were taken over a period of 11 weeks. In general, the repeatability of the measurements of the triplicate test cells is remarkably good for the high impedance measurements. The variations from week to week typically vary ±200 percent. Most of the initial readings tend to be lower than the subsequent

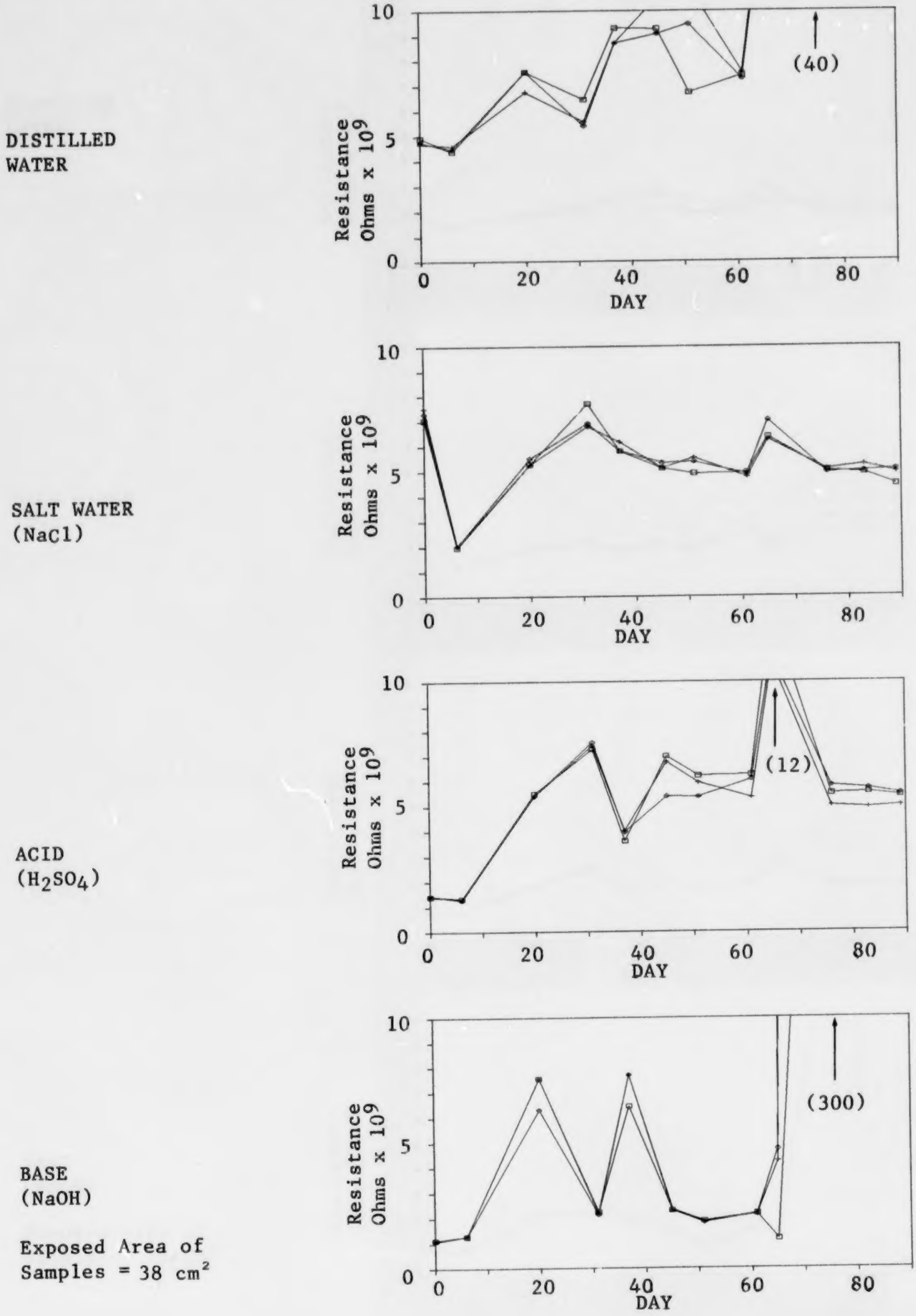

Figure 59. Resistivity versus time of 1.5 mm HDPE samples exposed to water, salt water, acid, and base.

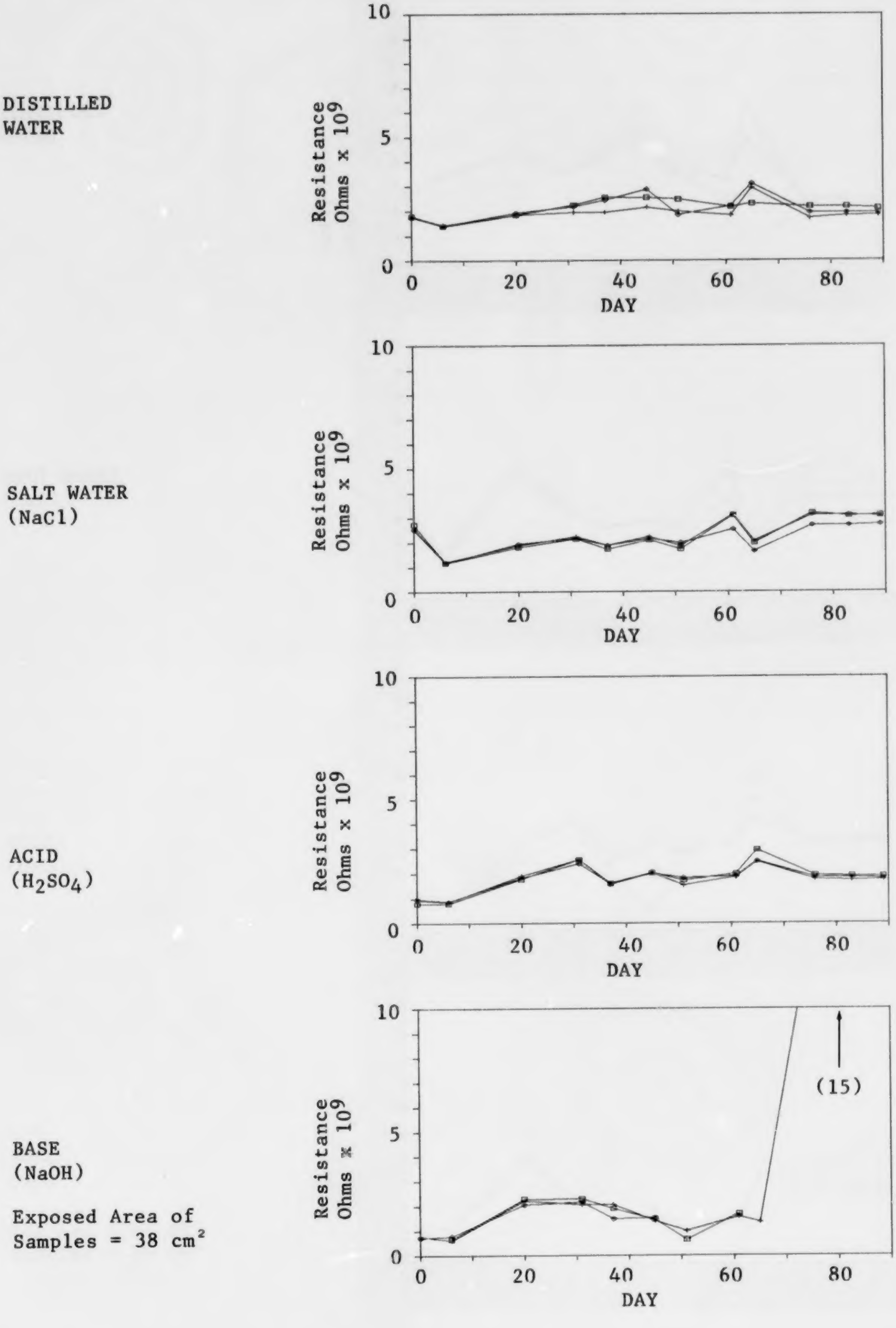

Figure 60. Resistivity versus time of 1 mm PVC samples exposed to water, salt water, acid, and base.

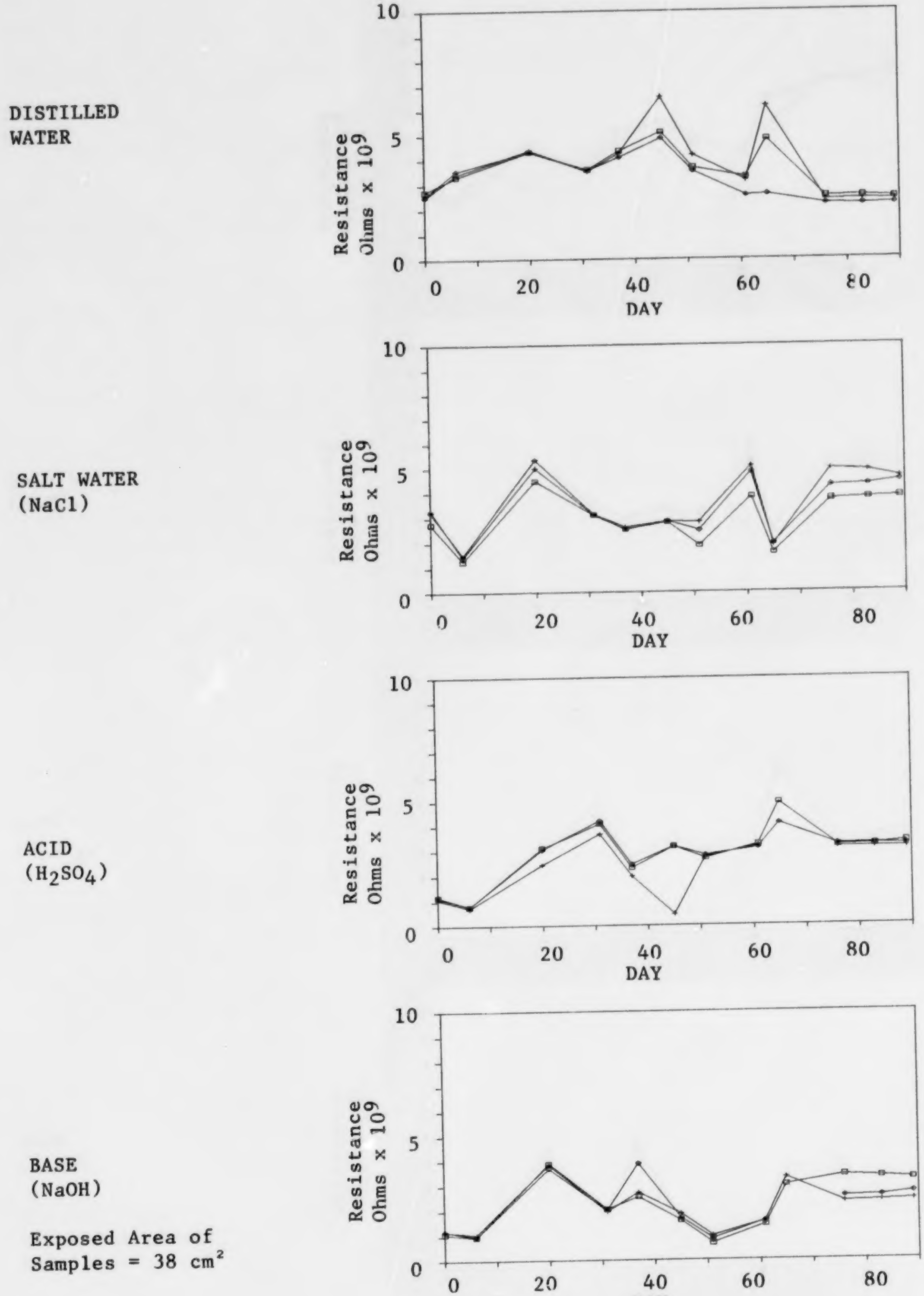

Exposed Area of Samples = 38 cm²

Figure 61. Resistivity versus time of 0.91 mm CPER samples exposed to water, salt water, acid, and base.

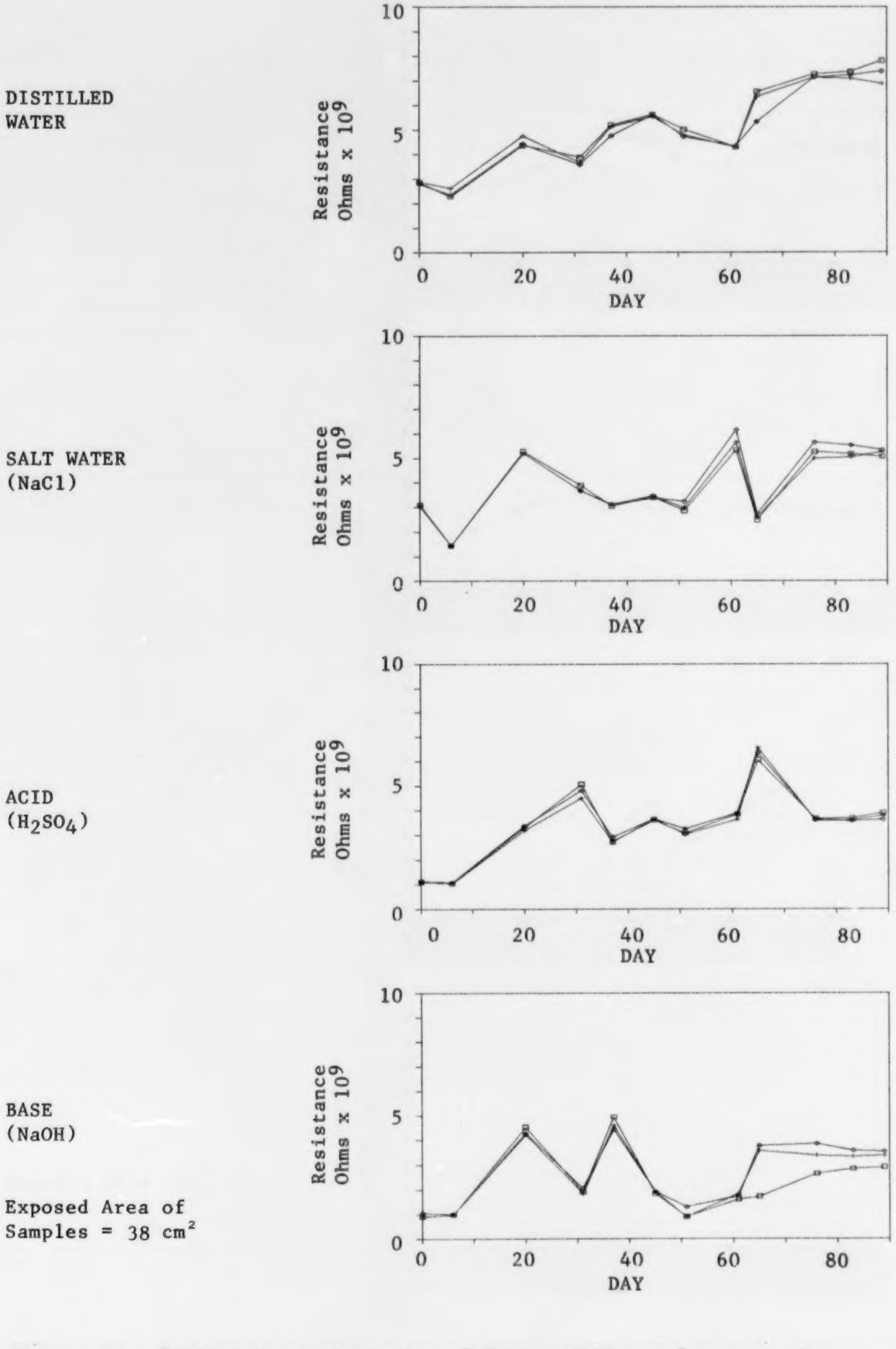

Exposed Area of Samples = 38 cm^2

Figure 62. Resistivity versus time of 0.91 mm CSPE samples exposed to water, salt water, acid, and base.

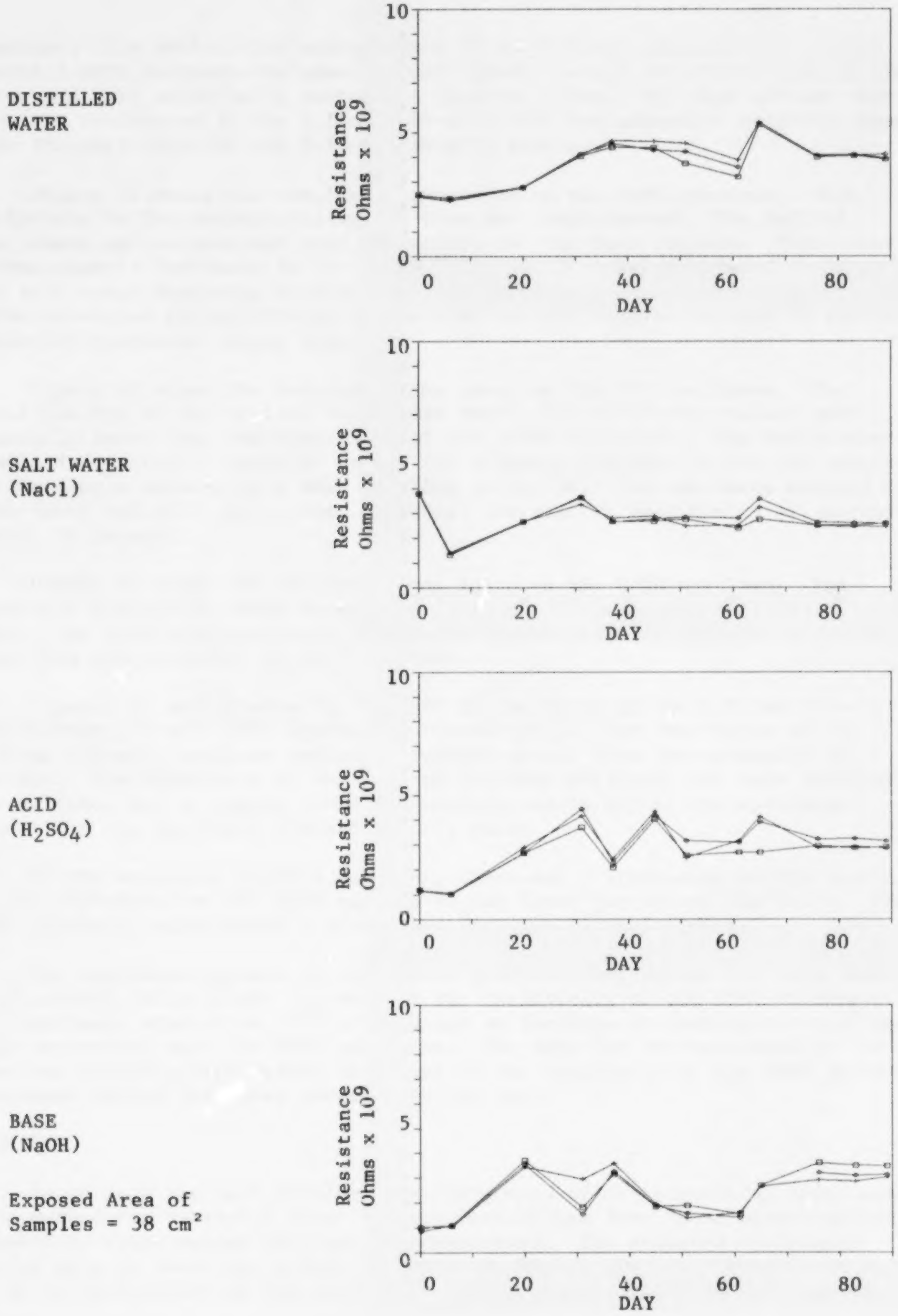
DISTILLED
WATER

SALT WATER
(NaCl)

ACID
(H_2SO_4)

BASE
(NaOH)

Exposed Area of
Samples = 38 cm^2

Figure 63. Resistivity versus time of 1.14 mm CSPE samples exposed to water, salt water, acid, and base.

readings. The resistivity measurements of the 0.91-mm (36-mil) and 1.14-mm (45-mil) CSPE followed the same general trends, except for differences in the water and salt water cells during the last two weeks. For some unknown reason, the resistance of the 1.14-mm (45-mil) CSPE was generally slightly lower than the resistance of the 0.91-mm (36-mil) samples.

Figure 59 shows the results of the tests on the HDPE specimen. Wide variations in the resistivity versus time were experienced. The initial resistance values were not very repeatable for the four liquids. There were sudden drastic increases in the resistivity of the samples exposed to water and salt water beginning with days 65 and 76. The samples exposed to the salt water decreased in resistivity versus time and the samples exposed to the acid generally increased versus time.

Figure 60 shows the results of the tests on the PVC specimens. The repeatability of the initial values was good. The resistance values were generally lower than the resistance of the other materials. The resistances remained essentially constant except for a sudden increase in the resistance of the sample exposed to a base starting at day 76. The specimens exposed to salt water and acid experienced a gradual increase in resistivity of approximately 50 percent.

Figure 61 shows the results of the tests on the CPER specimen. The specimens exposed to water experienced a slight decrease in resistance versus time. The remaining specimens experienced an increase in resistance versus time from approximately 40 to 70 percent.

Figures 62 and 63 show the results of the tests on the 0.91-mm (36-mil) and 1.14-mm (45-mil) CSPE specimens, respectively. The resistance of the 0.91-mm (36-mil) specimen typically trended upward from approximately 30 to 90 percent. The resistance of the 1.14-mm (45-mil) specimens was more constant versus time, but an upward trend was experienced in all of the specimens except for the specimens exposed to salt water.

Of the specimens exposed to water, there was a pronounced sudden increase in the resistance of the HDPE samples in the later portion of the tests. The CSPE specimens experienced a pronounced increase in resistivity.

The specimens exposed to salt water generally maintained the same resistance except for a slight increase in the resistivity of the CSPE specimens. The specimens exposed to acid experienced an increase in resistivity that was most pronounced with the HDPE specimens. The data for the specimens in the base was variable with sudden increases in the resistance of the HDPE and PVC specimens during the later portions of the test.

SUMMARY

Based upon the test results, the usefulness of the electrical leak location method for surveying liner systems constructed from these materials and exposed to these wastes will not be compromised. The measured resistance values were at least two orders of magnitude higher than the resistance needed to allow application of the electrical leak location method to impoundments of one hectare or more in area. Therefore, the relatively minor changes in electrical resistivity caused by various liquids will have no effect upon field application of the method.

Obviously, liner materials in service throughout the United States are exposed to a variety of waste materials far exceeding the four liquids included in this experiment. A valid determination of the usefulness of the technique for surveying a specific in-service liner system after long-term exposure to given waste liquids will require that these tests be performed using the specific liner material and waste liquid. Predictions of liner electrical property changes with waste exposure require a fundamental understanding of how different wastes alter the chemical and electrical properties of liner materials.

SECTION 9

FIELD DEMONSTRATION SURVEYS

BACKGROUND

Previous field tests of the electrical leak location method performed at Southwest Research Institute demonstrated the usefulness of the electrical leak location method under full-scale test conditions. The equipment required to measure surface potentials was assembled, and a survey methodology was established. A computer-controlled data acquisition program was developed and tested. Additional investigations were needed to define the performance of the technique under a wide variety of test conditions and to determine the required field operational procedures for surveying liner systems in industrial and municipal environments.

OBJECTIVE

The objectives of this project task were to: (1) demonstrate the electrical leak location method at a pre-service facility and at an in-service facility; (2) assess the existing field survey methodology as applied to these surveys and develop new procedures as required to improve the methodology; and (3) improve the quality of the data or performance of the data acquisition system based upon the results of the field survey activities.

RESEARCH APPROACH

Site Selection

Candidate surface impoundment field sites were identified and listed in two categories. The first category includes sites where a liner installation is planned or under construction. These sites allow survey technique testing before the liner is placed into service. Since the liner is readily accessible, leaks found during the survey can be verified. The sites include planned landfill and surface impoundment facilities. The second site category is in-service surface impoundments with installed liners.

Candidate lists for both categories were developed from many sources, including: (1) liner installation and manufacturing companies, (2) engineering design companies, (3) state regulatory agencies, (4) EPA records, and (5) owners of surface impoundment facilities. Prior to contacting any of the owners of these sites, this list was reviewed to select those sites which appeared to satisfy the project requirements, i.e., offered the most promising opportunity for demonstrating and testing the electrical leak location method.

The site information required to make a final selection included:

(1) Willingness of owner to authorize a survey;

(2) Willingness of liner installer to cooperate during testing; and

(3) Details regarding site geology, liner design, soil cover, etc.

The additional information needed for planned facilities or facilities under construction included:

(1) Liner installation status and schedule, and

(2) Willingness of owner to allow water flooding of the liner (required to test the liner).

The additional information needed for in-service impoundments included:

(1) Current condition of the liner, i.e., knowledge of existing leaks;

(2) Type and depth of liquid contained in the impoundment; and

(3) Ongoing monitoring activities, such as monitoring wells, leak detection systems, etc.

Site visits were made to discuss details of the survey with site owners and confirm the suitability of each site for project purposes. Backup sites were identified in the event that a survey at the primary site could not be arranged.

Results of Site Selection

Approximately 30 field sites were identified and evaluated for site surveys. The majority of these sites were new installations. Difficulties were experienced in locating in-service facilities for consideration because owners do not want to discover problems with their liner systems or they are reluctant to participate in an EPA-supported study.

Four site visits were made. Leak location surveys were completed at two of the sites. Both sites qualified as pre-service survey sites. The other two sites were unacceptable for technical reasons. The Cape May, New Jersey landfill site was unacceptable because access to the drainage layer between the two liners was limited, resulting in poor electrical contact with the current electrode. Also, the drainage layer was grounded to the earth, shunting current away from the liner. The Radford, Virginia acid waste equalization impoundment was filled with 1.5 to 2 m of calcium sulfate sludge and liquid with a pH of 1.5 to 2.0. A soil cover of graphite sand provided an electrical shunt from the liquid to ground. The first site selected was the EPA Land Treatment Research Demonstration Facility near Ada, Oklahoma. The second site selected was at a site in the San Antonio, Texas vicinity.

General Field Demonstration Test Procedures

At the time of each site visit, the owner was given a preliminary survey plan. This plan explained the procedures that would be followed and what might be required from the owner. After a site was selected, a specific site survey plan was prepared. If any equipment modifications were needed, the modified equipment was tested at the Southwest Research Institute test impoundment before being sent to the site. The site survey was completed according to the survey plan.

Tests at the EPA Land Treatment Research Demonstration Facility

Test Procedures--

A survey was performed at the EPA Land Treatment Research Demonstration Facility near Ada, Oklahoma. Appendix C contains the specific survey plan for the facility. The land treatment site includes two 0.6-hectare high-density polyethylene lined liquid impoundments. These serve as storage impoundments for surface runoff water from test plots. The primary liner of the impoundments was seeping water at rates of 2 to 6 liters per minute. The impoundments contain 60 cm to 120 cm of fresh water. Pumps are installed for transferring water from one impoundment to the other. The site manager agreed to pump each impoundment dry to allow verification of the results of a leak location survey. This site satisfied three important criteria for selection as a survey site: (1) a drainage collection layer was in place to verify the integrity of the liner; (2) the survey results could be verified after evacuation of the liquid; and (3) the primary liner was known to be leaking. In addition, the site manager was willing to cooperate to the fullest extent during the survey.

Results of Tests--

The survey was started on December 10, 1984. A mobile laboratory containing the necessary survey equipment was towed to the site. The south pond was surveyed first with the necessary equipment set up on the north side of the pond. The south pond was surveyed on 10-degree radials extending out from the current source electrode. Measurements were obtained along the 0-degree through the 180-degree radial lines, from the south berm back to within 3 m of the current electrode. To increase the data coverage along the berm, measurements were then taken along 5-degree radials from the berm back to within 15 m of the current electrode. Equipotential contour plots of these data are presented in Figures 64 and 65. These plots do not reveal the location of any leaks.

After surveys were complete from the north berm, the mobile laboratory and platform were moved to the south berm, and measurements were made along the 0-degree through 180-degree radials. This survey was performed to provide complete coverage of the liner along the north berm from the opposite direction. The results are shown in Figure 66.

The equipotential contour plots of these data did not reveal obvious leak locations. Presuming that a leak (or multiple leaks) existed, the conclusion

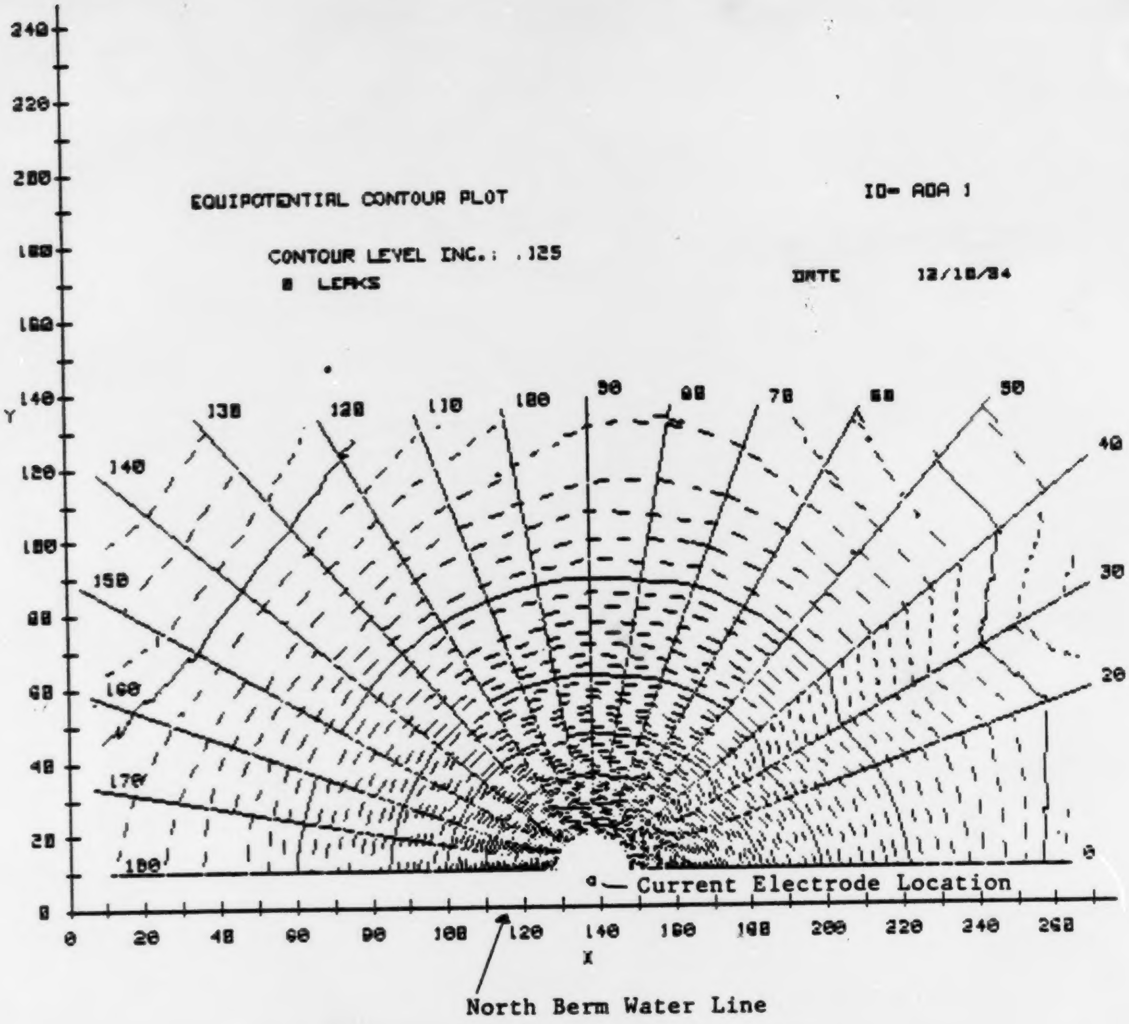

Figure 64. Equipotential contour plot of the conventional array data taken on 10 degree radials at the Ada South Pond.

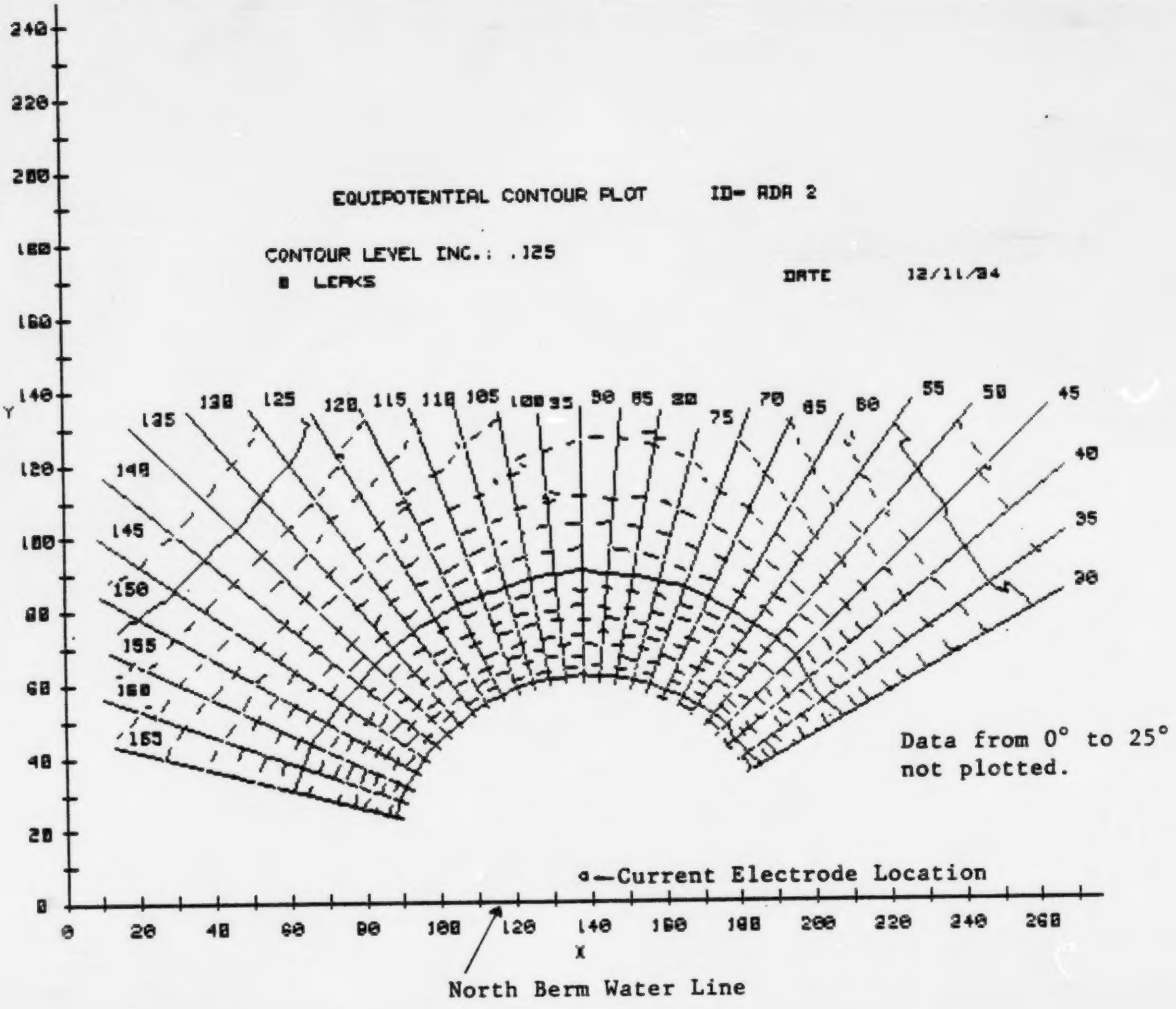

Data from 0° to 25° not plotted.

o—Current Electrode Location

North Berm Water Line

Figure 65. Equipotential contour plot of the conventional array data taken on 5 degree radials at the Ada South Pond.

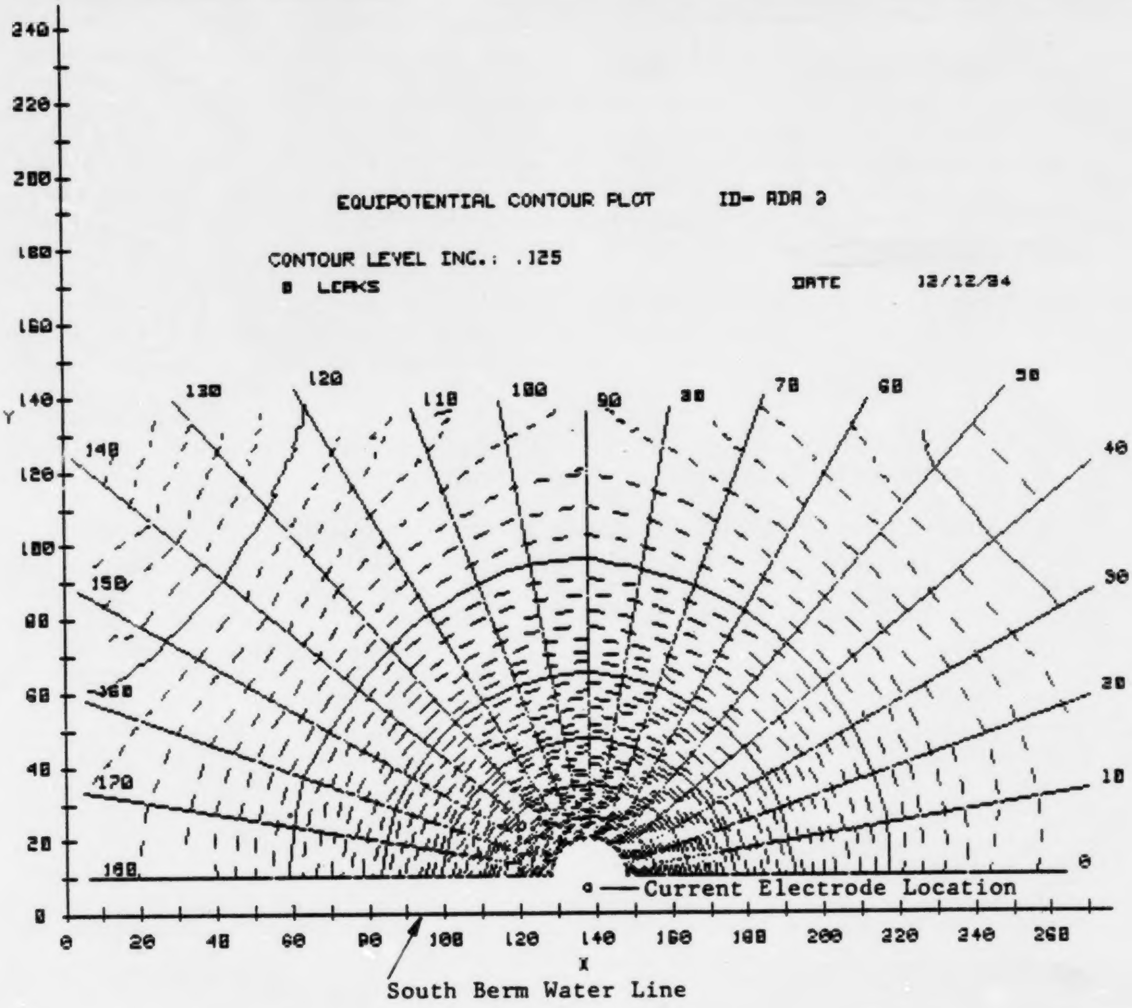

Figure 66. Equipotential contour plot of the conventional array data taken on 10 degree radials at the Ada South Pond.

was that either data had not yet been obtained close enough to the leak or that the leaks were so small as to not be distinguishable with the contour plotting data analysis technique. This conclusion was based on the absence of an obvious perturbation in the contour lines similar to what had been observed during tests conducted at Southwest Research Institute with a 5.1-square cm leak.

Measurements were then made using a simulated leak of a known size and location to assess the sensitivity of the technique under site conditions. A 3.2-square cm simulated leak was created by placing a grounded wire leak in the far corner of the pond on the bottom and along the 135-degree radial line. Measurements were made using the conventional electrode array and an experimental dipole array. The dipole probe measured the potential difference between two electrodes 1.83 m apart. Both electrodes moved together along the survey line. The conventional array includes one stationary electrode and one floating electrode with only the floating electrode moving along the survey radial. An AC signal generator was used as the current source.

The results of the simulated leak tests for the conventional and dipole arrays are presented in Figures 67 and 68, respectively. The actual location of the simulated leak is approximately 3.6 m away from the water line. The water line is located at the end of each radial survey line. The contour lines in Figure 67, while showing a small perturbation, do not close. The dipole array data plotted in Figure 68 clearly show the location of the simulated leak where the contour lines close in a concentric ring pattern.

These results indicated that the fixed dipole array was more sensitive to small leaks than was the variable array. The liner was suspected to have tears or punctures larger than the simulated test leak because of the quantity of water seeping into the collection system below the liner. The reasons why leaks were not detected using the conventional stationary electrode and single measurement electrode approach were that the holes were too small to be detected, or current flow through the leaks was not sufficiently large to produce a voltage drop measurable with the available equipment. The dipole probe test results were encouraging in that the signal-to-noise ratio was higher, which increases the sensitivity of the electrical technique.

A follow-up survey of the EPA Land Treatment Research Demonstration Facility land treatment storage ponds using the dipole was performed during the week of March 18, 1985. The purpose of this survey was to collect data on the south pond using the new dipole probe. The probe was tested to determine its sensitivity and resolution capabilities. In addition to this dipole probe, another dipole probe developed by Southwest Research Institute for commercial leak location surveys was taken. This probe differs from the first dipole probe in that it is hand-carried in the water rather than tethered to the shore by a logging cable. The hand-carried probe is used to manually search for leaks rather than to log data. The hand-carried probe system uses a DC current source instead of the AC source used with the conventional system.

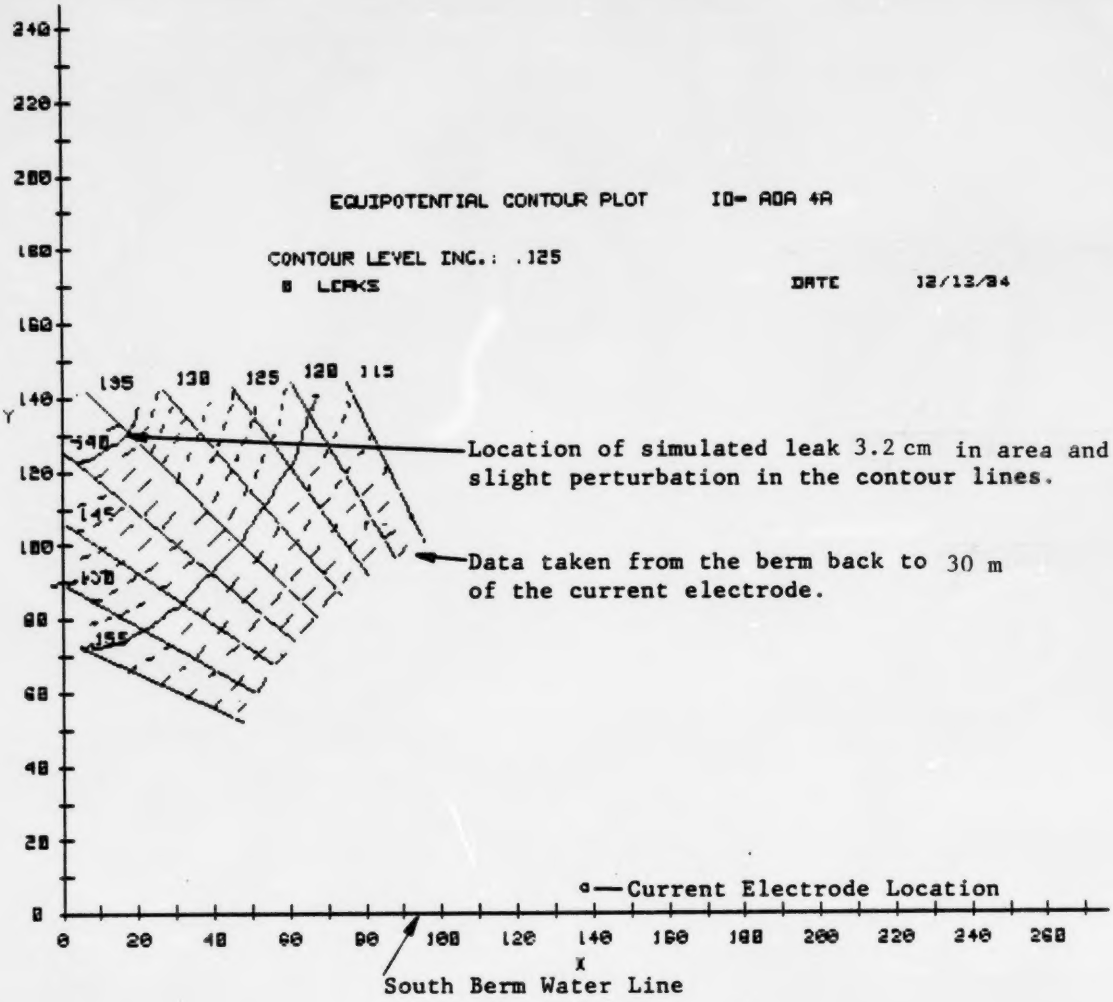

Location of simulated leak 3.2 cm in area and slight perturbation in the contour lines.

Data taken from the berm back to 30 m of the current electrode.

Current Electrode Location

South Berm Water Line

Figure 67. Equipotential contour plot of the conventional array data taken on 5 degree radials over a 3.2 cm^2 simulated leak. A slight perturbation occurred in the area of the leak, where the lines begin to curve around the leak location.

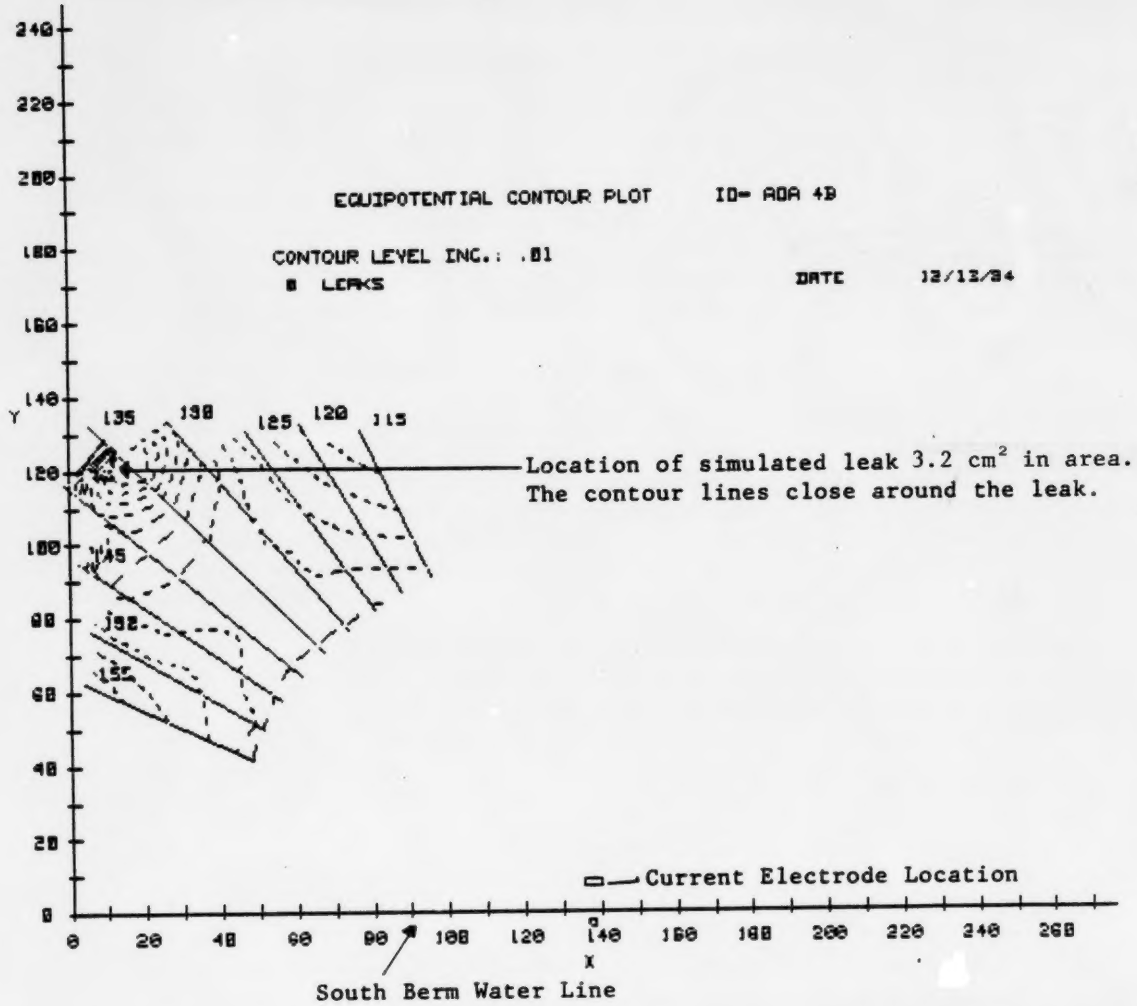

Location of simulated leak 3.2 cm^2 in area. The contour lines close around the leak.

Current Electrode Location

South Berm Water Line

Figure 68. Equipotential contour plot of the dipole array data taken on 5 degree radials over the simulated 3.2 cm^2 leak. The closed contour lines indicate the presence and location of the leak.

A survey of the north pond, which contained 1 m to 1.2 m of water, was made using the hand-held dipole probe. The tethered dipole system could not be used because the mobile laboratory could not be positioned near the pond because of muddy site conditions. Twenty-nine leaks were located and marked. Twenty-one of the leaks were at welded joints or patches. Two of the remaining leaks were between welded joints near the water line. These two leaks were verified, one visually and the other by touching. The leaks were each approximately 10 mm in diameter. The remaining leaks could not be verified at the time of the field survey.

The south pond was surveyed using both the hand-held dipole probe and the tethered dipole probe. Access to this pond with the mobile laboratory was limited; therefore, only the western half of the pond was surveyed using the tethered dipole probe. Numerous leaks were located using the hand-held probe. These leaks were generally located along welded joints. Two leaks located near the west end of the pond were verified with the tip of the hand-held probe. Twenty-five leaks were marked in the western half of the pond. The floating, tethered dipole probe was then used to measure surface voltage gradients over this area of the pond. A review of the data indicated that two leaks near the west berm were detected and located.

The results of the follow-up survey resulted in two very important conclusions. First, a DC power supply was preferable to the previously used AC source to increase the current flow through the leaks relative to the current flow through the liner. This was later documented in tests at the Southwest Research Institute test pond. With DC power, current flow through the capacitive reactance of the liner was eliminated; therefore, more of the current was available to flow through the leaks. Secondly, the signal-to-noise ratio of the dipole probe was excellent, increasing the sensitivity of the electrical leak location method.

In May 1985, a follow-up inspection of the EPA Land Treatment Research Demonstration Facility north pond was completed. The pond was drained to allow visual inspection of each leak location identified during March. Twenty-five of the twenty-nine suspected leak locations were visually verified to be holes or tears in the liner. The surface area of the three largest holes ranged between 0.6 and 1.9 square cm. The remaining 22 holes were smaller than 0.6 square cm. Four suspected leaks could not be verified by visual inspection in the field. These areas were cut out of the liner and sent by site personnel to Southwest Research Institute for further examination. Two of these specimens were verified as having leaks by examining the sample against a high-intensity lamp. Holes could not be verified in the remaining two specimens. Possibly the marker on each of these two areas had been misplaced during the survey or moved after it was placed, or the hole was so minute as to not be visible without magnification. Table 3 presents the results of the verification activity. The estimated leak areas were computed from field measurements and photographs.

TABLE 3. FIELD VERIFICATION RESULTS
ADA NORTH POND

	Location of Leak				Estimated
Leak No.*	On A Weld	On Flat Sheet	Field Verified	Lab Verified	Leak Area (mm^2)
1-CC	-	Yes	Yes	-	<190
1-A	Yes	-	Yes	-	<0.6
1-B	-	Yes	Yes	-	<0.6
1-BB	-	Yes	No	Yes	>65<130
2-AA	Yes	-	Yes	-	<6
2-C	Yes	-	Yes	-	<6
3-D	Yes	-	Yes	-	<2
3-E	Yes	-	Yes	-	<2
3-F	Yes	-	Yes	-	<6
3-Z	Yes	-	Yes	-	<6
4-G	-	Yes	Yes	-	<6
4-H	Yes	-	Yes	-	<13
5-I	Yes	-	Yes	-	<2
6-K	Yes	-	Yes	-	<6
6-J	-	Yes	Yes	-	<6
6-L	Yes	-	No	Yes	<2
6-Y	Yes	-	Yes	-	<6
7-M	Yes	-	Yes	-	<26
7-N	-	Yes	No	No	N/A
7-X	Yes	-	Yes	-	<6
8-O	Yes	-	Yes	-	<2
8-P	Yes	-	No	No	N/A
9-Q	Yes	-	Yes	-	<0.6
9-R	Yes	-	Yes	-	<0.6
9-W	-	Yes	Yes	-	<190
10-S	-	Yes	Yes	-	<6
10-V	Yes	-	Yes	-	<65
11-5	Yes	-	Yes	-	<0.6
13-U	Yes	-	Yes	-	<0.6

*Corresponds to weld number; welds numbered 1 to 13 from west to east.

Equipment and Survey Procedure Modifications

Modifications--

A series of tests was performed at the Southwest Research Institute test impoundment using survey equipment with design improvements identified during the EPA Land Treatment Research Demonstration Facility survey. The objective of these tests was to establish the performance of the equipment in detecting and locating small leaks. A new computer, data acquisition software, and contour plotting program were tested. The winch was modified for operation by one person instead of two people. The spacing of the electrodes on the dipole probe was modified to be adjustable from 60 cm to 180 cm. The electrodes were modified so that potential measurements could be taken at positions from the surface of the water to a maximum depth of 60 cm. These modifications provided the flexibility to survey in shallow water and to take more detailed survey data. Measurements were taken either along radial survey lines, as before, or along parallel survey lines.

Results of Equipment and Survey Procedure Modifications--

A survey of the Southwest Research Institute test impoundment was performed to determine if the technique can detect and locate four small circular leaks, each 0.79 mm in diameter. These leaks are one-sixteenth the diameter of the smallest leaks detected during the previous contract period using the old equipment. The survey was taken along 36 parallel lines, each 33.5 m long and spaced 60 cm apart. The total liner surface area surveyed was 21.3 m x 33.5 m. Figure 69 shows the location of the survey area and the leak locations. Line No. 10 crosses directly over three of the leaks. Line No. 29 crosses over the fourth leak. Measurements were taken every 15 cm along each line with the electrodes at a depth of 30 cm. The impoundment was filled with water to a depth of approximately 46 cm.

Figure 70 shows a plot of the potential measurements along line No. 10. Three dipolar anomalies indicate the presence of the three leaks. The voltage anomalies due to the leaks are detectable 1.5 m away from the leaks. The anomalies caused by the 0.79-mm diameter leaks are at least 10 times larger than the higher frequency measurement noise. The anomalies consist of adjacent peaks of opposite polarity. This response is as predicted by the computer simulation model. The approximate location of the leak is midway between the positive and negative peaks. Because the potential measurements were made only every 15 cm, the actual location accuracy was better than 15 cm when the electrodes were scanned 15 cm above the leak.

The peak-to-peak amplitude of the leak signatures differed even though the leaks were the same size. This variation can be explained by a difference in the electrical resistance of each leak due to different current return paths. The electrical resistance controls the current density and hence the resultant voltage anomaly of each leak.

Figure 71 is a plot of the voltage measurements along survey line No. 29 plotted with the same scale as Figure 70. The plot shows a similar, but smaller amplitude leak signature. Leak 4 was located approximately 36.6 m from the water line. The measurements indicated the leak to be located 37.2 m from the water line.

An equipotential contour plot was generated using the 8640 potential gradient measurements taken along 36 survey lines. Figure 72 shows this computer-generated plot with 0.05-volt contour intervals. Contour plots of potential gradient data must be interpreted differently than contour plots of absolute potential. With contour plots of absolute potential, a leak is indicated by a concentric circle pattern centered on or near the leak. With contour plots of potential gradient data, leaks are indicated by characteristic dipolar responses consisting of adjacent peaks and depressions with closely spaced contour lines between. The leak is located midway between the peak and the depression. Figure 72 graphically shows four of these patterns at locations corresponding to the locations of the four leaks. The closed contour

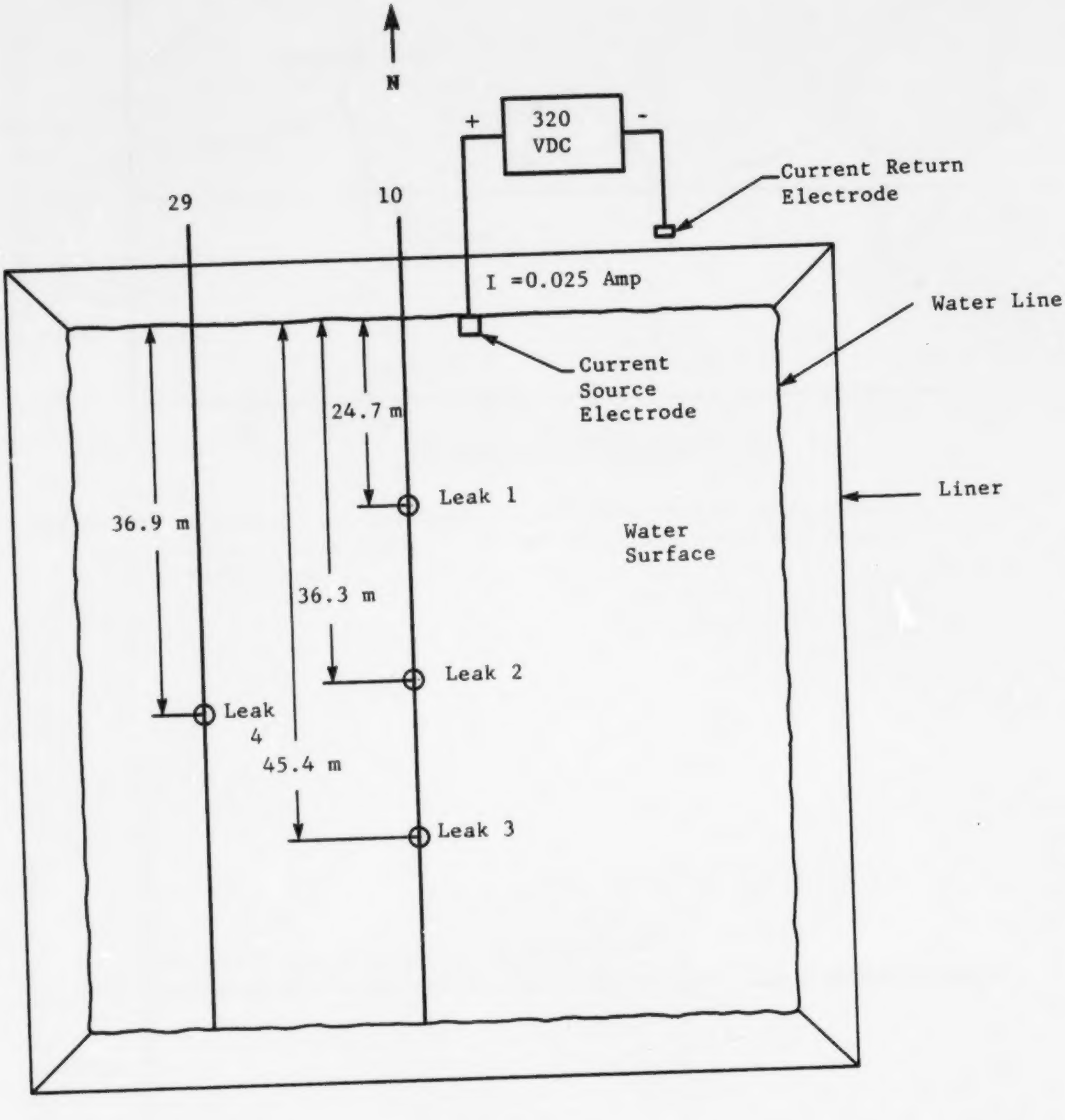
N
320
VDC
+
-
Current Return Electrode
29
10
I =0.025 Amp
Water Line
Current Source Electrode
24.7 m
Leak 1
Liner
36.9 m
Water Surface
36.3 m
Leak 2
Leak 4
45.4 m
Leak 3

Figure 69. A plan view of the test impoundment showing the location of four 0.76 mm diameter leaks, survey lines 10 and 29, and positions of the current source and return electrodes.

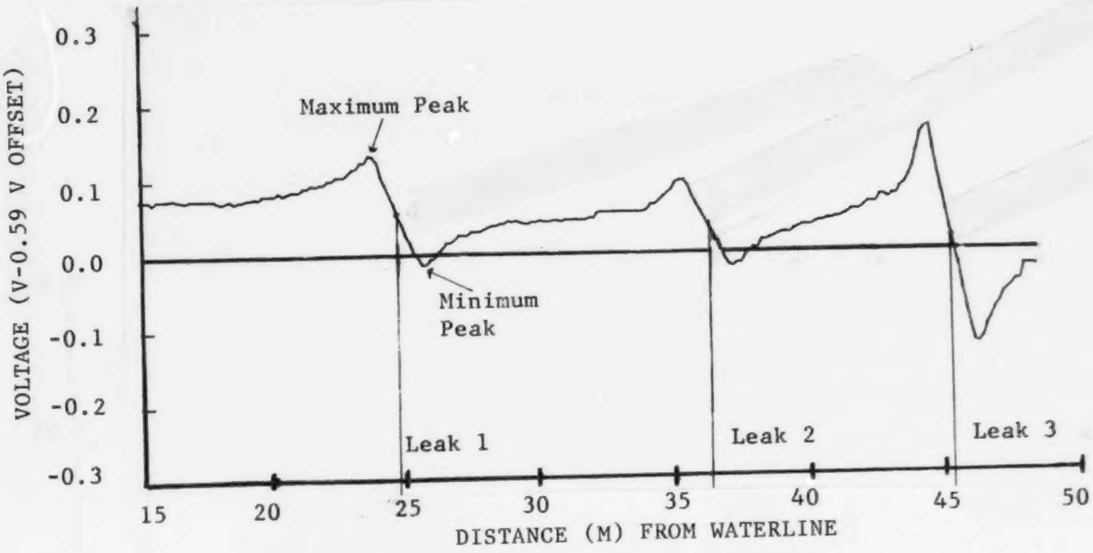

Figure 70. A plot of the potential measurements taken along survey line 10 over leaks 1, 2, and 3 clearly shows the leak signatures.

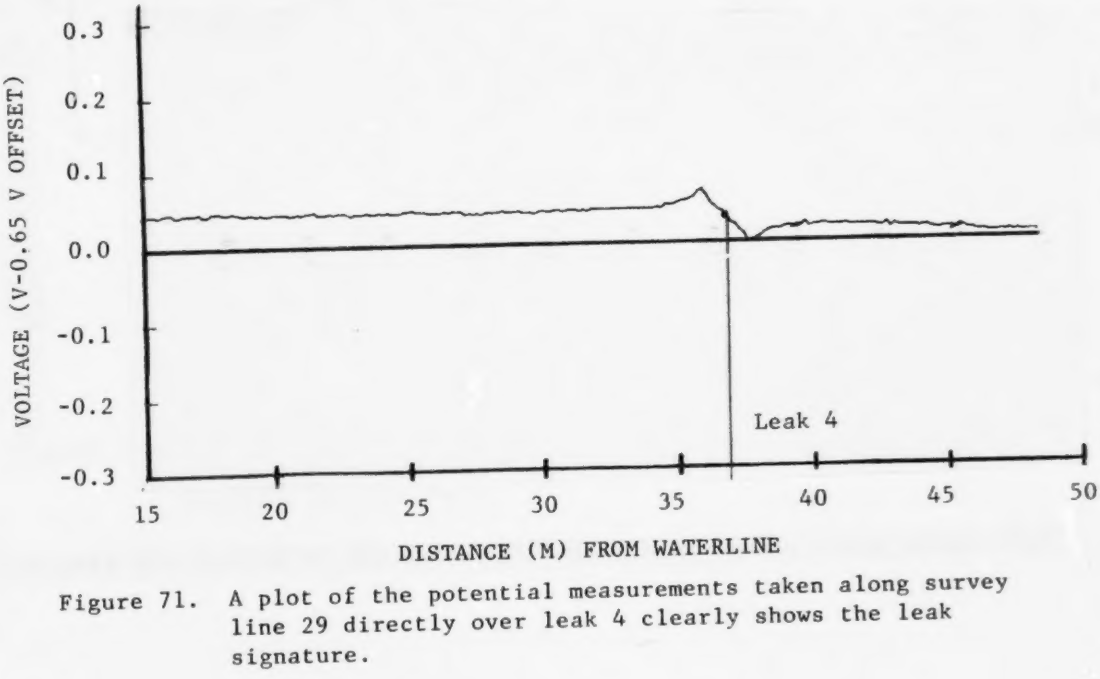

Figure 71. A plot of the potential measurements taken along survey line 29 directly over leak 4 clearly shows the leak signature.

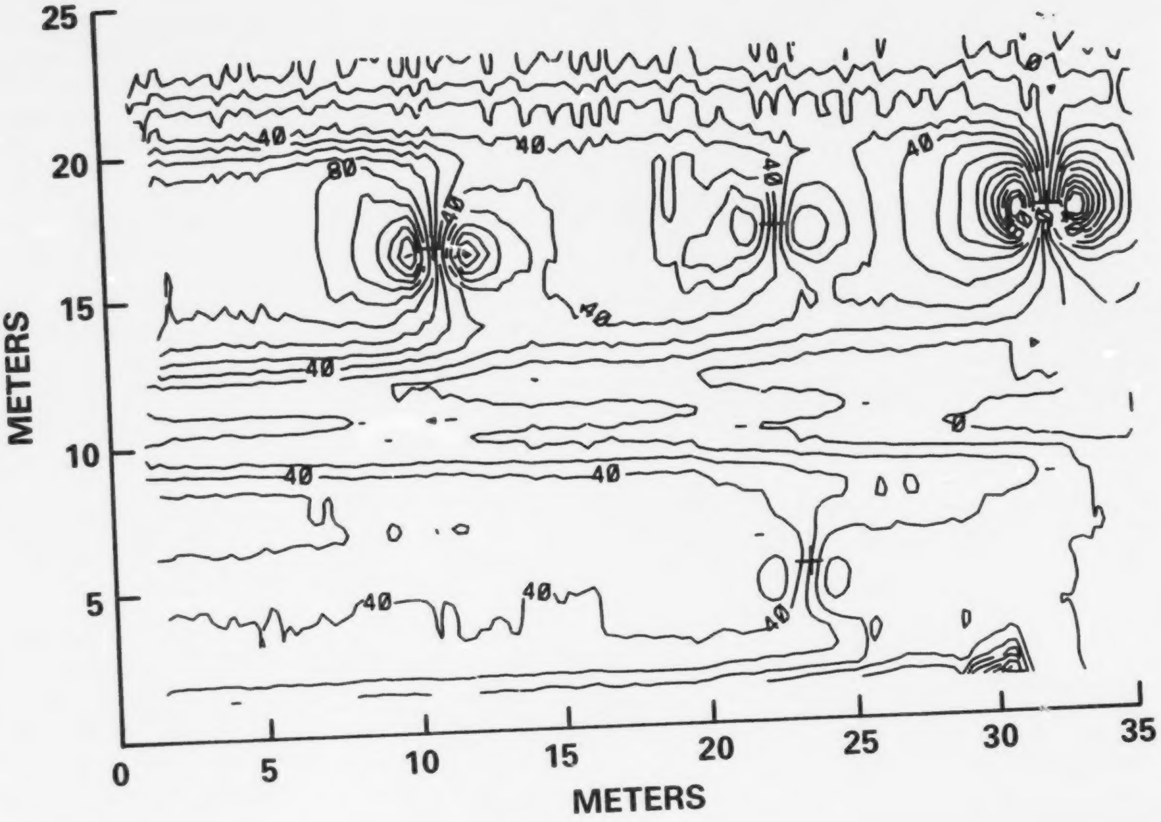

Figure 72. The locations of four 0.81 mm diameter leaks are indicated by electrical dipole patterns shown in the potential gradient contour data.

lines correspond to the opposite polarity peaks in the data plotted in Figures 70 and 71. The closely-spaced contour intervals correspond to the steep change in voltage between the peaks. The contour plot, together with the potential plots for each survey line, provide a straightforward means to analyze and interpret the data for leak detection and location purposes.

Tests at Facility in the Vicinity of San Antonio, Texas

Test Procedure--

The electrical leak location method was demonstrated at a full-scale impoundment in the San Antonio, Texas area. The full-scale field evaluations were conducted at a newly constructed lined impoundment where a double liner system was installed but not yet placed into service. Appendix D contains the specific site survey plan for the facility in the vicinity of San Antonio, Texas.

Only slight modifications to the site survey plan were necessary. These modifications were:

(1) Water was pumped into the impoundment to cover the bottom of the impoundment to a minimum depth of approximately 15 cm. The source of the water was not determined.

(2) There was no need to reference the survey line markings to nearby fixed permanent locations outside the impoundment.

(3) The potential electrode spacing was 192 cm.

(4) A list of the location of the leaks found was not necessary.

(5) A follow-up visit to the site after the impoundment was drained was not needed.

Figure 73 shows the instrumentation set-up for the field demonstration survey in the vicinity of San Antonio. The system control unit and computer are set up on a truck tailgate. The winch is mounted on a trailer towed by the truck. The dual-drum winch system with a four conductor cable and nylon rope were used to pull the sensor assembly back and forth across the pond. Figure 74 shows the dipole probe and isolation amplifier being towed along a survey line. The sensor assembly consisted of two flexible weighted electrodes connected to an isolation amplifier located on a floating electrode spreader assembly. The electrodes dragged on the bottom of the impoundment. A pulley was located near the water level at each end of the survey lines. An electronic odometer measured the distance traveled by the sensor. A Hewlett-Packard Model 226 computer and interface cards controlled the data acquisition and recorded the data on flexible magnetic disks. The computer plotted the data as the data was being acquired.

Figure 75 shows the plan view of the impoundment. The impoundment will have a double geomembrane liner constructed with 1.52 mm (60-mil) HDPE liner

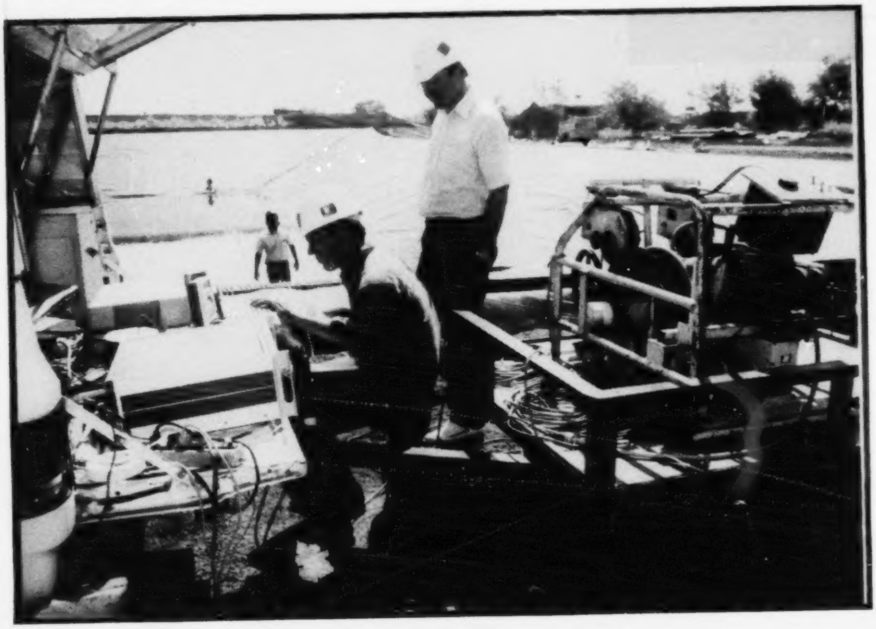

Figure 73. The instrumentation set-up for the full-scale tests in the vicinity of San Antonio included the system control unit, computer, and dual-drum winch.

Figure 74. The electrode assembly is being towed along a survey line.

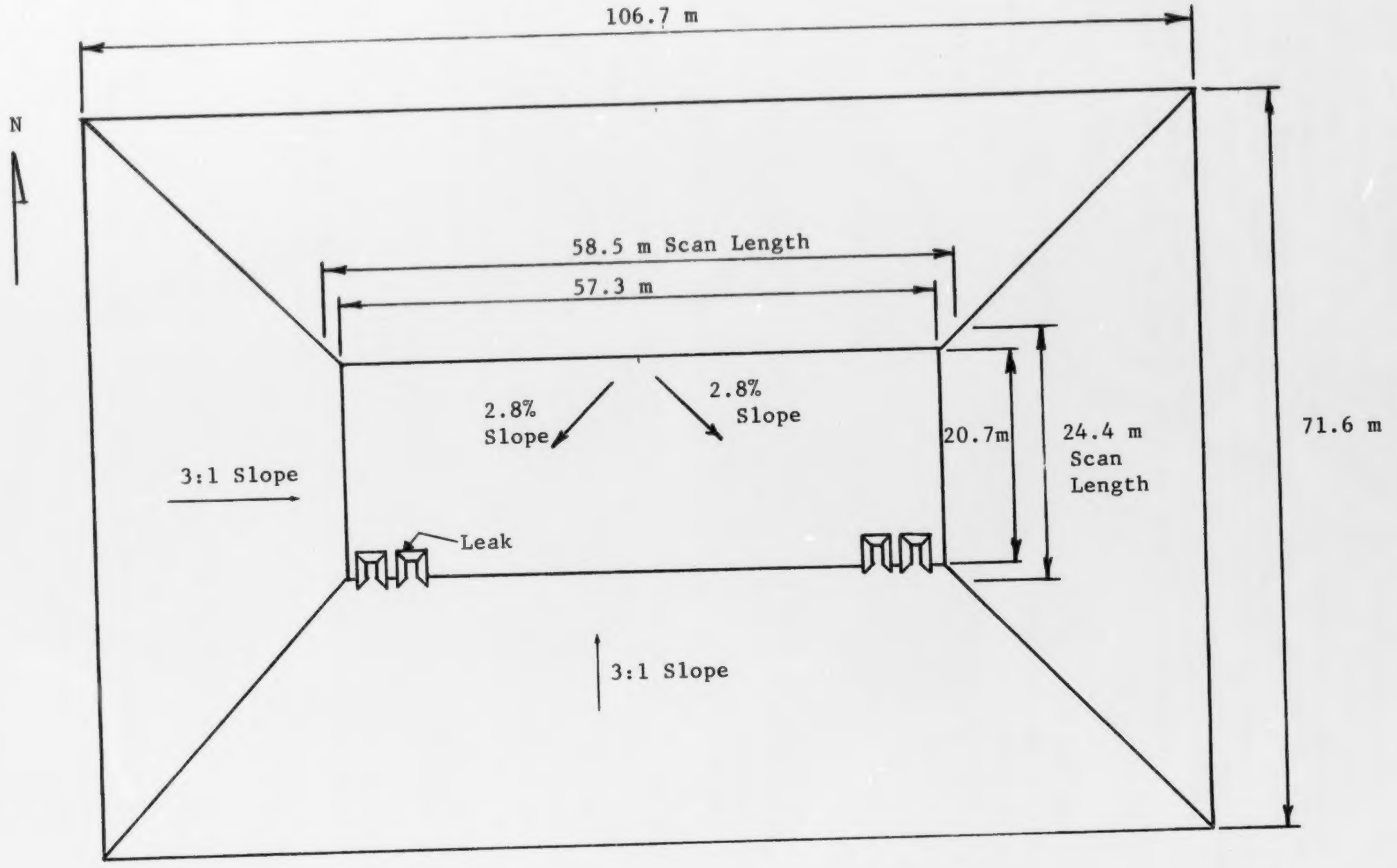
106.7 m
N
58.5 m Scan Length
57.3 m
2.8%
Slope
2.8%
Slope
20.7m
24.4 m
Scan
Length
71.6 m
3:1 Slope
Leak
3:1 Slope

Figure 75. Diagram of impoundment with leak located.

material. At the time of the tests, only the secondary liner was in place. The depth of the impoundment is approximately 5.5 m and the sidewall slopes are 3:1. The bottom of the secondary liner has a compound angle that slopes downward to two of the corners. The impoundment was filled only to cover the bottom with a minimum of 15 cm of water. The flooded area was approximately 24 m × 58 m. The maximum depth of the water was approximately 107 cm, not including the four sumps. The impoundment was ideal for the tests because the geomembrane liner had no electrical penetrations such as drain lines. All of the geomembrane liner except for the corners and sump corners had been tested for leaks using the vacuum box method. All of the leaks found with the vacuum box were repaired prior to the electrical leak location survey.

Results of Tests--

The leak location survey was started on September 3, 1987 and completed on September 5, 1987. Only one leak was found. The leak was in the inside corner of a sump as previously shown in Figure 75. The general location of the leak was 18.6 m south and 4.6 m east from the northwest corner of the pond. Figure 76 shows the very distinctive measured anomaly caused by the leak. The leak anomaly is clearly evident and no other anomalies are present. A manual leak location survey of approximately three-fourths of the seams and one-fourth of the remainder of the geomembrane liner did not locate any additional leaks.

The maximum anomaly measured was 1.65 volts peak-to-peak. The leak anomaly was detected on survey lines up to 1.5 m away from the leak. The DC power injected was 83 milliamperes at 100 volts nominally. The resistivity of the sample of the water was measured to be 1500 ohm-cm.

The leak consisted of two holes spaced approximately 32 mm apart on either side of a wide seam. Evidently, stress was concentrated adjacent to a heavy buildup of seam filler material, resulting in the leaks. One leak was parallel to the seam and approximately 20 mm long and 2.5 mm wide. The smaller leak was approximately 3.8 mm long and 1.0 mm wide. Because the impoundment had been tested using the vacuum box method and because subsequent follow-up tests revealed no additional leaks, the deduction was made that no ther leaks were present.

Because of regulatory restrictions, the impoundment operator would not allow the survey of the primary liner. If the drainage layer had been flooded as required to conduct the survey of the primary liner, residual water collected in the drainage system would have to be analyzed periodically to show that the water was not leachate.

SUMMARY

The EPA Land Treatment Research Demonstration Facility survey results demonstrated the usefulness of the electrical leak location method in an uncontrolled field environment. The need for additional design improvements and further tests of capabilities under controlled conditions was indicated, however.

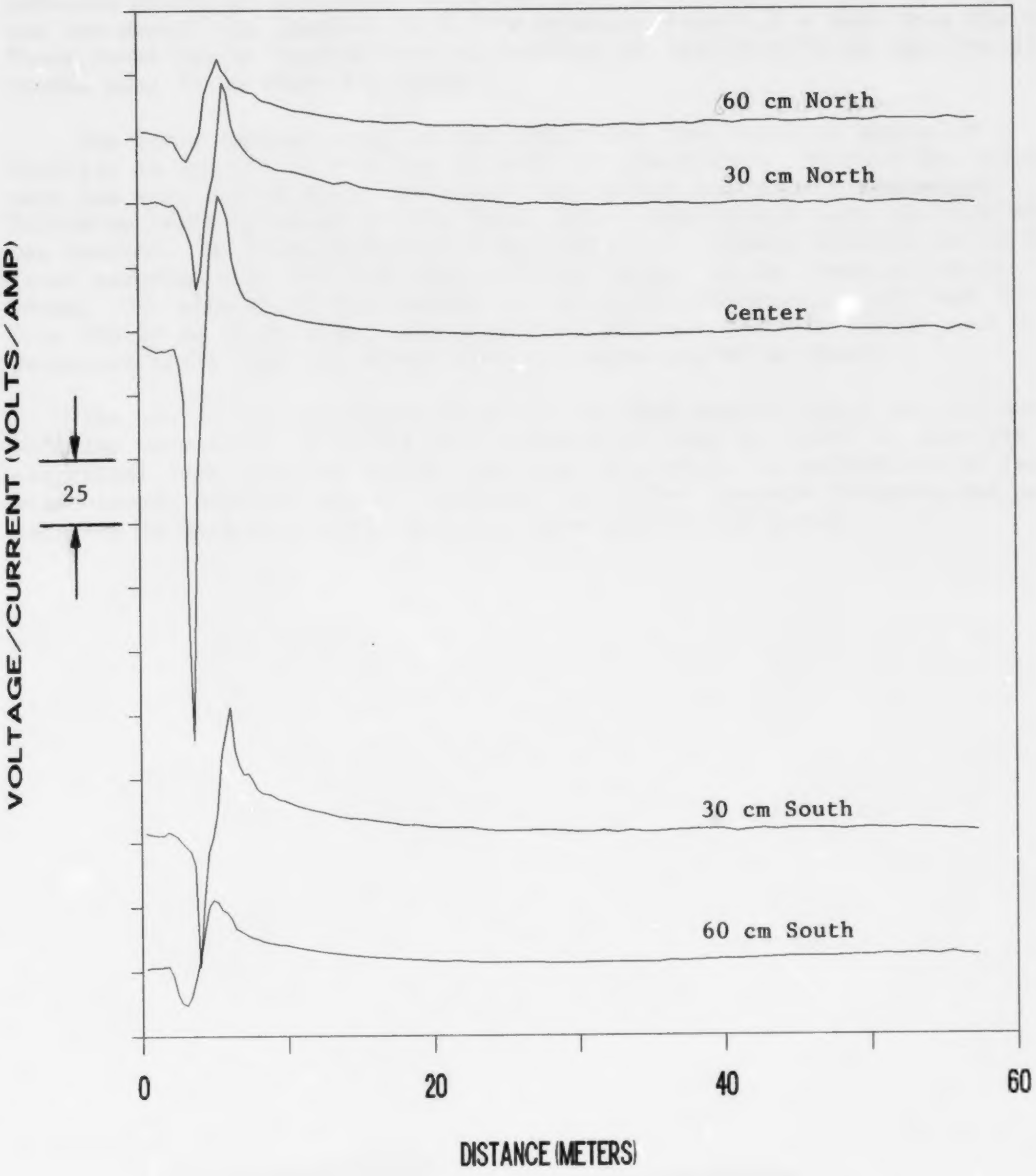

Figure 76. Scan data taken near leak.

The modified hardware and software were demonstrated to be an effective system for detecting and locating leaks in geomembrane liners. The equipment measures potential gradients, logs the data, and plots the results. The system can detect the presence of 0.8-mm diameter leaks 1.5 m away from the leak. These leaks can be located with an accuracy of less than 15 cm when the electrodes pass 15 cm above the leaks.

The field demonstration of the electrical leak location method at a facility in the vicinity of San Antonio was successful. Because the impoundment had been tested using the vacuum box method and because subsequent follow-up tests revealed no additional leaks, most likely only one leak area was present. No false indications were obtained. Visual examination of the liner revealed that the leak signature was caused by two close proximity leaks. The electrical leak survey did not differentiate a second leak 32 mm from the 20 mm crack leak. For practical purposes there is little need to delineate leaks that are closer than approximately 80 mm apart.

The system was successful in acquiring high quality data, but the survey was time consuming. A faster data acquisition rate is needed to make the electrical leak location method more cost effective. A combination of faster winch speed, multiple sensor channels, and faster computer hardware and software can be used to greatly increase data acquisition speed.

REFERENCE

Anderson, W.L., 1979, Numerical integration of related Hankel transforms of order 0 and 1 by adaptive digital filtering: *Geophysics*, 44, 1287-1305.

BIBLIOGRAPHY

Fitterman, D.V., 1979, Relationship of the self-potential Green's function to solution of controlled-source direct-current potential problems: Geophysics, 44, 1879-1881.

Parra, J.O., 1988, Electrical response of a leak in a geomembrane liner: To be published in Geophysics, 53.

Parra, J.O., and Owen, T.E., 1988, Model studies of electrical leak detection surveys in geomembrane-lined impoundments: To be published in Geophysics, 53.

Shultz, D.W., Duff, B.M., and Peters, W.R., 1984, Electrical resistivity technique to assess the integrity of geomembrane liners: Final Technical Report, U.S. Environmental Protection Agency, Contract 68-03-30331, SwRI Project 14-6289.

Shultz, D.W., Parra, J.O., and Darilek, G., 1986, Testing of the geomembrane survey technique: Interim Status Report, U.S. Environmental Protection Agency, Contract 811771-01-0, SwRI Project 14-8263.

APPENDIX A

GREEN'S FUNCTION FOR A LEAK IN A GEOMEMBRANE LINER

A liquid impoundment or landfill characterized by a waste material layer, a thin plastic liner, and a semi-infinite soil half-space may be simulated by a three-layer model. This model consists of a waste material medium of resistivity, ρ_w, and thickness, h; a geomembrane liner of resistivity, ρ_ℓ, and thickness, t; and an underlying semi-infinite soil medium of resistivity, ρ_s.

A point source of current is located at the position, $P_o(x_o, y_o, z_o)$, in the geomembrane liner layer, and the potential field is measured at the position, $P(x, y, z)$, in the waste material.

The Green's function for the electrical potential satisfies the following equations

$$\nabla^2 G_w(x,y,z;\ x_o,y_o,z_o) = 0; \text{ for } 0 < z < h, \tag{A-1}$$

$$\nabla^2 G_\ell^+(x,y,z;\ x_o,y_o,z_o) = -\delta(x - x_o)\delta(y - y_o)\delta(z - z_o);$$

$$\text{for } h < z < z_o, \tag{A-2}$$

$$\nabla^2 G_\ell^-(x,y,z;\ x_o,y_o,z_o) = -\delta(x - x_o)\delta(y - y_o)\delta(z - z_o);$$

$$\text{for } z_o < z < h + t, \tag{A-3}$$

and

$$\nabla^2 G_s(x,y,z;\ x_o,y_o,z_o) = 0; \text{ for } z > h + t, \tag{A-4}$$

where

$$\nabla^2 = \left(\frac{\partial^2}{\partial x^2} + \frac{\partial^2}{\partial y^2} + \frac{\partial^2}{\partial z^2}\right).$$

The Green's function for the electrical potential may be developed using the Hankel transform representation of the free-space Green's function in cylindrical coordinates defined by

$$G(r,z;\, r_o,z_o) = \int_0^\infty e^{-\lambda|z-z_o|}\, J_o(\lambda|r - r_o|)\, d\lambda. \tag{A-5}$$

Thus, the Green's functions for the regions of different electrical properties are:

For the region $0 < z < h$:

$$G_w = \int_0^\infty [f_w(\lambda)e^{-\lambda z} + g_w(\lambda)e^{\lambda z}]\, J_o(\lambda|r - r_o|)\, d\lambda; \tag{A-6}$$

For the region $h < z < z_o$:

$$G_\ell^+ = \int_0^\infty [e^{\lambda(z-z_o)} + f_\ell(\lambda)e^{-\lambda z} + g_\ell(\lambda)e^{\lambda z}]\, J_o(\lambda|r - r_o|)\, d\lambda; \tag{A-7}$$

For the region $z_o < z < h + t$:

$$G_\ell^- = \int_0^\infty [e^{-\lambda(z-z_o)} + f_\ell(\lambda)e^{-\lambda z} + g_\ell(\lambda)e^{\lambda z}]\, J_o(\lambda|r - r_o|)\, d\lambda. \tag{A-8}$$

For the region $z > h + t$:

$$G_s = \int_0^\infty f_s(\lambda)e^{-\lambda z}\, J_o(\lambda|r - r_o|)\, d\lambda; \tag{A-9}$$

where $|r - r_o| = [(x - x_o)^2 + (y - y_o)^2]^{1/2}$. The factors $f_\ell(\lambda)$, $g_\ell(\lambda)$, $f_w(\lambda)$, $g_w(\lambda)$, and $f_s(\lambda)$ are arbitrary functions of λ which render the integrals convergent and satisfy the following boundary conditions:

No vertical current flow out of the waste material surface

$$\left(\frac{\partial G_w}{\partial z}\right)_{z=0} = 0. \tag{A-10}$$

At the layer interfaces continuity of potentials and current densities are required:

$$[G_w]_{z=h} = [G_\ell^+]_{z=h}, \tag{A-11}$$

$$\frac{1}{\rho_w}\left(\frac{\partial G_w}{\partial z}\right)_{z=h} = \frac{1}{\rho_\ell}\left(\frac{\partial G_\ell^+}{\partial z}\right)_{z=h}, \tag{A-12}$$

$$[G_\ell^-]_{z=h+t} = [G_s]_{z=h+t}, \tag{A-13}$$

and

$$\frac{1}{\rho_\ell}\left(\frac{\partial G_\ell^-}{\partial z}\right)_{z=h+t} = \frac{1}{\rho_s}\left(\frac{\partial G_s}{\partial z}\right)_{z=h+t}. \tag{A-14}$$

From the first, second, and third conditions stated above,

$$g_\ell(\lambda)\chi + f_\ell(\lambda)e^{-2\lambda h} = -\chi e^{-\lambda z_o}, \tag{A-15}$$

where

$$\chi = -\frac{k_{\ell w} + e^{-2\lambda h}}{1 + k_{\ell w}e^{-2\lambda h}}, \tag{A-16}$$

in which

$$k_{\ell w} = \frac{\rho_w - \rho_\ell}{\rho_w + \rho_\ell}. \tag{A-17}$$

The second equation, which determines the unknown functions $g_\ell(\lambda)$ and $f_\ell(\lambda)$, can be obtained by applying the last two boundary conditions. Thus,

$$g_\ell(\lambda) + f_\ell(\lambda)\zeta\, e^{-2\lambda(h+t)} = -\,\zeta e^{-\lambda[2(h+t)-z_o]}, \tag{A-18}$$

where

$$\zeta = \frac{\rho_\ell - \rho_s}{\rho_\ell + \rho_s} = k_{s\ell}. \tag{A-19}$$

Upon solving the system of equations for the unknown coefficients $f_\ell(\lambda)$ and $g_\ell(\lambda)$, the resulting Green's function for the region above the leak may be derived and is given by

$$G_w = \int_0^\infty \frac{(1 + k_{\ell w})\,[e^{-\lambda z_o} - k_{s\ell}\, e^{-\lambda[2(h+t)-z_o]}]}{1 + k_{\ell w}\, k_{s\ell}\, e^{-2\lambda t} + (k_{\ell w} + k_{s\ell}\, e^{-2\lambda t})\, e^{-2\lambda h}}$$

$$\times\, [e^{\lambda z} + e^{-\lambda z}]\, J_o(\lambda|r - r_o|)\, d\lambda. \tag{A-20}$$

In a highly resistive and thin liner of thickness, t, and resistivity, ρ_ℓ, and with a current source at the position, $z_o = h$, the approximations $\rho_\ell \gg \rho_w$ and $\rho_\ell \gg \rho_s$ and $t \ll h$ reduce the Green's function G_w given by Equation (A-20) to

$$G_w \cong \int_0^\infty \frac{\rho_w}{\rho_\ell}\, \frac{2(\rho_s + \lambda t \rho_\ell)[e^{-\lambda(h+z)} + e^{-\lambda(h-z)}]}{[\rho_w + \rho_s + \lambda t \rho_\ell - (\rho_s - \rho_w + \lambda t \rho_\ell)e^{-2\lambda h}]}$$

$$\times\, J_o\,(\lambda|r - r_o|)\, d\lambda; \qquad \text{for } 0 \leq z \leq h. \tag{A-21}$$

In this equation, ρ_w, ρ_ℓ, and ρ_s are the resistivities of the waste material, the liner, and the soil, respectively; $\rho_\ell t$ is the total transverse resistance of the geomembrane liner.

APPENDIX B

ELECTRICAL POTENTIAL FOR A CURRENT SOURCE LOCATED IN A THREE-LAYER MEDIUM

For the case in which the current source is located in the upper layer of a three-layer half-space at the position (x_s, y_s, z_s). The solutions for the resulting potentials are:

For the region $0 < z < z_s$:

$$\phi_w^+ = \int_0^\infty [C_s e^{\lambda(z-z_s)} + A(\lambda)e^{-\lambda z} + B(\lambda)e^{\lambda z}]\ J_o(\lambda|r_s - r|)\ d\lambda; \qquad \text{(B-1)}$$

For the region $z_s < z < h$:

$$\phi_w^- = \int_0^\infty [C_s e^{-\lambda(z-z_s)} + A(\lambda)e^{-\lambda z} + B(\lambda)e^{\lambda z}]\ J_o(\lambda|r_s - r|)\ d\lambda; \qquad \text{(B-2)}$$

For the region $h < z < h + t$:

$$\phi_\ell = \int_0^\infty [C(\lambda)e^{-\lambda z} + D(\lambda)^{\lambda z}]\ J_o(\lambda|r_s - r|)\ d\lambda; \qquad \text{(B-3)}$$

For the region $z > h + t$:

$$\phi_s = \int_0^\infty E(\lambda)e^{-\lambda z}\ J_o(\lambda|r_s - r|)d\lambda; \qquad \text{(B-4)}$$

where $|r_s - r| = [(x - x_s)^2 + (y - y_s)^2]^{1/2}$ and $C_s = \dfrac{I_s\rho_w}{4\pi}$.

The boundary conditions require that no current flow out of the waste material surface

$$\left(\frac{\partial \phi_w^+}{\partial z}\right)_{z=0} = 0. \tag{B-5}$$

At the layer interface, the potentials and current densities must be continuous

$$[\phi_w^-]_{z=h} = [\phi_\ell^+]_{z=h}, \tag{B-6}$$

$$\frac{1}{\rho_w} \left(\frac{\partial \phi_w^-}{\partial z}\right)_{z-h} = \frac{1}{\rho_\ell} \left(\frac{\partial \phi_\ell}{\partial z}\right)_{z=h}, \tag{B-7}$$

$$[\phi_\ell]_{z=h+t} = [\phi_s]_{z=h+t}, \tag{B-8}$$

and

$$\frac{1}{\rho_\ell} \left(\frac{\partial \phi_\ell}{\partial z}\right)_{z=h+t} = \frac{1}{\rho_s} \left(\frac{\partial \phi_s}{\partial z}\right)_{z=h+t}. \tag{B-9}$$

These relationships lead to five linear algebraic equations to be solved for the unknown coefficients A, B, C, D, and E. The solution for the potential above and below the source current electrode is

$$\phi_p = \frac{I_s \rho_w}{4\pi} \quad \frac{1}{\sqrt{|r - r_s|^2 + (z + z_s)^2}} + \frac{1}{\sqrt{|r - r_s|^2 + (z - z_s)^2}}$$

$$+ \int_0^\infty R(\lambda) \frac{[e^{-\lambda(h+z_s)} + e^{-\lambda(h-z_s)}]}{1 - R(\lambda)\, e^{-2\lambda h}}$$

$$\times [e^{-\lambda(h+z)} + e^{-\lambda(h-z)}]\, J_o(\lambda|r - r_s|)\, d\lambda, \tag{B-10}$$

where:

$$R(\lambda) = -\frac{k_{\ell w} + k_{s\ell}\, e^{-2\lambda t}}{1 + k_{\ell w}\, k_{s\ell}\, e^{-2\lambda t}}\ , \tag{B-11}$$

in which $k_{\ell w}$ and $k_{s\ell}$ are given in Equations (A-17) and (A-19), respectively. For a thin, highly resistive liner of thickness, t, and resistivity, ρ_ℓ, the function, $R(\lambda)$, reduces to

$$R(\lambda) \approx \frac{\rho_s - \rho_w + \lambda t \rho_\ell}{\rho_s + \rho_w + \lambda t \rho_\ell}\ . \tag{B-12}$$

APPENDIX C

SITE SURVEY PLAN FOR FULL-SCALE FIELD TESTS FOR TESTING OF THE GEOMEMBRANE SURVEY TECHNIQUE - EPA LAND TREATMENT RESEARCH FACILITY

INTRODUCTION

Southwest Research Institute has developed an electrical technique for testing the physical integrity of geomembranes. The technique takes advantage of the high electrical insulating properties of geomembranes. For new installations, water is pumped into the facility, flooding the liner to be tested. Only the liner below the water is tested. A current source electrode is placed in the water above the liner, and a current return electrode is grounded outside the liner. If the membrane is punctured physically or separated, the electrical conductivity of the water and underlying soil form a current path at the leak point, increasing the current density at that point.

By mapping potentials across the surface of the water, the higher current density areas are identified, revealing the location of the leaks. Two floating measurement electrodes are used to measure voltage potentials in the water. An automatic data acquisition system is used to record measurements. An equipotential contour plotting program is used to analyze the measurements.

This specific site survey plan includes: (1) the planned layout of electrodes; (2) how the potential measurements are to be taken; (3) where the electronic equipment will be housed; and (4) the estimated manpower required to set up and conduct the survey.

FIELD DEMONSTRATION TEST PROCEDURES

Site Description

The EPA Land Treatment Research Demonstration Facility includes two 0.6 hectare high-density polyethylene lined liquid impoundments. These serve as storage impoundments for surface runoff water from test plots. The primary liner of the impoundments were seeping water at rates of 2 to 6 liters per minute. The impoundments contain 60 to 120 cm of fresh water. Pumps are installed for transferring water from one impoundment to the other.

General Test Procedures

Typical survey procedures followed after arrival at the site are:

(1) The Department of Geosciences mobile laboratory trailer is positioned adjacent to the impoundment. This lab contains the instrumentation, equipment, computer, and power supply necessary to conduct the survey.

(2) The remote current return electrode is installed near the impoundment and the current source electrode is installed in the liquid just below the liquid line.

(3) The electric winch used in previous tests at Southwest Research Institute is placed at the top of the berm. This winch is used to control the position of the measurement electrodes during data acquisition.

(4) Radial or rectilinear survey lines are established using a transit and tape measure. The liner is marked to correspond to radial lines 5 or 10 degrees apart. These marks are used to position the cable and measurement electrodes for measuring surface potentials.

(5) Surface potential measurements are taken along each survey line, beginning at the far edge of the impoundment and moving toward the source electrode. Survey procedures depend upon the specific site characteristics. The spacing of measurements along each line and the spacing between lines are based on the size of the site and depth of the liquid.

All measurements are recorded on magnetic disk using a Hewlett-Packard HP 9825 microcomputer located in the mobile laboratory. The computer is used to analyze the data on site and the results are plotted on a Hewlett-Packard 7475A printer plotter. The plotted data are inspected to determine if any areas of the impoundment need to be resurveyed in more detail. In this way, anomalies are identified and resurveyed immediately to assure a complete liner survey while the field crew is on site.

The minimum field crew consists of an engineer and a technician. The technician drives the truck and the mobile laboratory to the site and sets up for the survey. The engineer arrives prior to initiating the field measurements and remains until the survey is complete.

The site owner or responsible party receives a briefing on the results of the survey before the field crew leaves the site. Preliminary data analyses performed on site are presented to the owner and any questions are answered.

APPENDIX D

SITE SURVEY PLAN FOR FULL-SCALE FIELD TESTS FOR TESTING OF THE GEOMEMBRANE SURVEY TECHNIQUE - SITE IN THE VICINITY OF SAN ANTONIO, TEXAS

I. INTRODUCTION

Southwest Research Institute has developed an electrical survey technique to locate leaks in geomembrane liners for hazardous waste impoundments. If the liner is physically punctured or separated, the electrical conductivity of the liquid and underlying soil form a detectable current path by which the leak may be detected and located.

This site survey plan is for the full scale field evaluations of the electrical leak location technique at a newly constructed lined impoundment in the San Antonio vicinity where a double liner system has been installed but not yet placed into service.

II. OBJECTIVES OF THE SITE SURVEY PLAN

This site survey plan outlines the basic steps for conducting the tests. Because of the experimental nature of the investigations, and depending upon the initial findings, the plan may be modified as necessary in the field. The objective of this task is to verify the performance of the electrical leak detection and location equipment at a double-lined industrial facility. The survey results will be fully documented for the impoundment operator and for the Final Report for the EPA Project.

III. SITE DESCRIPTION

The impoundment to be surveyed is a double lined-impoundment lined with a 1.5 mm HDPE geomembrane. The depth of the impoundment is 5.5 m and the sidewall slopes are 3:1. The bottom of the bottom liner has a compound angle that slopes downward to two of the corners. With the impoundment filled to cover the bottom with a minimum of 75 mm of water, the covered area will be approximately 27 m × 59 m. The maximum depth of the water will be approximately 1 m.

IV. SITE SURVEY PLAN

The elements of the site survey plan are as follows:

(1) The tests will be conducted in a manner that will not require damage of the liner or other facilities at the site.

(2) The computer data acquisition system developed on the project will be used to conduct the survey.

(3) The calibration of the potential measurement system will be checked and recorded before and after the survey.

(4) River water will be pumped into the impoundment to cover the bottom of the impoundment to a depth of at least three inches.

(5) A 1-liter sample of the water will be taken in a plastic or glass bottle for liquid resistivity determination.

(6) All electrical paths between the water in the impoundment and the earth will be removed or insulated.

(7) The survey lines will spaced 30 cm apart.

(8) The survey lines will be parallel to the 59-m length of the impoundment.

(9) The liner near the edge of the water on the short edges of the impoundment will be marked with paint or yellow crayon to establish the parallel survey lines.

(10) Distinctive markings will be made at 1.5- and 3-m intervals.

(11) At least two of the line markings will be referenced to nearby fixed permanent locations outside the impoundment. (i.e. existing fence posts, buildings, structures)

(12) The injected current electrode will have a surface area of approximately 3600 square cm.

(13) The current return electrode will be placed in the ground outside of the impoundment. Measures will be taken to insure a good ground.

(14) The DC power to be injected will be limited to 1 ampere, 100 volts, or the level at which the potential measurement system overloads, whichever occurs first.

(15) The injected DC current and potential will be measured and recorded periodically.

(16) Operators will be stationed at the edge of the water on each end of the survey lines to move the scan cable sheaves.

(17) Field procedures will be adopted to eliminate the danger of electrical shock to the operating personnel. In particular, DC power will be disconnected before the operators come in contact with the water and any grounded item.

(18) Hard hats and safety glasses are required at the site.

(19) Non-conductive safety lines will be used to help the operators maneuver at the edge of the water.

(20) Survey scans will be made in both directions of winch travel.

(21) Data points will be taken every 15 cm along the survey lines.

(22) Weighted trailing electrodes will be used to make potential gradient measurements at the bottom of the impoundment.

(23) The potential electrode spacing will be 1 meter.

(24) All measurements will be recorded on flexible magnetic disks for on-site display and interpretation.

(25) Where feasible, any leaks found will be spot-checked with other leak location methods.

(26) Other leak location methods will be applied on a spot-check basis to make limited determinations if leaks were missed.

(27) Preliminary results will be used to direct the survey crew during the subsequent survey activities.

(28) The field crew for the survey will consist of a research scientist, staff technician, and technician.

(29) Detailed field notes will be maintained in a field log book. The field documentation required is to the level that the survey could be repeated to obtain the same results.

(30) Photographs of the field operations will be made to document the test procedures. The photographs will be composed so that the location, installer, or operator of the impoundment can not be identified.

(31) Relevant drawings of the impoundment will be requested from the impoundment operator, or the impoundment will be measured and sketched.

(32) A representative of the impoundment operator will receive a briefing and report on the results of the survey.

(33) A list of the location of any leaks found will be submitted to a representative of the impoundment operator before the survey crew leaves the site.

(34) If feasible, a follow-up visit to the site will be made after the impoundment is drained to assist in visually locating the leaks, and to verify, photograph, and document any leaks found.

(35) Any deviations from this survey plan will be documented.

From: V.NEWILL (EPA8000) Delivered: Fri 10-June-88 8:18 EDT Sys 163 (109)
Subject: Retirement - Dr. Thomas R. Hauser
Mail Id: IPM-163-880610-074771239

NOTE TO CORRESPONDENTS

FOR RELEASE: FRIDAY, June 10, 1988

Dr. Thomas R. Hauser, Director of EPA's Hazardous Waste Engineering Research Laboratory, has announced his retirement effective August 1, 1988 in order to accept an appointment as Research Professor of Civil and Environmental Engineering at the University of Cincinnati.

Dr. Hauser, whose outstanding Federal career has spanned more than 33 years, has served in a variety of important roles in the government's research and development efforts on problems of environmental pollution and the management and disposal of toxic and hazardous wastes. Dr. Hauser, in addition to his service as Laboratory Director at EPA's A.W. Breidenbach Environmental Research Center in Cincinnati, has also served as Deputy Director and then Director of EPA's Environmental Monitoring Systems Laboratory (EMSL) at EPA's major research complex in Research Triangle Park, North Carolina and as EPA's Senior Official for Research and Development at that location. Among a number of special assignments for which Dr. Hauser was responsible was his service as Field Director and Coordinator for all EPA environmental monitoring studies at Love Canal in upstate New York. In that role he coordinated the efforts of several EPA Laboratories, including his own, on studies to determine sources and amounts of contamination from hazardous wastes found at the Love Canal site. In late 1985 he also served briefly as EPA's Acting Deputy Assistant Administrator for Research and Development in Washington, D.C.

A native of Cincinnati, Hauser received his bachelors and masters degrees in chemistry from Xavier University and his doctorate in environmental engineering from the University of Cincinnati. He began his Federal career as a Commissioned Officer of the Public Health Service at the Taft Sanitary Engineering Center and, in 1958, joined the National Air Pollution Administration (NAPCA) as a research chemist. In 1970, he transferred to Research Triangle Park to become part of NAPCA's Health Effects Research Program. When NAPCA became a part of the U.S. Environmental Protection Agency in 1970, Hauser was named Deputy Director of EMSL. He was promoted to the post of Laboratory Director in 1977.

Dr. Hauser was named a charter member of the Federal government's elite Senior Executive Service in 1980. He is the author of over 50 articles in professional journals, books and EPA policy reports. His memberships include the American Chemical Society, the Air Pollution Control Association, the American Society for Testing Materials and the Sigma Xi honorary scientific society. He has held adjunct professorships at both North Carolina State University and the University of Cincinnati.

He and his wife, Jean, along with four of their five children, currently reside in Evendale, Ohio.